Mechanistic Insights into the Role of Bacterial Metabolites on Microbial-Induced Inflammation in Vaginal Epithelial Cells

Fabienne Danielle Hanton

November 2024

Department of Metabolism, Digestion and Reproduction

Imperial College, London

Declarations

Declaration of originality

I certify that all work presented in this thesis was performed by me unless stated otherwise.

Declaration of contribution

Statistical analysis was performed by Fabienne Hanton with assistance from Dr Katia Capuccini (VMET1 and FLIP-1 studies: Chapters 3 and 5). LC-MS protein data analysis was carried out by Dr Harry Whitwell. Proteomics data analysis using R, and AMICA was performed by Fabienne Hanton with assistance from Dr Sherrianne Ng (Chapter 7).

Copyright declaration

The copyright of this thesis rests with the author and is made available under a Creative Commons Attribution Non-Commercial 4.0 International Licence (CC BY-NC). Researchers are free to copy, distribute or transmit the thesis on the condition that they attribute it, that they do not use it for commercial purposes and that they do not alter, transform or build on it.

When reusing or sharing this work, researchers must ensure the licence terms are clear to others by naming the licence and linking to the licence text. Where work has been adapted, researchers should indicate that the work has been changed and describe those changes.

Please seek permission from the copyright holder for uses for this work that are not included in this licence or permitted under UK Copyright Law.

Abstract

The microenvironment of the lower female reproductive tract is a complex ecosystem composed of epithelial and immune cells and a diverse microbiota. Both host and microbial communities produce metabolites and immune mediators that regulate reproductive health and homeostasis. Disruption of this balance can lead to infection, infertility, miscarriage, preterm birth, and gynaecological disease. A healthy vaginal microbiome is usually dominated by *Lactobacillus* species, which produce lactic acid (LA) to maintain an acidic environment that protects against pathogens. Whereas, *Lactobacillus*-depletion, with greater bacterial diversity, is associated with elevated short-chain fatty acids and succinate, reduced acidity, inflammation, loss of epithelial barrier integrity, and greater risk of reproductive disorders. Although LA has been implicated in cytokine release from vaginal epithelial cells (VECs), its mechanisms remain unclear.

This thesis tested the hypothesis that LA is a key regulator of transcription factor activity and innate immune responses in VECs. The research aimed to characterise LA-mediated signalling in response to bacterial and viral agonists, identify potential lactate receptors, and examine the contribution of LA to epithelial barrier function. A proteomics approach was employed to identify novel pathways involved in LA-mediated VEC regulation.

Using a multilayered *in vitro* VEC model, LA was found to suppress inflammatory signalling, consistent with observations in cervicovaginal fluid samples collected from pregnant women. LA inhibited NFκB, AP-1, IRF3, and upstream kinases, with evidence for HCAR1 receptor involvement. Further support for LA's role in immune regulation was provided by studies of pregnant women, in whom therapeutic modulation of the vaginal microbiota towards *Lactobacillus* dominance was associated with increased LA levels and reduced inflammation. Proteomics analysis identified additional LA-responsive pathways related to cytoskeletal organisation, signalling, and metabolism. Overall, these findings provide new insight into the regulatory role of LA in inflammation of VECs and suggest broader implications for reproductive health and pregnancy outcomes.

Acknowledgements

A thesis in figures:

1 thesis

2 hands

7 years

309 pages

2 555 days

25 000 miles cycled

100 000 cells per well

First and foremost, I would like to express my deepest gratitude to my supervisors Professors David MacIntyre and Phil Bennett. David, I will always be grateful for your unwavering support and generosity with your time. You guided me patiently through challenges, answered my endless questions and even lent an extra pair of hands in the lab when things got hectic. Your patience with my evolving digital competence has been amazing. But above of all, your inspiring enthusiasm and dedication to preterm birth research have left a lasting impression.

I am also indebted to many brilliant scientists at Imperial College: Professor Aylin Hanyaloglu generously shared her deep expertise in GPCRs and their signalling pathways, always available to discuss ideas, offer thoughtful feedback, and encourage me throughout the project. Dr Alexiane Decout was a wonderful collaborator, and I was fortunate to have worked alongside her developing a VK2 reporter cell system, even though we ultimately lost it due to a freezer malfunction. I also thank Dr Harry Whitwell for introducing me to the fascinating world of proteomics.

To all my friends and colleagues on the 3rd floor, past and present: Alexiane, Belen, Beth, Denise, Hanine, Katia, Kim, Lucia, Lynne, Maria, Pamela, Sherrianne, Tanweer and Yooni, thank you for the camaraderie, encouragement, and all the smiles that carried me through the long days. Kim, Lucia and Aanya, thank you for teaching me so many lab skills with such patience. Katia and Sherrianne, your bioinformatics skills and support gave me the confidence to

organise the vast datasets and even venture into coding. I also extend my thanks to my Master's students, Maria, Jessica, Harriet, Guitar, Nathaniel, Hayley, Kate, and Katherine who contributed to this project.

Away from work, my heartfelt thanks go to Kim, Nathalie, Sharon, Rosalind, and the Dulwich Dodgers for keeping me sane. Meryl, thanks for travelling all the way from Australia, proof-reading chapters, sparking stimulating conversations, and keeping the home fires burning. And to Sharon and Lucia, despite your busy schedules, you became my most dedicated proofreaders; thank you.

Finally, to my family: thank you for your unwavering support, encouragement and love. Thomas, for asking insightful questions in a field we both care about; Oliver, for sharing advice from your own PhD journey; Angus and Julian, for countless cups of tea and constant support; and Peter, for much-needed distractions; and Florence and Max, for your curiosity and joy, and reminding me to step away from science from time to time.

Thank you all.

List of Publications and Presentations

Conference oral presentations

Hanton FD, Capuccini K, Ng S, Bayar E, Delgado-Diaz D, Tyssen D, Tachedjian G, Bennett PR and MacIntyre DA Bacterial metabolites mediate vaginal epithelial cell inflammation via pro-inflammatory transcription factor inhibition. Finalist for the 2025 John Gusdon New Investigator Award, American Society of Reproductive Immunology, St Paul, Minnesota, May 2025.

Hanton FD. Mechanistic insights into the role of lactate acidification on microbial-induced inflammation in vaginal epithelial cells. March of Dimes, London, June 2023.

Hanton FD, Hanyaloglu A, Bennett PR, MacIntyre DA. Mechanistic insights into the role of lactate acidification on microbial-induced inflammation in vaginal epithelial cells. 70th Annual Scientific Meeting for the Society for Reproductive Investigation, Brisbane, March 2023.

Hanton FD. Mechanistic role of lactate on microbial-induced inflammation of vaginal epithelial cells. Imperial College MDR Department Away Day, London, January 2023.

Hanton FD. Lactic acid and inflammatory mediation of vaginal epithelial cells. March of Dimes Annual Visit, London, November 2022.

Hanton FD, Gunstone H, Lee YS, Bennett PR and MacIntyre DA. Impact of lactate acidification on inflammatory pathway activation in vaginal epithelial cells. 4th Annual UK Preterm Birth Conference, Bristol, September 2018.

Conference poster presentations

Hanton FD, Bennett PR, MacIntyre DA. The role of lactate acidification on inflammatory pathway activation in vaginal epithelial cells. World of Microbiome, Milan, October 2019.

Hanton FD, Bennett PR, MacIntyre DA. The role of lactate acidification on microbial-induced inflammation in vaginal epithelial cells. British Society for Immunology - London Immunology Group, London, September 2019.

Hanton FD, Gunstone H, Chaitrakulthong N, Tay N, Lee YS, Bennett PR, MacIntyre DA. The role of lactate acidification on inflammatory pathway activation in vaginal epithelial cells. 66th Annual Scientific Meeting for the Society for Reproductive Investigation, Paris, March 2019.

Hanton FD, Foley J, Lee YS, Bennett PR, MacIntyre DA. Lactate acidification inhibits inflammatory pathway activation in vaginal epithelial cells. 3rd European Preterm Birth Conference, Edinburgh, September 2018.

Hanton FD, Foley J, Lee YS, Bennett PR, MacIntyre DA. Impact of lactate acidification on inflammatory pathway activation in vaginal epithelial cells. 65th Annual Scientific Meeting for the Society for Reproductive Investigation, San Diego, March 2018.

Hanton FD, Foley J, Lee YS, Bennett PR, MacIntyre DA. Inhibition of inflammatory pathway activation by lactate in vaginal epithelial cells. 3rd Annual UK Preterm Birth Conference, Leeds, September 2017.

Hanton FD, Lee YS, Bennett PR, MacIntyre DA. D-Lactic acid inhibits basal inflammatory pathways in human vaginal epithelial cells. 64th Annual Scientific Meeting for the Society for Reproductive Investigation, Orlando, March 2017.

Table of Contents

DECLARATIONS 2

ABSTRACT 3

ACKNOWLEDGEMENTS 4

LIST OF PUBLICATIONS AND PRESENTATIONS 6

TABLE OF CONTENTS 8

LIST OF FIGURES 14

LIST OF TABLES 20

ABBREVIATIONS 21

CHAPTER 1: INTRODUCTION 26

1.1 Scope of the problem 27

1.2 Cervicovaginal niche 27

1.2.1 Structure of the lower female reproductive tract 27

1.2.2 Cervicovaginal cell-microbe recognition 34

1.2.3 Signalling pathways 41

1.3 Vaginal microbiota and their importance in health and disease 48

1.3.1 Community state types: vaginal microbial communities 49

1.3.2 CST prevalence in health and disease 51

1.3.3 CST mediation of disease pathology 53

1.4 Microbiota and role of metabolites in vaginal mucosa interface 54

1.4.1 Lactic acid 55
1.4.2 Short chain fatty acids (SCFAs) 58
1.4.3 Receptor and transporter mediation of metabolite activity 61

1.5 LA and SCFA mediation of intracellular signalling pathways 62

1.6 Hypothesis and Aims 64

CHAPTER 2: MATERIALS AND METHODS 65

2.1 Materials 66
2.1.1 Cell lines and primary cells 66
2.1.2 Cell culture media, supplements and chemicals 66
2.1.3 Treatments, inhibitors and activators 67
2.1.4 Buffers and solutions 68
2.1.5 Western blotting reagents and materials 70
2.1.6 Antibodies 70
2.1.7 mRNA extraction, cDNA synthesis and qPCR reagents and materials 71
2.1.8 Kits 71
2.1.9 Instruments 72
2.1.10 Software 72

2.2 Methods 73
2.2.1 Cell culture 73
2.2.2 Assessment of cell viability and morphology 75
2.2.3 Acid acclimatisation experiments 76
2.2.4 Simulations of bacterial and viral infection using TLR agonists 76
2.2.5 MEK inhibition of VECs 77
2.2.6 Whole cell protein extraction 78
2.2.7 Protein analysis with SDS-PAGE and Western Blot analysis 79
2.2.8 mRNA extraction 80
2.2.9 DNase treatment and first-strand cDNA synthesis 80
2.2.10 Real-time PCR 81

2.2.11 Assessment of VEC barrier function using transepithelial electrical resistance (TEER) 83
2.2.12 Assessment of VEC G protein-coupled receptor (GPCR) function 83
2.2.13 Identification of lactate receptors and primer design 85
2.2.14 Metabolic profiling of cervicovaginal fluid by Desorption Electrospray Ionisation Mass Spectrometry (DESI-MS) 85
2.2.15 Lactin-V treatment of pregnant women 88
2.2.16 Proteomic profiling of VECs 90
2.2.17 Statistical analysis 94

CHAPTER 3: THE EFFECT OF LACTIC ACID ON ACTIVATION OF PRO-INFLAMMATORY TRANSCRIPTION FACTORS..... 96

3.1 Introduction 97

3.2 Results 98
3.2.1 Cervicovaginal microbial composition modulates metabolite composition in CVF of pregnant women affecting immune mediator production.....98
3.2.2 Epithelial cell culture model 101
3.2.3 Effect of acidity on inflammatory transcription factor activation in multilayered VECs 103
3.2.4 Effect of L-LA on transcription of pro-inflammatory immune mediators 105
3.2.5 Assessment of LA isoforms on pro-inflammatory mediators 108
3.2.6 Effect of D-LA and L-LA on TLR2/6-mediated transcription factor activation....109
3.2.7 Effect of L-LA on TLR3-mediated transcription factor activation 112
3.2.8 L-LA elicits an anti-inflammatory response in primary VECs 116
3.2.9 *L. crispatus* colonisation in pregnant women and its effect on LA concentration and inflammation.....117

3.3 Discussion 124

CHAPTER 4: LACTIC ACID MEDIATION OF TRANSCRIPTION FACTOR ACTIVATION IN VECS 132

4.1 Introduction 133

4.2 Results 135

4.2.1 Effect of L-LA on activation of kinases upstream of transcription factors 135

4.2.2 Inhibition of ERK activation 141

4.2.3 Effect of MEK inhibition on NF-κB and AP-1 142

4.2.4 Effect of MEK inhibition on vaginal epithelial cell barrier integrity 147

4.3 Discussion 149

CHAPTER 5: MEDIATION OF VEC INFLAMMATORY PATHWAYS BY SUCCINATE 154

5.1 Introduction 155

5.2 Results 156

5.2.1 Cervicovaginal microbial composition associates with succinate levels in CVF of pregnant women.....156

5.2.2 Effect of succinate on transcription factor activation in VECs treated with bacterial agonist 157

5.2.3 Effect of succinate on MAP kinase ERK activation in VECs treated with bacterial agonist 158

5.2.4 The effect of *L. crispatus* colonisation in pregnant women on CVF succinate concentration and inflammation 159

5.3 Discussion 164

CHAPTER 6: PRELIMINARY INVESTIGATION INTO LACTATE RECEPTORS..... 168

6.1 Introduction 169

6.2 Results 172

6.2.1 Identification of putative LA receptors and channels in VECs 172

6.2.2 Effect of L-lactate on $G\alpha_i$ signalling of HCAR1.....176

6.2.3 Effect of pertussis toxin (PTX) on GPCR signalling in VECs.....178

6.2.4 Effect of pertussis toxin on inflammatory transcription factors NFκB and AP-1, and MAP kinase ERK 180

6.3 Discussion 184

CHAPTER 7: PROTEOMIC-BASED CHARACTERISATION OF VEC RESPONSE TO LACTIC ACID 191

7.1 Introduction 192

7.2 Results 194

7.2.1 Generation of proteomics data 194

7.2.2 Impact of acidification on protein abundance in VECs 198

7.2.3 Effect of inhibiting MEK/ERK on protein abundance 213

7.2.4 Characterisation of LA-associated proteins regulated by MEK/ERK inhibition ..222

7.2.5 Further consideration of selected pathways and proteins 234

7.3 Discussion 240

CHAPTER 8: FINAL SUMMARY AND DISCUSSION 250

8.1 Summary of key findings 251

8.1.1 Lactic acid's anti-inflammatory effects 251

8.1.2 Role of microbiome modulation 251

8.1.3 Mechanistic insights into LA's action 252

8.1.4 Receptor signalling 253

8.1.5 Succinate and inflammatory pathways in VECs 253

8.1.6 Proteomics data 254

8.2 Implications for reproductive health and translational outcomes 254

8.2.1 Microbiome-targeted therapies 256

8.2.2 LA as a therapeutic agent 256

8.3 Limitations 258

8.4 Future Directions 259

8.5 Final Conclusions 261

CHAPTER 9: SUPPLEMENTARY 264

9.1 SWATH windows used in proteomics data 265

9.2 FLIP-1 patient pregnancy outcome data for patients that transition from CST IV to CST I 268

9.3 FLIP-1 patient pregnancy outcome data for patients that do not transition following Lactin-V treatment 269

9.4 IKK activation is suppressed by LA 1 hour after TLR agonist stimulation 270

9.5 LA-mediation of p38 phosphorylation following 30 minutes treatment with TLR agonists 271

9.6 LA-induced ERK activation following bacterial agonist stimulation for 30 minutes, 1 hour and 2 hours treatments 272

CHAPTER 10: REFERENCES 273

List of Figures

Figure 1.1 Overview of lower female reproductive tract (FRT) anatomy and components of mucosal immunity....28
Figure 1.2 Schematic of tight junctions in vaginal epithelial cells. 31
Figure 1.3 TLR receptors and their associated MAMPs. 36
Figure 1.4 Overview of TLR signalling pathways. 38
Figure 1.5 Simplified overview of classical NF-κB pathway. 43
Figure 1.6 Overview of MAPK signalling pathways. 44
Figure 1.7 Overview of TBK1-IRF3 signalling pathway. 47
Figure 1.8 Simplified metabolic pathways of L. crispatus in the vaginal mucosa. 56
Figure 1.9 Schematic of short-chain fatty acid metabolism....59
Figure 1.10 Metabolite profile of cervicovaginal fluid from healthy women and women with BV....60
Figure 2.1 Schematic of optimised Transwells® multilayered cell culture of VECs. 74
Figure 2.2 Study design and longitudinal sampling of cervicovaginal swabs collected from pregnancy cohort VMET1. 87
Figure 2.3 Study design showing longitudinal sampling and workflow of women enrolled in the FLIP-1 study (n = 62; 362 samples). 89
Figure 2.4 Workflow for the generation of proteomics data. 94
Figure 3.1 Distribution of community state types (CST) in the VMET1 cohort samples (n = 160 subjects). 101
Figure 3.2 VECs cultivated in Transwells® remain viable when exposed to physiological concentrations of L-LA (30 mM). 103
Figure 3.3 Exposure of VECs to acidic medium (pH 3.9 HCl, D-LA or L-LA) results in a temporary “acidic shock” which returns to baseline levels after 2 hours. 104
Figure 3.4 LA inhibits pro-inflammatory immune mediator production prior to gene transcription. 105
Figure 3.5 L-LA inhibits the production of pro-inflammatory immune mediators following stimulation with a bacterial agonist FSL-1 at a stage prior to gene transcription. 106

Figure 3.6 L-LA inhibits the production of pro-inflammatory immune mediators following stimulation with a viral agonist PIC at a stage prior to gene transcription. 107
Figure 3.7 Suppressive effect of LA inhibiting pro-inflammatory immune mediator decreases over time in the multilayered VECs model. 108
Figure 3.8 Pro-inflammatory immune mediators following stimulation with a bacterial agonist FSL-1 are inhibited by both isomers D-LA and L-LA. 109
Figure 3.9 Bacterial agonist FSL-1 induces a temporal change in transcription factor activation which is suppressed by LA. 111
Figure 3.10 L-LA suppresses viral agonist-induced activation of transcription factors NF-κB and AP-1. 113
Figure 3.11 Viral agonism of VECs activates transcription factor IRF3 which is suppressed by L-LA. 115
Figure 3.12 Microscopy showing formation of multilayers in primary vaginal epithelial cells. 116
Figure 3.13 L-LA suppresses viral and bacterial agonist-induced activation of transcription factors NF-κB and AP-1 in primary cells. 117
Figure 3.14 LA levels are higher when Lactobacillus species are dominant in cervicovaginal fluid. 118
Figure 3.15 Following treatment with Lactin-V levels of lactate decrease in samples that are Lactobacillus-deplete. 119
Figure 3.16 Lactate levels increase or remain the same in paired samples following Lactin-V treatment whereas IL-1β levels decrease. 120
Figure 3.17 Lactate levels increase or remain the same in paired samples transitioning from CST IV to CST I following treatment with Lactin-V whereas IL-1β levels decrease or remain the same. 121
Figure 3.18 Failure to transition to CST I leads to lower levels of lactate and high levels of IL-1β levels. 123
Figure 4.1 IKK is rapidly activated by the bacterial agonist in VECs, and LA suppresses this activation 136
Figure 4.2 FSL-1 activation of TBK1 in VECs is inhibited by LA. 137

Figure 4.3 LA-mediation of p38 and JNK phosphorylation in VECs treated with FSL-1 or PIC. 139
Figure 4.4 ERK is rapidly and strongly activated by LA. 141
Figure 4.5 ERK activation by LA is suppressed by MEK inhibitor U0126. 142
Figure 4.6 NF-κB and AP-1 activation are independent of ERK activation by LA. 143
Figure 4.7 Methanol activates NF-κB in acidic conditions. 144
Figure 4.8 ERK activation by LA is suppressed by MEK inhibitor U0126 solubilised in Cyrene™. 145
Figure 4.9 Cyrene and KSF medium have less impact on the confluence of the VEC monolayer treated with MEK inhibitor U0126. 146
Figure 4.10 NF-κB and AP-1 activation and inhibition are independent of ERK activation. ..147
Figure 4.11 L-LA attenuates barrier disruption by a MAPK-dependent mechanism in vaginal epithelial cells. 149
Figure 5.1 Assessment of CVF succinate concentration during pregnancy using direct on-swab desorption electrospray ionisation mass spectrometry (DESI-MS). 157
Figure 5.2 Succinate suppresses bacterial agonist-induced activation of transcription factors NFκB and AP-1. 158
Figure 5.3 ERK activation by succinate is reduced when the VECs have been exposed to a bacterial agonist. 159
Figure 5.4 Following treatment with Lactin-V levels of succinate increase in cervicovaginal fluid samples that are Lactobacillus-deplete. 160
Figure 5.5 Succinate levels show an upward trend in the paired samples following Lactin-V treatment. 161
Figure 5.6 Succinate levels change when CVF microbial community transitions from CST IV to CST I following Lactin-V treatment. 162
Figure 5.7 Failure to transition to CST I following Lactin-V treatment leads to changes in succinate levels. 163
Figure 6.1 Overview of receptor- and channel-mediated mechanisms regulating LA signalling pathways in different cellular systems. 169
Figure 6.2 LA ligand inhibits cAMP signalling pathways via HCAR1 receptor. 171

Figure 6.3 mRNA gene expression levels of lactate receptor GPR81 (HCAR1) are increased in the presence of L-LA levels. 175
Figure 6.4 L-LA decreases forskolin-induced intracellular cAMP levels at pH 7.4. 177
Figure 6.5 Intracellular cAMP levels are affected by low pH. 178
Figure 6.6 Pertussis toxin (PTX) significantly decreases concentrations of intracellular cAMP at pH 7.4. 179
Figure 6.7 Effect of forskolin on cAMP levels in VECs. 180
Figure 6.8 Pertussis toxin suppresses phosphorylation of p65, c-Jun and ERK in VECs. 181
Figure 6.9 L-LA activation of ERK is reduced but not absent when VECs have been pre-treated with pertussis toxin. 182
Figure 6.10 Differential effects of cAMP regulation of inflammatory pathways. 183
Figure 7.1 General workflow of analysis using bioinformatics in MS-based proteomics. 193
Figure 7.2 Examination of data quality and robustness generated by LC-MS for different VEC treatments. 195
Figure 7.3 Protein abundance quantification across replicates. 196
Figure 7.4 Sample LLA.2 was excluded from the final data set used for analysis based on the different protein abundance patterns compared to the other replicates. 197
Figure 7.5 Proteomic differences in VECs exposed to different pH conditions with or without L-LA. 199
Figure 7.6 Differentially expressed proteins in VECs exposed to acidity were predominantly enzymes or involved in cellular structure and mapped to cytoskeletal regulation pathways as well as inflammatory signalling pathways. 200
Figure 7.7 Exposure of VECs to acidity altered the abundance of relatively few proteins. ...202
Figure 7.8 Differences in protein abundance in VECs exposed to pH 7.4 or LLA. 203
Figure 7.9 STRING protein-protein interaction (PPI) network of the differentially expressed proteins that changed in abundance when VECs were treated with L-LA. 204
Figure 7.10 Proteins upregulated by L-LA are predominantly enzymes or involved in cellular structure and map to cytoskeletal regulation pathways as well as inflammatory signalling pathways. 205
Figure 7.11 Protein-protein interaction network of the differentially expressed proteins that increase in abundance relative to pH 7.4 when VECs were treated with L-LA. 206

Figure 7.12 Protein-protein interaction network showing key protein clusters and important pathways for differentially expressed proteins significantly decreased by L-LA. relative to pH 7.4.....208
Figure 7.13 Protein abundance differences in VECs exposed to pH 3.9 or L-LA.....209
Figure 7.14 L-LA upregulated 105 proteins that did not increase in abundance with acidity alone. 210
Figure 7.15 L-LA upregulated proteins associated with cytoskeletal regulation. 211
Figure 7.16 Downregulation of 71 unique proteins by L-LA exposure. 212
Figure 7.17 L-LA downregulated signal transduction pathway proteins at the plasma membrane.....213
Figure 7.18 Heatmap of proteins differentially expressed following MEK inhibition at pH7.4. 214
Figure 7.19 Proteins whose abundance changed when MEK was inhibited at pH 7.4 showed few interactions. 215
Figure 7.20 Key pathways for proteins upregulated by MEK inhibition at pH 7.4. 216
Figure 7.21 Proteomic differences in vaginal epithelial cells exposed to pH 3.9 with or without MEK inhibition. 218
Figure 7.22 MEK Inhibition at pH 3.9 led to the upregulation of 10 proteins which showed few protein-protein interactions.....219
Figure 7.23 Downregulation of proteins involved in cytoskeletal regulation and inflammatory signalling pathways following MEK inhibition at pH 3.9. 220
Figure 7.24 Fewer proteins changed in abundance in VECs exposed to L-LA with MEK inhibition at pH 3.9. 221
Figure 7.25 No clustering was observed in proteins that changed in abundance in VECs exposed to L-LA with MEK inhibition. 222
Figure 7.26 MEK inhibition in the presence of L-LA upregulated 141 proteins and downregulated 15 proteins compared to pH 7.4. 223
Figure 7.27 MEK inhibition in the presence of L-LA led to the upregulation of 42 proteins and downregulation of 26 proteins compared to pH 3.9. 224
Figure 7.28 Overlap of proteins that changed in abundance in the presence of L-LA with or without MEK inhibitor at (A) pH 7.4 and (B) pH 3.9. 225

Figure 7.29 L-LA upregulated 92 proteins that failed to be upregulated when MEK was inhibited at pH 7.4. 228
Figure 7.30 Protein-protein interaction network for 37 proteins downregulated by L-LA but no longer abundant when MEK was inhibited at pH 7.4. 229
Figure 7.31 Protein-protein interaction network and key pathways for L-LA-upregulated proteins no longer detected when MEK was inhibited at pH 3.9. 231
Figure 7.32 Key pathways for proteins downregulated by L-LA but no longer abundant when MEK was inhibited at pH 3.9. 233
Figure 7.33 Protein clusters of L-LA-regulated proteins no longer detected when MEK was inhibited at both pH 7.4 and pH 3.9. 234
Figure 7.34 Protein-protein interaction network of the 22 cytoskeletal proteins with significantly altered abundance in VECs exposed to L-LA. 236
Figure 7.35 Cytoskeletal protein abundance is differentially regulated by L-LA and MEK inhibition. 238
Figure 7.36 L-LA significantly increases the abundance of Flightless-I (Flii). 238
Figure 7.37 Changes in the abundance of integrin-binding proteins talin, vinculin and paxillin in response to L-LA. 239
Figure 7.38 Changes in the abundance of integrin-binding proteins integrin-β1 (ITB1), focal adhesion kinase 1 (FAK1) and Flight I-associated protein 1 (FLAP1) with L-LA. 240
Figure 7.39 Putative role of LA, Flii, nucleoredoxin and MyD88 in TLR signalling in VECs. ...247
Figure 8.1 Overview of treating women with a Lactobacillus-deplete vaginal microbiome with Lactin-V. 252
Figure 8.2 Schematic summarising the modulation of inflammatory signalling pathways in VECs by LA and succinic acid. 262
Figure 9.1 IKK activation continued to be suppressed by LA 1 hour after TLR agonist stimulation. 270
Figure 9.2 LA-mediation of p38 phosphorylation in VECs treated with FSL-1 or PIC for 30 minutes. 271
Figure 9.3 ERK continues to be strongly activated by LA after 4 hour's exposure. 272

List of Tables

Table 1.1 Summary of vaginal microbiome community state types using VALENCIA classification. 51
Table 2.1 Media composition for apical treatment of multilayered VECs. 76
Table 2.2 Sequences of primers used in real time PCR. 82
Table 2.3 Gradient elution programme used in HPLC. 92
Table 3.1 Demographics of patients in the VMET1 study. 99
Table 3.2 Distribution of community state types (CST) in the VMET1 cohort samples (n = 160 subjects, 455 samples). 100
Table 6.1 Potential receptors for LA identified by BLAST search and literature review. 174
Table 7.1 Different VEC treatments used for proteomics study 194
Table 7.2 Proteins no longer abundant when MEK is inhibited at pH 7.4 or pH 3.9 in presence of L-LA 226
Table 7.3 Differentially expressed cytoskeletal proteins when L-LA is present 235
Table 9.1 SWATH windows used in proteomics data 265
Table 9.2 FLIP-1 patient pregnancy outcome data for women that transition from CST IV to CST I. 268
Table 9.3 FLIP-1 patient pregnancy outcome data for women that do not transition following Lactin-V treatment. 269

Abbreviations

AC	Adenylate cyclase
AIM2	Absent in melanoma-2
ALI	Air-liquid interface
ALR	AIM2-like receptor
AMPs	Antimicrobial Peptides
ANOVA	Analysis of variance
AP-1	Activator protein 1
APC	Antigen presenting cell
APS	Ammonium peroxydisulfate
ATF	Activating transcription factor
ATP	Adenosine triphosphate
BSA	Bovine serum albumin
BV	Bacterial vaginosis
CAMP	Commensal-associated molecular pattern
cAMP	Cyclic adenosine monophosphate
CARD	Caspase activation and recruitment domain
CCKR	Cholecystokinin receptors
cDNA	Complementary deoxyribonucleic acid
cGAS	cyclic GMP-AMP synthase
CLR	C-type lectin receptor
CREB	Cyclic adenosine monophosphate response element-binding protein
CST	Community state type
CVF	Cervicovaginal fluid
DAMP	Damage-associated molecular pattern
DAPI	4’,6-diamidino-2-phenylindole
DEP	Differentially expressed protein
DEPC	Diethyl pyrocarbonate

D-LA	D-lactic acid
DMEM	Dulbecco's modified Eagle's medium
DMSO	Dimethyl sulfoxide
DNA	Deoxyribonucleic acid
dNTP	Deoxynucleoside triphosphate
DTT	Dithiothreitol
E-cadherin	Epithelial cadherin
ECL	Enhanced chemiluminescence
EDTA	Ethylenediaminetetraacetic acid
EGF	Epidermal growth factor
EMMPRIN	Extracellular matrix metalloproteinase inducer
EPAC	Exchange protein directly activated by cAMP
ERK	Extracellular signal-regulated kinase
FBS	Foetal bovine serum
Flii	Flightless I protein
FRT	Female Reproductive Tract
GAPDH	Glyceraldehyde 3-phosphate dehydrogenase
GDE	Glycogen-degrading enzyme
GDP	Guanosine diphosphate
GEF	Guanine nucleotide exchange factor
GO	Gene Ontology
GPCR	G protein-coupled receptor
GRK	G protein-coupled receptor kinase
GTP	Guanosine triphosphate
HCAR	Hydroxycarboxylic acid receptor
HIV	Human immunodeficiency virus
HPV	Human papillomavirus
IBMX	3-isobutyl-1-methylxanthine
IFN	Type I interferon
Ig	Immunoglobulin

IκB	Inhibitor of κB
IKK	IκB kinase
IL	Interleukin
IL-1β	Interleukin 1β
IL1-Ra	Interleukin 1 receptor antagonist
IRAK	Interleukin-1 receptor associated kinase
IRF3	Interferon regulatory factor 3
JAM	Junctional adhesion molecule
JNK	c-Jun N-terminal kinase
L-LA	L-lactic acid
LA	Lactic acid
LPS	Lipopolysaccharide
LRR	Leucine-rich repeat
MAL	MyD88 adaptor-like
MAMP	Microorganism-associated molecular pattern
MAPK	Mitogen-activated protein kinase
MAPKK	MAP kinase kinase
MAPKKK	MAP kinase kinase kinase
MAVS	Mitochondrial antiviral signalling protein
MCT	Monocarboxylate transporter
MEF2	Myocyte-enhancer factor 2
MEK	Mitogen-activated protein kinase kinase
MIP3	Macrophage inflammatory protein 3
MMP	Matrix metalloproteinase
mRNA	Messenger ribonucleic acid
MS	Mass spectrometry
mTOR	Mammalian target of rapamycin
MyD88	Myeloid differentiation primary response 88
NEMO	NF-κB essential modulator
NF-κB	Nuclear factor kappa-light-chain-enhancer of activated B cells

NIK	NF-κB inducing kinase
NLR	NOD-like receptors
NLRP	NOD-like pyrin domain-containing protein
NOD	Nucleotide-binding oligomerisation domain
NXN	Nucleoredoxin
PBS	Phosphate buffered saline
PCR	Polymerase chain reaction
PDGF	Platelet-derived growth factor
PI3K	Phosphoinositide 3-kinase
PKA	Protein kinase A
PKC	Protein kinase C
PMSF	Phenylmethylsulfonyl fluoride
PPI	Protein-protein interaction
PPROM	Premature prelabour rupture of membranes
PRR	Pattern recognition receptors
PTB	Preterm birth
PTL	Preterm labour
PTX	Pertussis toxin
PVDF	Polyvinylidene difluoride
RANTES	Regulated on activation, normal T cell expressed and secreted
Rel	Proto-oncogene c-Rel
RIG-I	Retinoic acid-inducible gene I
RIPA	Radioimmunoprecipitation assay
RLR	RIG-I-like receptors
SC	Stratum corneum
SCFA	Short-chain fatty acid
SDS	Sodium dodecyl sulphate
SEM	Standard error of the mean
SLPI	Secretory leukocyte protease inhibitor

SMCT	Sodium monocarboxylate transporter
sPTB	Spontaneous preterm birth
STAT3	Signal transducer and activator of transcription 3
STI	Sexually transmitted infection
STING	Stimulator of interferon genes
TAK1	TGFβ-activated kinase 1
TBK1	TANK-binding kinase 1
TBS	Tris-buffered saline
TEMED	Tetramethylethylenediamine
TF	Transcription factor
TIR	Toll-IL-1 receptor
TIRAP	TIR-domain-containing adaptor protein
TLR	Toll-like receptor
TNF	Tumor necrosis factor
TRAF	Tumor necrosis factor receptor-associated factor
TRAM	TRIF-related adaptor molecule
TRIF	TIR-domain-containing adaptor protein inducing interferon β
VECs	Vaginal epithelial cells
UTI	Urinary tract infection
ZO-1	Zonula occludens-1

Chapter 1: Introduction

1.1 Scope of the problem

Microbial-induced inflammation in the lower female reproductive tract (FRT) represents a significant clinical challenge, contributing to conditions such as bacterial vaginosis (BV), adverse pregnancy outcomes, and increased susceptibility to sexually transmitted infections (STIs). Disruptions in the vaginal microbiota, including depletion of *Lactobacillus* species and an increase in short-chain fatty acids (SCFAs) production, are associated with heightened inflammatory responses. Although substantial progress has been made in characterising the composition of the FRT microbiota, the mechanistic role of bacterial metabolites in driving inflammation remains poorly defined. Bacterial metabolites such as lactic acid (LA) and SCFAs can interact directly with host epithelial and immune cells, modulating cytokine secretion and compromising mucosal barrier integrity (1, 2). Elucidating the mechanisms by which these metabolites influence host immune pathways is essential for developing targeted diagnostics and therapies aimed at restoring homeostasis, rather than merely suppressing pathogenic microorganisms (3-5).

1.2 Cervicovaginal niche

1.2.1 Structure of the lower female reproductive tract

The FRT is an important physical and immunological barrier to exogenous pathogens. It is composed of two distinct regions: upper and lower. The upper FRT is composed of the endocervix and the uterus while the lower region is composed of the vagina and the ectocervix (Figure 1.1).

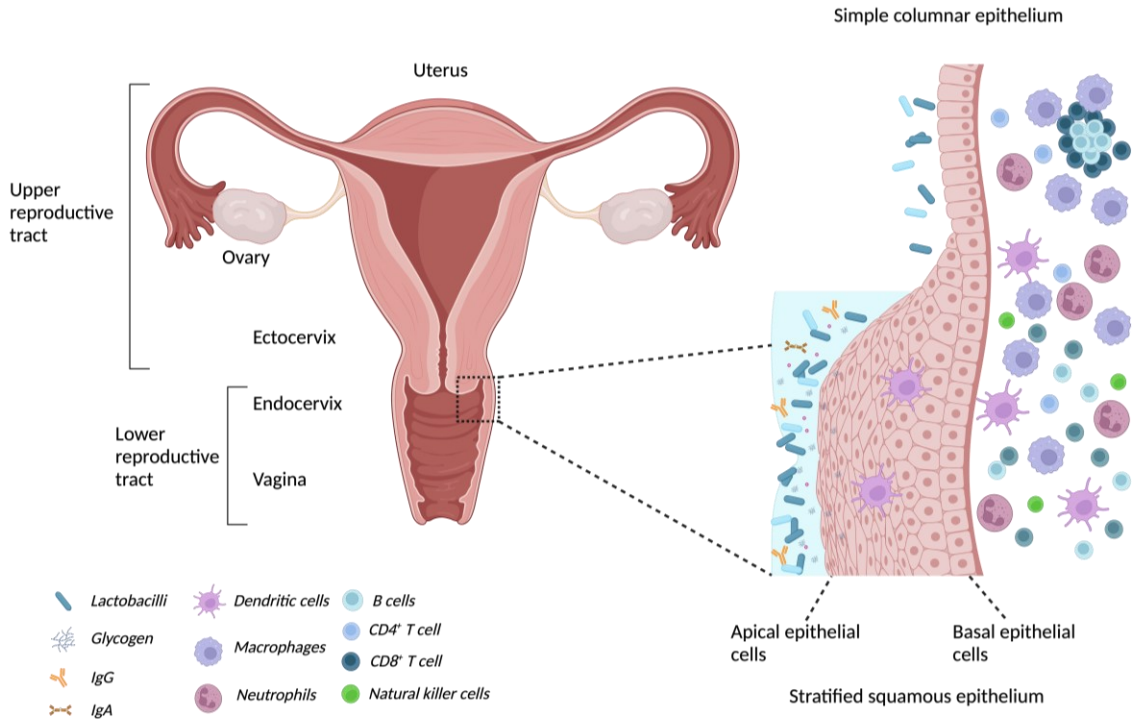

Figure 1.1 Overview of lower female reproductive tract (FRT) anatomy and components of mucosal immunity

The lower FRT is lined with a stratified squamous epithelium resting on a lamina propria containing progenitor and immune cells such as macrophages, natural killer cells, and T cells. The apical surface of the epithelium consists of glycogen-rich, denucleated, flattened cells. This surface is covered by a mucosal layer containing innate immune factors, such as antimicrobial peptides (AMPs), mucins and immunoglobulins, as well as commensal bacteria such as *Lactobacilli,* which help prevent the passage of pathogens through the epithelial barrier (6-8)**.** Adapted from Plesniarski *et al. Created with BioRender.com*.

The vaginal and ectocervical mucosa are contiguous and histologically similar, lined with stratified squamous epithelial cells and covered in cervicovaginal fluid (CVF), whereas the endocervix is formed of a simple columnar epithelium. The FRT maintains a unique immunological environment, tolerating the presence of commensal bacteria, sperm and fertilised ova, yet retaining the ability to respond to mount effective responses to pathogens and adverse conditions.

1.2.1.1 Structure of the epithelial barrier

Epithelial tissues are composed of tightly packed cells joined by intercellular junctions that form a semipermeable barrier (9). They line internal and external surfaces, ducts and secretory units of glands, regulating the exchange of molecules and protecting underlying tissues. The structure of the epithelial tissue varies with function. The vaginal epithelium is a keratinised stratified squamous epithelium composed of three layers: basal (*stratum basale*), suprabasal, and apical (*stratum corneum,* SC) layers (10, 11). The basal epithelial cells sit on a lamina propria, resembling the gut epithelium, which harbours a dense immune cell population and functions as a major effector site of immune activity. Cells in the SC are flattened, denucleated, depleted of organelles, and enriched in cytoplasmic glycogen. These uppermost layers lack tight junctions, making them permeable and central to complex interactions between immune mediators and microbes (7, 12).

The vaginal epithelium is dynamic and responsive to hormonal and environmental changes (7). Prior to the onset of puberty, the epithelium is thin and lacks the SC layer (13). During reproductive years, the vaginal epithelium thickens and a distinct apical cornified layer develops. While its thickness varies modestly with hormonal changes, glycogen content stores fluctuates substantially in response to oestrogen levels (14). Lower progesterone levels are associated with increased concentrations of free glycogen (15). After menopause, the vaginal epithelium becomes thinner, and glycogen levels decrease (15-17).

1.2.1.2 Intercellular junctions and epithelial mucosal barrier

The mucosal surface of the FRT is the primary site of entry for cellular and molecular immune mediators, as well as many invading pathogens. Molecules or pathogens can cross the epithelium either transcellularly, requiring hydrophobicity or specific transport mechanisms, such as channels, pumps, or cotransporters or paracellularly, which is regulated by intercellular junctions which help maintain the integrity and organisation of cells in the mucosal barrier. Three types of intercellular junctional molecules are involved: tight junctions, adherens junctions and desmosomes (12). Tight junctions consist of transmembrane proteins,

such as occludin, claudins and junctional adhesion molecules (JAMs) that connect epithelial cells and control paracellular permeability by allowing ions and leukocytes to pass through while blocking pathogens (Figure 1.2) (18). Adherens junction proteins such as E-cadherin connect actin filaments between cells, supporting tissue integrity (19). Desmosomes, including JAM3, desmoglein and desmocollin anchor keratin intermediate filaments to create a strong elastic structural framework (18, 20, 21). Tight junction integrity is signalling pathways involving mitogen-activated protein kinases (MAPKs), G-proteins, protein kinase C (PKC), protein kinase A (PKA), myosin light chain kinase, Rho, and secondary messengers such as calcium and cyclic adenosine 3',5'-monophosphate (cAMP) (21, 22). For instance, phosphorylation of occludin by MAPKs attenuates its interaction with the tight junction protein, zonula occludens-1 (ZO)-1, thereby reducing integrity of the epithelial barrier (23).

The most robust junctions are located in the parabasal layer where adherens junction proteins are abundant, whereas the upper layers are more permeable and lack of tight junctions (12).

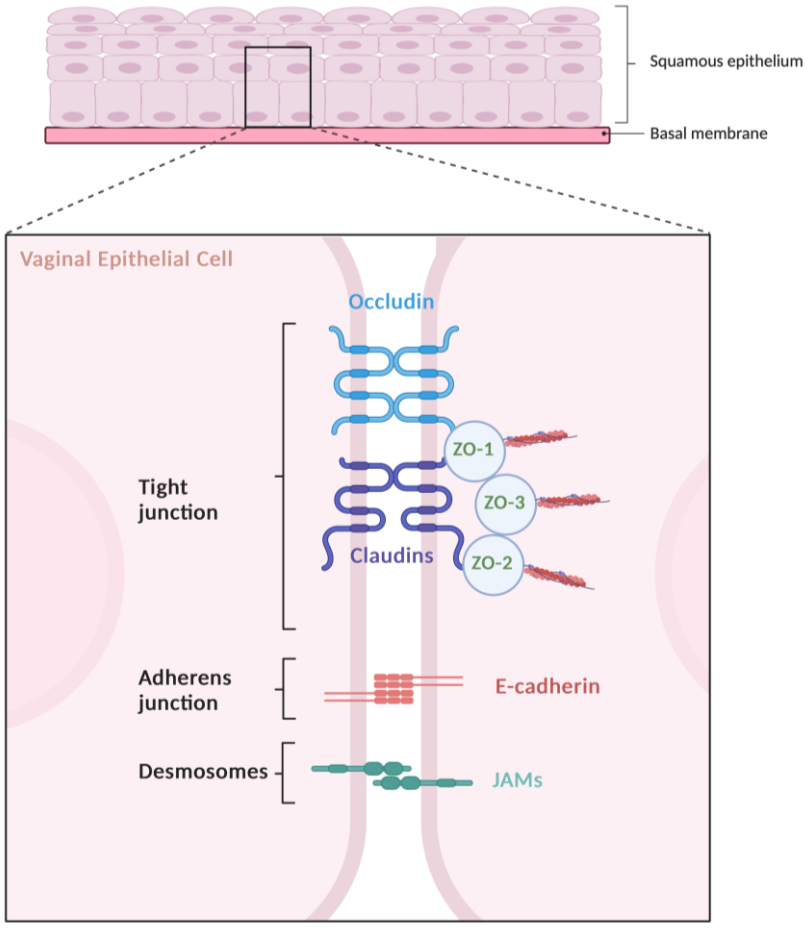

Figure 1.2 Schematic of tight junctions in vaginal epithelial cells.

Tight junctions, located in the basal layers, are formed by integral membrane proteins occludin and the claudins interacting laterally and linking to cytoplasmic proteins zonula (ZO)-1, -2 and -3. Integrity decreases progressively towards the apical surface, where cells slough into the vaginal lumen. Below the tight junctions, adherens junctions, mainly E-cadherin maintain cell-cell adhesion, and desmosomes anchor keratin intermediate filaments to the plasma membrane forming a strong elastic structural framework. *Created with BioRender.com*.

Tight junctions respond dynamically to stimuli such as hormones, cytokines, pathogens, growth factors, and calcium. For example, oestrogen reduces the tight junction protein occluding, increasing permeability, in a primary cervicovaginal epithelial cell model (24, 25). Apical vaginal and ectocervical epithelial cells have fewer tight junctions, facilitating regular sloughing (12). This process of exfoliation happens approximately every 4 hours (26) and contributes to displacement of pathogens and release of glycogen from the cells as they disintegrate and liberate their contents into the vaginal lumen. This releases an essential

energy source for the commensal bacteria, especially *Lactobacilli* and glycogen is used to produce LA, maintaining an acidic pH (27-29).

The epithelium is coated in CVF, the properties of which provide an ideal habitat for commensal bacteria whilst suppressing colonisation of pathogens (30). CVF is a complex mixture of cervical mucus, secretions from sebaceous glands, sweat glands, Bartholin's and Skene's glands, plasma transudate and exfoliated cells (31). The gel-forming mucins are N- and O-glycosylated proteins which forming disulphide-linked long polymers through their amino- and carboxy-terminal regions. These are secreted into the cervicovaginal lumen and form a heterogenous protein matrix (32) that varies during the menstrual cycle, with MUC5B peaking at ovulation (33, 34). CVF also contains immune components such as antibodies, defensins, secretory immunoglobulin A (IgA), IgG, lactoferrin and lysozymes, along with bacterial products and exfoliated cells (7, 30, 35).

CVF enhances the adhesion of commensal vaginal microbes, whilst trapping exogenous pathogens (30, 36). Evidence from the intestinal tract has revealed that antibodies such as IgA play an important role in maintaining a healthy diversified microbial composition (37). In the lower FRT, bacterial IgA is enriched in women with a *Lactobacillus crispatus*-dominant microbiota, suggesting an anti-inflammatory role (38). Antibodies in the mucus are tightly bound and contribute to the pathogen-trapping properties of the mucus (39).

1.2.1.3 Mucosal immunity in the cervicovaginal niche

Immune cells in the lower FRT have complex roles in that they must protect against pathogens, while tolerating commensal species and exogenous factors such as sperm and in later stages of reproduction, the semi-allogenic foetus. The vaginal and cervical tissues contain mainly antigen presenting cells (APCs), including macrophages, natural killer cells and dendritic cells and T cells, with fewer immune cells found in the vaginal tissues (40). The lower vagina contains high concentrations of $CD8^+$ T cells in the lamina propria with very few $CD4^+$ T cells. Macrophages and dendritic-like cells are also detected in the lamina propria and epithelium (41).

Antimicrobial molecules in the mucosa are strongly influenced by oestrogen levels and spatially regulated. For example, high oestrogen levels correlate with increased IgA, IgG, lactoferrin, β-defensin 2, elafin, secretory leukocyte protease inhibitor (SLPI) and α-defensin1-3 (HNP1-3) in the upper FRT, and comparatively lower levels in the lower FRT. Unlike other mucosal sites where IgA predominates, IgG is the most abundant immunoglobulin in CVF (42-44). Oh *et al.* showed that circulating memory B cells are the source of IgG antibodies in the CVF (45). Levels of IgA and IgG appear to be hormonally regulated, peaking immediately before ovulation and reaching lowest levels during menstruation (46).

In addition, the concentrations of pro-inflammatory cytokines IL-6 and IL-8 decrease in the vagina when oestrogen levels are at their highest, creating an environment conducive to sperm survival in the periovulation period (47).

1.2.1.4 *In vitro* models of the vaginal epithelium

To improve mechanistic understanding of the cervicovaginal epithelia, several *in vitro* model systems have been developed. The first immortalised vaginal cell lines were established and characterised by Fichorova *et al.* (48). The vaginal epithelial cell line VK2/E6E7 was found to closely resemble its tissue of origin as well as primary cell cultures. The immortalised cells displayed similar phenotypes to their tissue of origin even after a year in continuous culture. The addition of calcium to the growth medium promoted the formation of intercellular cadherin and desmosomal junctions.

Initially, *in vitro* models using 2D monolayer cultures of vaginal epithelial cells were widely used. These provide quick and inexpensive systems for study; however, they differ substantially from cervicovaginal tissue in several key ways. Monolayer models display different rates of cell differentiation and proliferation compared to *in vivo* tissue as well as differences in protein expression, and perhaps most importantly, they do not form multilayers and therefore multidirectional cell junctions (49, 50). The human vaginal environment is unique in having an acidic pH and so animal models are inadequate. To address these

shortcomings, *in vitro* 3D cell culture models have been developed. One of the first of these involves the seeding of epithelial cells onto a Transwell®, a semipermeable membrane, which permits the formation of polarised and differentiated multilayers using an air-liquid interface (ALI) (51). The ALI model simulates a mucosal environment where the cells obtain their nutrients on the basal surface and the apical surface of the epithelium is exposed to air which triggers cellular differentiation and the formation of tight junctions (52). In 2022, a "vagina-on-a-chip" model using hydrogels and microfluidics was described, however high technical variability and expense currently limits its utility (53-55). As such, a recent review of vaginal cell culture systems concluded that the ALI-VK2 model was most useful for studying multilayers, epithelial integrity and tight junction formation (6).

1.2.2 Cervicovaginal cell-microbe recognition

Cervicovaginal epithelial cells detect and respond to both commensal and pathogens through pattern recognition receptors (PRRs) expressed on the surface and within the cytoplasm of the cells, triggering an innate immune response (56-59).

PRRs detect microorganism-associated molecular patterns (MAMPs) or host-derived ligands that cause inflammation without infection called damage associated molecular patterns (DAMPs) (60-63). Some PRRs can also detect commensal-associated molecular patterns (CAMPs) (64). Recognition of commensal bacteria by PRRs is critical for maintaining host–microbe interactions and homeostasis.

PRRs are made up of three domains: ligand recognition domain, intermediate domain and effector domain. When a ligand binds to the ligand recognition domain, adaptor molecules are recruited by the effector domains which then trigger a cascade of signalling pathways. Six main classes of PRRs have been described including Toll-like receptors (TLRs), nucleotide-binding oligomerisation domain (NOD)-like receptors (NLRs), retinoic acid-inducible gene I (RIG-I)-like receptors (RLRs), C-type lectin receptors (CLRs), absent in melanoma-2 (AIM2)-like receptors (ALRs) and cyclic GMP-AMP synthase (cGAS) (65-69). TLRs and CLRs are

transmembrane receptors found both on the cellular plasma membrane as well as intracellular membranes. The others reside in intracellular compartments (70-72).

The immune system has evolved to protect the host from pathogens but in the vaginal niche the ability to generate an inflammatory response by BV-associated bacteria is much lower than in the endocervical cells (73). Gerson *et al.* showed that a TLR2-mediated immune response is activated by high doses of bacteria regardless of whether the bacterial species is beneficial or detrimental to female reproductive tract health (74). This is important because vaginal epithelial cells may be exposed to a much higher bacterial load than further up the reproductive tract; it was postulated that this immune response could be a regulatory mechanism by the cervicovaginal epithelium to control bacterial overgrowth. Immunoglobulins found in the mucosa and CVF can bind to pathogens and interact with the mucosal layer allowing clearance from the FRT (75).

1.2.2.1 Toll-like receptors

Toll-like receptors (TLRs) are type I transmembrane proteins made up of a horseshoe-shaped extracellular or cytoplasmic leucine-rich repeat (LRR) domain and an intra-cytoplasmic toll/IL-1 receptor (TIR) domain which are connected by a single transmembrane domain. Ligand recognition occurs in the LRR domain whilst intracellular signal transfer happens via the TIR domain (76). Ten TLRs have been identified in humans: TLR1, TLR2, TLR4, TLR , TLR6, and TLR10 are expressed on the cell surface where they recognise extracellular microbes and ligands, while TLR3, TLR7, TLR8, and TLR9 are intracellular and localised in endosomal compartments within the cytosol where they detect pathogen-derived nucleic acid sequences (Figure 1.3) (61-63, 70, 76-81). TLR2 forms a heterodimers with either TLR1 or TLR6 to recognise MAMPs of pathogens, including lipoproteins, peptidoglycans, lipoteichoic acid, zymosan, mannan and some glycoproteins (82). TLR3 recognises double-stranded RNA (dsRNA) (83). TLR4 and the secreted glycoprotein myeloid differentiation factor 2 (MD-2) form a heterodimer that acts as a receptor for lipopolysaccharide (LPS) molecules found on the surface of Gram-negative bacteria (84). TLR5 identifies bacterial flagellin (85). TLR7 and TLR8 detect single-stranded RNA (61, 78). TLR9 recognises CpG-enriched double-stranded DNA (78, 86). TLR10, which lacks a

clearly defined ligand, exhibits both pro-inflammatory and anti-inflammatory properties (87-89).

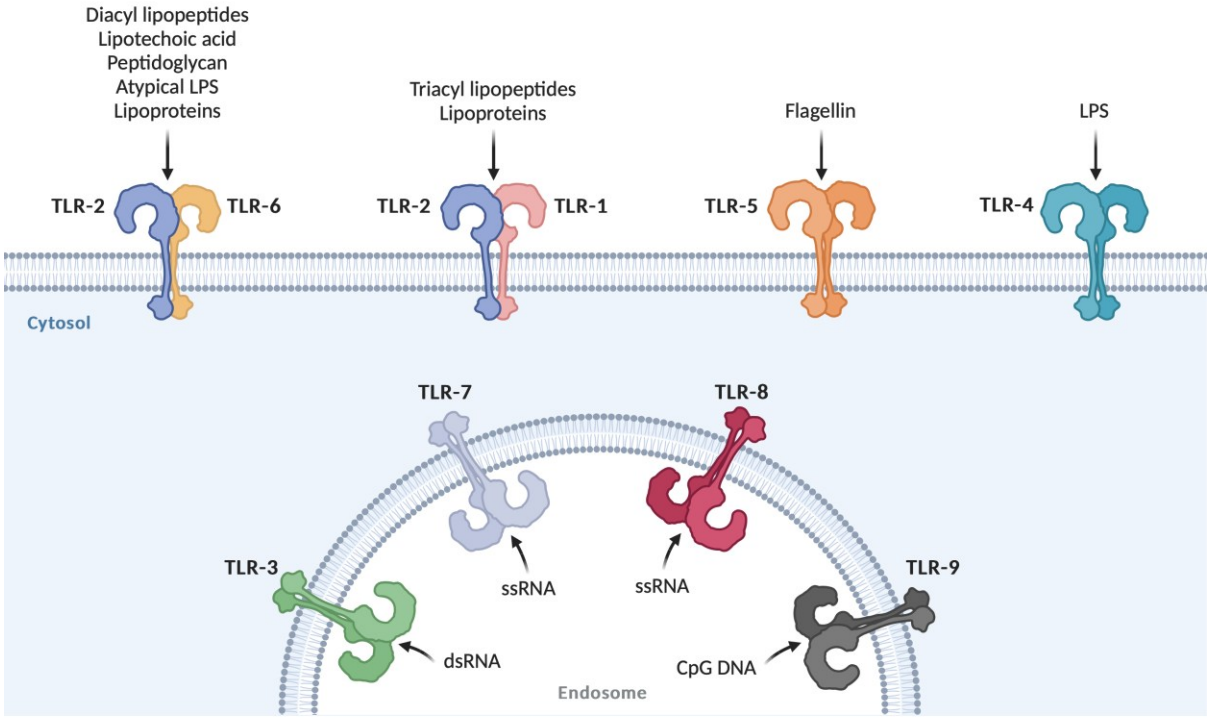

Figure 1.3 TLR receptors and their associated MAMPs.

TLRs recognise one or more MAMPs through their LRR domain. They can form homo- or heterodimers and recruit adaptor molecules with the same TIR domain to transmit signals. Adapted from Mantovani *et al.* (90) *Created with BioRender.com*.

When TLRs are activated, a signalling cascade is initiated leading to the production of pro-inflammatory cytokines, antimicrobial peptides, induction of interferon genes as well as activation of the adaptive immune response (70, 91-93). This inflammatory response is the immune system's response to harmful stimuli and is a vital defence mechanism for a healthy environment.

As represented in Figure 1.3, when a ligand binds to the LRR domain of the TLR, the TLR forms either a homo- or a heterodimer. The resulting conformational change in the TIR domain enables interactions between the TIR domains of adjacent TLRs and the recruitment of cytosolic adaptor proteins which mediate signal transduction (94, 95). The signal is transferred internally to the cell via a variety of adaptor molecules all of which contain a TIR domain

including the cytosolic face of each TLR (96). There are five TIR domain-containing signalling adaptor proteins: MyD88 (myeloid differentiation primary-response protein 88); MAL (MyD88 adaptor-like); TIRAP (TIR-domain-containing adaptor protein); TRIF or TICAM1 (TIR-domain-containing adaptor protein inducing interferon β); and TRAM or TICAM2 (TRIF-related adaptor molecule) (97). MyD88 can be used by all TLRs to activate NF-κB and MAPKs, TIRAP is involved in the attachment of MyD88 to the membrane-bound TLRs, TRIF is attached to TLR3 or TLR4 and activates an alternative signalling pathway involving activation of IRF3, NF-κB and MAPKs whilst TRAM connect TRIF to TLR4 (98).

Depending on the adaptor protein involved, TLR signalling is divided into two main pathways: the MyD88-dependent and the MyD88-independent TRAM/TRIF pathway. MyD88 signalling activates nuclear factor NF-κB and induces many cytokines, including tumour necrosis factor α (TNFα) and IL-6 whereas stimulation of TRIF signalling pathway activates the interferon (IFN) regulatory factor (IRF) family to induce production of type I IFNs (69, 76) (Figure 1.4).

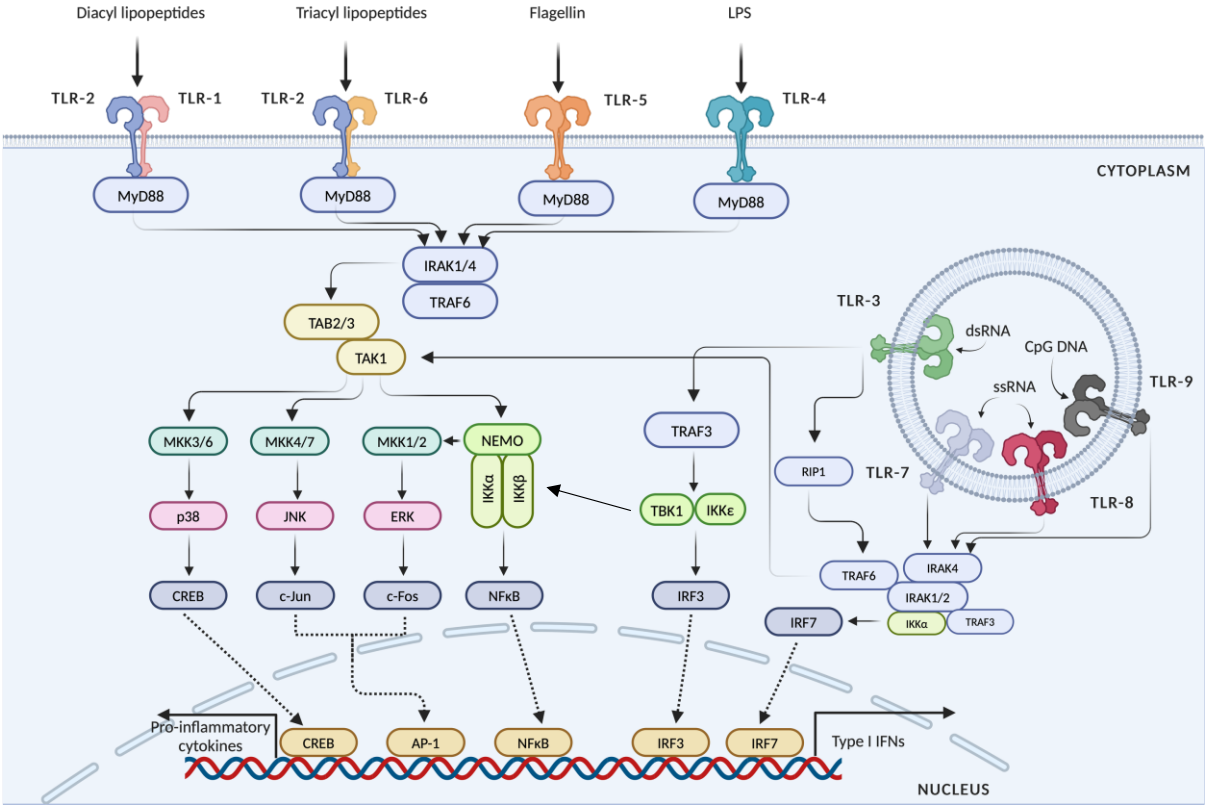

Figure 1.4 Overview of TLR signalling pathways.

TLRs found on the cell surface such as TLR4, TLR5 and heterodimers TLR1/2 or TLR2/6 recognise membrane components of pathogens, whereas TLR3, TLR7, TLR8 and TLR9 localise to endosomes where they detect microbial nucleic acids. Dimerisation of the receptors leads to the engagement of the TIR domain with TIRAP and MyD88 or with TRAM and TRIF. Activated MyD88 recruits downstream signalling molecules to form the Myddosome which is formed of MyD88, IRAK4 and IRAK1/2. Kinase activity of the IRAKs activates TRAF6 to synthesise the K63-linked polyubiquitin chains leading to the recruitments of the TAK1 complex. Activated TAK1 phosphorylates and activates the canonical IKK complex as well as the MAPKs, leading to the activation of important pro-inflammatory transcription factors NF-κB, AP-1 and cyclic AMP-responsive element-binding (CREB) which results in the induction of pro-inflammatory cytokines. TRIF-dependent signalling also promotes TRAF3/TBK1-mediated activation of IRF3 to produce predominantly type I interferons (IFNs). Adapted from Chen *et al.* (99) *Created with BioRender.com.*

Recruitment of MyD88 to the TIR domain facilitates the formation of the Myddosome, a signalling complex that includes the IL-1 receptor-associated kinases (IRAKs), Tollip and tumour necrosis factor receptor (TNF)-associated factor 6 (TRAF6), which then activates transforming growth factor TGFβ-activated kinase 1 (TAK1), and the TAK1 binding proteins TAB1 and TAB2. TAK1 phosphorylates and activates IKKα/β which form the IKK complex with NEMO/IKKɣ. Phosphorylation of the inhibitor of NF-κB (IκB) by the IKK complex results in its

polyubiquitination and proteasomal degradation which releases the inhibited p65 and p50 NF-κB subunits to translocate to the nucleus enabling transcription of NF-κB-targeted genes (100, 101). These include genes encoding pro-inflammatory cytokines, but also costimulatory molecules important for APCs, and the maturation of naive dendritic cells. The binding of microbial ligands to TLRs is therefore a key step in the acute inflammatory response. In the TRIF-dependent pathway activated TRIF binds to TRAF3 and TANK-binding kinase 1 (TBK1), leading to the activation of IRF3 and the production of type I interferons (IFNs). TRIF can also interact with TRAF6 to stimulate the MAPKs and NF-κB independently of MyD88.

Vaginal epithelial cells express TLRs 1-6, and TLR9 but expression of TLR2 and TLR4 is highest (5, 68, 102). The profile of TLRs and NLRs is differentially expressed as the reproductive tract is ascended, likely in response to the concurrent decrease in bacterial load. Although the function of TLRs has been well studied there is little data on the temporal expression of TLRs. One study reported that in the placenta where all 10 TLRs are expressed, levels of TLR expression is dynamic over gestation (103, 104). Early in pregnancy when the developing foetus is particularly vulnerable to infection, expression of TLRs is high. As pregnancy progresses, TLR expression reduces. This may prevent an excessive immune response leading to activation of inflammatory pathways that could cause miscarriage or preterm birth.

1.2.2.2 NOD-like receptors

The NLR family of receptors are cytoplasmic sensors predominantly expressed in immune cells but also in epithelial and mesothelial cells. They sense molecules associated with microbial infection and stress that have entered the cell (105). Similar to TLRs, NLRs have three domains: a central nucleotide-binding domain NACHT that brings about the self-oligomerisation following activation by a ligand; the LRR domain for ligand detection; and a variable N-terminal homotypic protein-protein interaction domain, which is essential for downstream signalling (106, 107). Nucleotide-binding oligomerisation domains (NODs) are well characterised NLRs, as well as NOD-like pyrin domain-containing proteins (NLRPs). NOD1 and NOD2 were the first NLRs identified and detect peptidoglycan components from bacterial cells. Specifically, NOD1

detects mesodiaminopimelic acid (meso-DAP) whereas NOD2 detects muramyl dipeptide (MDP) and can recognise single-stranded RNA (ssRNA) from viruses (108).

Expression levels of NOD1 and NOD2 are highest in the upper FRT (58). It remains unclear whether NLRs bind ligands directly or detect pathogens and other signals indirectly. Regardless, oligomerisation of NODs leads to activation of the three major signalling pathways: NF-κB, MAP kinases and inflammatory caspases to stimulate the production of pro-inflammatory cytokines (58).

1.2.2.3 Other pattern recognition receptors

Compared to TLRs and NLRs, the remaining PRRs are comparatively less characterised within the FRT. RLRs recognise viral RNA and induce an antiviral response of pro-inflammatory cytokines and IFNs (109). Retinoic acid-inducible gene I (RIG-I), melanoma differentiation-associated gene 5 (MDA5) and laboratory of genetics and physiology 2 (LGP2) are the three currently known members of the RLR family (110). They are located in the cytoplasm of cells although recent research has reported RLRs in the cell nucleus (111). Upon RNA binding, RLRs bind to PACT (protein kinase R activator) leading to a conformational change which triggers the release of CARD (caspase activation and recruitment domain) domains which can then bind regulatory molecules such as PP1A or PP1ɣ (112). The CARD domains are dephosphorylated allowing the RIG-I receptor to interact with proteins such as TRIM (tripartite motif protein) and RNF135. The transformed RIG-I receptor can then bind to MAVS (mitochondrial antiviral signalling protein) and the resulting signalling complex can activate several signalling pathways such as NF-κB and IRF3 (113). However, lactate was shown to bind directly to the transmembrane domain of the MAVS, thereby inhibiting its aggregation and blocking RLR signalling (114).

CLRs are phagocytic receptors that recognise carbohydrates on the surface of pathogens, facilitating their internalisation to cytoplasmic vesicles for direct digestion and removal (115-117). They can function as either transmembrane or secretory receptors. Notable examples of CLRs include the dendritic cell-specific intercellular adhesion molecule-3-grabbing non-

integrin (DC-SIGN), the sialic acid-binding Ig-like lectin (Siglec) receptor family, mannose receptors and dendritic cell-associated C-type lectins, Dectin-1 and Dectin 2 (118-120). These receptors are predominantly expressed on macrophages, dendritic cells and certain tissue cells. A recent study showed that vaginal *Lactobacilli* expressing surface layer proteins (SLPs) interact with the anti-inflammatory receptor DC-SIGN (121).

ALRs act as intracellular sensors recognising intracellular DNA in infected or stressed cells (122). They promote the formation of inflammasomes and the release of IL-1β and IL-18 (123). In human cells examples include AIM2, IFI16 (interferon-inducible protein 16), PYHIN1 (pyrin and HIN domain family member 1), and MNDA (myeloid cell differentiation antigen).

cGAS is a recently identified PRR responsible for the recognition of cytosolic DNA, including host-derived self-DNA (124-127). Upon binding of dsDNA, cGAS dimers activate stimulator of interferon genes (STING) leading to the phosphorylation and activation of TBK1 and NF-κB signalling pathways (128, 129).

1.2.3 Signalling pathways

Recognition of microbes by PRRs leads to the activation of downstream signal transduction pathways that involve three main types of molecules: protein kinases, adaptor proteins and transcription factors. While PRRs are activated by specific ligands in different subcellular locations and via diverse mechanisms, the signal transduction molecules exhibit similar structures and functions. Consequently, there is cross talk between the signals that they transmit which can converge into several common signalling pathways which include NF-κB, MAPK, mTOR and the inflammasome.

1.2.3.1 NF-κB signalling

The transcription factor NF-κB is an important regulator of inflammation that controls the expression of inflammatory cytokines and chemokines which in turn activate innate and adaptive immune responses and remodel epithelial cell barrier integrity enabling pathogen invasion and immune cell entry. It is activated by pro-inflammatory cytokines or pathogen exposure recognised by receptors on the cell surface (130, 131). NF-κB is composed of heteromeric dimers from the Rel/NF-κB family: p65/RelA, C-Rel, RelB, p50/NF-κB1, and p52/NF-κB2 (132). These proteins share a conserved N-terminal region called the Rel homology domain (RHD) which mediates the binding of the NF-κB complex to DNA as well as its nuclear translocation and the interaction of NF-κB with inhibitors of κB (IκB). Nuclear translocation of NF-κB is prevented when inactivated NF-κB dimers in the cytoplasm associate with IκB proteins. The IκB kinase (IKK) complex, composed of IKKα, IKKβ and the scaffold protein NF-κB essential modifier (NEMO or IKKɣ), controls NF-κB by phosphorylating IκB, triggering its ubiquitin-dependent proteasomal degradation and releasing NF-κB which rapidly and transiently translocates to the nucleus (132-135).

Two distinct pathways are involved in NF-κB activation: the classical (or canonical) pathway and the noncanonical pathway, each with different activating mechanisms and resulting in different outcomes (136). The classical pathway is more rapidly activated and involves NF-κB dimers composed of p65, c-Rel and p50 subunits as well as the degradation of IKK target proteins IκBα, IκBβ, and IκBε, and p50 precursor, p150 (Figure 1.5). The IKKs are especially important as they act rapidly, leading to classical IκB degradation by the 26S proteasome (137, 138). The IKK complex is activated by transforming growth factor beta-activated kinase 1 (TAK-1) which is downstream of TLRs including both TLR2/6 and TLR3. IκBα can also regulate the duration of the NF-κB-dependent response by translocating to the nucleus where it blocks NF-κB binding to the DNA by binding to the NF-κB dimers (139).

The noncanonical NF-κB pathway controls genes important in homeostatic pathways, and tends to be activated more slowly by members of the tumour necrosis factor receptor (TNFR)

superfamily leading to translocation to the nucleus where it initiates transcription of target genes (133, 140, 141).

The majority of NF-κB target genes encode pro-inflammatory proteins such as cytokines, chemokines, cell adhesion molecules and proteins involved in antigen presentation (142). However, NF-κB also activates transcription of genes involved in cervical ripening, foetal membrane remodelling and uterine contractions (143).

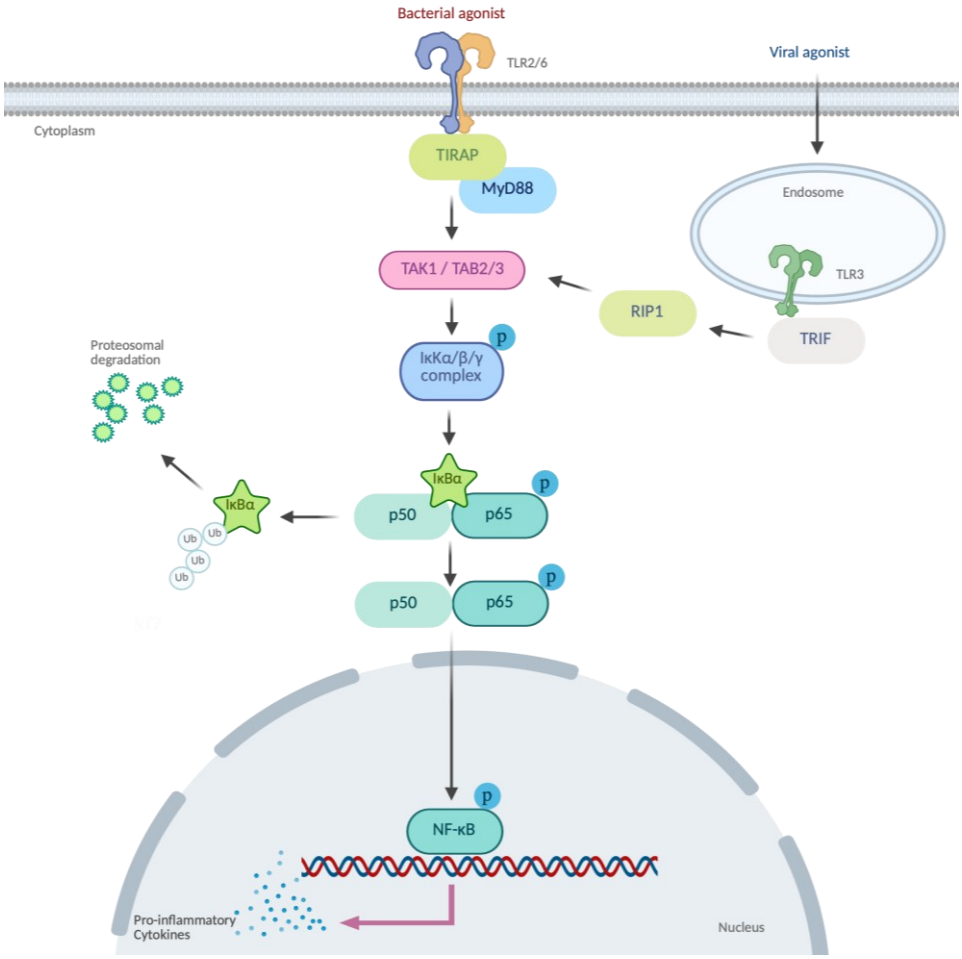

Figure 1.5 Simplified overview of classical NF-κB pathway.

Following recognition of TLR ligands, MyD88 promotes activation of the IκK complex via TRAF6 and TAK1, which mediates IκB phosphorylation. Phosphorylation of IκB triggers its ubiquitination and degradation and releases NF-κB to translocate to the nucleus where it can transcribe its target genes many of which are related to inflammation such as TNFα and IL-1β. Adapted from Yu *et al* (144). Created *with BioRender.com.*

1.2.3.2 Mitogen-activated protein kinase (MAPK) signalling

Mitogen-activated protein kinases (MAPKs) are a group of highly conserved enzymes involved in intracellular signalling cascades that transduce cell-surface signals to the nucleus to induce target gene expression. There are three main subfamilies of MAPKs: extracellular signal-regulated kinases (ERK1, ERK2 and ERK5), c-Jun N-terminal kinase (JNK1, JNK2, and JNK3) and p38 (p38-α, p38-β, p38-ɣ, and p38-δ). Activation of each MAPK signalling pathway follows a three-tiered cascade where a MAP3K (MAPK kinase kinase) phosphorylates and activates a MAP2K (also known as MAPK kinase or MEK) which in turn phosphorylates and activates a MAPK, following signals from membrane-bound receptors (Figure 1.6).

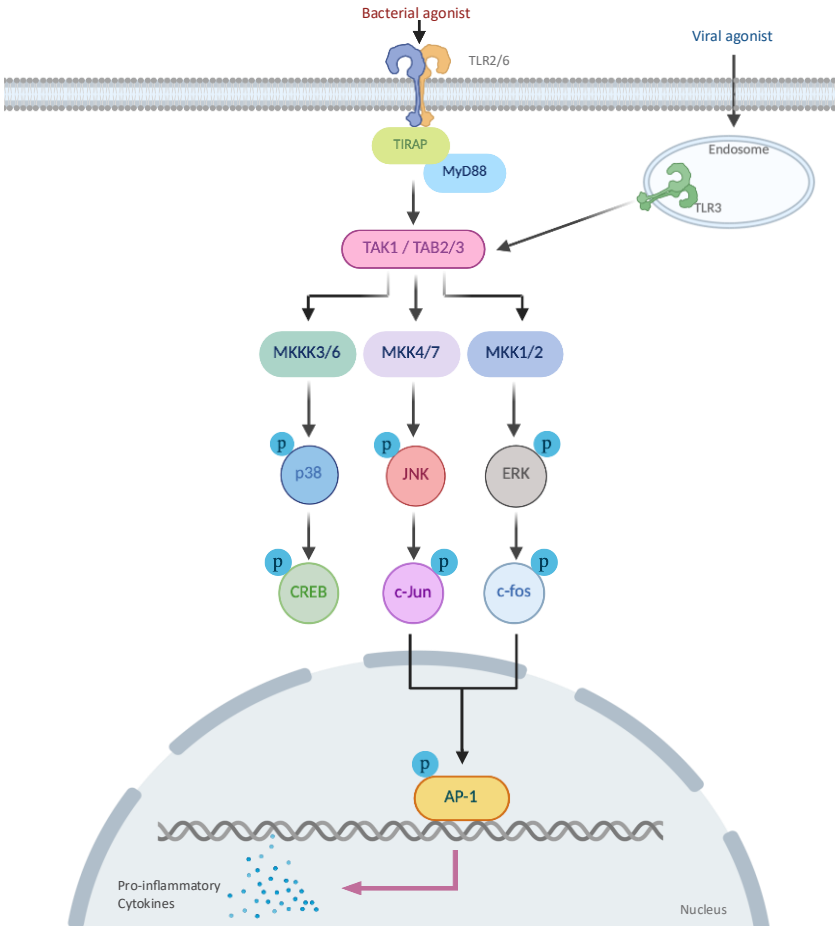

Figure 1.6 Overview of MAPK signalling pathways.

Upon ligand binding, receptors activate the MAP kinase pathways (p38, JNK and ERK) leading to phosphorylation of transcription factor subunits, which mediate their translocation to the nucleus and activation of target gene transcription. Adapted from Chen *et al.* (99). *Created with BioRender.com*.

The pathways differ in their sensitivity to external stimuli: all respond to growth factor stimulation or cytokines. In endothelial cells G protein-coupled receptors (GPCRs) activate the p38 MAPK via a non-canonical TAB1-TAB2- and TAB1-TAB3-dependent pathway (145). ERK1/2 is activated by multiple stimulants such as GPCR ligands, mitogens, oncogenes, and viruses as well as growth factors (146). Small G proteins Ras and downstream Raf kinase, and MEK1/2 are key molecules in the ERK MAPK signalling pathway. Typically, ERK signalling is associated with control of cell proliferation, survival and differentiation, whereas JNK and p38, which are also known as stress-activated protein kinases (SAPKs) are associated with apoptosis and cell cycle arrest (147, 148). The MAPKs play a crucial role in phosphorylating transcription factors downstream of TLRs. ERK1/2 predominantly activates c-Fos to facilitate inflammatory cytokine production (149, 150). Upon activation, ERK1/2 phosphorylates and activates a wide range of cytoplasmic substrates such as RSK (p90 ribosomal S6 kinase), MSK (stress-activated kinase) and MNK (MAPK-interacting kinase) as well as many nuclear proteins including transcription factors. ERK activation can also mediate tight junction integrity in a cell type- and differentiation state-specific manner. For example, in intestinal epithelial cells ERK was shown to destabilise tight junctions in under-differentiated cells but protect tight junction integrity in differentiated epithelial cells (151). c-Jun, on the other hand, is primarily phosphorylated by JNK which also facilitates the nuclear translocation of activating transcription factor 4 (ATF4) to form heterodimers with c-Jun for AP-1 activation (152-154). p38 phosphorylates members of the myocyte-enhancer factor 2 (MEF2) family of transcription factors, MEF2A and MEF2C which control production of anti-inflammatory cytokine IL-10 as well as stimulating AP-1-mediated cytokine production via stimulating expression of c-Jun (155-158).

Similar to NF-κB, AP-1 contains transcriptional regulator binding sites for most inflammatory mediators. It can also independently bind promoters of inflammatory mediators during inflammation. AP-1 is a ubiquitous dimeric protein complex characterised by a basic leucine zipper (bZip) domain and composed of four different subfamilies of DNA-binding proteins: Jun family (c-Jun, JunB, v-Jun, and JunD), Fos family (c-Fos, FosB, Fra-1, and Fra-2), ATF/cyclic AMP-responsive element-binding (CREB) (ATF1-4, ATF-6, b-ATF, and ATFx) and Maf family (c-Maf, MafA, MafB, MafG, MafF, MafK, and Nrl) (159-164). The Jun proteins form homo- and hetero-dimers, whereas the Fos and ATF proteins can only form heterodimers with Jun proteins. AP-

1 transcription factors respond rapidly to external stimuli and regulate a variety of cellular processes including inflammation, proliferation or apoptosis.

Even though the underlying regulatory mechanisms of NF-κB and AP-1 differ, they can be activated simultaneously by the same stimuli. This cross-communication can take place at many levels from the plasma membrane to the nucleus and involves components that are in common pathways. The cAMP pathway is one of the best-characterised signalling pathways in MAPK activation. It can differentially regulate the MAPKs depending on cell and receptor type. The small G proteins Rap1, Rac and Cdc42 play an important role in this. The key point of divergence for activation of NF-κB and AP-1 signalling pathways are the TNFR-associated factors (TRAFs) that not only activate IKKs but also signal to other pathways (165). Importantly TRAF6-activated TAK1 can also induce MAPK signalling leading to activation of AP-1 (166).

1.2.3.3 TANK-binding kinase 1-interferon regulatory factor 3 signalling

Interferon regulatory factor 3 (IRF3) is a transcription factor that plays an important role in the antiviral immune response in cells by promoting the synthesis of IFN. Two innate immune signalling pathways can activate IRF3: either the TLR3/TLR4-TRIF or RIG-I-MAVS (Figure 1.7) (167, 168). Phosphorylation of IRF3 in the cytoplasm promotes homodimerisation, and subsequent translocation to the nucleus and activation of IFN genes such as IFNα and IFNβ. Interferons are typically coordinately activated with NF-κB. When the TRIF adaptor protein binds to the TIR domain on TLR3 it phosphorylates TRAF3 leading to the activation of the TBK1-IKKε heterodimer kinase complex. This complex is then the pivotal point for separately activating the IRF3 and NF-κB pathways.

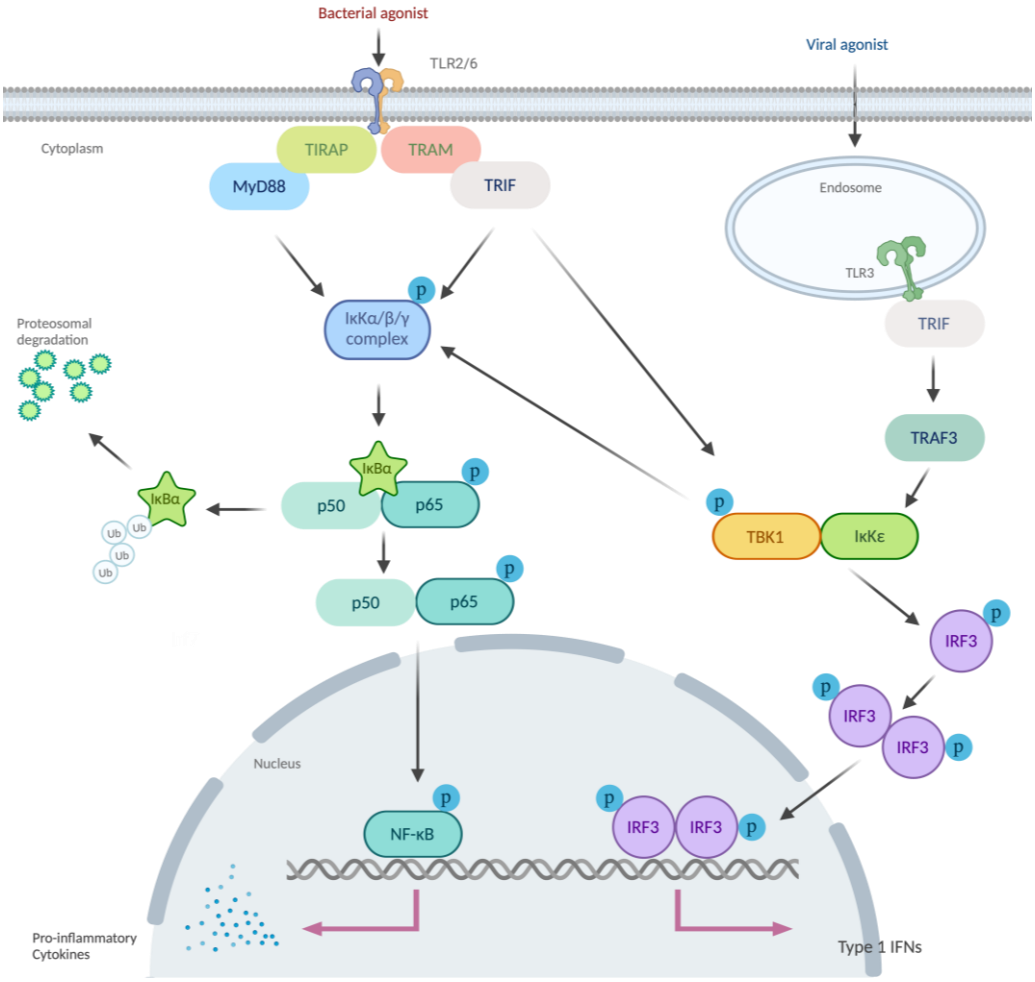

Figure 1.7 Overview of TBK1-IRF3 signalling pathway.

TBK1 is activated by pathogenic stimulation of TLRs and RLRs. A variety of adaptor proteins convey signals from the plasma membrane receptors leading to the assembly of the TBK1-IKKε heterodimer which phosphorylates interferon regulatory factors such as IRF3 leading to its homo- or heterodimerisation and subsequent nuclear translocation. TBK1 and IKKε also target the IκK complex which activates the NF-κB pathway. Adapted from Kawai *et al. (169) Created with BioRender.com.*

1.2.3.4 Other inflammatory signalling pathways

Other cellular inflammatory signalling pathways include the inflammasome, multi-protein complex assembled by PRRs in the cytoplasm, which forms an important part of the innate immune system (170). The inflammasome can recognise MAMPs or DAMPs and recruit and activate Caspase-1 with the adaptor protein ASC (apoptosis-associated speck-like protein containing a CARD) leading to activation of pro-inflammatory cytokines IL-1 and IL-18 (171, 172).

In other cell types, the mTor signalling pathway has been linked to TLR4 stimulation leading to either NF-κB or PI3K activation (173, 174). Berard *et al.* used an integrated multi-omics approach and identified that, in BV, mTOR underlies epithelial dysfunction and inflammation (175). This study also showed that the mTOR pathway is activated by numerous signalling pathways including upstream Wnt and TLR induction of NF-κB as well as downstream signalling of RhoA, integrin and ARP2/3.

The signalling pathways mediate the interaction between the woman's epithelial cells and immune system, and the vaginal microbiota. These interactions play a vital role in protecting against opportunistic pathogens and maintaining a healthy vaginal environment.

1.3 Vaginal microbiota and their importance in health and disease

The human lower female reproductive tract plays host to a functionally important microbial community. Unlike other body niches such as the gut, where high diversity microbial communities are associated with health, the optimal female reproductive tract composition is widely considered to be low in diversity and dominated by only one or a few *Lactobacillus* species especially during the reproductive years (176-179). Reduced levels of *Lactobacillus* species and increased microbial diversity of strict or facultative anaerobes such as *Gardnerella, Prevotella* and *Atopobium* species are characteristic of a dysbiotic vaginal microbiome and are linked to increased risk of urinary tract infections (UTIs) (180, 181), susceptibility to human immunodeficiency virus (HIV) (182-186) and other STIs (187-190), gynaecological cancers (191), infertility (192), preterm birth (193-195) and miscarriage (183, 196, 197).

Over the last couple of decades, application of new molecular-based methodologies has permitted improved understanding of microbial composition in the vaginal niche as they enable identification of microbes that are difficult to cultivate. Two major methodological

approaches being used include (1) metataxonomics in which targeted microbial taxonomic marker genes such as the 16S ribosomal RNA gene are amplified and sequenced, and (2) metagenomics which uses bioinformatics to assemble microbial genomes from shotgun sequencing of all the DNA extracted from a sample (198). These methods have limitations in providing direct information about microbiota-host interactions, such as the molecular signalling pathway or functional responses influenced by the microbiota. This gap highlights the value of emerging mass spectrometry (MS)-based -omics approaches like metaproteomics and metabolomics, which can assess functional responses by analysing proteins and metabolites, bridging the understanding of microbiota-host dynamics.

1.3.1 Community state types: vaginal microbial communities

In 2011 Ravel *et al.,* undertook one of the first large-scale metataxonomic studies of the vaginal microbiome in reproductive age women (199). The resulting vaginal bacterial profiles permitted samples to be classified into five distinct vaginal community state types (CSTs). *Lactobacillus* species dominate four of these CSTs: CST I (*Lactobacillus crispatus*), CST II (*Lactobacillus gasseri*), CST III (*Lactobacillus iners*), and CST V (*Lactobacillus jensenii*). In contrast, CST IV is characterised by a highly diverse microbial community which is *Lactobacillus*-deplete. Subsequently, it was shown that this group could be further subdivided into CST IV-A which contains various species of strictly anaerobic bacteria such as *Anaerococcus, Corynebacterium, Finegoldia or Streptococcus* as well as low levels of *Lactobacillus* species and CST IV-B which is enriched with *Atopobium*, *Gardnerella, Prevotella, Sneathia, Mobiluncus, Parvimonas* or *Peptoniphilus* species and little to none *Lactobacillus* (200). However, another key finding of the original Ravel study was that CST IV is commonly found in healthy Black and Hispanic women, highlighting ethnic differences in vaginal microbiota composition (200).

More recently a new system of vaginal microbiota classification was developed in an attempt to facilitate cross-comparison of studies. The VALENCIA (VAginaL community state typE Nearest CentroId clAssifier) algorithm was trained using data from approximately 13,000 samples collected from populations throughout the world (201). This approach allowed for

the microbiota profile to be classified into seven major CSTs which can be further subdivided into thirteen classifications as outlined below: CST I *L. crispatus*, CST II *L. gasseri*, CST III *L. iners*, and CST V *L. jensenii* which are rich in *Lactobacillus* species. An additional three CSTs do not have a high relative abundance of *Lactobacilli*: CST IV-A high in *Candidatus Lachmocurva vaginae*, CST IV-B high in *Gardnerella vaginalis* and CST IV-C which has an abundance of facultative anaerobic bacteria and is further split into eight sub-groups based on bacterial dominance: CST IV-C0-homogenous community with a moderate level of *Prevotella,* CST IV-C1—*Streptococcus*, CST IV-C2—*Enterococcus*, CST IV-C3—*Bifidobacterium*, CST IV-C4—*Staphylococcus*, CST IV-C5—*Escherichia coli*, CST IV-C6—*Fusobacterium nucleatum*, CST IV-C7—*Prevotella timonensis*, and CST IV-C8—*Veillonella atypica* (201, 202) (Table 1.1). While CST profiling provides a means to broadly classify vaginal microbiota composition, it does not capture sub-species diversity. Ma *et al.* recently showed that populations of *Lactobacilli* are typically not made up of a single strain and that vaginal communities contain far more intraspecies diversity than captured by CSTs, although the functional significance of this remains unclear (203).

Table 1.1 Summary of vaginal microbiome community state types using VALENCIA classification.

Community State Types (CSTs) of the Vaginal Microbiome		
CST Group	**Dominant bacteria**	***Lactobacillus*-dominance**
CST IA	*L. crispatus* (dominant focal species)	Yes
CST IB	*L. crispatus* (lower moderate abundance)	Yes
CST II	*L. gasseri*	Yes
CST IIIA	*L. iners* (dominant focal species)	Yes
CST IIIB	*L. iners* (lower moderate abundance)	Yes
CST IVA	high *Candidatus Lachmocurva vaginae* and low *Gardnerella vaginalis*	No
CST IVB	high *G. vaginalis* and low *Ca. L. vaginae*	No
CST IVC	facultative anaerobic bacteria	No
CST IV-C0	homogenous community with moderate levels of *Prevotella*	No
CST IV-C1	*Streptococcus*	No
CST IV-C2	*Enterococcus*	No
CST IV-C3	*Bifidobacterium*	No
CST IV-C4	*Staphylococcus*	No
CST IV-C5	*Escherichia coli*	No
CST IV-C6	*Fusobacterium nucleatum*	No
CST IV-C7	*Prevotella timonensis*	No
CST IV-C8	*Veillonella atypica*	No
CST V	*L. jensenii*	Yes

1.3.2 CST prevalence in health and disease

As previously described, microbial recognition and interaction with the vaginal epithelium and host immune cells influences physiology and immune function in the lower female reproductive tract (177). CST IV vaginal microbiota compositions depleted of commensal

Lactobacilli and enriched for potential pathogens are associated with several pathological and disease states including miscarriage, preterm birth and progression of cervical cancers (204-206). However, it is increasingly clear that not all *Lactobacillus* species have the same capacity to protect against infection and inflammation in the lower reproductive tract. For example, *L. crispatus* dominance (CST I) of the cervicovaginal niche provides protection against UTIs, HIV infection and other STIs, and is associated with term gestation and healthy pregnancy outcomes (194, 207-211). Mechanisms by which *L. crispatus* contributes to host protection includes lowering the vaginal pH more effectively than other *Lactobacillus* species leading to reduced inflammation and through competitive inhibition of pathogen colonisation via nutrient utilisation and production of antimicrobial compounds (212-214). In contrast, *L. iners* (CST III) is often associated with transition to higher diversity CSTs (e.g. CST IV) that are linked to adverse health outcomes (215-217). This is likely due to evolutionary pressure conferred by a small genome. While the *L. crispatus* genome is on average 2.25 Mbp, the *L. iners* genome is 1.28 Mbp, meaning that it does not encode several genes required for efficient activity in the niche (218). In response, it has evolved to tolerate the presence of other bacteria that produce the necessary nutrients and proteins, and to adapt more readily to low or high pH (215, 218, 219). Accordingly, it is often detected in both BV-positive and BV-negative women and is considered the most common and persistent *Lactobacillus* species in the vaginal niche (201, 220, 221).

Vaginal microbial community composition is dynamic. It is affected by many external and internal factors such as ethnicity, age, pollutants, exercise and BMI, endogenous hormones, contraception, hygiene practices, the menstrual cycle, pregnancy, and sexual behaviour (186, 199, 200, 222). The influence of oestrogen in shaping microbiota composition is evident throughout a women's life span. Relative abundance of *Lactobacillus* increases at the onset of puberty and then fluctuates during menses, increasing during the follicular and luteal phases as levels of oestradiol increase (200, 223). In the highly oestrogenic state of pregnancy, *Lactobacillus* levels are further increased although late in pregnancy microbial diversity increases and *Lactobacillus* levels more resemble those of nonpregnant women (224-226). Post-menopause there is a decreased in *Lactobacillus* species with a shift towards CST IV and increased bacterial diversity (227, 228).

Shifts in vaginal CSTs are implicated in pathology and disease states including in pregnancy where *L. iners* (CST III) has been associated with increased risk of preterm birth. In contrast, *L. crispatus* (CST I) provides protection against preterm birth (210, 229, 230). *Lactobacillus*-depleted microbial communities (CST IV), are associated with upregulated expression of TLRs and NF-κB, increased production of cytokines and chemokines and activation of immune cells (1), and increased risk of premature prelabour rupture of foetal membranes (PPROM) and spontaneous preterm birth (sPTB) (231-233). However, merely possessing an optimal vaginal microbial profile does not ensure a healthy pregnancy outcome. Women with a high abundance of *L. crispatus* may still experience preterm delivery, and many pregnant women with BV do not. It is probable that an individual's host immune response to the microbial environment plays a pivotal role in determining pregnancy outcomes (234).

1.3.3 CST mediation of disease pathology

Transition of the vaginal microbiome from an optimal CST I state to CST IV *in vivo* is associated with inflammation, including increased levels of IL-1α, IL-1β, and TNFα (1). Microbial-induced inflammation correlates with decreased epithelial integrity and altered barrier properties of the cervicovaginal mucosa (235-237). However, the host response varies depending on the specific composition of the vaginal microbiota and the disease state. For instance, in women with aerobic vaginitis (AV), distinct patterns of inflammatory activation are observed across CSTs (238).

CST IV is frequently linked with BV and multiple adverse gynaecological outcomes. While BV is not associated with clinical inflammation in the lower FRT, it has been associated with inflammation in the upper FRT contributing to an increased risk of PTB, pelvic inflammatory disease, and the acquisition of STIs such as HIV and human papillomavirus (208, 239-242). During pregnancy, women with CST III or CST IV vaginal microbiota, who later experienced sPTB, exhibited dysregulated innate and adaptive immune responses characterised by excessive activation of the lectin-mediated and classical complement pathways and increased levels of pro-inflammatory cytokines (42).

The relationship between CST and inflammation has been recapitulated *in vitro*. Vaginal epithelial cells (VECs) exposed to *Lactobacillus* species show reduced levels of pro-inflammatory cytokines, such as IL-6, IL-8 and TNFα (51). Similarly, PRRs on VECs *in vitro* are not activated in the presence of *L. crispatus* (243). Conversely, exposure to CST IV-associated bacteria, such as *G. vaginalis* (73) and *Atopobium vaginae* (244), induces the production of pro-inflammatory cytokines and chemokines, such as IL-6, IL-8, RANTES, and MIP1β in VECs (1, 51). Recently, Anton *et al.,* demonstrated that *G. vaginalis*-mediated immune activation can be mitigated by blocking TLR2 (74).

Although CST IV is generally associated with pro-inflammatory conditions and a higher risk of reproductive complications, it is not universally pathological. Some women with CST IV microbiota may experience no adverse effects. Further research is needed to understand the factors, such as host genetics, hormonal environment or microbial activity, that differentiate benign CST IV states from those linked to disease.

1.4 Microbiota and role of metabolites in vaginal mucosa interface

Metabolic activity of vaginal bacteria is closely linked to the host response (245). Metabolic profiles can be rapidly acquired, in less than 3 minutes, using direct on-swab desorption electrospray ionisation mass spectrometry (DESI-MS) which requires minimal sample preparation or chemical extraction from vaginal swabs (246, 247). The most abundant metabolites in the vaginal niche are LA, short chain fatty acids (SCFAs), amines, organic acids, nitrogenous bases and monosaccharides. It is important to note that many of these metabolites can also be produced by epithelial cells as well as microbes (248-251).

1.4.1 Lactic acid

At low pH, lactate exists in its protonated form LA. The role of LA in preventing pathogen colonisation and infection in the FRT is now widely acknowledged (28). Originally described in the 1800s as a waste product, LA is now recognised as a vital energy source, a precursor of gluconeogenesis, and a signalling molecule with autocrine, paracrine and endocrine effects (252-255). For example, cardiac myocytes take up lactate and oxidise it as fuel (256) and in the brain, astrocytes and neurons employ it for oxidative metabolism (257, 258). LA can be produced in one cell and consumed in another, a process known as the lactate shuttle theory. As a signalling molecule, LA plays a significant role in mediating immune responses. It inhibits antitumour immunity by negatively regulating innate and adaptive immune cells, prevents monocytes from differentiating into dendritic cells, thereby suppressing antigen-presenting capabilities, and promoting the infiltration of immunosuppressive cells. These include M2-like tumour-associated macrophages, N2-like tumour-associated neutrophils, myeloid-derived suppressor cells, and regulatory cells (259).

Production of LA in the vaginal niche is largely dependent on glycogen availability. Glycogen is a large multibranched glucose polysaccharide made up of α-1,4-glycosidic-linked glucose units, with periodic α-1,6-glycosidic branches and containing small amounts of phosphate and glucosamine. It accumulates in VECs, which are then sloughed off into the vaginal lumen, where they are lysed by bacteria (15, 260). Glycogen-degrading enzymes (GDEs) break it down into complex oligosaccharides such as maltose and maltotriose, which can then be preferentially metabolised by *Lactobacilli* to produce LA (261-264). The mechanism by which vaginal bacteria metabolise glycogen remains unclear with recent evidence suggesting the involvement of both bacterial and human enzymes. In 2019, van der Veer *et al.,* identified an amylopullulanase encoding gene *pulA* in *L. crispatus* which enables direct metabolism of glycogen for growth (265-267) (Figure 1.8).

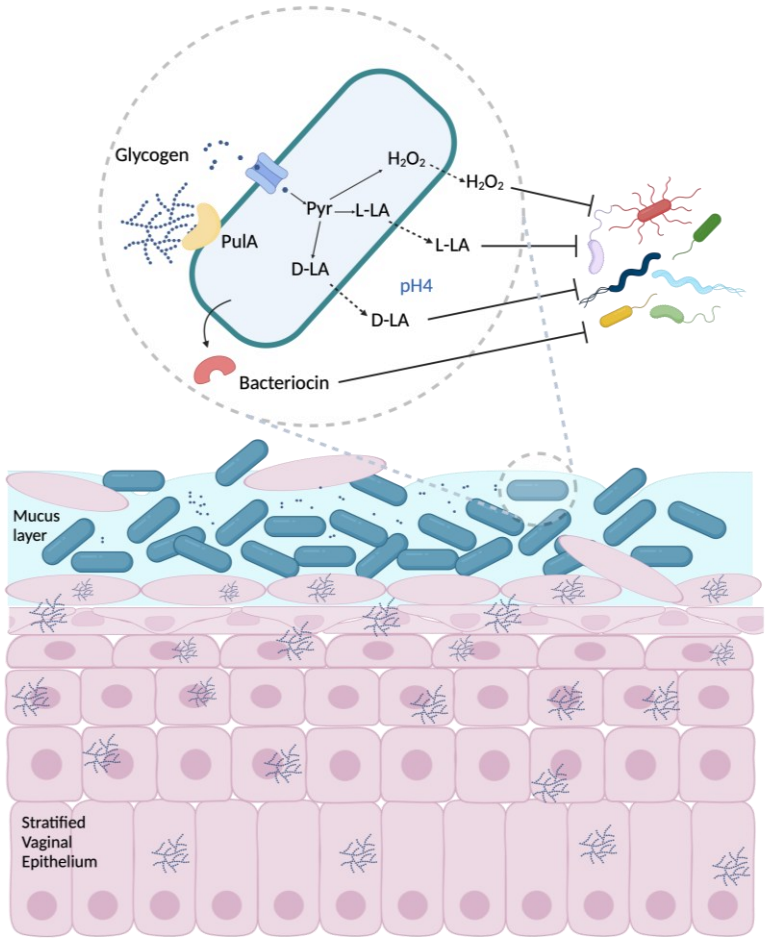

Figure 1.8 Simplified metabolic pathways of L. crispatus in the vaginal mucosa.

L. crispatus produces both D- and L-LA isomers through fermentation of glycogen using the recently identified amylopullulanase PulA enzyme which acidifies the environment to a pH < 4 and suppresses the growth of less beneficial bacteria. Adapted from France 2022 *et al.* (268). *Created with BioRender.com***.**

Since then, several bacterial and host-derived GDEs have been identified in CVF, including putative pullulanases from *L. iners* and *G. vaginalis,* suggesting that these enzymes are not limited to *L. crispatus* (268). These enzymes have distinct substrate preferences, and recently, Navarro *et al.* showed that the activity of these enzymes is pH-dependent, for example, the enzymes from *G. vaginalis* have almost no activity at pH 4 (269). The GDEs from *L. crispatus* and *L. iners* are better adapted to a low pH environment (270). This may explain why *Lactobacillus*-dominant communities have a competitive advantage for metabolism of host-derived glycogen at low pH (269). However, glycogen degradation has not been reported for

L. gasseri or *L. jensenii* and no PulA homologues were identified in their genomes, leaving unanswered questions about how CST II and CST V bacteria may be accessing and utilising glycogen (270).

The human vaginal niche contains both isomers of LA: D-lactic acid (D-LA), and L-lactic acid (L-LA. L-LA can be produced by VECs, *Lactobacilli* and other LA-producing bacteria whereas D-LA is almost exclusively produced by bacteria (271). In healthy women, LA concentrations can reach 110 mM which creates a pH of about 3.5 (261, 272). LA is in its protonated form at pH < 3.9, which appears to be important for its antimicrobial and immunomodulatory properties (261, 273-275). Incubation of VECs in physiologically relevant concentrations of LA inhibits production of pro-inflammatory cytokines and chemokines (276). This anti-inflammatory effect is LA-specific and is not seen when cells are exposed to HCl (276).

LA plays a crucial role in maintaining vaginal health by inhibiting the colonisation of bacteria associated with BV, such as *G. vaginalis* and *A. vaginae* (273, 277-279). In addition, LA demonstrates antimicrobial properties against a range of pathogens, including STIs. For example, LA has been shown to inactivate HIV by disrupting the viral envelope and reducing its infectivity (274-276). Similarly, it exhibits antiviral activity against herpes simplex virus (HSV) by altering the viral structure and preventing attachment to host cells (280, 281). LA is also effective against human papillomavirus (HPV) where it may impair viral replication and inhibit infection (282). Beyond its antiviral properties, LA has demonstrated bactericidal effects against *Neisseria gonorrhoeae*, the causative agent of gonorrhoea, by interfering with its growth and survival in the vaginal niche (283). Likewise, LA inhibits *Chlamydia trachomatis*, a common bacterial STI, by disrupting its ability to infect epithelial cells and replicate within host tissues (190, 284).

L. crispatus, L. gasseri, and *L. jensenii* all produce D-LA; however, *L. iners* does not as its genome lacks the gene encoding the enzyme, D-lactate dehydrogenase (218, 271). Consequently, the ratio of D-LA:L-LA in cervicovaginal fluid reflects the relative abundance of different *Lactobacillus* species present in the niche (28). This ratio appears to be functionally significant (276, 285). D-LA influences the viscosity and properties of the vaginal mucosa,

playing a crucial role in trapping of viruses and protecting the upper reproductive tract (250, 271, 286) . VECs produce extracellular metalloproteinase inducer (EMMPRIN) also known as CD147, a major inducer of matrix metalloproteinase-8 (MMP-8). MMP8 is an enzyme that degrades the extracellular matrix and reduces the structural integrity of the cervix, facilitating the passage of bacteria through the endocervix (271, 287). D-LA inhibits EMMPRIN and, therefore MMP-8, which is implicated in UTIs and preterm birth risk (271, 288, 289). In contrast to these findings, the L-LA isomer has been reported to have a 17-fold greater HIV-1 virucidal activity than D-LA at pH 4.0 (274).

While the link between LA and inhibition of vaginal inflammation has now been firmly established, the precise signalling pathways by which LA mediates inflammation remain poorly understood (276).

1.4.2 Short chain fatty acids (SCFAs)

SCFAs are carboxylic acids containing six or fewer carbon molecules and include acetate, propionate, butyrate, pentanoate (valerate) and hexanoate (caproate). In the gut, they are the product of fermentation of non-digestible carbohydrates and proteins, whereas in the FRT they are metabolised from glycogen released by VECs (290, 291) (Figure 1.9).

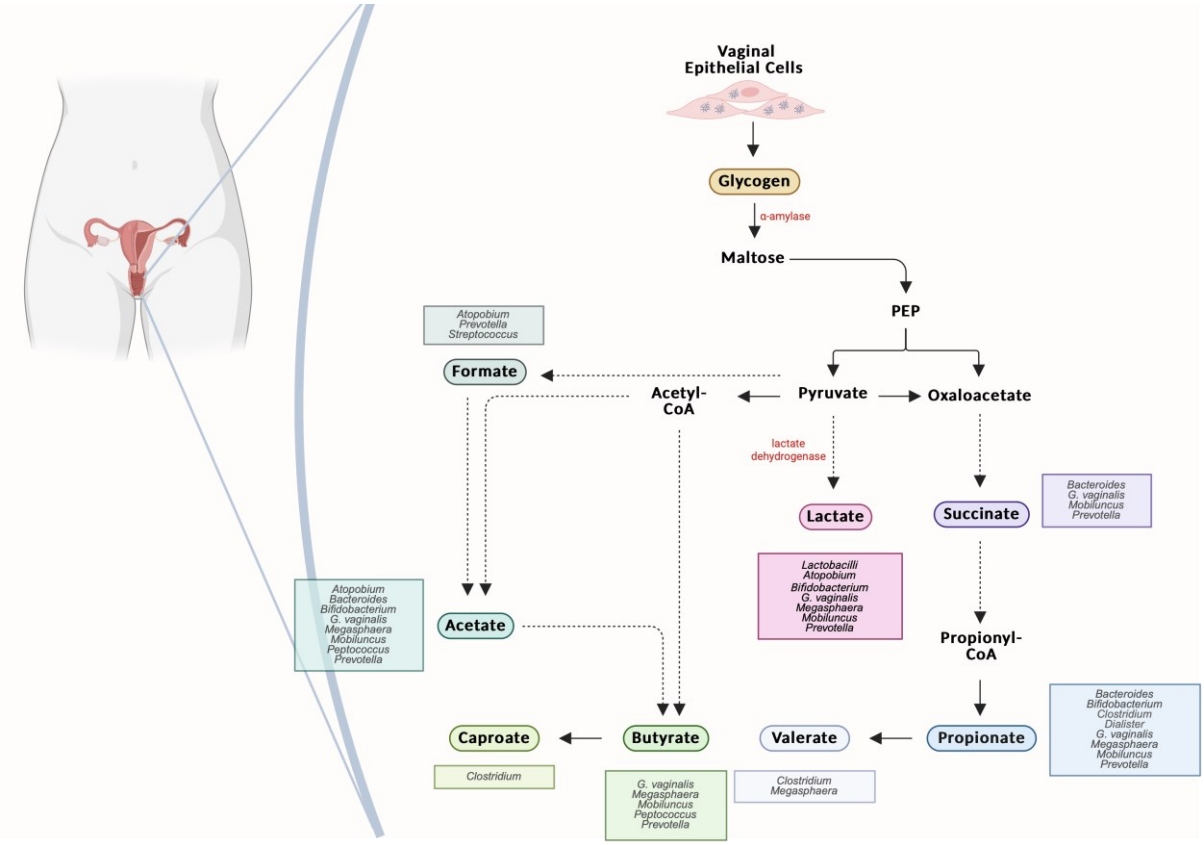

Figure 1.9 Schematic of short-chain fatty acid metabolism.

Vaginal microbes and pathways for the biosynthesis of short-chain fatty acids in the vaginal niche. Figure adapted from Baldewijns 2021 *et al.* and Amabebe 2020 *et al.* (245, 292). *Created with BioRender.com.*

Decreased levels of *Lactobacillus* species in the vagina correspond with increased pH (> 4.5) and increased bacterial diversity (272). Consistent with this, women with BV have significantly higher vaginal levels of SCFAs (293, 294) including acetate, butyrate, propionate and succinate, in addition to biogenic amines such as putrescine, cadaverine and trimethylamine (1, 186, 246, 249, 272, 295). In the vaginal environment, SCFAs are associated with reduced antimicrobial activity and a pro-inflammatory environment, which contrasts with SCFAs in the gut mucosa (1, 175, 245, 296). In the gut, SCFAs reduce mucosal inflammation, enhance mucus production, stimulate antimicrobial peptide synthesis, increase the expression of epithelial tight junction proteins to preserve the integrity of the epithelial barrier, and serve as an energy source for colonocytes (297-303). Many of these effects are mediated through GPCR signalling, specifically via the receptors GPR41, GPR43, and GPR109 (304).

While vaginal SCFA production is predominately associated with BV-associated microbes, several *Lactobacillus* species were shown to produce SCFAs and other carboxylic acids (248, 305-307). For example, *L. jensenii* produces acetate and succinate, and *L. crispatus* and *L. gasseri* have been positively correlated with succinate levels (292). A comparison of CVF concentrations of LA and SCFAs is presented in Figure 1.10.

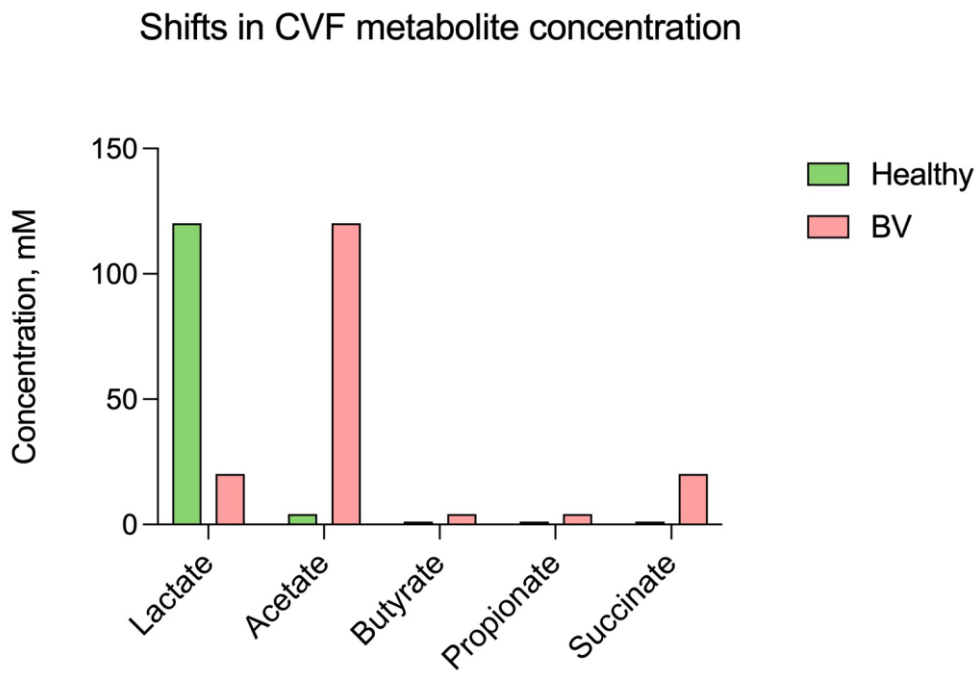

Figure 1.10 Metabolite profile of cervicovaginal fluid from healthy women and women with BV.

Data were sourced from Aldunate 2015 *et al.* (272).

Despite their association with an inflammatory state *in vivo*, Delgado-Diaz *et al.* recently reported in a cervicovaginal epithelial cell monolayer model that acetate, propionate, butyrate and succinate exposure at concentrations and a pH reflective of BV, did not strongly drive inflammation (308). It was also shown that LA's ability to dampen VEC inflammation and promote epithelial barrier proteins is maintained in the presence of SCFAs (296). These results highlight the gap in understanding of the immunomodulatory roles of SCFAs produced by vaginal microbes.

1.4.3 Receptor and transporter mediation of metabolite activity

To date, receptors involved in mediation of metabolite activity in VECs are poorly characterised. LA receptors and transporters have not been described in VECs however, in other epithelial cells, their identity and function are well characterised (309-315). LA can be transported across the plasma membrane by monocarboxylate transporters (MCTs). MCTs are transmembrane proteins made up of 12 helices, which form a channel for transporting carboxylic acids (316). MCT1 (SLC16A1) and MCT4 (SLC16A3), mainly involved in lactate transport, form heterodimers with the glycoprotein CD147 (basigin) which is essential for the active configuration of the transporter. MCTs play a key role in tumour cell metabolism in excreting LA produced by high levels of glycolysis via MCT4. LA can then enter oxidative tumour cells through MCT1 where it is used as an energy source in the tricarboxylic acid cycle (317).

A second class of plasma membrane monocarboxylate transporters has been identified, which mediate the cellular uptake of monocarboxylates in a sodium-coupled manner. Sodium-coupled monocarboxylate transporters, SMCT1 and SMCT2, have been detected in epithelial cells in the gastrointestinal tract, kidney, thyroid, brain and retina where they enable cellular uptake of lactate (318-320). They are formed of seven transmembrane domains. The kinetics of SMCT1 tend to favour the import of lactate rather than its export but little is known about these transporters (321).

Many metabolites signal directly through GPCRs (322), integral membrane proteins with seven transmembrane α-helical domains, one extracellular N-terminal domain and one intracellular C-terminal domain, which is coupled to a heterotrimeric G protein. The extracellular domain is responsible for ligand recognition and exhibits the greatest inter-receptor diversity. The heterotrimeric G protein complex consists of three subunits: alpha (α), beta (β) and gamma (ɣ). When a ligand binds to its GPCR, it induces a conformational change in the receptor which can then act as a guanine nucleotide exchange factor (GEF) and there is an exchange of GDP to GTP on the alpha subunit. This enables the Gα-GTP subunit to

dissociate from the Gβɣ dimer and from the receptor. Both Gα-GTP and Gβɣ can then activate different signalling cascades and effector proteins.

G protein-coupled receptor 81 (GPR81) was part of a family of orphan GPCRs coupled to G_i-type G proteins which are inhibitory and have a high homology to SCFA receptors GPR109Aand GPR109B. It was first identified in 2001 as an orphan GPCR and in 2008 as the only known endogenous receptor of lactate (309, 310). Now renamed HCAR1, it is linked to a variety of physiological functions with lactate playing roles in metabolic processes and modulation of inflammatory responses. The G protein's $G\alpha_i$ subunit inhibits the enzyme adenylate cyclase (AC) which increases the rate of conversion of adenosine triphosphate (ATP) to cAMP thereby reducing levels of cAMP (309, 310, 323, 324). cAMP is a second messenger molecule and mediates a variety of biological responses such as cell migration, differentiation, proliferation and apoptosis (325, 326). Other lactate-sensitive GPCRs include GPR4, GPR65, GPR68 and GPR132, however they have been largely localised to the tumour microenvironment. GPR132 and GPR65 have also been described in macrophages (327, 328). Where it has been characterised, lactate signalling in the intracellular space is mediated by lactate-activated GPCR HCAR1 (304, 329). HCAR1 is expressed in intracellular organelles as well as the plasma membrane (310).

1.5 LA and SCFA mediation of intracellular signalling pathways

In many cellular and tissue environments, high concentrations of LA are associated with pathological conditions such as tumorigenesis, microbial infection, and pro-inflammatory response (330-335). The effect of LA on the MAPK and NF-κB signalling pathways has been extensively studied in the context of inflammation of joints and pathologies such as rheumatoid arthritis (333, 336-338). Both D-LA and L-LA were shown to increase ERK1/2 and p38 phosphorylation in an animal model (333). Inhibition of these kinases decreases the expression of pro-inflammatory cytokines IL-6 and IL-8, suggesting that LA could be regulating the cytokines via the MAPK and NF-κB pathways.

A recent review of the pleiotropic role of lactate on inflammatory signalling pathways suggests that lactate exerts different effects depending on the metabolic status, the cell type being studied and the pathological process analysed (339). Lactate uptake through MCT1 in endothelial cells induces the activation of the NF-κB pathway and in lymphocytes increases expression of pro-inflammatory cytokine IL-17 through the PKM2/STAT3 pathway (258, 259). But in macrophages and mast cells, LA has an anti-inflammatory effect when it activates the HCAR1 receptor leading to inhibition of the NF-κB and inflammasome pathways (332, 340, 341). Extracellular LA has been found to suppress activation of NF-κB in LPS-stimulated monocytes and regulate TLR-mediated induction of the NLRP3 inflammasome and production of IL-1β (342, 343). LA-induced acidity plays an important role in immune cell-specific effects of LA which can have opposing effects, for example in macrophages LA reduces the expression of pro-inflammatory genes but increases the expression of pro-inflammatory genes such as IL-23 (344).

In the gut, the anti-inflammatory effects of SCFAs are mediated by the inhibition of TLR signalling through the downregulation of adaptor protein expression (345-347). Additionally, SCFAs such as acetate, propionate and butyrate enhance the integrity of the epithelial barrier by promoting tight junction formation and inhibiting the NLRP3 inflammasome, thereby preventing tissue damage (301, 348, 349). In comparison to other mucosal sites, understanding of metabolite-mediated signalling pathways in the cervicovaginal mucosa remains limited. However, recent studies have identified signalling pathways involved in regulating the vaginal epithelial barrier. For instance, Berard *et al.* identified the activation of mTOR and NF-κB signalling pathways in *Lactobacillus*-depleted microbiomes (175). Furthermore, LA was found to counteract the inflammatory effects of dysbiotic bacterial metabolite mixtures by suppressing NF-κB activation and TNFα production in VECs (296).

Despite significant advances in understanding the roles of metabolites in various physiological processes, there remains a notable lack of comprehensive information regarding their mediation of inflammatory pathways in VECs. This gap in knowledge hampers being able to fully elucidate the mechanisms by which metabolites influence inflammation and immune

responses in the female lower reproductive tract. Addressing this gap is critical, as inflammation in VECs plays a pivotal role in conditions such as BV, STIs, and other gynaecological disorders.

1.6 Hypothesis and Aims

The vaginal microbiota and its production of metabolites are fundamental in modulating the immune response at the mucosal surface of the lower FRT. A healthy vaginal microbiome, dominated by *Lactobacillus* species is associated with increased levels of LA, an acidic environment and protection against pathogens and disease. In contrast, a vaginal microbiome dominated by diverse microbial species which is *Lactobacillus*-deplete is associated with increased levels of SCFAs and succinate, a less acidic environment, increased inflammation and disruption of the epithelial barrier, and susceptibility to gynaecological and reproductive disorders.

This thesis sets out to test the hypothesis that bacterial metabolites are key mediators of host innate immune responses, specifically vaginal epithelial cell inflammatory activation. It is hypothesised that LA, the most abundant bacterial metabolite in the vaginal niche of healthy reproductive-age women, inhibits TLR-mediated MAPK activation and downstream activation of pro-inflammatory transcription factors.

The major aims of this thesis were to:

- Characterise LA inflammatory signalling pathways in VECs
- Understand the mechanism underlying LA signalling during bacterial and viral infection
- Investigate and characterise potential lactate receptors on vaginal epithelial cells
- Examine the role of LA on epithelial cell barrier integrity
- Identify significant pathways and proteins regulated by LA using a proteomics approach

Chapter 2: Materials and Methods

2.1 Materials

2.1.1 Cell lines and primary cells

Cell line	Catalogue Number	Supplier
VK2 E6E7	CRL-2616	ATCC Boston USA
V19	Special arrangement with Burnet Institute	MatTek
HVEC	Special arrangement with Burnet Institute	MatTek

2.1.2 Cell culture media, supplements and chemicals

Compound	Catalogue Number	Supplier
Ammonium Bicarbonate	09830	Sigma-Aldrich
Ammonium Persulphate (APS)	A3678	Sigma-Aldrich
Bovine Pituitary Extract	13028-014	Life Technologies
Bovine Serum Albumin (BSA)	A7906	Sigma-Aldrich
Calcium Chloride	CC-3235	Lonza
2-Chloroacetamide (CAA)	C0267	Sigma-Aldrich
DEPC-Treated Water	AM9906	Ambion
Dulbecco's Modified Eagle's Medium - high glucose	D5671	Sigma-Aldrich
Human Recombinant Epithelial Growth Factor (EGF)	10450-013	Life Technologies
Ethanol	20821.330	AnalaR®
Foetal Bovine Serum	10270-098	Gibco
Glycerol	101 M	AnalaR®
Hydrochloric Acid (HCl)	CHE2166	Scientific Laboratory Supplies
Keratinocyte Serum-Free Medium (KSFM)	17005-034	Invitrogen
L-Glutamine Solution	G7513	Sigma-Aldrich
Methanol	20847.307	AnalaR®
Penicillin-Streptomycin	P0781	Sigma-Aldrich
RNAse Zap™	AM9780	Invitrogen

Sodium Dodecyl Sulphate (SDS) 10%	1610302	Bio-Rad
Sodium Chloride (NaCl)	10241AP	AnalaR®
Sodium Hydroxide (NaOH)	221465	Sigma-Aldrich
N,N,N'N'-Tetramethyletylenediamine (TEMED)	T7024	Sigma-Aldrich
Trifluoroacetic Acid, 98% Pure	471670250	Thermo Scientific
Tris Base	BP152-1	Fisher Bioreagents
Tris (2-carboxyethyl)phosphine Hydrochloride, 95%, 0.5M Solution in Water (TCEP)	H51864.AA	VWR
Tris HCl	10812846001	Sigma-Aldrich
Triton X-100	T-8787	Sigma-Aldrich
Tween 20	P9416	Bio-Rad
Transwell® Permeable Supports	3450	Corning
Trypan Blue Solution (0.4%)	T8154	Sigma-Aldrich
Trypsin-EDTA Solution	T3924	Sigma-Aldrich
Trypsin/LysC	V5073	Promega
Urea	15604	Sigma-Aldrich

2.1.3 Treatments, inhibitors and activators

Compound	**Catalogue Number**	**Supplier**
Cremophore EL	HY-Y1890	Cambridge Bioscience
Cyrene™	807796	Sigma-Aldrich
D-Lactic Acid (D-LA)	L0625	Sigma-Aldrich
DL-Dithiothreitol	D9779	Sigma-Aldrich
DMSO (Dimethyl Sulfoxide)	D4540	Sigma-Aldrich
Forskolin	Ab120058	abcam
FSL-1	Tlrl-fsl	Invivogen
3-Isobutyl-1-Methylxanthine (IMBX)	PHZ1124	Life Technologies
JNK Inhibitor (SP600125)	8177	Cell Signaling
L-Lactic Acid (L-LA)	L6402	Sigma-Aldrich
Oligo$(dT)_{23}$, Anchored	O4387	Sigma-Aldrich
Pertussis Toxin	3097	Tocris
Phosphatase Inhibitor Cocktail II	P5726	Sigma-Aldrich

Phosphatase Inhibitor Cocktail III	P0044	Sigma-Aldrich
Phenylmethanesulfonyl Fluoride (PMSF)	P7626	Sigma-Aldrich
Protease Inhibitor	P8340	Sigma-Aldrich
Polyinosinic:polycytidylic Acid (PIC)	P9582	Invivogen
RNase Inhibitor	R2520	Sigma-Aldrich
Sodium Acetate	S7545	Sigma-Aldrich
Sodium Chloride	10241	BDH
Succinic Acid	S9512	Sigma-Aldrich
U0126 (MEK Inhibitor)	9903	Cell Signaling

2.1.4 Buffers and solutions

2.1.4.1 Protein extraction buffers

Buffer	**Recipe**
Modified RIPA buffer	1% (v/v) Triton X-100 1% (w/v) Sodium Deoxycholate 0.1% (v/v) SDS 15 mM NaCl 10 mM Tris, pH 7.4 1 mM EDTA
1 M AmBic (100 ml)	7.906 g Ammonium Bicarbonate (AmBic) 80 ml ddH_2O Make up to 100ml once Ambic has dissolved
8 M urea	120.12 g urea 25 g 1M AmBic 100 ml ddH_2O Make up to 250 ml when urea is dissolved

2.1.4.2 Western blotting buffers

Buffer	**Recipe**
Blocking Buffer 5% Milk	5% (w/v) Non-fat Milk in TBS-T
Blocking Buffer 5% BSA	5% (w/v) Bovine Serum Albumin in TBS-T
Tris-glycine/SDS-PAGE Running Buffer	25 mM Tris-base 250 mM Glycine 0.1% (w/v) SDS pH 8.3
Transfer Buffer	39 mM Glycine54 48 mM Tris-base 20% (v/v) Methanol
TBS	1.21 g Tris 8.77 g NaCl pH 7.4 2.5 ml 20% Tween 80
TBS-T (washing buffer for Western Blotting)	0.01% (v/v) Tween-20 in TBS
Protein Loading Dye (reducing)	3% (v/v) SDS 3% (v/v) Glycerol 1% Bromophenol Blue β-Mercaptoethanol

2.1.4.3 Other buffers

Buffer	**Recipe**
Phosphate Buffered Saline	140 mM NaCl 2.5 mM KCl 1.5 mM KH_2PO_4 10 mM Na_2HPO_4 pH 7.2

2.1.5 Western blotting reagents and materials

Compound	Catalogue Number	Supplier
Ammonium Persulphate	AA0307	VWR
Clarity™ Western ECL Substrate	170-5061	Bio-Rad
Luminata™ Forte Western HRP Substrate	WBLUF0500	Millipore
Mini-PROTEAN® TGX™ Gels	#4561036	Bio-Rad
Pierce™ ECL Western Blotting Substrate	32209	Thermo Scientific
PVDF Membrane	IPVH00010	Millipore
Skimmed Milk Powder	84615.0500	VWR
Thermo Scientific PageRuler™ Prestained Protein Ladder	26616	Thermo Scientific
N,N,N'N'-Tetramethyletylenediamine (TEMED)	T7024	Sigma-Aldrich
Trans-Blot® Turbo™ Midi PVDF Transfer Pack	#1704157	Bio-Rad

2.1.6 Antibodies

2.1.6.1 Primary antibody

Antibody Epitope	Dilution used	Catalogue number	Supplier
β-actin	1:50,000	ab6276	Abcam
Phospho-c-Jun (Ser73)	1:1,000	9164	Cell Signaling
Phospho-p65 (Ser536)	1:1,000	3033	Cell Signaling
Phospho-IKKα (Ser176)/IKKβ (Ser177)	1:1,000	2078	Cell Signaling
Phospho-JNK (Thr183/Tyr185)	1:2,000	9251	Cell Signaling
Phospho-ERK1/2 (Thr202/Tyr204)	1:2,000	9101	Cell Signaling
Phospho-p38 (Thr180/Tyr182)	1:1,000	9211	Cell Signaling
Phospho-IRF3 (Thr202/Tyr204)	1:1,000	4947	Cell Signaling
Phospho-TBK1	1:1,000	5483S	Cell Signaling
E-cadherin	1:1,000	24E10	Cell Signaling

2.1.6.2 Secondary antibody

Goat Anti-Mouse IgG-HRP	1:12,500	sc-2005	Santa Cruz
Goat Anti-Rabbit IgG-HRP	1:2,000	7074	Cell Signaling
Donkey Anti-Goat IgG-HRP	1:2,000	Sc-2020	Santa Cruz

2.1.7 mRNA extraction, cDNA synthesis and qPCR reagents and materials

Compound	**Catalogue Number**	**Supplier**
DNase I (Amplification Grade)	AMPD1	Sigma-Aldrich
M-MLV Reverse Transcriptase	M1302	Sigma-Aldrich
Deoxynucleotide Mix, 10 mM	D7295	Sigma-Aldrich
Oligo(dT)23, Anchored	O4387	Sigma-Aldrich
Ribonuclease Inhibitor Human	R2520	Sigma-Aldrich
SYBR® Green JumpStart™ Taq ReadyMix	S4438	Sigma-Aldrich
Platinum® SYBR® Green qPCR SuperMix-UDG	11733-046	Invitrogen
PrimeStar Max DNA Polymerase	R045	Clonetech

2.1.8 Kits

Compound	**Catalogue Number**	**Supplier**
cAMP Gs Dynamic Kit	62AM4PEB	CisBio
Phospho-Total Protein Lysis Buffer 1 (4 x)	760007B	CisBio
DC Protein Assay Kit Reagent A	#5000113	Bio-Rad
DC Protein Assay Kit Reagent B	#5000114	Bio-Rad
DC Protein Assay Kit Reagent S	#5000115	Bio-Rad
QiAmp Mini DNA Kit	51304	Qiagen
QIAshredder Kit	79656	Qiagen
RNeasy Mini Kit	74106	Qiagen

2.1.9 Instruments

Instrument	**Manufacturer**
Countess™ Automated Cell Counter	Invitrogen
ImageQuant LAS4000 Luminescent Image Analyser	GE Healthcare
Leica SP5 Confocal Microscope	Leica
NanoDrop® ND-1000	Thermo-Fisher
BMG PHERAstar	BMG Labtech
StepOnePlus Real Time PCR Systems	Applied Biosystems
TE2000-U Confocal Microscope	Nikon
M Class (HPLC)	Waters

2.1.10 Software

Compound	**Supplier**
Amica v3.0.1 (350)	Max Perutz Labs
GraphPad Prism 10	GraphPad Software
ImageQuant TL v8.1	GE Healthcare
Leica Application Suite Advanced Fluorescence Lite 2.6.0	Leica
PANTHER 18.0	National Science Foundation
PheraStar Data Analysis	BMG Labtech
QCapture	
QuikChange Primer Design	Agilent
Reactome	Reactome
R Studio	R Foundation for Statistical Computing
StepOne Software v2.3	Applied Biosystems

2.2 Methods

2.2.1 Cell culture

2.2.1.1 VK2/E6E7 vaginal epithelial cell culture models

The immortalised vaginal epithelial cell line VK2/E6E7, which resembles its tissue of origin both in morphology and immunochemical characteristics, was obtained from ATCC, Boston, USA (48). This is a vaginal epithelial cell line established in 1996 from a 32-year-old premenopausal woman who had anterior-posterior vagina repair surgery as part of a treatment for endometriosis. The cells were taken from normal mucosal tissue and are widely used as an *in vitro* model of VECs. The viability and inflammatory response of these cells to *Lactobacillus* species and *Staphylococcus epidermis* are similar to primary cells (51).

Cells were cultured in keratinocyte serum-free (KSF) medium (Invitrogen, Carlsbad, CA) supplemented with 0.1 ng ml^{-1} human recombinant epithelial growth factor, 50 mg ml^{-1} bovine pituitary extract (Life Technologies, Carlsbad, CA), 0.4 mM calcium chloride, 50 U ml^{-1} penicillin, and 50 µg ml^{-1} streptomycin, at 37°C under a humidified 5% CO_2 atmosphere. Medium was refreshed every 2-3 days. These conditions were maintained for 7 days until 70-80% confluency was reached. Vaginal epithelial cells were grown as either monolayers or multilayers as described below.

Monolayered VEC culture

For monolayered cultures, VECs were seeded (10^5 ml^{-1}) into 6-well tissue culture plates and maintained in supplemented KSFM until reaching 90% confluency. At this stage, cells were used in experimental models.

Multilayered VEC culture

A multilayered cell culture was generated by seeding 10^5 ml^{-1} VK2/E6E7 cell line onto 24 mm diameter polyester Transwell® inserts with 0.4 µm pores (Corning, Corning, NY) in 6-well tissue culture plates. Cultures were incubated at 37°C under a humidified 5% CO_2 atmosphere for 24-36 hours to create a confluent monolayer before removing the apical medium to form an air-liquid interface (ALI) (51). Medium in the basal chamber was refreshed regularly every 2-3 days and multilayers were considered mature at day 12 after creating the ALI. Fresh medium was added to the basal chamber before starting any experiment (Figure 2.1).

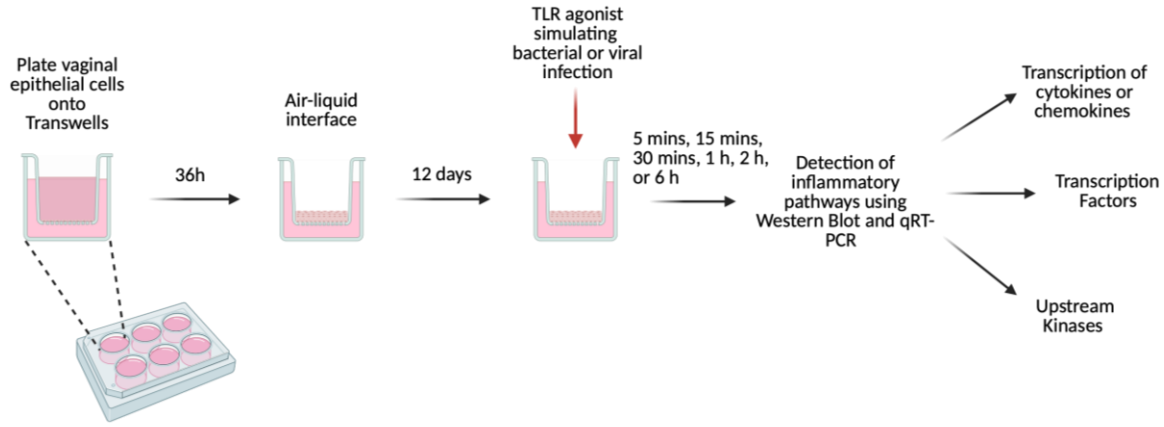

Figure 2.1 Schematic of optimised Transwells® multilayered cell culture of VECs.

Cells were seeded onto Transwells®, allowed to form a confluent monolayer before an ALI was created to encourage formation of a multilayer over the course of 12 days. Cells were then treated with bacterial agonist fibroblast-stimulating lipopeptide (FSL-1) or viral agonist polyinosinic:polycytidylic acid (PIC) over a time course in the presence or absence of 30 mM L-LA (pH 3.9), or media alone (pH 7.4) as indicated. Proteins and mRNA were extracted and used to detect inflammatory pathways using Western Blotting and RT-PCR. *Created with BioRender.com*.

2.2.1.2 Primary vaginal epithelial cell culture

Primary vaginal epithelial cell culture was performed by collaborators in the Burnet Institute, Melbourne, Australia. For this, primary human vaginal-ectocervical cells (HVEC) were obtained from MatTek Corp (Ashland, MA). The cells were derived from discarded surgical tissue from the reproductive tract of premenopausal, healthy women undergoing hysterectomies for benign indications. HVECs were maintained at 37°C under a humidified 5% CO_2 atmosphere in supplemented KSF medium. Medium was refreshed every 2-3 days until 70-80% confluency was reached (approximately 10-12 days).

HVECs were then seeded onto Transwells® and when a confluent monolayer was formed an ALI was applied in the apical chamber to promote the formation of multilayers as described above (Section 2.2.1.1).

2.2.2 Assessment of cell viability and morphology

Cell viability was assessed using the Countess™ Automated Cell Counter (Invitrogen). Cells were gently lifted using Trypsin-EDTA, centrifuged at 125 x *g* for 5 minutes and the supernatant was carefully removed from the resulting cell pellet. Cells were then resuspended in 250 µl PBS and 250 µl of trypan blue stain was added. Sample mixture (10 µl) was added to the chamber port on one side of the Countess™ cell counting chamber slide. The cell count and viability were determined on the Countess™ Automated Cell Counter.

To assess the impact of LA treatment on VEC morphology, representative images were captured with the TE2000-U Confocal microscope (Nikon) using white light imaging at x10 magnification. QCapture software was used to acquire the images.

2.2.3 Acid acclimatisation experiments

The effect of low pH on VECs was assessed by culturing cells with KSF medium adjusted to pH 3.9 with HCl (pH 3.9-HCl) or with L-LA or D-LA at physiological concentrations of 30 mM and pH 3.9 (pH 3.9-LLA or -DLA). A third condition of culture in KSF at pH 7.4 was included for comparison. The three different media conditions were added separately to the apical side of the multilayered cultures in a 6-well plate, which were left to acclimate at 37°C for 2 hours under a humidified 5% CO_2 atmosphere. Volumes of each of the three-treatment media used for the acid acclimatisation are presented in Table 2.1.

Table 2.1 Media composition for apical treatment of multilayered VECs.

	KSF	HCl	L-LA or D-LA
pH 7.4	1.5 ml	—	—
pH 3.9-HCl	1.5 ml	34.8 µl	—
pH 3.9-LLA	1.5 ml	6.75 µl	45 µl

Cells were then collected, proteins extracted (Section 2.2.6.1) and processed (Section 2.2.7) following 30 minutes, 1 hour and 2 hours of incubation.

2.2.4 Simulations of bacterial and viral infection using TLR agonists

After allowing the multilayered VECs to acclimatise at 37°C for 2 hours, a bacterial or viral agonist prepared in KSF at pH 7.4, pH 3.9-HCl or pH 3.9-LLA or -DLA was added to the apical chamber. TLR agonists used to treat the cells in these experiments included the TLR2/6 agonist, fibroblast stimulating ligand-1 (FSL-1; 1.0 µg ml^{-1}, Invivogen) and the TLR3 agonist, polyinosinic:polycytidylic acid (PIC; 20 µg ml^{-1}, Invivogen), chosen following previous work carried out in the MacIntyre and Bennett laboratory and by Rose *et al.* (51, 351). The concentration of the bacterial agonist was determined using a dose response experiment in which the following concentrations were tested: 0.01 µg ml^{-1} , 0.1 µg ml^{-1}, and 1.0 µg ml^{-1} as experiments in the existing literature were on VEC monolayers (51). The FSL-1 concentration

of 1.0 µg ml^{-1} was chosen as it activated two inflammatory transcription factors NF-κB and AP-1 significantly. The concentration of the viral agonist had been previously established in multilayered VECs in the existing literature (276).

Cells were exposed to the TLR agonists for 5 minutes, 15 minutes, 30 minutes, 1 hour, 2 hours, 6 hours or 24 hours at 37°C under a humidified 5% CO_2 atmosphere. All cell culture experiments were stopped by placing plates on ice and washing cells with ice cold PBS. Plates were frozen immediately at -80°C. Whole cell protein extraction (Section 2.2.6) and mRNA extraction (Section 2.2.8) were carried out and samples were stored at -80°C.

2.2.5 MEK inhibition of VECs

2.2.5.1 Optimising the solvent for MEK inhibitor, U0126

Initial experiments with MEK Inhibitor U0126 dissolved in dimethyl sulfoxide (DMSO) (manufacturer recommended), or methanol indicated that these solvents may activate NF-κB pathways. Multilayered VECs were treated for 30 minutes with 10 mM MEK Inhibitor U0126 resuspended in DMSO or methanol. Following a 2-hour acclimatisation in KSF medium at pH 7.4, pH 3.9-HCl or pH 3.9-LLA, multilayered VK2 cells were treated with bacterial (1.0 µg ml^{-1} FSL-1) or viral agonists (20 µg ml^{-1} PIC) for 30 minutes. Whole cell proteins were extracted as described below and probed for p-ERK, p-p65 and p-cJun. Both DMSO and methanol were found to activate NF-κB pathways. Therefore, as an alternative, the solvent Cyrene™ was also tested (352). VK2 cells were acclimatised in KSF (pH 7.4), KSF (pH 3.9-HCl) or KSF (pH 3.9-LLA) containing Cyrene™ (1 µl ml^{-1}).

2.2.5.2 Inhibition of MEK

Multilayered VECs were treated for 30 minutes with 10 mM MEK Inhibitor U0126 resuspended in Cyrene™. Following the 2 hours media acclimatisation at pH 7.4, pH 3.9-HCl or pH 3.9-L-LA, the VK2 cells were treated with bacterial or viral agonists FSL-1 or PIC for 30 minutes. Whole cell proteins were extracted as described below and probed for p-ERK, p-p65, and p-cJun.

2.2.6 Whole cell protein extraction

Samples were split equally for whole cell protein extraction and mRNA extraction. For this, cells were gently resuspended in 500 µl ice-cold PBS with protease inhibitor (10 µl ml^{-1}) before being divided equally into 250 µl aliquots. The cells were then pelleted by centrifugation at 4°C for 5 minutes at 3,000 x *g*. The supernatant was discarded, and the resulting pellet used for protein or mRNA extraction as described below.

2.2.6.1 Whole cell protein extraction with modified RIPA buffer

For whole cell protein extraction, the pelleted VECs were lysed on ice for 5 minutes in 80 µl protein extraction buffer containing modified radio-immunoprecipitation assay (RIPA) buffer with phosphatase and protease inhibitors (0.5% v/v), 1 mM phenylmethylsulphonyl fluoride (PMSF) (1% v/v), protease inhibitor (0.5% v/v), phosphatase inhibitor cocktail II (1% v/v) and phosphatase inhibitor cocktail III (1% v/v) and collected in 1.5 ml microcentrifuge tubes. Cell lysates were centrifuged at 13,500 x *g* for 10 minutes at 4°C. The supernatant containing the extracted proteins was then removed and stored at -80°C or used immediately for immunodetection using Western Blotting.

2.2.6.2 Whole cell protein extraction with 8 M urea

Pelleted cells were washed with 500 µl PBS and centrifuged at 500 x *g* for 3 minutes at 4°C and the supernatant discarded. The cells were then lysed for 10 minutes on ice in 80 µl 8 M urea lysis buffer followed by sonication in a water bath at 4°C for 10 minutes. Samples were then centrifuged at 10,000 x *g* at 4°C for 10 minutes. The resulting supernatant was transferred to protein maximum recovery tubes and stored at -80°C or used immediately in the protein digestion step.

2.2.7 Protein analysis with SDS-PAGE and Western Blot analysis

Equal volumes of extracted protein samples were denatured with protein loading dye consisting of 3% glycerol, 3% SDS, 1% bromophenol blue, and β-mercaptoethanol at 80°C for 10 minutes. Prepared protein sample (30 µL) was resolved by SDS-polyacrylamide gel (SDS-PAGE) initially through a 5% stacking gel (5.5 ml distilled water, 1.3 ml 30% acrylamide mix, 1 ml 1.0M Tris pH 6.8, 0.08 ml 10% SDS, 0.08 ml 10% ammonium persulphate, and 0.008 ml TEMED) and then through a 10% resolving gel (7.9 ml distilled water, 6.7 ml 30% acrylamide mix, 5 ml 1.5M Tris pH 8.8, 0.2 ml 10% SDS, 0.2 ml 10% ammonium persulphate, and 0.008 ml TEMED) at 100 V for 10 minutes and 130 V for 60-70 minutes before being transferred to a polyvinylidene difluoride (PVDF) membrane (Immobilon®-P, Millipore, Billerica, MA) using Bio-Rad Transblot Turbo Blotting System. The membranes were then incubated in either 5% [w/v] BSA in Tris-buffered saline with 0.1% Tween-20 or 5% [w/v] non-fat milk powder in Tris-buffered saline with 0.1% Tween-20 for 1 hour at room temperature. Following two washes in TBS-T, the membranes were incubated overnight in primary antibodies at 4°C (see Section 2.1.6 for dilution concentrations).

The membranes were then washed once for 10 minutes and three times for 5 minutes in TBS-T and incubated with horseradish peroxidase (HRP)-conjugated secondary antibody (1:2,000 in 1% milk-TBST) for 1 hour at room temperature. Detection of immunoreactive proteins was carried out using 1:1 mixture of Clarity™ Western ECL Substrate (Bio-Rad) or Luminata™ Forte Western HRP Substrate (Millipore). Immunoreactive protein bands were imaged on an

ImageQuant LAS4000 Luminescent Image Analyser (GE Healthcare). To confirm equal loading, the membranes were stripped and re-probed for β-actin. Densitometric analysis was performed using ImageQuant TL v8.1 (GE Healthcare) and the values were normalised to β-actin.

2.2.8 mRNA extraction

VEC pellets were homogenised using a QIAShredder column (Qiagen, Hilden, Germany) before extracting mRNA with the RNeasy mini kit (Qiagen). Cells were lysed using lysis buffer Buffer RLT and centrifuged through a QIAShredder homogeniser column to simultaneously remove insoluble elements and reduce any viscosity in the lysates. Ethanol was added to the lysate to promote selective binding of mRNA to the RNeasy membrane. The samples were then applied to the RNeasy mini spin column so that contaminants could be washed away, and mRNA was eluted in RNase-free water. The concentration and purity of the extracted mRNA was assessed using a Nanodrop 1000 spectrophotometer (ThermoScientific, Waltham, MA) by measuring OD_{260} and OD_{280}, with a 260/280 absorbance ratio of 2.0 indicative of highly pure samples. mRNA was then either immediately stored at -80°C or used for synthesis of cDNA.

2.2.9 DNase treatment and first-strand cDNA synthesis

Prior to cDNA synthesis, any potential DNA contamination was removed by DNase I treatment (Invitrogen). The DNase I-treated mRNA was used for cDNA synthesis with the M-MLV reverse transcriptase kit (Sigma-Aldrich). With a total reaction volume of 10 µl, 2 µg of mRNA was digested with 1 µl of DNaseI (Sigma-Aldrich) in 10 x DNaseI buffer at room temperature for 15 minutes. Once the digestion was complete, the reaction was stopped by adding 1 µl of Stop solution, which binds calcium and magnesium ions and inactivates the DNaseI, by incubating the solution at 70°C for 10 minutes and subsequently chilling it on ice.

First-strand cDNA was synthesised using the M-MLV reverse transcriptase kit (Sigma-Aldrich) and oligo (dT) primers. The DNase-treated mRNA was incubated at 70°C with 1 µl dNTP mix

(10 mM each of dATP, dTTP, dGTP, and dCTP) and 1 µl oligo(dT) for 10 minutes before being placed on ice for 1 minute. Following the addition of 2 µl 10 x reverse transcriptase buffer (Invitrogen), 1 µl M-MLV reverse transcriptase, 0.5 µl RNase inhibitor and DEPC-treated water to attain a total reaction volume of 20 µl, the reaction mix was incubated at room temperature to ensure elongation of oligo dT primers before incubating at 37°C for 50 minutes, the temperature at which reverse transcriptase is active. The reverse transcription was terminated by heating the sample between 80 to 94°C for 10 minutes. The resulting cDNA was then stored at -20°C until further analysis.

The cDNA was optimised for each primer using a pooled sample of the treatments in order to determine the optimal concentration of cDNA to use for each primer. The dilution that showed an amplification curve with Ct values between 17 and 28 was used.

2.2.10 Real-time PCR

Assessment of gene expression was performed by quantitative real-time polymerase chain reaction (RT-PCR) carried out in 96-well plates on the StepOnePlus™ Real Time PCR system (Applied Biosystems) using SYBR® Green JumpStart™ Taq ReadyMix (Sigma-Aldrich). As SYBR Green dye fluoresces when incorporated into double-stranded DNA, an increase in the accumulation of PCR product generates a higher fluorescence which can be detected by the RT-PCR system throughout the cycle. Amplification was carried out using specific primers for the target cDNA (Table 2.2).

Each reaction mix (total volume 20 µl) contained 10 µl SYBR® Green JumpStart™ Taq ReadyMix™, 0.2 µl ROX reference dye, 0.6 µl forward primer, 0.6 µl reverse primer, 4.6 µl DEPC-treated water and 4 µl diluted cDNA. Reactions were run in triplicate using DEPC-treated water as a negative control. The following cycle condition were used: 2 minutes at 50°C, 2 minutes at 95°C, 40 cycles of 15 sec at 95°C, 30 sec at 60°C; melt curve: 15 sec at 85°C, 1 minute at 60°C and 15 sec at 95°C.

Table 2.2 Sequences of primers used in real time PCR.

Gene	Forward Sequence	Reverse Sequence	Supplier
GAPDH	CTTTTGCGTCGCCAG	TTGATGGCAACAATATCCAC	Sigma-Aldrich
L19	CAGAAGATACCGTGAATCTAAG	TGTTTTTGAACACATTCCCC	Sigma-Aldrich
IL-6	AAGATTCCAAAGATGTAGCC	ACATGTCTCCTTTCTCAGG	Sigma-Aldrich
IL-8	GCCTTCCTGATTTCTGCAGC	CGCAGTGTGGTCCACTCTCA	Invitrogen
IL-1β	CTAAACAGATGAAGTGCTCC	GGTCATTCTCCTGGAAGG	Sigma-Aldrich
IL-1Ra	CTGGAGGCTGATAAATGC	TTTGTGTTGATGAATCCTGG	Sigma-Aldrich
TNFα	CTCAGCCTCTTCTCCTTC	AGAAGATGATCTGACTGCC	Sigma-Aldrich
RANTES	ATCTGCCTCCCCATATTC	AAGAGTTGATGTACTCCCG	Sigma-Aldrich
IRF3	ATTCTGGATGAGTTACTGGG	AAGGTAATCAGATCTTCCCC	Sigma-Aldrich
IRF7	TCTTCTTCCAAGAGCTGG	CTATCCAGGGAAGACACAC	Sigma-Aldrich
MIP-3α	GCGCAAATCCAAAACAGACT	CAAGTCCAGTGAGGCACAA	Invitrogen
MCT1 p1	TGGATGGAGAGGAAGCTTTCTAAT	CACACCAGATTTTCCAGCTTTC	Sigma-Aldrich
MCT1 p3*	ACAAGCAAACGAGGCAGCGA	CCTCCAACTGCTGGTGGCATT	Sigma-Aldrich
MCT4 p1	CACGGCATCGTCACCAACT	ACAGCCTGGATAGCAACGTACAT	Sigma-Aldrich
GPR81 p1	AATTTGGCCGTGGCTGATTTC	ACCGTAAGGAACACGATGCTC	Sigma-Aldrich
GPR81 p5*	GCATCTGTGCCATTGTGGGG	CACGACCCGTTGTACATGGC	Sigma-Aldrich
SMCT1 p1	TCCGAGGTCTACCGTTTTG	GGGCAGGGGCATAAATAAC	Sigma-Aldrich
SMCT1 p2*	CTGCGCTGGCGTCACTTATG	GCCATCAGACCAACAACTGCT	Sigma-Aldrich
SMCT2 p1	GATATATAGCCATGGAGGTGAAGAACTTTG	CGTCTAGATGTGCATTCATACAGGTATTG	Sigma-Aldrich
SMCT2 p2*	TGGAATTGGGGTGTTCTTTGCC	AAGGATGCCCCAAAGCGGTA	Sigma-Aldrich

* denotes optimised primer used.

Baseline of fluorescence was determined using StepOnePlus™ Software v2.3 and a baseline-subtracted amplification plot was generated by calculating a mathematical trend of the normalised fluorescent reporter signal. The cycle number at the point of the amplification plot where it crossed the threshold, defined as the Ct value, was used as a quantitative measurement of the input target. A decrease in the Ct value was seen as an increase in the target cDNA. Expression levels were assessed using the comparative ΔΔCt method and the target Ct values were normalised to ribosomal proteins L-19 and GAPDH for analysis (353).

Any significant changes in target cDNA level were determined using one-way ANOVA with Tukey's *post hoc* test.

2.2.11 Assessment of VEC barrier function using transepithelial electrical resistance (TEER)

Changes in VEC barrier function were quantified using transepithelial electrical resistance (TEER) measured according to the method described by Hidalgo *et al.* using the Millicell® electrical resistance system (Millipore) (354, 355). First the basal medium was refreshed and apical medium added (1.5 ml). "Chopstick"-type electrodes were placed in the medium on either side of the Transwell® membrane, a small AC current was applied passing from one electrode to the other. The TEER measurement quantifies the barrier integrity by measuring how much this electrical signal is blocked by the layer of cells. Three measurements were made for each well. The resistance was calculated by multiplying the observed value minus the background resistance by the surface area of the membrane.

2.2.12 Assessment of VEC G protein-coupled receptor (GPCR) function

2.2.12.1 Pertussis toxin (PTX) treatment

To investigate if LA may be signalling via a GPCR in VECs, PTX was used to inhibit potential G-protein heterotrimer interactions, thus blocking receptor coupling. For this, multilayered VECs were treated apically and basally for 24 hours with 200 ng ml^{-1} PTX. The medium was then removed, and cells were acclimatised to fresh KSF medium at pH 7.4 or pH 3.9 +/-L-LA, +/- 200 ng ml^{-1} PTX for 2 hours. The cells were then treated with 1.0 µg ml^{-1} FSL-1 for 30 minutes. Proteins were extracted and probed for p-ERK, p-p65 and p-cJun as previously described (Section 2.2.6 and 2.2.7).

2.2.12.2 cAMP signalling assays

Multilayered VECs were pre-treated basally and apically with 0.5 mM 3-isobutyl-1-methylxanthine (IBMX) for 15 minutes at 37°C. Fresh KSF medium at pH 7.4, or pH 3.9 +/- L-LA containing 0.5 mM IBMX was then added apically. Forskolin (3 µM) was used in some experiments to enhance the accumulation of cAMP by activating the adenylate cyclase enzyme. To quench the experiment, cells were washed in ice cold PBS and lysed in Cisbio cAMP lysis buffer on a shaker at room temperature for 15 minutes. Plates were scraped, and lysates transferred to 1.5 ml tubes. Samples were centrifuged at 14,500 x *g* for 10 minutes before supernatants were collected in fresh tubes.

cAMP accumulation was detected using cAMP Gs Dynamic kit (CisBio). The assay is a competitive immunoassay involving a cAMP-specific antibody labelled with Europium Cryptate and d2-labelled cAMP. Cryptate acts as an energy acceptor for which cAMP produced by the cells competes with d2-labelled cAMP. This decreases the FRET ratio and so the specific signal is inversely proportional to the concentration of cAMP in the sample. Using a 384-well white bottom plate, 10 µl of sample, 5 µl cAMP-d2 and 5 µl anti-cAMP Europium Cryptate were added and incubated in the dark for 1 hour.

Plates were read using the PHERAstar FSX equipped with a HTRF 337 optic module. The 665/620 nm fluorescence ratio was used to calculate results and lysates were normalised to protein concentration as determined by the Pierce Coomassie (Bradford) Protein Assay (Section 2.2.16.1).

Finally, VK2 multilayers were treated overnight with or without pertussis toxin PTX (200 ng ml^{-1}) in KSF before treatment. The cells were then stimulated with 3 µM forskolin alone at pH 7.4 or with 3 µM forskolin at pH 3.9 with or without 30 mM L-LA in KSF and incubated for 5 minutes or 1 hour at 37°C. Levels of cAMP accumulation were detected as described above.

2.2.13 Identification of lactate receptors and primer design

Potential lactate receptors were identified through a detailed literature review using PubMed and analysis of the National Centre for Biotechnology Information (NCBI) website and the NCBI Basic Local Alignment Search Tool (BLAST).

An assessment was made of the characteristics of each receptor which included confirmed or proposed mechanism of function, the number and quality of previous publications, ability to transport lactate, tissue type expression or location to reproductive tissue or epithelial cells. A prospect ranking system was developed based on these criteria: category A represented receptors matching all or most criteria examined, category B matched two or more criteria and category C matched at least one criterion.

Primers were selected using a combination of known primers from the literature search as well as designing primers using the NCBI primer design tool. Target human genes were selected, and the NCBI's Primer BLAST tool was used to generate potential primers. Selection of primers was performed following consideration of estimated product size (~150 bp), primer length (15-22 bp), melting temperature (59-65°C), GC content (50-60%), presence of GC clamp, nucleotide repeats (< 4), self-complementary binding and spanning of potential exon-exon regions.

2.2.14 Metabolic profiling of cervicovaginal fluid by Desorption Electrospray Ionisation Mass Spectrometry (DESI-MS)

In collaboration with Dr Katia Capuccini from the MacIntyre Laboratory, cervicovaginal fluid swab samples were collected from the posterior fornix using BD BBL™ CultureSwab™ MaxV Liquid Amies swabs (Becton, Dickinson and Company, Oxford, UK) from pregnant women with a singleton pregnancy (n = 165, 455 samples), with and without risk factors for preterm birth at up to five time points throughout pregnancy (8-16, 16-20, 20-26, 26-30, and 30-37 weeks). These samples were collected as part of the Vaginal Microbiome and Metabolome in

Pregnancy 1 (VMET1) study, which was conducted with approval of the NHS National Research Ethics Service (NRES) Committees London-City and East (REC 12/LO/2003) and London–Stanmore (REC 14/LO/0328), and by the North of Scotland Research Ethics Service (REC 14/NS/1078). Experiments were performed in accordance with the approved institutional guidelines after written informed consent was provided by all participants. Pregnant women were recruited at four major hospitals: Queen Charlotte's and Chelsea, and St Mary's Hospitals (Imperial College Healthcare NHS Trust, London, UK), Chelsea & Westminster Hospital (NHS Foundation Trust, London, UK), University College London Hospital (NHS Foundation Trust, London, UK) and the Royal Infirmary of Edinburgh (Scotland, UK).

Two swabs were collected at each visit - one dry swab for metabolomic studies and one liquid Amies swab for microbiome studies. After collection, swabs were placed in either Amies transport medium or a sterile microcentrifuge tube on ice, before long-term storage at −80°C. The vaginal swabs were thawed on ice and vortexed to resuspend the secretions in the Amies medium, yielding about 500 µl. Dry swabs were resuspended in 500 µl phosphate buffer saline (PBS). Whole genomic bacterial DNA was extracted from the swabs using the QiAmp Mini DNA kit (Qiagen) after enzymatic and mechanical extraction. The V1 - V3 hypervariable regions of 16S rRNA genes were amplified for sequencing using a forward and reverse fusion primer. The resulting amplicons were sequenced using an Illumina MiSeq platform (Illumina Inc.) at RTL Genomics (Lubbock, Texas, USA), as previously described (233, 247, 356, 357). Samples were classified into five CSTs following the 2011 Ravel classification, as well as defined as *Lactobacillus*-dominant (> 75% relative abundance *Lactobacillus* species; CST I, II, III and V), or *Lactobacillus*-deplete (< 75% *Lactobacillus* species; CST IV) (199). Metabolic profiling of cervicovaginal fluid (CVF) was performed using direct swab analysis by DESI-MS. A pneumatically assisted electrospray of charged aqueous droplets was directed onto a rotating swab. Methanol/water (95:5, v/v) was used as the solvent spray. This formed a liquid film that desorbed and ionised molecules from the swab, which was transferred directly to the mass spectrometer via an atmospheric pressure ion-transfer line. Full-scan mass spectra (m/z 50-1000, resolution = 30,000 FWHM) were acquired in both positive and negative ion modes. A metabolic profile was obtained in less than 3 minutes (247, 358) (Figure 2.2).

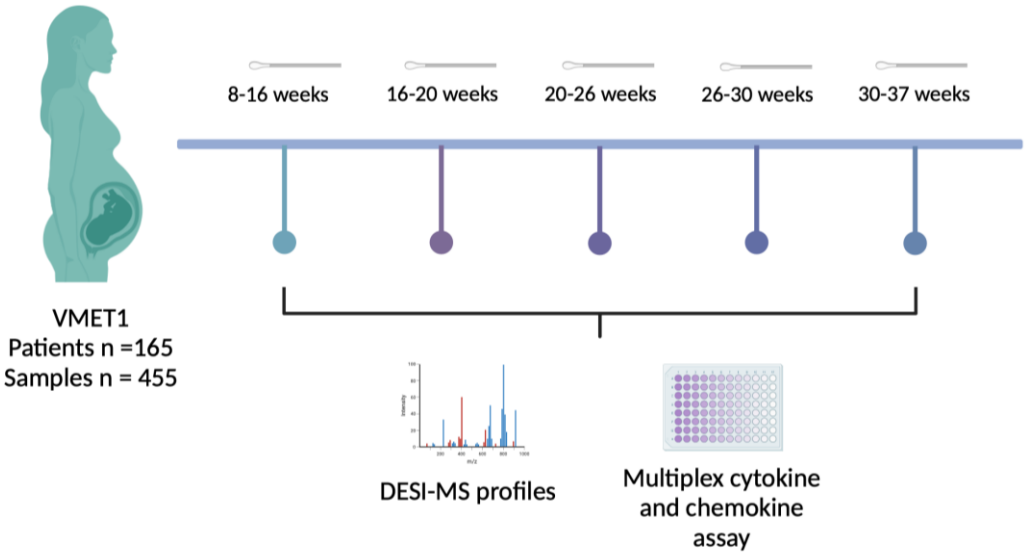

Figure 2.2 Study design and longitudinal sampling of cervicovaginal swabs collected from pregnancy cohort VMET1.

Cervicovaginal fluid swabs were collected from pregnant women (n = 165, 455 swabs) at up to five different time points (8-16, 16-20, 20-26, 26-30 and 30-37 weeks). Bacterial DNA was extracted and 16s rRNA amplicons were sequenced to determine bacteria present. DESI-MS was used to profile metabolites in CVF. *Created with BioRender.com*.

Raw spectral files (.raw) were converted to .mzML format using ProteoWizard msConverterGUI and processed in Python 3.5 with the pymzml package and in-house scripts (359). Data were imported at 0.01 Δm/z resolution, and an average mass spectrum was obtained from the first 30 spectra. Putative metabolite identification was achieved through accurate mass and isotopic pattern matching against the METLIN and LIPID MAPS databases.

For the inflammatory profiling of the cervicovaginal samples, the swabs were thawed on ice and resuspended in 350 µl PBS containing protease inhibitor (5 µl ml^{-1}). Samples were centrifuged at 7,000 x *g* for 10 minutes to remove cellular debris, and the supernatant was kept for analysis. Cytokine and chemokine concentrations were quantified using customised multiplex assays (R&D Systems) on a Bio-Plex 200 system. For this study, IL-1β was selected as a representative pro-inflammatory marker but the panel also included IL-2, IL-4, IL-5, IL-6, IL-8, IL-10, IL-18, IFNγ, granulocyte-macrophage colony-stimulating factor, and TNFα.

2.2.15 Lactin-V treatment of pregnant women

Metabolic profiling was performed on vaginal swab samples collected from women enrolled in the FLIP-1 study, which evaluated the safety, tolerance, and acceptability of live biotherapeutic *L. crispatus* (Lactin-V) use in a cohort of pregnant women at risk of preterm birth (360). Recruitment took place between September 2019 and April 2021 at Queen Charlotte's and Chelsea Hospital (Imperial College Healthcare NHS Trust, London, UK). The study was conducted in accordance with the Declaration of Helsinki and ethical approval was granted by the London Surrey Borders Research Ethics Committee (IRAS 262987). Health Research Authority and Health and Care Research Wales Approval was given (Phillip Bennett (2019)). The FLIP-1 Study: feasibility, safety, tolerance, and assessment of Lactin-V use in a cohort of pregnant women at increased risk of preterm birth. Reference 19/LO/1018. Retrieved from https://www.hra.nhs.uk/planning-and-improving-research/application-summaries/research-summaries/flip-1-study-v1/). This study was performed by Dr Erna Bayar, as part of her PhD project under the supervision of Professors David MacIntyre and Phillip Bennett. Eligible participants were selected from patients referred to the Prematurity Prevention Service at Imperial Healthcare NHS Trust due to their increased risk of PTB. The inclusion criteria comprised a series of well-established risk factors for PTB, such as a previous history of PTB, PPROM, mid-trimester loss, caesarean section at full cervical dilatation, trachelectomy, previous cervical tear or congenital uterine anomaly, a short cervix in a previous pregnancy, or having previously undergone a large loop excision of the transformation zone of the cervix. Inclusion required women to be over 18 years of age, between 11- and 15+6-weeks' gestation, and able to provide informed consent. Exclusion criteria included HIV positivity and the use of antibiotic therapy within one week prior to recruitment.

Participants received instruction on Lactin-V use at their initial visit. This was supplied in pre-filled applicators containing $2x10^9$ colony-forming units of *L. crispatus* CTV-05. Women were advised to refrigerate the product and abstain from sexual intercourse during the first 14 days and for 48 hours before each follow-up visit. Lactin-V doses were administered vaginally by the participants (n = 62, 362 samples) over five days at 14 weeks' gestation, followed by a

weekly maintenance dose until 20 weeks' gestation (Figure 2.3). Two cervicovaginal fluid swab samples were collected from the posterior fornix using BD BBL™ CultureSwab™ MaxV Liquid Amies swabs (Becton, Dickinson and Company, Oxford, UK) and one using Transwab®MW170 with rayon bud type (Medical Wire & Equipment, Corsham, UK) at six time points through the pregnancy (14, 15, 18, 20, 28, 36 weeks) and at delivery for 16S rRNA amplicon-based metataxonomic, immune and metabolite profiling (Figure 2.3). The samples collected at the first timepoint (T0) were pre-intervention and participants started Lactin-V administration the following day. At the 28-week visit, CVF was collected using a sterile disposable menstrual disc (Softdisc™, Instead Inc.), which was weighed before and after use to determine the fluid volume. As with the VMET1 study, samples were matched to five CSTs and levels of metabolites were determined using DESI-MS. For this study the focus was on women that started with a CST different from CST I (n = 28).

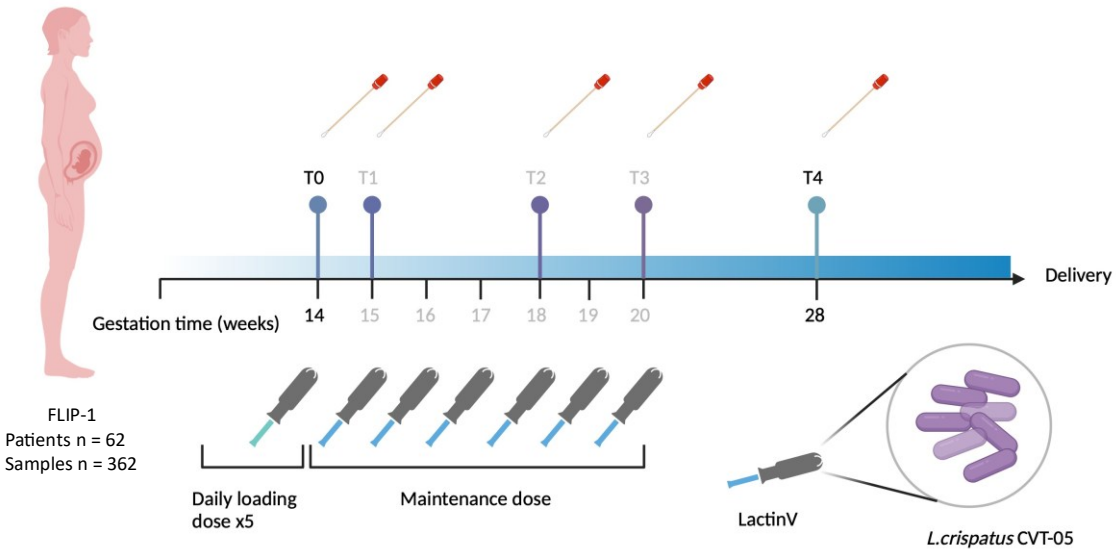

Figure 2.3 Study design showing longitudinal sampling and workflow of women enrolled in the FLIP-1 study (n = 62; 362 samples).

A dose of *L. crispatus* biotherapeutic Lactin-V was administered at 14 weeks' gestation over five consecutive days followed by six weekly maintenance doses. Vaginal swab samples were collected from pregnant women (n = 62, 362 swabs) at six time points (14, 15, 18, 20, 28, 36 weeks and at delivery). The first timepoint (T0) samples were taken pre-intervention. Bacterial DNA was extracted and 16s rRNA amplicons were sequenced to determine bacteria present. DESI-MS was used to profile metabolites in CVF. *Created with BioRender.com.*

2.2.16 Proteomic profiling of VECs

2.2.16.1 Treatment of VECs

A total of six different treatment groups (n = 5) were investigated in this study. First, the differential effect of acidity or 30 mM L-LA at pH 3.9 was compared to cells treated apically with medium at pH 7.4. A multilayered VEC culture was treated apically with KSF medium at pH 7.4 or pH 3.9, with or without 30 mM L-LA, for 6 hours. Then, in order to identify changes in the abundance of proteins regulated by LA-induced activation of the MEK/ERK signalling pathway, the VECs in these three conditions were also set up in the presence of a MEK inhibitor as described in Section 2.2.5.2. Proteins were extracted using 8 M urea (Section 2.2.6.2).

2.2.16.2 Protein concentration determination

VEC proteins were extracted using 8 M urea as previously described (Section 2.2.6.2). Total protein concentration was determined using the Pierce Coomassie (Bradford) Protein Assay Kit. In this method, Coomassie dye binds to positive charges found on proteins resulting in a change in colour proportional to the protein concentration within a sample. For both standards and samples, 5 µl was added in triplicate to a 96-well plate followed by 25 µl Reagent A and Reagent S (20 µl S in every 1 ml A) and 200 µl Reagent B. The plate was gently agitated and left at room temperature for 20 minutes. Absorbances were read at 595 nm. A calibration curve was produced using BSA standards and the concentrations of the samples was determined.

2.2.16.3 One step urea lysate protein digestion

Having quantified the amount of protein in each sample, 20 µg of protein were combined with 100 mM AmBic, 10 mM TCEP, 40 mM CAA and 0.2 µg of sequencing-grade modified trypsin; the volume was adjusted to 60 µl with ddH_2O. The final concentration of urea was < 1 M for

all samples. The samples were left to digest overnight at 37°C before quenching with 0.5% (V/V) tri-fluoroacetic acid (TFA). The following day the samples were either frozen or desalted.

2.2.16.4 Peptide desalting

Acidified peptides (0.5% (V/V) TFA) were kept at 4°C. A HLB µElution plate 30 µm (Waters) was equilibrated by drawing 100 µl 0.1% (V/V) TFA under vacuum for 45 sec. This was repeated twice ensuring that all the buffer had passed through the plate for the final wash. The digested peptides were then added and drawn through the plate with the vacuum controlled by the user to ensure all the sample had passed through. The plate was then washed three times with 100 µl 0.1% (V/V) TFA under vacuum for 1 min for the first two washes and 2 minutes for the third wash. Peptides were eluted into a 96-well Max-Quant 700 µl (Waters) sample plate placed under the HLB µElution plate by adding 50 µl 60% (V/V) acetonitrile (ACN) manually drawn through the plate under vacuum, followed by 100 µl 60% ACN. The samples were then dried in a Speedyvac (Eppendorf) at 60°C until completely dry (90-120 minutes).

The samples were then ready to be analysed using liquid chromatography-mass spectrometry (LC-MS). LC-MS and proteomic analysis were performed at the National Phenome Centre in collaboration with Dr Harry Whitwell.

2.2.16.5 Liquid Chromatography (LC) and Mass Spectrometry (MS)

A 150 x 0.3 mm Kinetex 2.6 µm XC-C18 column (Phenomenex) was connected to the M-class HPLC system (Waters) and the column temperature was set to 40°C to ensure consistent chromatographic performance. Buffer A was prepared by adding 0.1% formic acid to high purity water and Buffer B by adding 0.1% formic acid to high purity acetonitrile. The column was equilibrated with 3% Buffer B for 5 minutes before injecting the first sample into the HPLC system with the mobile phase composition set to 3% Buffer B. Table 2.3 shows the gradient elution programme used:

Table 2.3 Gradient elution programme used in HPLC.

Time	Buffer B (%)	Buffer A (%)
0-30	3	97
30-60	3 to 30	97 to 70
60-80	30 to 80	70 to 20
80-82	80	20
82-87	3	97

The eluted samples were detected using a SWATH mass spectrometry data-independent approach (DIA) strategy: Zeno SWATH DIA (361). The ions were detected in positive mode and the mass range was 400-1,500 m/z with an accumulation time of 0.1 sec. The declustering potential was set at 80 V.

For MS/MS, the mass range was set to 140-1,800 m/z with an accumulation time of 0.013 sec, enabling dynamic collision energy. MS/MS data were collected across 85 variable SWATH windows spanning 400–904 m/z (Supplementary 9.1; Table 9.1). The method was run over 29 minutes.

2.2.16.6 Data analysis

Using DIA.NN v1.8.1 software the raw LC-MS/MS data were matched against a spectral library based on a HeLa digest with annotation from the Human UniProtKB/Swiss-Prot Canonical Sequence downloaded 8.9.2022. To generate the spectral library, a highly fractionate HeLa proteome (40 fractions) was searched in-house using FragPipe v19 specifying cysteine carbamidomethylation and variable methionine oxidation. Peptides and proteins were filtered to 0.01 false discovery rate (FDR).

2.2.16.7 Proteomics bioinformatics pipelines and data visualisation

Resulting proteomic data were analysed using several open-source bioinformatics pipelines. Amica (v3.0.1), an open-source web-based proteomics platform was used to analyse, visualise and interpret the proteomics data generated (350).

The PANTHER (Protein Analysis Through Evolutionary Relationships) classification system (version 18.0) provided access to phylogenomic analyses of thousands of protein families (362) and was used to annotate each protein investigated by Protein Class, Molecular Function (using GO terms) and Pathways (curated by PANTHER and Reactome).

Reactome (V89) was used to look at biological pathways and processes (363-365). This is an open source, open access relational database of signalling and metabolic molecules and how they relate to each other within biological pathways and processes. Entities, including proteins, that react with each other are grouped into pathways.

Protein-protein interactions were visualised using the STRING database (https://string-db.org/) which collects and integrates both physical and functional protein-protein interactions data from a number of sources: computational text mining of the relevant scientific literature, interaction predictions from co-expression of proteins and databases on interaction experiments, and known complexes and pathways from curated sources (366).

The functional analysis of the relevant differential proteins may unmask pathways, interactions, post-translational modifications relevant for the biological question of interest. This *in silico* information can be used to formulate new hypotheses that could be eventually used to interrogate the biological system again.

A summary of the proteomics workflow is shown in Figure 2.4.

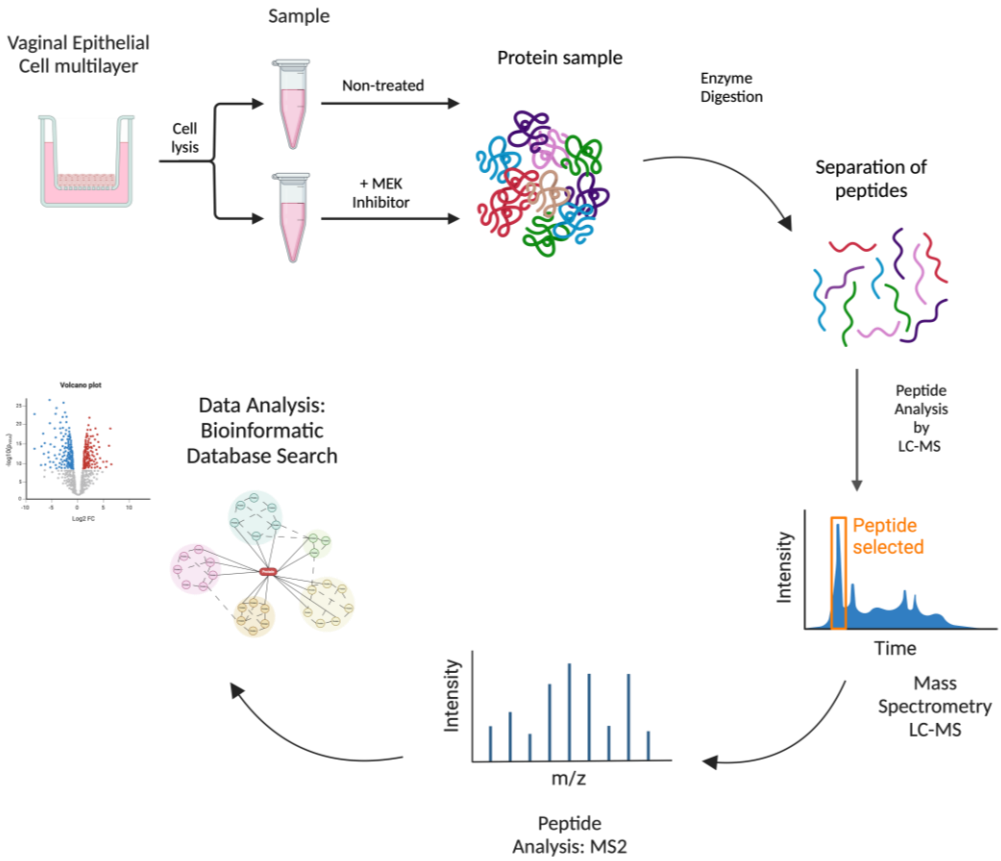

Figure 2.4 Workflow for the generation of proteomics data.

Samples of interest were subjected to 8 M urea protein extraction and trypsin digestion. The resulting peptides were separated by chromatography and directly electro sprayed into the mass spectrometer, where their mass-to-charge ratio and fragmentation spectra were recorded. MS data were analysed to identify and quantify the detected peptides and reassemble it to proteins. Resulting proteomic data were analysed using several open-source bioinformatics pipelines.

2.2.17 Statistical analysis

Statistical analyses of cytokines, inflammatory pathway proteins, receptors and cytoskeletal proteins from VECs were performed using GraphPad Prism 10.0 software (GraphPad Software, San Diego, CA, USA). All data were tested for normality using the Shapiro-Wilk normality test. Where appropriate the student's t-test for paired or unpaired data were used to calculate the significance of the differences of the means. Non-parametric data were analysed using Wilcoxon matched pairs test for paired data and Mann Whitney-U test for unpaired data when

comparing two groups. Differences between three or more groups were analysed using one-way ANOVA for parametric data or Kruskal-Wallis test for non-parametric data. Tukey's or Dunnett's *post hoc* multiple comparisons test was used for parametric data, and Dunn's for non-parametric data. Each experiment was repeated > 3 and data sets were presented with standard error mean (SEM) unless otherwise stated. Values of $P < 0.05$ were considered statistically significant.

Cytokine statistical analyses and data visualisation were additionally performed using R (v4.0.0) (367). Heatmaps were visualised with the pheatmap package (v1.0.12) (368).

Boxplots of the lactate and succinate levels were produced with the R package ggplot2 (v3.4.0). Comparisons between women with *Lactobacillus*-dominant and *Lactobacillus*-deplete vaginal microbiota were performed with t two-tailed Wilcoxon-Mann-Whitney tests, using the default R base function wilcox.test.

For AMICA proteomics, the logFC was computed by dividing the mean of conditions then converting to log base 2. Statistical significance was generated using the Mann-Whitney Test and adjusted with Bonferroni corrections (350).

Chapter 3: The Effect of Lactic Acid on Activation of Pro-inflammatory Transcription Factors

3.1 Introduction

Inflammation in the lower reproductive tract is associated with a breakdown of the vaginal epithelial barrier leading to increased risk of STI acquisition, and in pregnancy is associated with an increased risk of preterm birth (2, 369-371). Immune function within the lower female reproductive tract is highly influenced by the microbiota colonising the vaginal epithelium (177). A delicate balance is required between host tolerance of commensal microbes while still recognising and removing pathogenic microbes. VECs detect and respond to microbes via PRRs found in or on the epithelial cells, triggering an immune response (56-58). This initiates a complex cascade of signalling pathways leading to the production of immune mediators. Commensal bacteria tolerated by the host immune system, such as *L. crispatus,* do not activate PRRs *in vitro* whereas bacteria commonly associated with BV, such as *G. vaginalis* do (1, 74, 242, 372).

In vivo, the presence of BV-associated bacteria is associated with the production of pro-inflammatory cytokines, which are transcriptionally regulated by transcription factors such as NF-κB and AP-1 (1, 232, 233, 373). In contrast, low diversity vaginal bacterial communities enriched for *Lactobacillus* species are generally associated with reduced levels of inflammatory cytokines. Consistent with these findings, exposure of VECs *in vitro* to BV-associated bacteria causes an upregulation of pro-inflammatory cytokines and chemokines such as RANTES and IL-8. Surprisingly, it has been reported that exposure of VECs to some *Lactobacillus* strains *in vitro* induces NF-κB signalling although this does not lead to a significant increase in the production of pro-inflammatory cytokines such as IL-8, IL-6 or TNFα (243, 374). This may be accounted for by the metabolic activity of *Lactobacillus* species. Glycogen-rich VECs provide an energy source that can be preferentially utilised by *Lactobacillus* species, which produce LA as the primary metabolic end product (15, 269). LA, which acidifies the vagina, has both immunomodulatory and antimicrobial properties (250, 261, 375, 376). Several studies have shown that, when in its protonated state, LA directly modulates the inflammatory response via TLR agonism in VECs characterised by the reduction

of pro-inflammatory cytokines and chemokines and an increase in anti-inflammatory cytokine IL-1Ra (190, 272, 273, 276, 281, 283, 377).

Despite these findings, the mechanism by which LA mediates inflammatory pathway signalling in VECs remains poorly defined. It was hypothesised that LA inhibits the activity of pro-inflammatory transcription factors in VECs that are otherwise stimulated by bacteria via TLR recognition. To test this, the first aim was to validate the relationship between vaginal LA concentration and pro-inflammatory cytokine levels *in vivo* in a cohort of pregnant women, where vaginal microbiota composition is implicated in inflammatory pathway activation and preterm birth risk. Secondly, to establish a robust VEC culture model that facilitated characterisation of inflammatory response to bacterial and viral agonism, and mediation of these pathways by LA at a physiologically relevant pH. Finally, to determine if modulation of the vaginal microbiota *in vivo* towards a *Lactobacillus*-dominant state led to an increase in LA and thus, reduced levels of pro-inflammatory cytokines.

3.2 Results

3.2.1 Cervicovaginal microbial composition modulates metabolite composition in CVF of pregnant women affecting immune mediator production

To confirm that LA concentration in the cervicovaginal mucosal niche in pregnancy is associated with bacterial composition, data from the VMET1 study, published in Nature Communications, was interrogated in collaboration with Dr Katia Cappucini from the MacIntyre laboratory (247). Direct swab analysis by DESI-MS was used to longitudinally assess relative concentrations of CVF metabolites of interest throughout pregnancy in 160 women (n = 455 swabs) enrolled in a high-risk preterm birth clinic. Five timepoints during the pregnancy (8-16, 16-20, 20-26, 26-30, and 30-37 weeks of gestation) were assessed and key demographics of participants, including maternal age, time of delivery, BMI and gravida were

collected (Table 3.1). A total of 29/160 (18%) women had a spontaneous preterm birth (sPTB) and 131 (82%) experienced term deliveries. As described previously (247), the mean BMI of women with sPTB was significantly higher (mean kg/m^2 ±SD range; 26.2±4.4 vs 24.2±4.4; *P* = 0.0002) and they were more likely to have had a history of mid-trimester loss or preterm birth (67%; *P* = 0.00004).

Table 3.1 Demographics of patients in the VMET1 study.

Demographics	sPTB	Term	Total	p-value
Subject, n	29 (18%)	131 (82%)	160	
Sample swabs taken, n	79	376	455	
Mean maternal age, years (± SD range)	32.2	22.7	22.5	0.17
Mean sample gestation, weeks (± SD range)	21.8 ± 6.8	33.0 ± 5.0	32.9 ± 5.3	0.15
Mean BMI, kg/m^2 (± SD range)	26.2 ± 4.4	24.2 ± 4.4	24.5 ± 4.5	0.0002
Ethnicity, n/N (%)				
Caucasian	17/113 (15%)	96/113 (85%)	113/160 (71%)	0.14
Asian	1/11 (9%)	10/11 (91%)	11/160 (7%)	
Black	11/35 (31%)	24/35 (69%)	35/160 (22%)	
Other	0/0 (0%)	0/0 (0%)	0/160 (0%)	
Not recorded	0/1 (0%)	1/1 (100%)	1/160 (0%)	
Gravida				
0	2/50 (4%)	48/50 (96%)	50/160 (31%)	0.01
1	8/34 (24%)	26/34 (76%)	34/160 (21%)	
2	5/26 (19%)	21/26 (81%)	26/160 (17%)	
> 3	14/50 (28%)	36/50 (72%)	50/160 (31%)	
Previous mid trimester loss or PTB				
No	24/147 (16%)	123/147 (84%)	147/160 (92%)	0.00004
Yes	5/13 (38%)	8/13 (62%)	13/160 (8%)	

sPTB = spontaneous preterm birth; BMI = Body Mass Index; Data presented as a number (%) (247).

P values: Student's t-test for maternal age, sample gestation and BMI, and two-sided Pearson's chi-squared test for ethnicity, gravida and previous mid-trimester loss/PTB.

The vaginal microbiota of patient samples were assessed using metataxonomics and were subsequently grouped into five CSTs consistent with previous studies: CST I (*L. crispatus*); CST II (*L. gasseri*); CST III (*L. iners*); CST IV (diverse microbial composition of anaerobic bacteria); and CST V (*L. jensenii*); (199). Samples were also classified into *Lactobacillus*-dominant (Ldom) by grouping samples from CST I, II, III, and V or *Lactobacillus*-deplete (Ldep), which consisted of samples from CST IV (Table 3.2).

Table 3.2 Distribution of community state types (CST) in the VMET1 cohort samples (n = 160 subjects, 455 samples).

CSTs	n, swabs	%, swabs
Sample n	455	100%
CST I, *L. crispatus*	188	41%
CST II, *L. gasseri*	53	12%
CST III, *L. iners*	102	22%
CST IV, diverse	51	11%
CST V, *L. jensenii*	55	12%

Comparison of LA levels across the five vaginal CST groups indicated that the highest levels of lactate were identified in women with either a *L. crispatus* (CST I)- or a *L. iners* (CST III)-dominant microbiota composition followed by *L. jensenii* (CST V) and *L. gasseri* (CST II). However, significantly lower levels of LA were observed in women with a CST IV profile compared with the four *Lactobacillus*-dominant CSTs ($P < 0.001$, 0.05, 0.01 and 0.01, respectively; Figure 3.1B). At genera level, this was similarly reflected by *Lactobacillus*-deplete samples having a significantly lower concentration of lactate compared to *Lactobacillus*-dominant samples ($P = 0.00045$; Figure 3.1A).

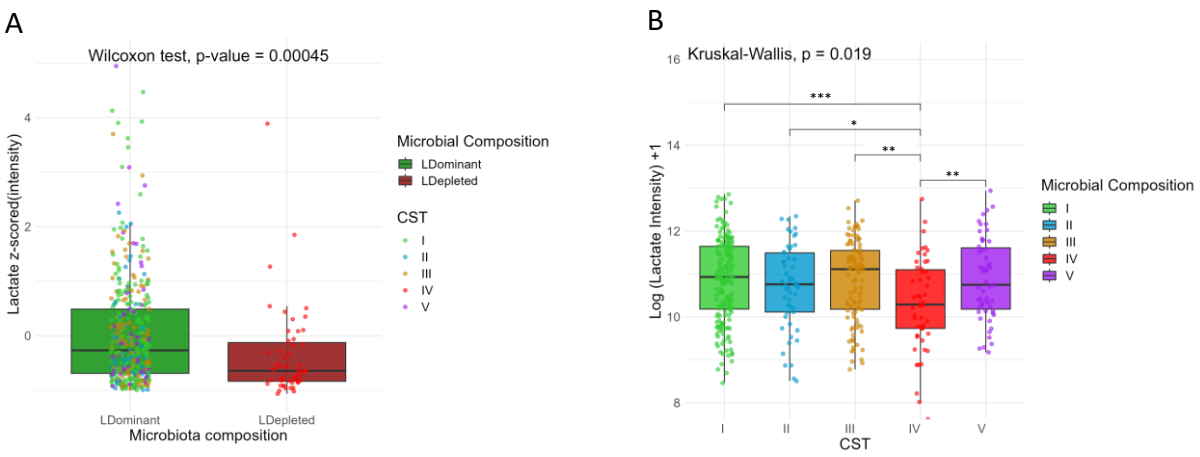

Figure 3.1 Distribution of community state types (CST) in the VMET1 cohort samples (n = 160 subjects).

(A) Levels of lactate (calculated z-score) in women with *Lactobacillus*-dominant (green, n = 404) were significantly higher than women with *Lactobacillus*-deplete (red, n = 51) vaginal microbiota ($P < 0.001$; Wilcoxon rank-sum test). **(B)** Levels of lactate (calculated z-score) in women with a CST IV-dominant vaginal microbiota (red, n = 51) were significantly lower than CST I (green, n = 188; *P < 0.001*), CST II (blue, n = 53; *P < 0.05*), CST III (mustard, n = 102; *P < 0.01*), and CST V (purple, n = 55; *P < 0.01*). Statistical significance was tested using one-way ANOVA Kruskal-Wallis test, with Dunn's *post hoc* test. *, ** and *** denote $P < 0.05$, 0.01 and 0.001, respectively.

3.2.2 Epithelial cell culture model

Using two different cell culture models, a 2D monolayer model and a 3D multilayered model, the morphology and viability of the immortalised VEC line VK2/E6E7 were compared. In the 2D model, VECs were grown in a monolayer as described by Fichorova *et al.* and treated with 2.5 mM, 5 mM, 10 mM, 15 mM and 25 mM LA for 30 minutes, 2 hours, 6 hours and 24 hours (48). This was compared with the Air-Liquid Interface (ALI) culture model developed by Rose *et al.*, optimised to enable treatment of VECs at low pH (51, 276). Once multilayered VEC cultures were established, they were treated apically with LA concentrations up to 30 mM at pH 3.9.

3.2.2.1 Morphology & viability of VK2s

To assess the impact of LA treatment on VEC morphology, representative images were acquired of confluent VK2 monolayers and multilayers. Indications of stress or apoptosis in the monolayers were characterised by a change in cellular morphology: the cells became less elongated, the nuclei became more translucent and granular, and there was an increase in cell debris. No difference in morphology was observed between multilayered cells exposed to pH 7.4 or pH 3.9 (Figure 3.2A).

Cell viability was assessed following apical exposure of VEC monolayers and multilayers with KSF medium at pH 7.4 or pH 3.9 with 30 mM L-LA at timepoints 30 minutes, 2 hours, 6 hours and 18 hours or 24 hours. Viable cell counts were determined by the Countess™ Automated Cell Counter (Invitrogen). VECs grown as a monolayer retained > 90% viability with concentrations of LA up to 15 mM. When treated with 25 mM LA the cells lost 50% of their viability (Figure 3.2B). Whereas VEC multilayers can be treated with 30 mM LA and show a < 25% loss in viability (Figure 3.2C).

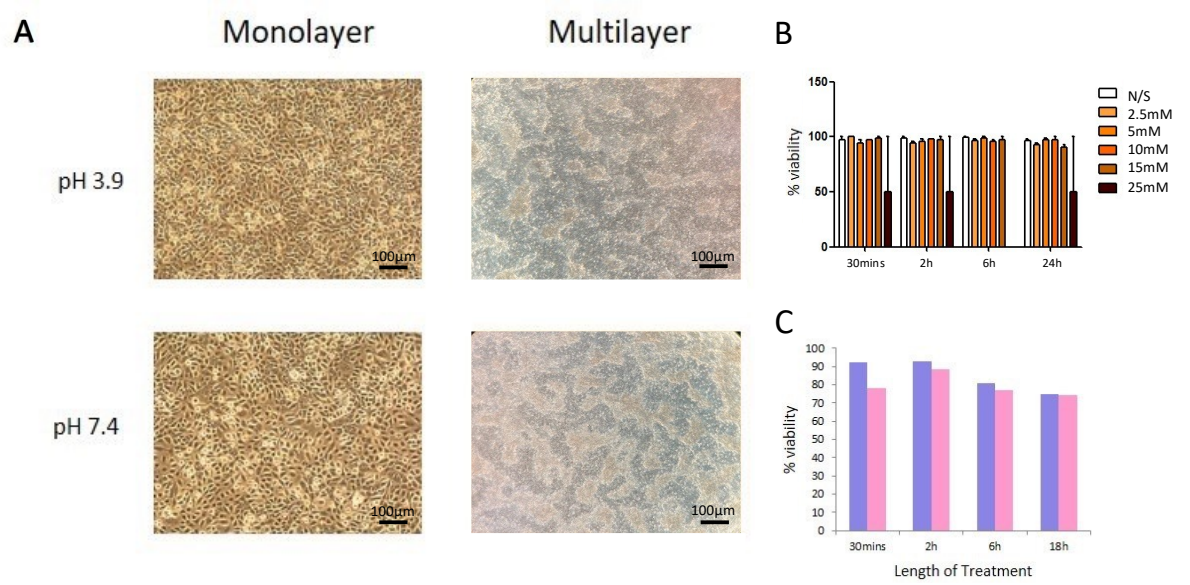

Figure 3.2 VECs cultivated in Transwells® remain viable when exposed to physiological concentrations of L-LA (30 mM).

(A) VECs grown as a monolayer in cell culture plates have a different morphology when grown in acidified media. The nuclei become more translucent and granular, and viability decreases significantly. This change in morphology is not seen in VECs grown as multilayer in Transwells®. 10 x images; scale bars represent 100 µm. **(B)** Viability of VECs grown as a monolayer decreased to 50% when treated with 25 mM L-LA for 30 mins, 2 hours, 6 hours and 24 hours (n = 3). **(C)** The viability of multilayered VECs grown in Transwells® following 30 mins, 2 hours, 6 hours and 18 hours treatment with 30 mM L-LA (pH 3.9, pink) and KSF medium (pH 7.4, purple) was determined by Countess™ Automated Cell Counter (Invitrogen) (n = 3).

3.2.3 Effect of acidity on inflammatory transcription factor activation in multilayered VECs

Acidosis has been demonstrated to impact transcription factor activation (378-380). To determine if exposure of multilayered VECs to an acidic environment augments the activation status of pro-inflammatory transcription factors, phosphorylation of the p65 NF-κB (p-p65) and cJun AP-1 (p-cJun) subunits were assessed by immunoblotting. A significant increase in p-p65 levels (3-4-fold above basal) was detected after 1 hour in VECs exposed to media acidified to pH 3.9 with either HCl or LA (Figure 3.3A and C). Levels of p-p65 returned to below basal levels after 2 hours treatment. In contrast, culture of VECs in acidified media led to significant and persistent reduction of p-cJun during all timepoints (Figure 3.3B and C). These results indicated that VECs experience an initial stage of acidic shock, leading to increased NF-κB, and

requiring approximately 2 hours to return to basal activation levels. A 2-hour step of acclimatisation to acidified media was thus incorporated into all experimental procedures unless otherwise stated.

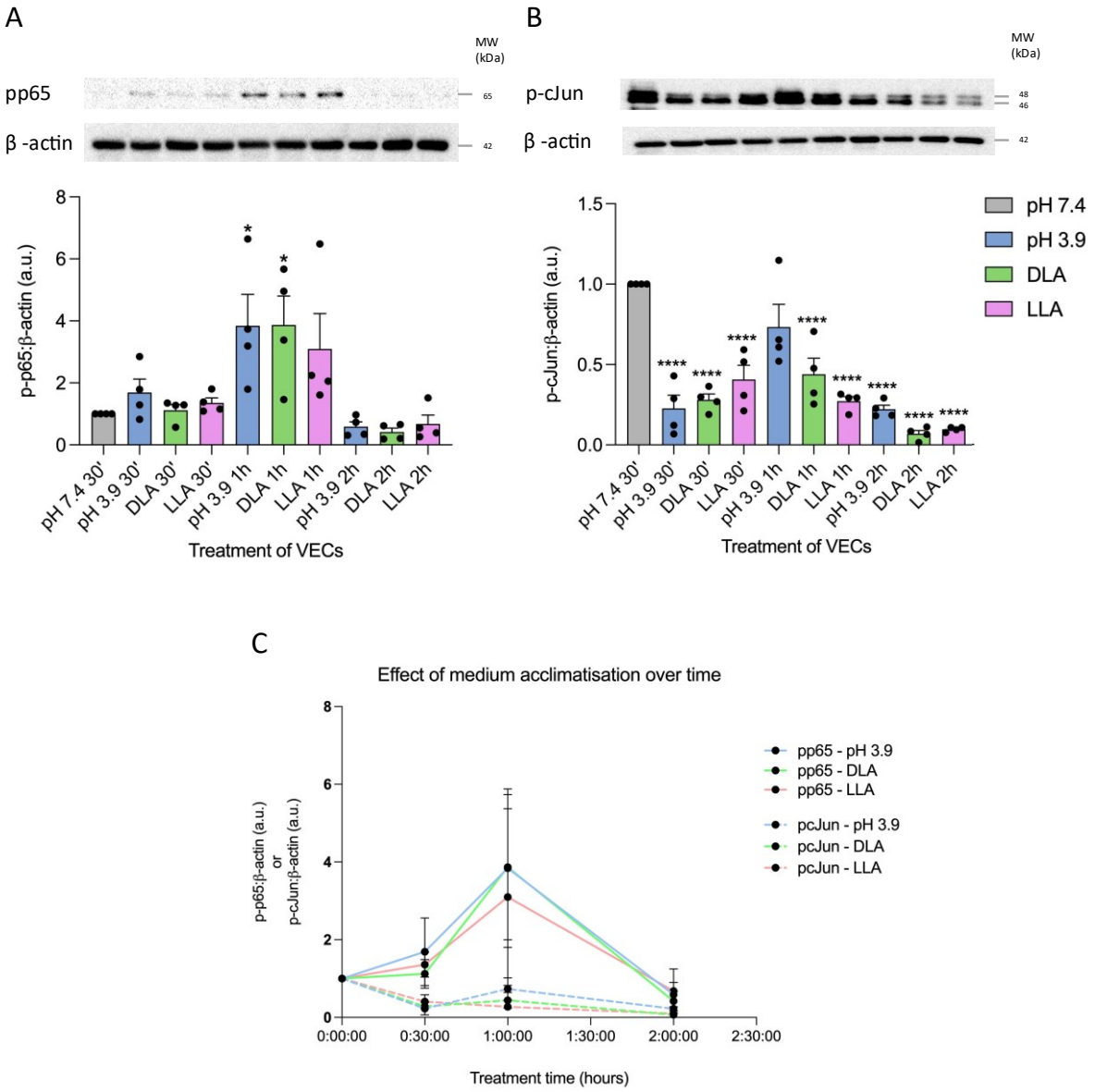

Figure 3.3 Exposure of VECs to acidic medium (pH 3.9 HCl, D-LA or L-LA) results in a temporary "acidic shock" which returns to baseline levels after 2 hours.

Multilayered VECs were cultured to confluence in Transwells® and exposed apically to media at pH 7.4 or pH 3.9 in the absence or presence of 30 mM LA for 30 mins, 1 hour and 2 hours as indicated. Whole cell protein extracts were probed for **(A)** p-p65 and **(B)** p-cJun and compared to the pH 7.4 control. β-actin was used as a loading control. **(C)** The acidic shock seen at 1 hour does not go above basal levels with AP-1. Graphs show SD from at least three independent experiments. Statistically significant differences between the different conditions and treatments were tested using one-way ANOVA and Dunnett's *post hoc* test. *and **** denote $P < 0.05$ and 0.0001, respectively.

3.2.4 Effect of L-LA on transcription of pro-inflammatory immune mediators

Transcription of key inflammatory mediators produced in response to bacterial (FSL-1) or viral (PIC) agonism was examined in multilayered VECs cultured in media acidified to pH 3.9 with HCl (pH 3.9) or L-LA (LLA). The expression of key anti- and pro-inflammatory factors IL-1Ra, IL-1β, RANTES, MIP-3α, IL-6, IL-8 and TNFα was measured using qRT-PCR (Figure 3.4).

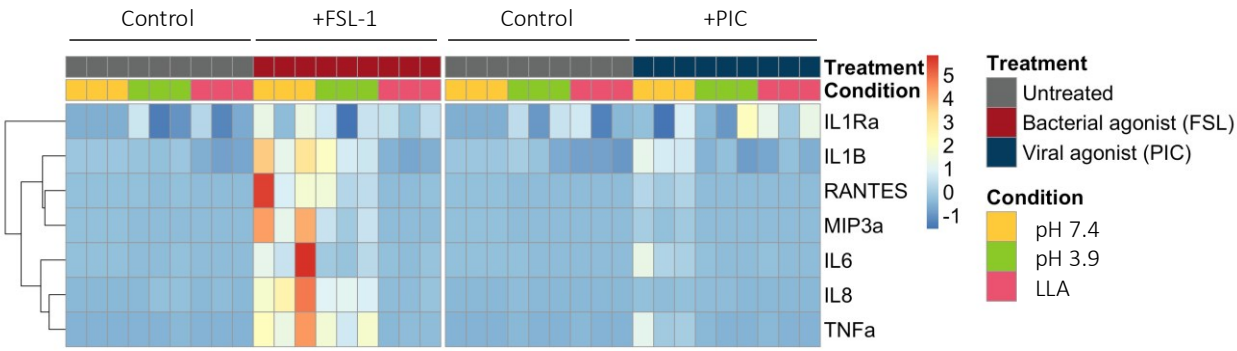

Figure 3.4 LA inhibits pro-inflammatory immune mediator production prior to gene transcription.

Heatmap of immune mediator gene expression *Il-1Rα*, *Il-1β*, *Rantes*, *Mip-3α*, *Il-6*, *Il-8* and *Tnfα* as measured by quantitative RT-PCR following 2-hour stimulation with bacterial agonist FSL-1 (1.0 μg ml^{-1}) or viral agonist PIC (20 μg ml^{-1}). Gene expression was standardised to housekeeping genes *Gapdh* and *L19* and expressed as a fold change over untreated cells using the $\Delta\Delta C_T$ method (353). The heatmap displays data as Z-scores, representing values ranging from +5 (red) to -1 (blue) standard deviations from the mean, based on three independent experiments (n = 3).

A detailed analysis of the changes in gene expression across time following exposure to a bacterial agonist showed a significant increase in IL-6, IL-8, IL-1β, RANTES, MIP-3α, and TNFα at 2 hours following treatment (Figure 3.5). This activation was suppressed by acidity, but most potently by L-LA. This was most notable with IL-1β and TNFα (Figures 3.5B and 3.5G).

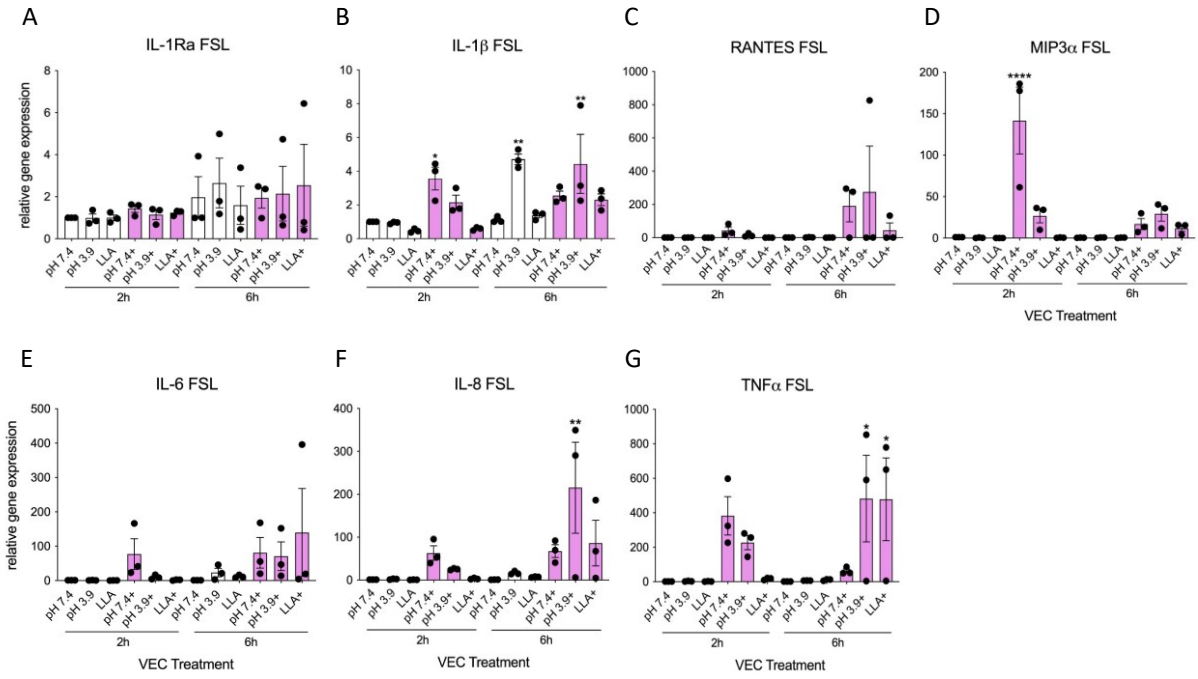

Figure 3.5 L-LA inhibits the production of pro-inflammatory immune mediators following stimulation with a bacterial agonist FSL-1 at a stage prior to gene transcription.

Multilayered VECs were acclimatised for 2 hours in the absence or presence of 30 mM L-LA (pH 3.9) or medium alone (pH 7.4) and then stimulated with TLR agonist FSL-1 (TLR2/6) 1.0 µg ml^{-1} for 2 hours and 6 hours. mRNA was isolated from the cells and expression of **(A)** *Il-1Ra,* **(B)** *Il-1ß,* **(C)** *Rantes,* **(D)** *MIP-3*α, **(E)** *Il-6,* **(F)** *IL-8*, and **(G)** *Tnf*α genes was measured by quantitative RT-PCR. Gene expression was standardised to the housekeeping genes *L19* and *Gapdh* and expressed as a fold change using the $\Delta\Delta C_T$ method (353). Graphs show SEM from at least three independent experiments (n = 3), compared to the 2-hour VEC treatment at pH 7.4. Statistical significance was tested using one-way ANOVA with Dunnett's *post hoc* test. *, ** and **** denote $P < 0.05$, 0.01 and 0.001, respectively.

Treatment of the multilayered VECs with a viral agonist also increased transcription of these immune mediators although to a lesser extent than bacterial agonism (Figure 3.6). L-LA and acidity similarly suppressed transcription of viral agonist-induced inflammatory mediators.

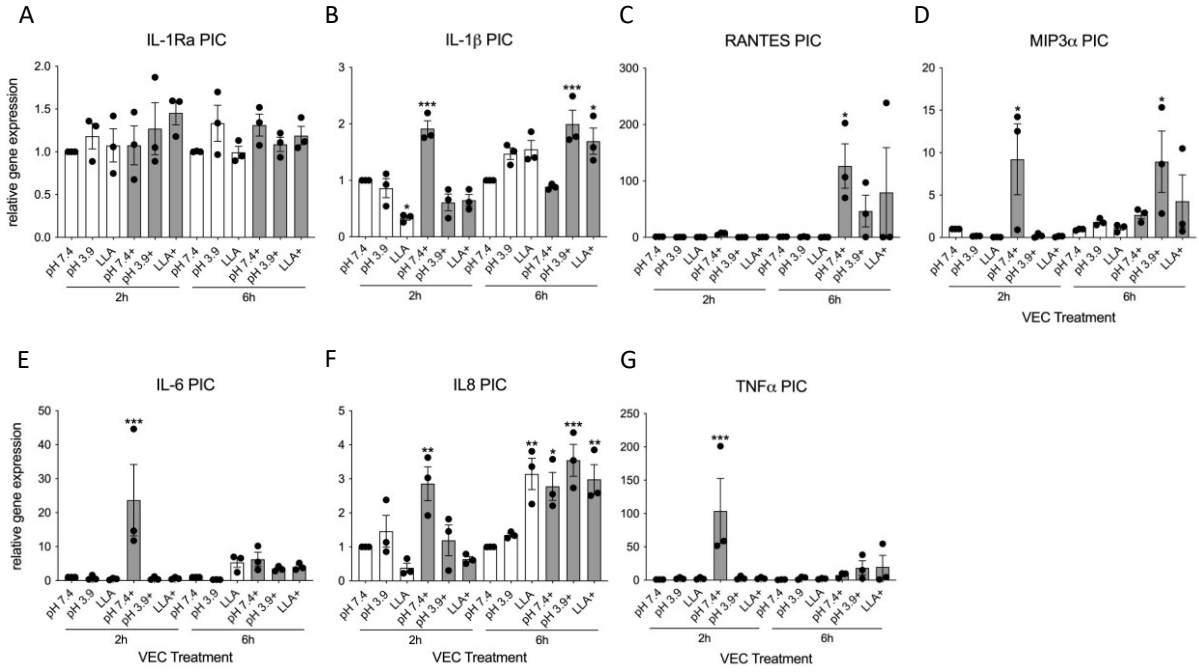

Figure 3.6 L-LA inhibits the production of pro-inflammatory immune mediators following stimulation with a viral agonist PIC at a stage prior to gene transcription.

Multilayered VECs were acclimatised for 2 hours in the absence or presence of 30 mM L-LA (pH 3.9) or medium alone (pH 7.4) and then stimulated with TLR agonist PIC (TLR3) 20 μg ml^{-1} for 2 hours and 6 hours. mRNA was isolated from the cells and expression of **(A)** *Il-1Ra,* **(B)** *Il-1ß,* **(C)** *Rantes,* **(D)** *MIP-3*α, **(E)** *Il-6,* **(F)** *IL-8,* and **(G)** *Tnf*α genes was measured by quantitative RT-PCR. Gene expression was standardised to the housekeeping genes *L19* and *Gapdh* and expressed as a fold change using the $\Delta\Delta C_T$ method (353). Graphs show SEM from at least three independent experiments (n = 3), compared to the 2-hour VEC treatment at pH 7.4. Statistical significance was tested using one-way ANOVA with Dunnett's *post hoc* test. *, ** and *** denote $P < 0.05$, 0.01 and 0.001, respectively.

The capacity for both HCl and L-LA to supress FSL-1-induced inflammation was reduced over a longer time period of 6 hours. However, at 6 hours both FSL and PIC (at pH 7.4 and pH 3.9-HCl) are having a strong, albeit variable effect, on RANTES expression which only reaches statistical significance at pH 7.4. Variations in acidity-mediated suppression were illustrated in the spider plot in Figure 3.7B, providing a clear visualisation of all the immune mediators within a single graphic. Fold change of relative gene expression was compared to 2-hour pH 7.4 samples.

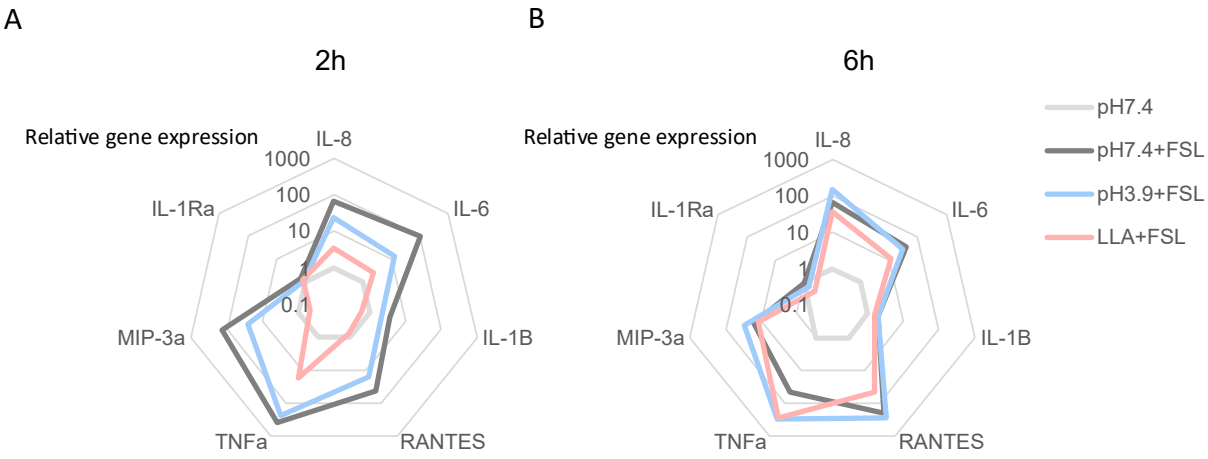

Figure 3.7 Suppressive effect of LA inhibiting pro-inflammatory immune mediator decreases over time in the multilayered VECs model.

Spider plot showing the suppressive effect of L-LA on expression of pro-inflammatory immune mediators Il-8, IL-6, IL-1β, RANTES, TNFα, MIP-3α, and IL-1Ra after a **(A)** 2-hour treatment with bacterial agonist FSL-1 (1.0μg ml^{-1}) and **(B)** 6-hour treatment with bacterial agonist FSL-1 (1.0μg ml^{-1}). By 6 hours treatment, the suppressive effect of LA is reduced, for example as shown by RANTES increasing almost 60-fold and TNFα increasing 30-fold. Data is compared to the 2-hour treatment at pH 7.4.

3.2.5 Assessment of LA isoforms on pro-inflammatory mediators

LA exists as two isoforms, D-LA and L-LA, both which are found in the lower reproductive tract (28, 261). To assess whether isomers of LA have a differential effect on inflammatory pathway activation, VECs were cultured in KSF media acidified with either D-LA or L-LA, stimulated with FSL-1, and mRNA levels of immune mediators examined. As presented in Figure 3.8, the capacity of both LA isomers to inhibit TLR2/6 mediated transcription of pro-inflammatory mediators IL-6, IL-8, IL-1β, TNFα, and RANTES was comparable.

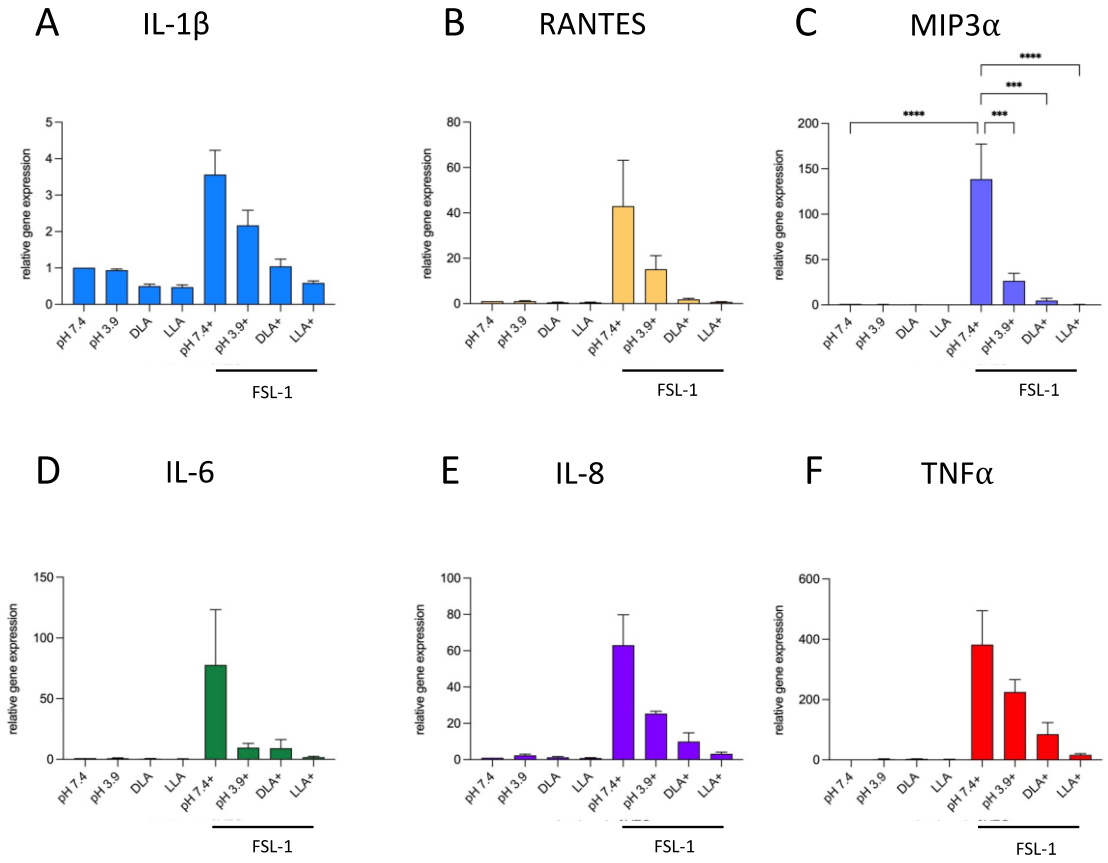

Figure 3.8 Pro-inflammatory immune mediators following stimulation with a bacterial agonist FSL-1 are inhibited by both isomers D-LA and L-LA.

Multilayered VECs were acclimatised for 2 hours in the absence or presence of 30 mM L-LA (pH 3.9) or medium alone (pH 7.4) and then stimulated with TLR agonist FSL-1 (1.0 µg ml^{-1}) (TLR2/6) for 2 hours. mRNA was isolated from the cells and expression of **(A)** *Il-1β,* **(B)** *Rantes,* **(C)** *MIP-3α,* **(D)** *Il-6*, **(E)** *IL-8,* and **(F)** *Tnfα* genes was measured by quantitative RT-PCR. Gene expression was standardised to the housekeeping genes *L19* and *Gapdh* expressed as a fold change using the $\Delta\Delta C_T$ method (353). Graphs show SEM from at least three independent experiments, compared to pH 7.4. Statistical significance was tested using one-way ANOVA with Dunnett's *post hoc* test. *** and **** denote $P < 0.001$ and 0.0001, respectively.

3.2.6 Effect of D-LA and L-LA on TLR2/6-mediated transcription factor activation

Next, FSL-1-induced phosphorylation of NF-κB (p-p65), and AP-1 (p-cJun) was assessed in VECs cultured in KSF (pH 7.4), KSF (pH 3.9-HCl) or KSF (pH 3.9-L-LA or -D-LA). FSL-1 treatment in VECs led to a strong increase (> 20-fold) in levels of p-p65 when cultured in KSF (pH 7.4) or KSF (pH 3.9-HCl) ($P < 0.01$ and $P < 0.05$, respectively; Figure 3.9A) before reducing to baseline

levels after 2 hours of treatment. However, culture of VECs in either isoform of LA significantly inhibits FSL-1-induced phosphorylation of NF-κB (D-LA, $P < 0.05$ and L-LA, $P < 0.05$). This effect was due to LA and not acidity.

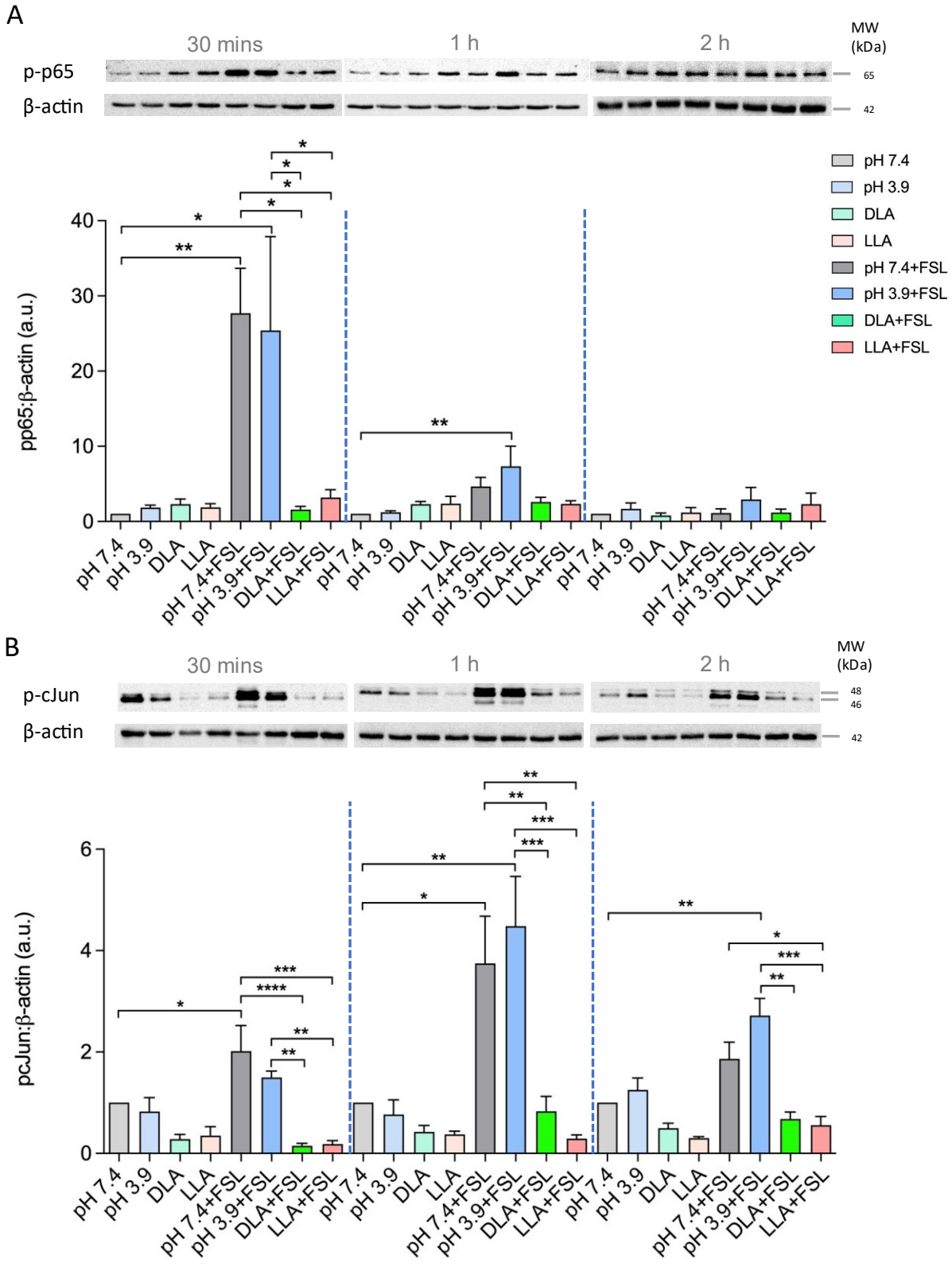

Figure 3.9 Bacterial agonist FSL-1 induces a temporal change in transcription factor activation which is suppressed by LA.

Multilayered VEC multilayers acclimatised in KSF (pH 7.4), KSF (pH 3.9-HCl) or KSF (pH 3.9-L-LA or -D-LA) for 2 hours were stimulated with bacterial agonist FSL-1 (1.0 µg ml^{-1}) for 30 mins, 1 hour and 2 hours as indicated. Whole cell protein extracts were probed for **(A)** p-p65 and

(B) p-cJun. β-actin was used as a loading control. Graphs show SD from at least four independent experiments (n = 4). Statistically significant differences between the different conditions and treatments were tested using one-way ANOVA and Tukey's post hoc test. *, **, *** and **** denote $P < 0.05$, 0.01, 0.001 and 0.0001, respectively. All data were standardised to untreated cells at pH 7.4 for each timepoint.

FSL-1-induced activation of p-cJun was detected at 30 minutes ($P = 0.0561$), peaking at 1-hour post-treatment ($P < 0.05$). Both basal ($P < 0.01$) and FSL-1 ($P < 0.001$) induced AP-1 phosphorylation were supressed by D- and L-LA and again not by acidity (Figure 3.9B). Collectively, these results indicated that both LA isomers equally attenuate VEC inflammatory pathway activation. In consideration of this and the high cost of D-LA, further examination of VEC inflammatory mediation was restricted to L-LA.

3.2.7 Effect of L-LA on TLR3-mediated transcription factor activation

The above experiments were repeated using the TLR3 agonist PIC to determine potential L-LA modulation of viral agonism of transcription factor activation in VECs. Neither NF-κB or AP-1 were significantly activated by the viral agonist PIC, however L-LA again supressed basal phosphorylation of both NF-κB ($P < 0.05$; Figure 3.10B) and AP-1 ($P < 0.0001$; Figure 3.10C) throughout the experimental time course. Following treatment with PIC, the acidity control pH 3.9 was also observed to significantly suppress both NF-κB ($P < 0.01$; Figure 3.10B; 2 hours) and AP-1 ($P < 0.01$; Figure 3.10C; 30 minutes).

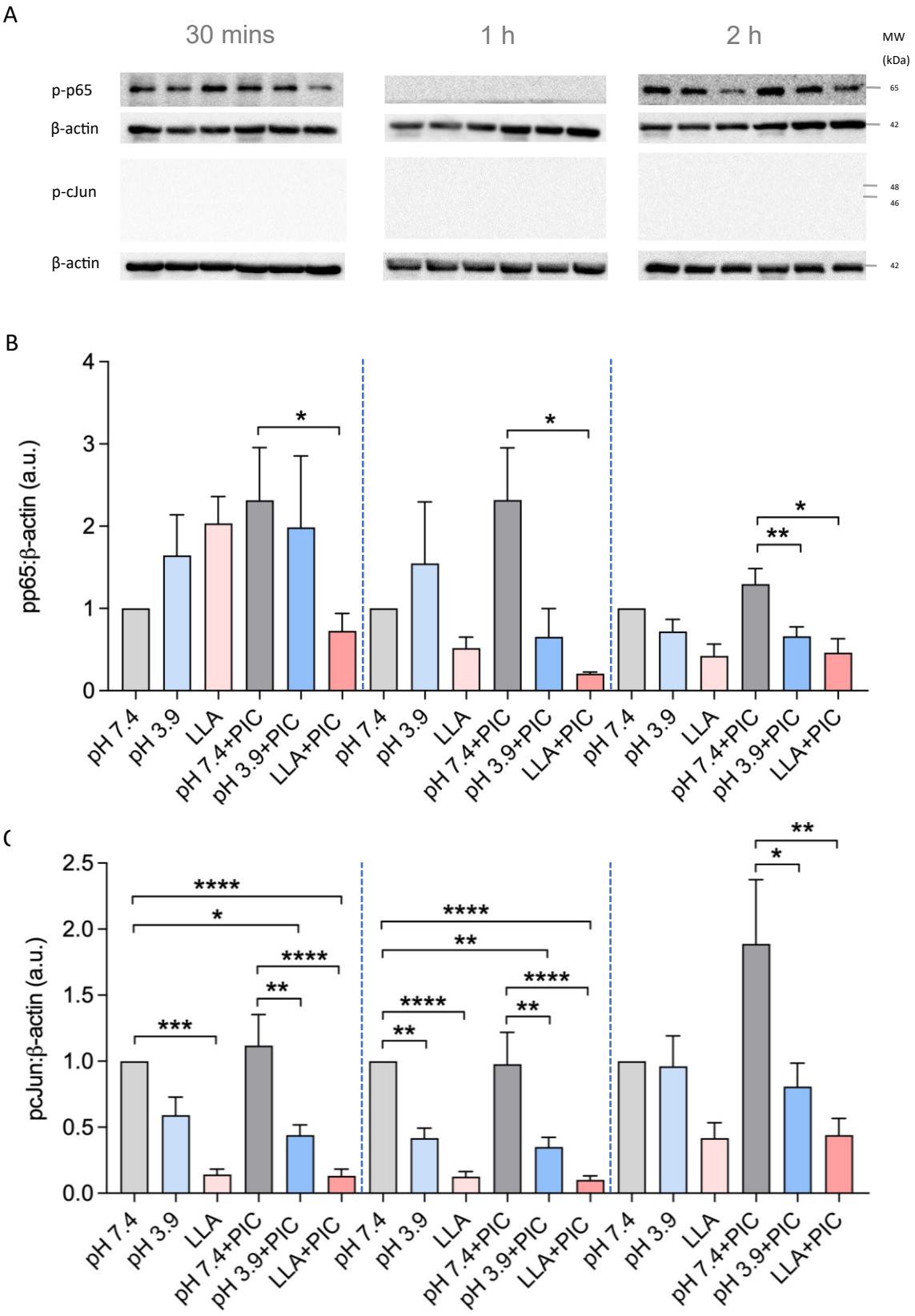

Figure 3.10 L-LA suppresses viral agonist-induced activation of transcription factors NF-κB and AP-1.

Multilayered VECs acclimatised for 2 hours in medium at pH 7.4 or acidified to pH 3.9 in the presence or absence of 30 mM L-LA were stimulated with viral agonist PIC (20 μg ml^{-1}) for 30 mins, 1 hour and 2 hours as indicated. **(A)** Immunoblotting of p-p65 and p-cJun expression levels in whole cell protein extracts using β-actin as a loading control. The protein expression profile was quantified using densitometry for (**B)** p-p65 and **(C)** p-cJun. Graphs show SD from at least three independent experiments (n = 3). Statistically significant differences between the different conditions and treatments were tested using one-way ANOVA and Tukey's post hoc test. *, **, *** and **** denote, $P < 0.05$, 0.01, 0.001 and 0.0001 respectively. All data were standardised to untreated cells at pH 7.4 for each timepoint.

Agonism of TLR3 was shown to drive phosphorylation and activation of IRF3 leading to upregulation of pro-inflammatory mediator transcription in several cell types (59, 381, 382). Thus, examination of p-IRF3 was also undertaken in treated VECs. As presented in Figure 3.11, PIC treatment caused a significant increase in p-IRF3 after 1 hour ($P < 0.05$), which was significantly suppressed by LA ($P < 0.01$). IRF3 was not significantly activated by the bacterial agonist FSL-1 (Figure 3.11B). A trend toward suppression of PIC-induced p-IRF3 was also observed for HCl-treatment but this did not reach statistical significance (Figure 3.11A). LA-induced suppression of p-IRF3 was maintained 2 hours following PIC treatment ($P < 0.001$), as was suppression by HCl ($P < 0.005$).

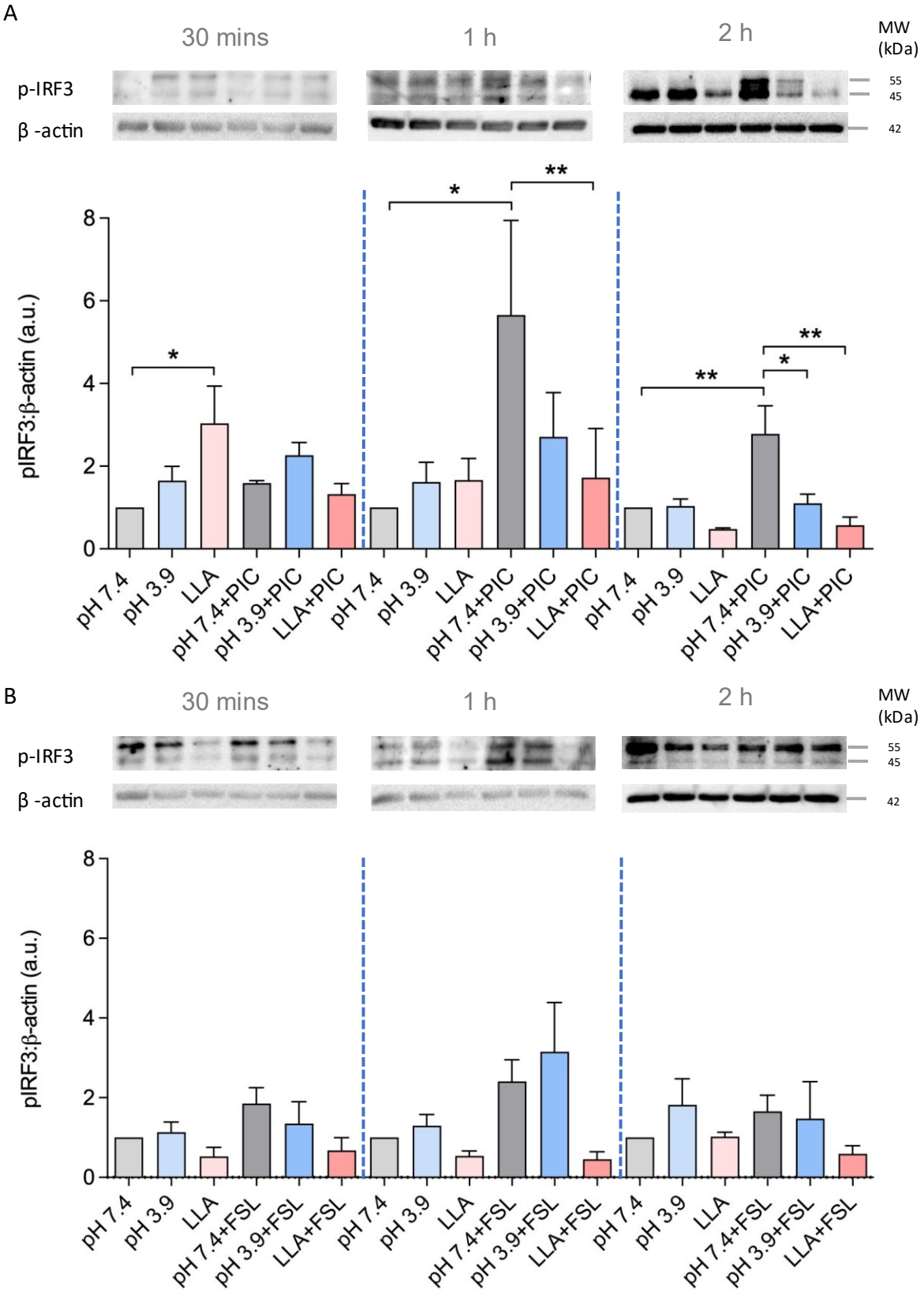

Figure 3.11 Viral agonism of VECs activates transcription factor IRF3 which is suppressed by L-LA.

Multilayered VECs acclimatised for 2 hours in medium at pH 7.4 or acidified to pH 3.9 in the presence or absence of 30 mM L-LA were stimulated with **(A)** viral agonist PIC (20 µg ml^{-1}) or **(B)** bacterial agonist FSL-1 (1.0 µg ml^{-1}), for 30 mins, 1 hour and 2 hours as indicated. Whole cell protein extracts were probed for p-IRF3 using β-actin as a loading control. Graphs show SD from at least three independent experiments (n = 3). Statistically significant differences between the different conditions and treatments were tested using one-way ANOVA and Tukey's post hoc test. * and ** denote $P < 0.05$ and 0.01, respectively. All data were standardised to untreated cells at pH 7.4 for each timepoint.

3.2.8 L-LA elicits an anti-inflammatory response in primary VECs

The anti-inflammatory action of LA was next investigated in a primary VEC model. This work was done in collaboration with Professor Gilda Tachedjian's group at the Burnet Institute, Melbourne who have expertise in culturing lower female reproductive tract primary cells. Primary VECs were cultured on Transwells® as described previously and confirmation of the transition of cells from monolayers (Figures 3.12A and B) to multilayers (Figures 3.12C and D) was performed using white light microscopy.

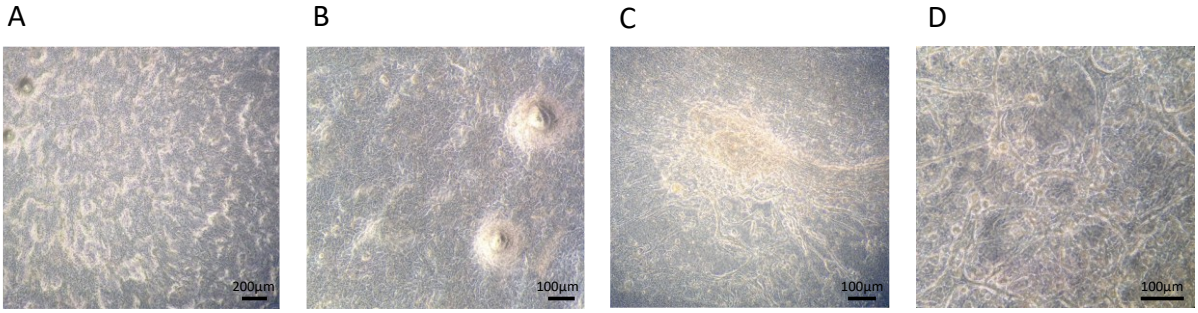

Figure 3.12 Microscopy showing formation of multilayers in primary vaginal epithelial cells.

Primary human vaginal-ectocervical cells (HVEC) were grown in KSF medium on Transwells® to form multilayers. When a confluent monolayer **(A)** 4 x image (scale bar represents 200 µm) and **(B)** 10 x image (scale bar represents 100 µm) was formed, the apical medium was removed to promote the formation of multilayers **(C)** 10 x image (scale bar represents 100 µm) **(D)** Fewer multilayers formed at the edge of the Transwells®; 20 x image (scale bar represents 100 µm).

Once multilayers had formed, VECs were treated with TLR agonists PIC (20 µg ml^{-1}) and FSL-1 (1.0 µg ml^{-1}) for 1 hour following the refined protocol developed for the VK2 cell line. Whole cell proteins were extracted, and Western blotting performed to assess the phosphorylation status of transcription factors (Figure 3.13). Consistent with results observed in the VK2 cell

line, the bacterial agonist FSL-1 significantly increased NF-κB and AP-1. Phosphorylation of both was suppressed by L-LA (Figure 3.13A and B). PIC treatment led to a trend increase in phosphorylation of NF-κB and AP-1, and this was again inhibited by L-LA.

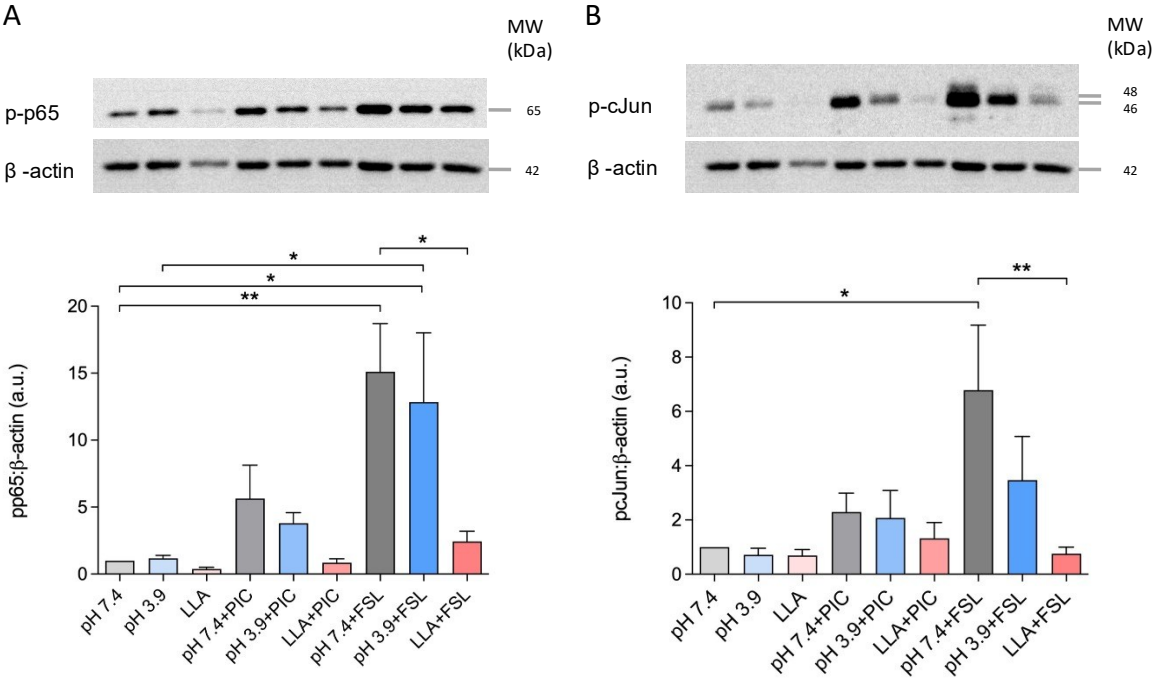

Figure 3.13 L-LA suppresses viral and bacterial agonist-induced activation of transcription factors NF-κB and AP-1 in primary cells.

Multilayered primary vaginal epithelial cells, acclimatised for 2 hours in medium at pH 7.4 or acidified to pH 3.9 in the presence or absence of 30 mM L-LA, were stimulated with **(A)** viral agonist PIC (20 µg ml^{-1}) or **(B)** bacterial agonist FSL-1 (1.0 µg ml^{-1}), for 1 hour as indicated. Whole cell protein extracts were probed for p-p65 and p-cJun. β-actin was used as a loading control. Graphs show SD from at least three independent experiments. Statistically significant differences between the different conditions and treatments were tested using one-way ANOVA and Tukey's *post hoc* test. * and ** denote $P < 0.05$ and $P < 0.01$, respectively. All data were standardised to untreated cells at pH 7.4.

3.2.9 *L. crispatus* colonisation in pregnant women and its effect on LA concentration and inflammation

Having demonstrated an anti-inflammatory effect for L-LA in both the VK2 cell line and primary VECs *in vitro*, the next step was to investigate whether modulation of the cervicovaginal microbiome towards a *Lactobacillus*-dominant state would lead to an increase in levels of lactate and subsequently, a decrease in immune mediators. This work was

performed in collaboration with PhD student Erna Bayar, from the MacIntyre and Bennett laboratory, who conducted a first in-pregnancy trial of the *L. crispatus* biotherapeutic, Lactin-V. The trial was referred to as the FLIP-1 study and involved vaginal administration of Lactin-V daily for 5 days from 14 weeks' gestation, followed by a weekly maintenance dose until 20 weeks' gestation (360). Vaginal swab samples were collected at seven time points (14 weeks (T0), 15 weeks (T1), 18 weeks (T2), 20 weeks (T3), 28 weeks (T4), 36 weeks (T5) and delivery (T6)). As with the VMET1 study data, samples were classified into *Lactobacillus*-dominant (Ldom, n = 333) by grouping samples from CST I, II, III and V or *Lactobacillus*-deplete (Ldep, n = 29), which consisted of samples from CST IV. Across all timepoints, significantly higher levels of LA were found in *Lactobacillus*-dominant samples compared to *Lactobacillus*-deplete samples (P = 0.0006; Figure 3.14A). At a CST level, the highest levels of lactate were found in women with either a *L. crispatus*- or a *L. iners*-dominant microbiota composition followed by *L. jensenii* and *L. gasseri*. However, as expected there were significantly lower levels of LA identified in women who were carrying CST IV (n = 29) compared with CST I samples (n = 333; P < 0.001; Figure 3.14B).

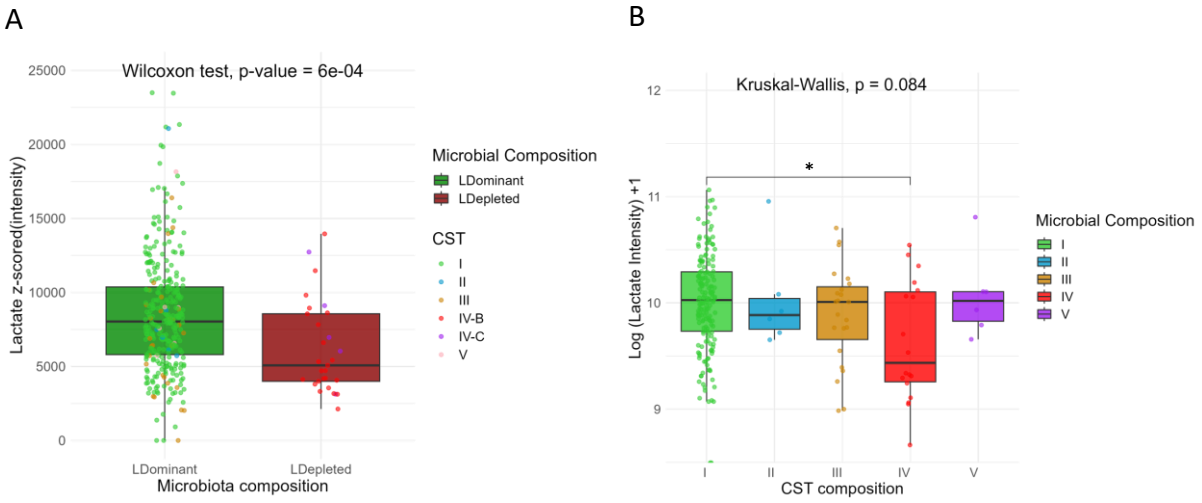

Figure 3.14 LA levels are higher when Lactobacillus species are dominant in cervicovaginal fluid.

(A) Boxplots comparing levels of lactate (calculated z-score) in *Lactobacillus*-dominant states (green, n = 333) with *Lactobacillus*-deplete (red, n = 29). Statistical significance was tested using Wilcoxon rank-sum test: *P*-value = 4.65e-06. **(B)** Boxplots showing levels of lactate (calculated z-score) in CST I (green, n = 292), CST II (blue, n = 6), CST III (mustard, n = 29), CST IV (red n = 29) and CST V (purple, n = 6). Statistical significance was tested using one-way ANOVA Kruskal-Wallis test, with Dunn's *post hoc* test. * denotes P < 0.05.

Comparison of LA levels following Lactin-V treatment between T0 and T4 indicated that concentrations were higher in women whose microbial composition had remained or transitioned to *Lactobacillus*-dominance (Figure 3.15). In comparison, LA levels between *Lactobacillus*-dominant and *Lactobacillus*-deplete samples at T0 were not significantly different, which may have been due to some CST IV bacteria producing lactate themselves. Only two of the 28 women did not transition from CST IV to a different CST with both maintaining lower levels of lactate and increased levels of IL-1β (Figure 3.15A) and one transitioned to CST III.

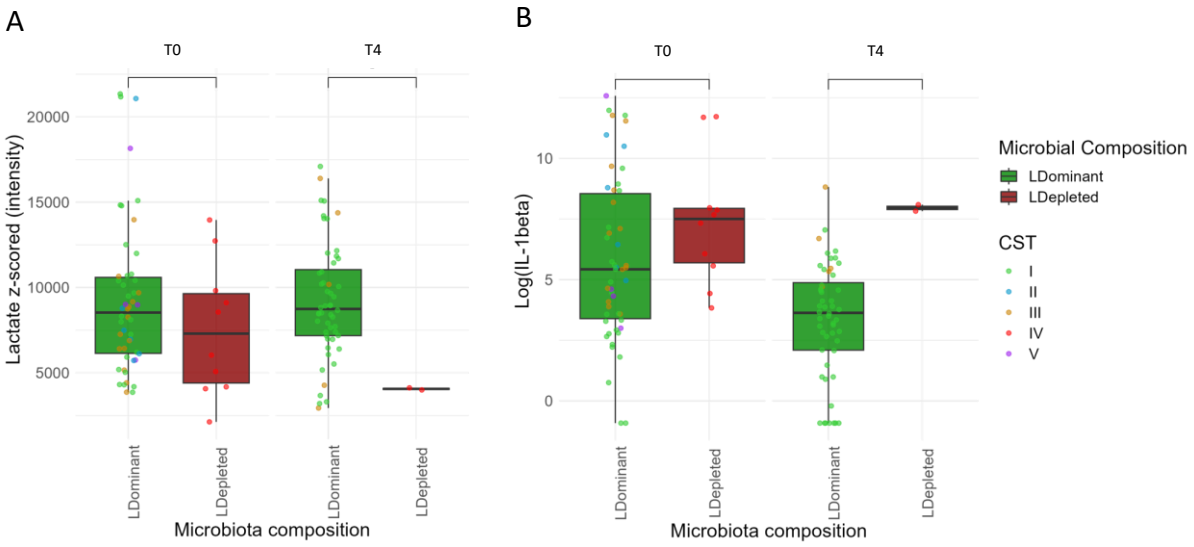

Figure 3.15 Following treatment with Lactin-V levels of lactate decrease in samples that are Lactobacillus-deplete.

Levels of **(A)** lactate and **(B)** IL-1β were measured using DESI-MS in paired samples following treatment with *L. crispatus* biotherapeutic Lactin-V from time point zero (T0 = 14 weeks) and time point 4 (T4 = 28 weeks; n = 28). Statistical significance was tested using a paired t-test. * denotes $P < 0.05$.

At T0 levels of IL-1β were lower in *Lactobacillus*-dominant samples but did not reach statistical significance. IL-1β levels decreased further in *Lactobacillus*-dominant samples following Lactin-V treatment when measured at T4. In contrast, levels of IL-1β in women with *Lactobacillus*-depletion remained high (Figure 3.15B). Based on our *in vitro* data, it was hypothesised that *L. crispatus* dominance associated with Lactin-V treatment would increase cervicovaginal concentrations of LA leading to a concurrent decrease in IL-1β. Consistent with this, LA levels, as measured by DESI-MS, in women who transitioned from a non-CST I

microbiome (n = 28) at baseline, to a CST I microbiome (n = 23) at T4, were consistently higher at this timepoint with the exception of sample F071 where lactate levels were reduced by 50% (Figure 3.16A). IL-1β levels were significantly decreased at T4 in these transitioning women and patient F071 did not show a marked increase in IL-1β despite lactate levels decreasing (Figure 3.16B). No patients showed a large increase in IL-1β levels following Lactin-V treatment.

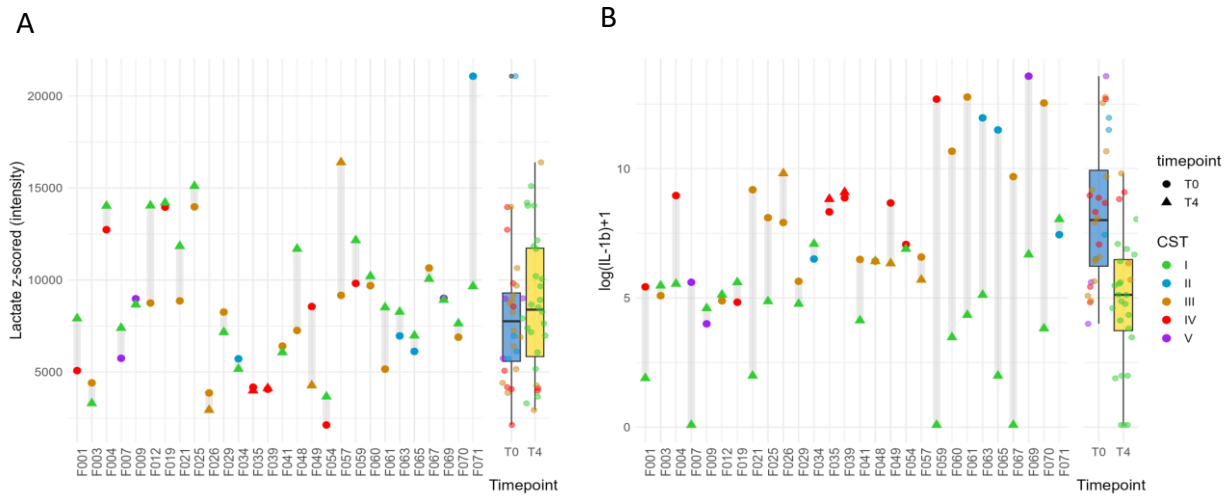

Figure 3.16 Lactate levels increase or remain the same in paired samples following Lactin-V treatment whereas IL-1β levels decrease.

Levels of **(A)** lactate and **(B)** IL-1β were measured using DESI-MS in paired samples (n = 28) following treatment with *L. crispatus* biotherapeutic Lactin-V. from time point zero (T0 = 14 weeks) to time point 4 (T4 = 28 weeks).

To examine if the relationship between LA and immune regulation could be partly attributed to a shift in microbiota composition, a sub-analysis was performed on patients that had transitioned from CST IV to CST I: F001, F004, F019, F054 and F059 (n = 5). In 4/5 cases, transition to CST I was associated with increased LA levels at T4 and a concurrent decrease of IL-1β (Figures 3.17A and B). A stacked bar chart displaying relative abundance of vaginal bacteria before and after treatment is presented in Figure 3.17C.

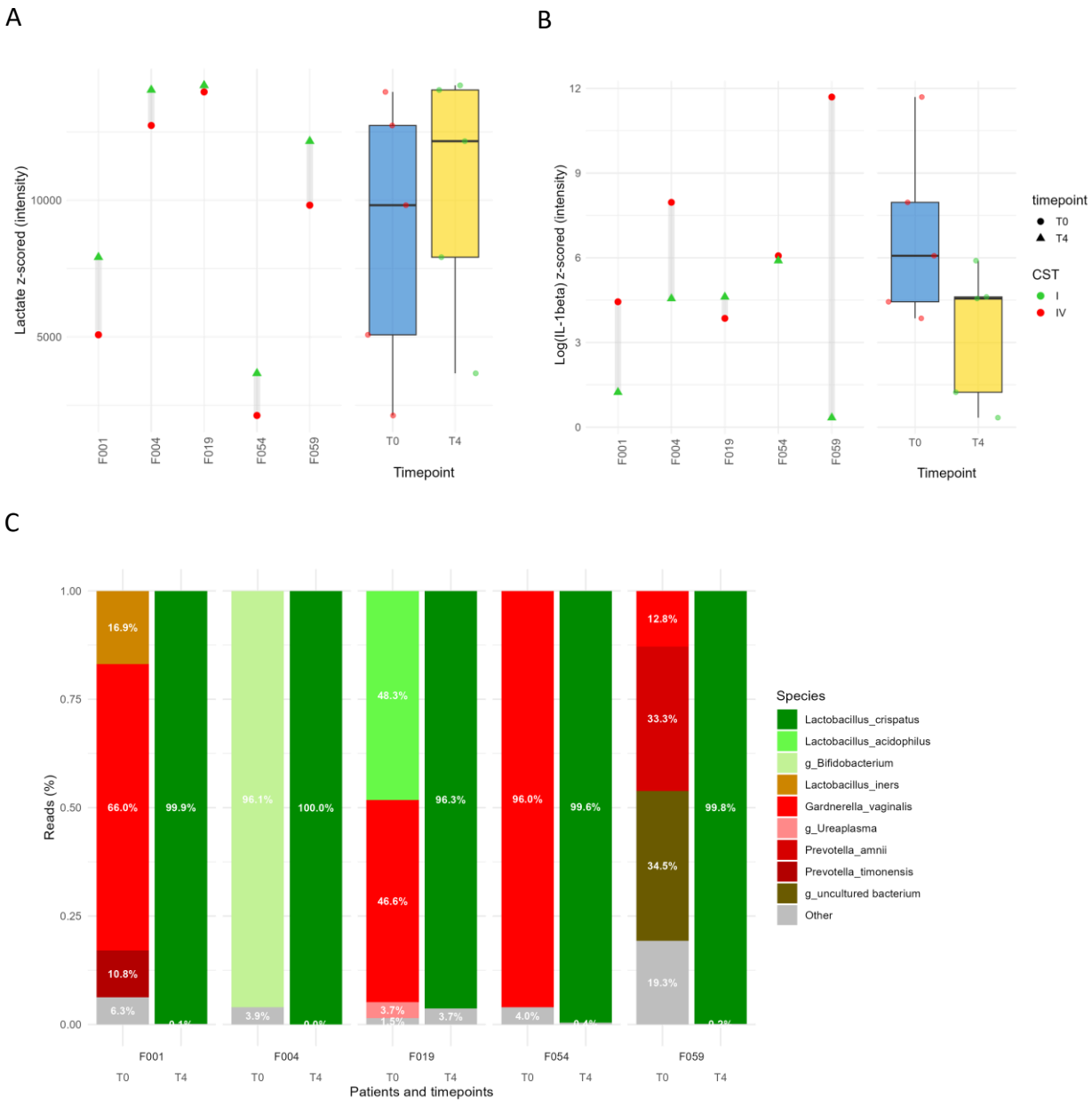

Figure 3.17 Lactate levels increase or remain the same in paired samples transitioning from CST IV to CST I following treatment with Lactin-V whereas IL-1β levels decrease or remain the same.

Using DESI-MS, levels of **(A)** lactate and **(B)** IL-1β were measured in paired samples that had transitioned from CST IV to CST I following treatment with *L. crispatus* biotherapeutic Lactin-V (n = 5). **(C)** Stacked bar chart of relative abundance of vaginal microbial composition by species for each individual sample at timepoint T0 and T4.

Patients F001 and F054 started with low levels of lactate and were predominantly colonised by *G. vaginalis* (66.0% and 96.1% respectively). F001 was also colonised by *L. iners* (16.92%) and *P. timonensis* (10.79%). Levels of lactate increased in both samples following Lactin-V

treatment but IL-1β levels only decreased in sample F001, while for F054, IL-1β levels remained the same. Patients F004, F019 and F059 all started treatment with relatively high levels of LA. Patient F004 had a microbiota dominated by lactate-producing bacterium *Bifidobacterium* (96.1%) and patient F019 had *L. acidophilus* present (48.3%) as well as *G. vaginalis* (46.6%). The dominant bacterial species in patient F059 was undetermined, but *P. amnii* (33.3%) and *G. vaginalis* (12.8%) were both present, indicative of a BV-associated microbial composition. At T0 levels of IL-1β were high in both F059 and F004, whereas patient F019 started with low levels of IL-1β. All five pregnancies went to term (Supplementary 9.2; Table 9.2).

Within the study cohort, there were five patients who did not transition to CST I following Lactin-V treatment: F026, F035, F039, F049, and F057 (Figure 3.18). Two patients began and finished treatment with CST III. Two patients maintained a CST IV microbiota throughout the treatment as well as low levels of LA. IL-1β levels in these patients slightly increased. The fifth patient transitioned from CST IV to CST III during the treatment and both LA and IL-1β levels decreased (Figures 3.18A and B).

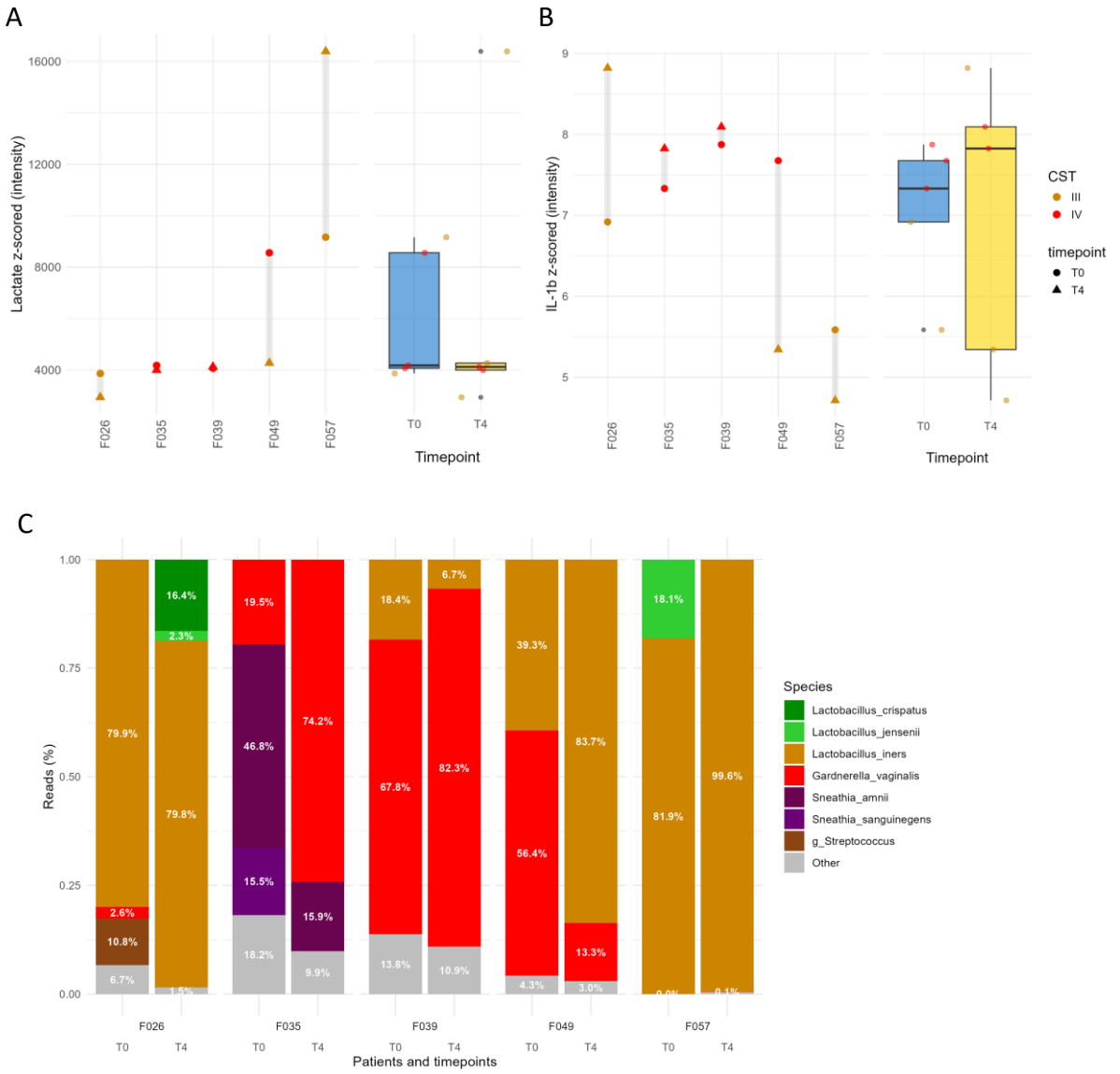

Figure 3.18 Failure to transition to CST I leads to lower levels of lactate and high levels of IL-1β levels.

Using DESI-MS, levels of **(A)** lactate and **(B)** IL-1β were measured in paired samples that did not transition to CST I following treatment with *L. crispatus* biotherapeutic Lactin-V (n = 5). **(C)** Stacked bar chart of relative abundance of vaginal microbial composition by species for each individual sample at timepoint T0 and T4.

Despite appearing to be "non-responders", these patients still experienced changes in the relative abundance of bacterial species between T0 and T4 timepoints. Patient F026 was initially predominantly colonised by *L. iners* (79.9%) which continued to dominate the niche at T4 (79.8%). However, *Streptococcus* (10.8%) and *G. vaginalis* (2.6%) at T0 were replaced with *L. crispatus* (16.4%) and *L. jensenii* (2.3%). Despite this, LA levels decreased by T4 with a concurrent increase in IL-1β levels. Patient F035 started treatment predominantly colonised

by *Sneathia amnii* (46.8%), *G. vaginalis* (19.5%) and *Sneathia sanguinegens* (15.5%). Following Lactin-V treatment, *G. vaginalis* (74.2%) dominated the niche with *S. amnii* (15.9%). At T0, patient F039 had a microbiota colonised by *G. vaginalis* (67.8%) and *L. iners* (18.4%). By T4 *G. vaginalis* dominated the niche (82.3%) although a low relative abundance of *L. iners* was still detected (6.75%). In both these patients, LA levels remained comparatively low and IL-1β levels comparatively high. Patient F049 was initially dominated by *G. vaginalis* (56.40%) and *L. iners* (39.4%) at T0, before transitioning to *L. iners* (83.7%) dominance at T4, with relatively low *G. vaginalis* (13.3%; Figure 3.18C). *L. iners* was the dominant bacterium in patient F057 and continued to dominate the niche after Lactin-V treatment. Unlike patient F026 which was also colonised by *L. iners*, a substantial increase in LA levels was detected (> 50%), which was associated with a decrease in IL-1β levels. The pregnancy outcomes of these "non-responder" patients were generally poor, with only 2/5 reaching term and 3/5 experiencing preterm deliveries (2 induced, 1 spontaneous; Supplementary 9.3; Table 9.3).

3.3 Discussion

The relationship between LA in the vaginal niche and microbiota composition is well established, particularly in non-pregnant women; *Lactobacillus* dominance of the niche associates with high LA concentrations, low inflammation and high epithelial barrier integrity (179, 208, 235, 243, 272, 383). Less data exists for women in pregnancy, where loss of *Lactobacillus* and a shift toward a high diversity bacterial composition is associated with increased levels of pro-inflammatory cytokines and chemokines and heightened risk of poor pregnancy outcomes such as preterm birth. Expression of chemokines and cytokines in gestational tissues such as the cervix and foetal membranes is regulated by pro-inflammatory transcription factors such as NF-κB and AP-1 (42, 143, 384). These transcription factors also regulate expression of pro-tissue remodelling enzymes and pro-contractile proteins implicated in cervical ripening and foetal membrane rupture. It is feasible that one of the mechanisms by which *Lactobacillus*-dominant microbiota in pregnancy protect against preterm birth is via production of LA, which may inhibit inflammatory pathways. Consistent with these findings, DESI-MS metabolic profiling of vaginal swabs collected from a pregnancy

cohort revealed an association between vaginal LA concentrations and bacterial composition. Women with *Lactobacillus*-depleted, high diversity microbiota had significantly lower concentrations of LA compared to those with *Lactobacillus*-dominant microbiota. Previous studies have shown that women with *Lactobacillus*-depleted, high diversity vaginal microbiota have significantly higher levels of pro-inflammatory cytokines and chemokines in CVF (207, 208, 385, 386).

Investigation into how LA may modulate inflammation in the vaginal niche has predominately relied on the use of monolayer cell culture models. More recently 3D multilayer models have been developed using immortalised vaginal (VK2), ectocervical (Ect1) and endocervical (End1) epithelial cell lines for studying reproductive health and VEC function (48). These models are more representative of the vaginal epithelia, both morphologically and functionally, but are more time consuming and expensive (6). In this study, VK2/E6E7 vaginal epithelial cell line monolayer cultures were initially used to examine the potential immune-modulatory effects of LA. However, viability of the cells dropped significantly when the LA concentration was 15 mM or above. It has been estimated that LA in the vaginal mucosa can reach a concentration of 110 mM with a pH range of 2.8 to 4.2 thus, to enable assessment of LA at functionally relevant concentrations, experiments were transitioned to a 3D multilayer model (261). Further, in this model, VECs could be cultured with viability remaining high for at least 18h. This dual chamber model enables cells to process and metabolise more readily. LA can diffuse through the cellular layer and membrane into the neutral basal medium which can be regularly refreshed, mimicking the *in vivo* vaginal epithelium (276).

In several cell culture systems, exposure to low pH was shown to activate NF-κB inflammatory pathways (378-380, 387, 388). Despite this, previous studies investigating LA inhibition of pro-inflammatory mediators in VECs have not investigated acidic shock as a potential confounder of results. The results in this study indicate that VECs indeed experience a transient “acidic shock” characterised by increased NF-κB phosphorylation that returns to basal levels after 2 hours of acclimatisation to acidic media. It is likely that this initial period of transcriptional activity would lead to an upregulation of several genes and proteins, leading to spurious

interpretation of results. To avoid this, a 2-hour period of acclimatisation was incorporated into all the experiments undertaken in this thesis unless otherwise stated.

Earlier work by Delgado-Diaz *et al*. reported that in ectocervical epithelial cells, there is a decrease in pro-inflammatory immune mediators such as IL-6, IL-8, IL-1β, RANTES and TNFα when cultured in L-LA at pH 3.9. However, this study relied on a monolayer cell model and cells were only exposed to L-LA for 1 hour before being cultured for a further 4 hours at pH 7.4 (276, 308). This study design poorly recapitulates exposure to LA *in vivo*. More recently, similar results have been reported by Schwecht *et al.* in a multilayer cell culture system where VECs were exposed to bacterial metabolites for 24 hours (296). A limitation of both studies is that assessment of LA on inflammatory pathways in VECs was restricted to measurement of cytokines with characterisation of upstream transcriptional regulation by LA yet to be elucidated.

Data presented in this chapter shows that agonism of viral- (TLR3) and bacterial- (TLR2/6) mediated inflammatory pathways in VECs involves rapid, transient activation of the inflammatory transcription factors, NF-κB, AP-1 and IRF3. Phosphorylation of either basal- or agonist-induced activation of both NF-κB and AP-1 were equally inhibited by D-LA and L-LA isomers. It has been previously reported that LA-isomers may have differed capacity to modulate microbiota-host interactions in the lower reproductive tract. For example, D-LA produced by *Lactobacillus* species is associated with increased vaginal mucosal viscosity, which enhances viral particle trapping (286). Further, the ratio of L-LA to D-LA has also been implicated in the regulation of vaginal extracellular matrix metalloproteinase inducer (EMMPRIN), a key inducer of MMP8 (271). The results in this study indicate that the anti-inflammatory action of LA is isomer independent. This may provide an explanation for why some high diversity vaginal bacterial communities avoid activating inflammation in the vaginal niche. If sufficient L-LA is produced by VECs and LA-producing bacteria, including non-*Lactobacillus* species, it is feasible that sufficient levels of L-LA could be reached inhibiting TLR-mediated inflammatory activation in VECs.

The findings in this chapter also confirm and extend earlier observations of LA-specific inhibition of certain cytokines (276, 341, 343). For example, inhibition of FSL-1-induced activation of both IL-1β and TNFα was only observed in VECs treated with LA, and not in VECs treated with HCl. Similar observations have been reported in monocytes where LA was shown to selectively inhibit the degradation of IκB proteins bound to cytosolic NF-κB complexes, thereby preventing nuclear translocation of NF-κB and subsequent activation of TNFα, IL23 and other pro-inflammatory cytokines and chemokines (343). Consistent with these findings, we observed that LA inhibited FSL-1-induced activation of NF-κB after 30 minutes of treatment but HCl did not. These results indicate that LA-mediation of inflammatory pathways in VECs is carefully regulated, potentially by specific receptors or channels, and not simply a result of acidification of the surrounding environment. Such a mechanism has been demonstrated in the liver and pancreas of mice where LA-mediated inhibition of IL-1β was shown to be regulated via the receptor, HCAR1 (342).

It has been well described that immortalised cell lines, such as the VK2 cells used in these studies, can express unique transcription patterns not observed in the primary cell type *in vivo* (48, 389). This can cause immortalised cells to have non-relevant characteristics or functions. Therefore, to validate the finding that LA mediates pro-inflammatory transcription factor activation in primary VECs, a collaboration was established with Professor Gilda Tachedjian in the Burnett Institute (Melbourne, Australia). Using an identical protocol as developed here in Imperial College for VK2 cells, primary VECs were stimulated with viral and bacterial agonists in acidic (HCl and LA) and neutral pH conditions. As observed in VK2 cells, LA suppressed NF-κB and AP-1 activation of primary VECs stimulated with bacterial and viral TLR agonists. This result provided evidence that the multilayer VK2 cell model recapitulates LA-mediated inhibition of inflammation as observed in primary cells and thus further characterisation and experimentation was performed using this cell model. In both cell lines and primary cells, LA was less effective in inhibiting inflammation in longer term (6 hours) exposure to TLR ligands. It is estimated that *in vivo*, the top layer of cells in the vaginal epithelium is sloughed off every 4 hours. Extrapolation of our *in vitro* findings to the *in vivo* setting suggests that the underlying layer of cells being freshly exposed to LA would result in a continuation of suppression of inflammation within the vaginal niche (7).

AP-1 exhibits highly specific differential signalling, being suppressed by both L-LA and D-LA isomers but not by acidity. In several systems, NF-κB activation is considered a "fast response" mechanism, rapidly inducing the production of pro-inflammatory cytokines such as IL-1. These cytokines can subsequently feed back into the AP-1 signalling pathway, or AP-1 may be independently activated by the TLR signalling pathways, though this is a slower response. Many genes require the coactivation of both NF-κB and AP-1, which work synergistically to enhance transcription (390-392). Fujioka *et al.* also demonstrated that NF-κB can regulate AP-1 activity through Elk-1 expression levels (393). This presents a promising direction for future research, as Elk-1, like AP-1, is activated by the MAPKs.

The study by Roselletti provides corroborative evidence, showing that epithelial cells from BV-positive women (characterised by a low LA environment) are positively correlated with activation of both AP-1 and NF-κB pathways. Their work examined apoptosis in epithelial cells from patients, using c-fos and IKK as markers (394). A subsequent theory to explore is whether LA, *in vivo*, can downregulate inflammatory pathways known to negatively impact female reproductive health outcomes and how this is influenced by changes in microbial composition. Using data collected in the MacIntyre and Bennett laboratory, the impact of treating pregnant women with the biotherapeutic Lactin-V over a 5-week period was assessed. Lactate levels were measured using DESI-MS metabolic profiling of vaginal swabs, while inflammation was evaluated by detecting the pro-inflammatory marker IL-1β.

Data from the FLIP-1 study confirmed that a *Lactobacillus*-dominant vaginal microbiota is associated with high lactate levels and low IL-1β levels in contrast to a *Lactobacillus*-deplete state. Amongst the 28 samples with a non-CST I microbiota composition at baseline, 82.1% transitioned to CST I following Lactin-V treatment. Initially, most patients (78.6%) had lactate levels around 50% lower than the highest observed and high IL-1β levels in 89.3%. After treatment, lactate levels increased in 75% of cases, while IL-1β decreased or remained unchanged. Notably, when lactate increases were minimal despite a shift to CST I, IL-1β levels did not decrease, suggesting that lactate exerts anti-inflammatory effects *in vivo*. This aligns

with our *in vitro* findings that lactate directly modulates inflammatory transcription factors, linking microbial composition shifts to increased lactate levels and reduced inflammation.

Five out of the eight women with CST IV microbiota at baseline transitioned to CST I, with four showing increased lactate and reduced IL-1β. However, not all CST IV samples had low lactate levels initially. For instance, samples F004 and F019 had relatively high LA levels at baseline due to the dominant presence of LA-producing CST IV bacteria, such as *Bifidobacterium* and *L. acidophilus,* which are typically gut-associated bacteria but can produce LA (395, 396). *L. acidophilus* is rarely found in the vaginal niche and as it is not classified in CST I, II, III or V by the VALENCIA algorithm used, it has been placed in CST IV but it is still a *Lactobacillus* species (201). Another sample, F059, was dominated by an uncultured bacterium which potentially could have been a LA-producing bacterium, alongside *P. amnii*, which does not produce LA (397). These findings highlight a limitation in grouping all CST IV bacteria together, as some compositions will be LA producers. A larger sample size would allow further exploration of bacterial compositions susceptible to transitioning to CST I after Lactin-V treatment.

Of the five women who did not transition to CST I, two remained in CST III, two stayed in CST IV and one transitioned from CST IV to CST III. *G. vaginalis* dominant in two of these women, while *L. iners* dominated in three. *L. iners*, often considered a transitional species, has an unclear role in adverse health outcomes or restoration of healthy cervicovaginal bacterial species (216, 229, 398). *In vitro* it does have an inhibitory effect against *G. vaginalis* (399). Notably, patient F049 shifted from *G. vaginalis*-dominance (56.4%) to *L. iners*-dominance (83.7%) post-treatment, with IL-1β levels decreasing despite lower lactate levels. *L. iners* is also not necessarily associated with inflammation. Lower levels of IL-1β were observed in 2/3 patients who transitioned to CST III. However, in cases where CST IV persisted, LA levels remained low and IL-1β levels stayed high. While this study was underpowered, the findings suggest trends that warrant further investigation.

Importantly, all five pregnancies that transitioned from CST IV to CST I reached term while only 40% of “non-responder” women did, with the remainder delivering preterm (two induced and one spontaneous; Supplementary 9.3; Table 9.3). Although the sample sizes were small, this

trend supports previous research linking between vaginal microbiota and pregnancy outcomes have shown an increased risk in preterm delivery in mothers with reduced levels of *Lactobacilli* and an increase in bacteria from CST IV (225, 233). Lower increases in LA concentration were observed when baseline levels were already high, suggesting an optimal LA range may exist. O'Hanlon *et al.* reported a lactate concentration of 111±22 mM in women with *Lactobacillus*-dominant microbiota, raising the question of whether baseline lactate levels should be screened to identify women most likely to benefit from Lactin-V treatment (261).

This work has demonstrated for the first time *in vivo* that modulation of the vaginal microbiota towards *L. crispatus* dominance is accompanied by an increase in lactate concentrations which is correlated to low levels of inflammation measured by levels of an inflammatory marker that is a known marker of risk for PTB, STI acquisition and other negative reproductive tract health outcomes. However, the pH of the samples was not measured, and this could be a useful addition for future investigations.

The main limitation of the FLIP-1 study was its small sample size which restricted the statistical power to analyse the outcomes assessed. As the study was was not designed to detect differences in clinical outcomes, a larger study is needed to determine whether Lactin-V reduces the risk of sPTB. The small sample size also limited the ability to explore the influence of ethnicity on response to LAVTIN-V and to perform subgroup analyses, such as among women with sPTB, PPROM or prior antibiotic use. Finally, several potential confounding factors, including ethnicity, sexual intercourse, vaginal douching, use of lubricants, and smoking, were not controlled for in the analysis.

Further, the anti-inflammatory action of LA is mediated via inhibition of pro-inflammatory transcription factors such as NF-κB, AP-1 and IRF3 known to be implicated in signalling pathways leading to adverse health outcomes in female reproductive health such as PTB, STIs, HIV acquisition and cancer. The biotherapeutic introduction of *Lactobacilli* in pregnancy may be able to reduce the risk of premature labour and stillbirth.

In conclusion, the findings presented demonstrate the crucial role of LA in modulating inflammation in VECs and within the cervicovaginal niche. The observed correlation between high levels of LA and diminished inflammation *in vivo* suggests its potential as a therapeutic target for inflammatory conditions. Moreover, the anti-inflammatory mechanisms attributed to LA, particularly its inhibition of pro-inflammatory transcription factors NF-κB, AP-1, and IRF3, elucidate the intricate pathways through which LA exerts its beneficial effects. Notably, the transition of microbial composition from CST IV to CST I demonstrates a tangible link between microbial dynamics and LA levels, further emphasising the interplay between microbiota and host physiology in maintaining inflammatory homeostasis.

Chapter 4: Lactic Acid Mediation of Transcription Factor Activation in VECs

4.1 Introduction

After demonstrating that the anti-inflammatory action of LA in VECs involves inhibition of NF-κB, AP-1 and IRF3, the next logical step was to investigate and characterise the role of upstream kinases mediating these effects, specifically those responsible for the phosphorylation and activation of these transcription factors. By focusing on these kinase-driven processes, this research aimed to elucidate the precise molecular cascades driving LA's anti-inflammatory properties, thereby advancing our understanding of immunoregulation in the reproductive mucosal tissues. Identifying the specific kinases involved could also reveal novel therapeutic targets for modulating inflammation in the FRT, enabling more targeted and effective treatments.

At a basal state, NF-κB subunits form inactive dimers in the cell cytoplasm by associating with IκB proteins. Upon activation by a variety of stimuli, the IκK complex, composed of IκKα, IκKβ and the NEMO regulatory subunit, phosphorylates the IκB proteins, marking them for ubiquitination and proteasomal degradation. This allows NF-κB dimers to translocate to the nucleus and activate target gene expression (400, 401) (Figure 1.5; Chapter 1).

The MAPK cascades regulate diverse biological processes, including responses to extracellular stress, proliferation, apoptosis, and immune response (402-406). These cascades involve three sequentially activated kinases: MAP3K (also called MAPKKK), MAP2K (MAPKK), and MAPK. Distinct scaffolding proteins assemble spatially localised signalling complexes that facilitate and propagate the signal through the cascade (407, 408). In mammalian cells, three major MAPK pathways have been characterised: ERK1/2, JNK, and p38 (409-411) (Figure 1.6; Chapter 1). ERK1/2 is predominantly activated by growth factors, hormones, and pro-inflammatory stimuli, while JNK and p38 respond primarily to cellular and environmental stress as well as pro-inflammatory signals (147, 409). Although the activation mechanisms differ between these pathways, cross-regulation is well documented, and many stimuli can activate more than one MAPK pathway.

The ERK1/2 pathway is mostly initiated at plasma membrane receptors, where ligand binding to a receptor tyrosine kinase (RTK), G-coupled protein receptor (GPCR) or ion channel activates the cascade. These receptors recruit adaptor proteins. Such as growth factor receptor-bound protein 2 (Grb2), and exchange factors like son of sevenless (SOS), which activate the small G-protein Ras. Ras subsequently activates the serine/threonine kinase Raf, (a MAP3K), which phosphorylates and activates the MAP2K, MEK. MEK then phosphorylates and activates ERK1/2 (412-415).

The kinase p38 plays an important role in inflammatory responses and is activated by both cellular stress and pro-inflammatory cytokines (416, 417). Upon stimulation, signalling through adaptor proteins such as TRAF2, TRAF3, or TRAF6, or alternatively through Rho family GTPases, activates upstream MAP3Ks, including MEKK1, ASK1 or TAK1. These MAP3Ks phosphorylate and activate the MAP2Ks, MKK3, and MKK6, which in turn activate p38 (418).

The JNK pathway has context-dependent and sometimes opposing roles in cellular processes such as growth control, transformation and apoptosis, depending on the cell type and the activity of other signalling pathways, (419, 420). JNK is activated by the MAP2Ks MKK4 and MKK7, which phosphorylate JNK in response to stress and cytokine signalling. Activated JNK then phosphorylates the AP-1 subunit c-Jun, enabling its nuclear translocation and transcriptional activity (421).

TBK1 is a serine/threonine kinase of the non-canonical IκB kinase (IKK) family, activated by MAMPS, inflammatory cytokines and oncogenic kinases. TBK1 mediates the production of inflammatory cytokines through activation of IRF3/7 activation and NF-κB signalling pathways (Figure 1.7; Chapter 1). Many proteins interact with TBK1, including adaptor molecules such as TANK (TRAF family member-associated NF-κB activator), post-translational regulators, and diverse substrates involved in IRF/IFN signalling and NF-κB signalling.

In this chapter, the kinase activity upstream of transcription factors NF-κB, AP-1 and IRF3 was examined by determining the phosphorylation status of IKK (upstream of NF-κB), p38, JNK and ERK1/2 (all upstream of AP-1), and TBK1 (upstream of IRF3) following bacterial and viral

agonism of VECs. The effect of LA exposure on the activation of these upstream kinases was also assessed.

4.2 Results

4.2.1 Effect of L-LA on activation of kinases upstream of transcription factors

As demonstrated in Chapter 3, bacterial and viral agonism of TLRs in VECs led to rapid activation of pro-inflammatory transcription factors within 30 minutes. Therefore, assessment of upstream kinase pathway activation was undertaken at 5 and 15 minutes following a 2-hour acclimatisation.

4.2.1.1. Effect of L-LA on IKK

Phosphorylation of IKK was significantly increased by FSL-1 as early as 5 minutes after treatment in VECs ($P < 0.05$; Figure 4.1). Stimulation with the viral agonist PIC also led to increased activation of IKK, but this failed to reach statistical significance. Agonist-induced activation of IKK was suppressed by LA ($P < 0.01$) but not by acidity.

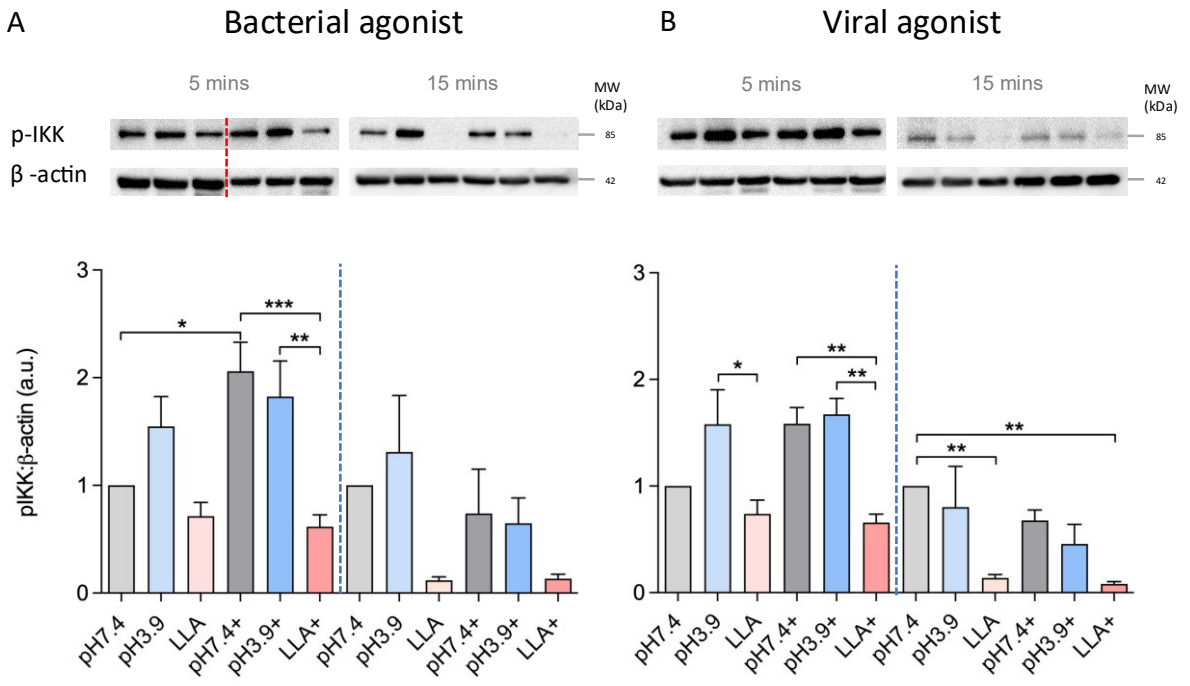

Figure 4.1 IKK is rapidly activated by the bacterial agonist in VECs, and LA suppresses this activation.

Multilayered VECs, acclimatised for 2 hours in medium at pH 7.4 or acidified to pH 3.9 in the presence or absence of 30 mM L-LA, were stimulated with **(A)** bacterial agonist FSL-1 (1.0 µg ml^{-1}) or **(B)** viral agonist PIC (20 µg ml^{-1}) for 5 mins and 15 mins in the presence or absence of 30 mM L-LA (pH 3.9), or media alone (pH 7.4) as indicated. Whole cell protein extracts were probed for p-IKK. Cutting point of blots to remove blots where cells were treated with the viral agonist is indicated by the red line. Graphs show mean ±SD from at least three independent experiments (n = 3). Statistically significant differences between the different conditions and treatments were tested using one-way ANOVA and Tukey's *post hoc* test. *, **, and *** denote $P < 0.05$, 0.01, and 0.001, respectively. All data were standardised to untreated cells at pH 7.4.

Assessment at later timepoints showed that the LA-induced suppression of TLR agonist-activated IKK is maintained 1 hour after treatment. PIC was shown to activate IKK 3-fold after 1 hour treatment ($P < 0.01$) but again this was suppressed specifically by LA ($P < 0.001$), and not acidity alone (Supplementary 9.4; Figure 9.1). Basal levels of IKK phosphorylation were also shown to be suppressed by LA in untreated cells.

4.2.1.2 Effect of L-LA on TBK1

FSL-1 treatment of VECs significantly increased phosphorylation of TBK1 within 15 minutes ($P < 0.01$). This activation was suppressed by both acidity ($P < 0.01$) and LA ($P < 0.01$; Figure 4.2A). PIC treatment did not lead to a significant increase in TBK1 phosphorylation (Figure 4.2B), despite IRF3 being activated by PIC at 1 hour and 2 hours as presented in the previous chapter.

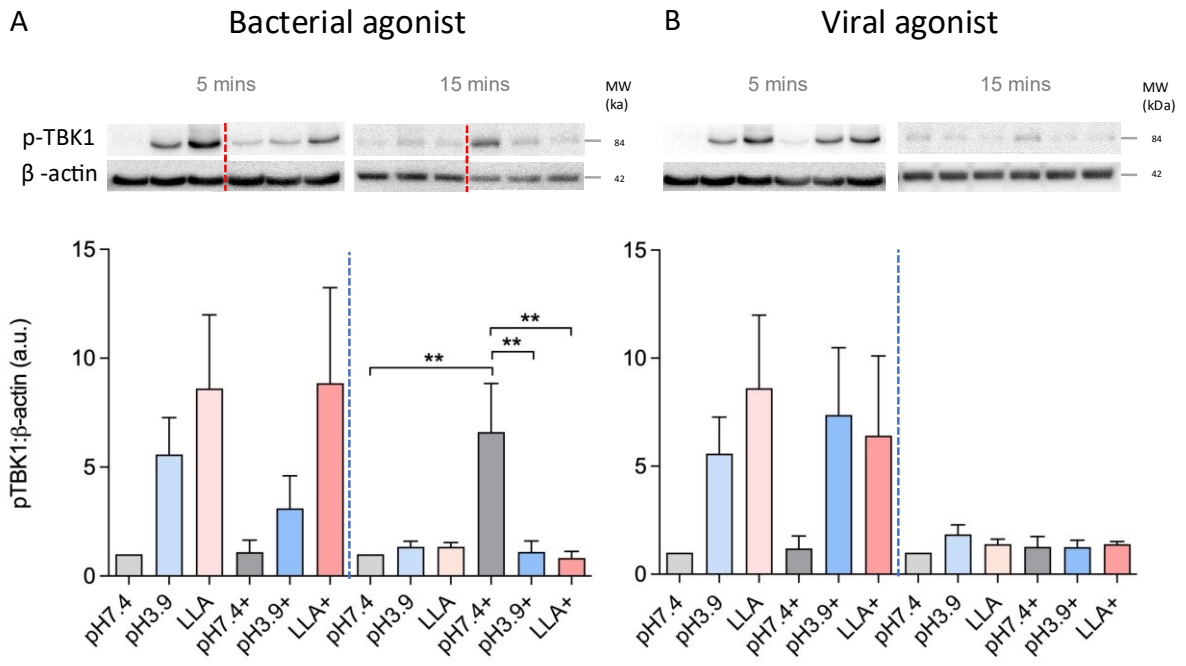

Figure 4.2 FSL-1 activation of TBK1 in VECs is inhibited by LA.

Multilayered VECs, acclimatised for 2 hours in medium at pH 7.4 or acidified to pH 3.9 in the presence or absence of 30 mM L-LA, were stimulated with **(A)** bacterial agonist FSL-1 (1.0 µg ml^{-1}) or **(B)** viral agonist PIC (20 µg ml^{-1}) for 5 mins and 15 mins in the presence or absence of 30 mM L-LA (pH 3.9), or media alone (pH 7.4) as indicated. Whole cell protein extracts were probed for p-TBK1. Cutting point of blots to remove blots where cells were treated with the viral agonist is indicated by the red line. Graphs show mean ±SD from at least three independent experiments (n = 3). Statistically significant differences between the different conditions and treatments were tested using one-way ANOVA and Tukey's *post hoc* test. ** denotes $P < 0.01$, respectively. All data were standardised to untreated cells at pH 7.4.

4.2.1.3 LA mediation of JNK and p38 activation

Exposure of VECs to LA culture conditions initially increased phosphorylation of p38 and JNK within 5 minutes, although this did not reach statistical significance (Figure 4.3). A significant increase in JNK phosphorylation was observed at 5 minutes in VECs cultured at pH 3.9-HCl treated with FSL-1 ($P < 0.05$) or PIC ($P < 0.01$; Figures 4.3C and D). There was no activation of p38 or JNK at 15 minutes and acidity and LA reduced the activation below basal levels.

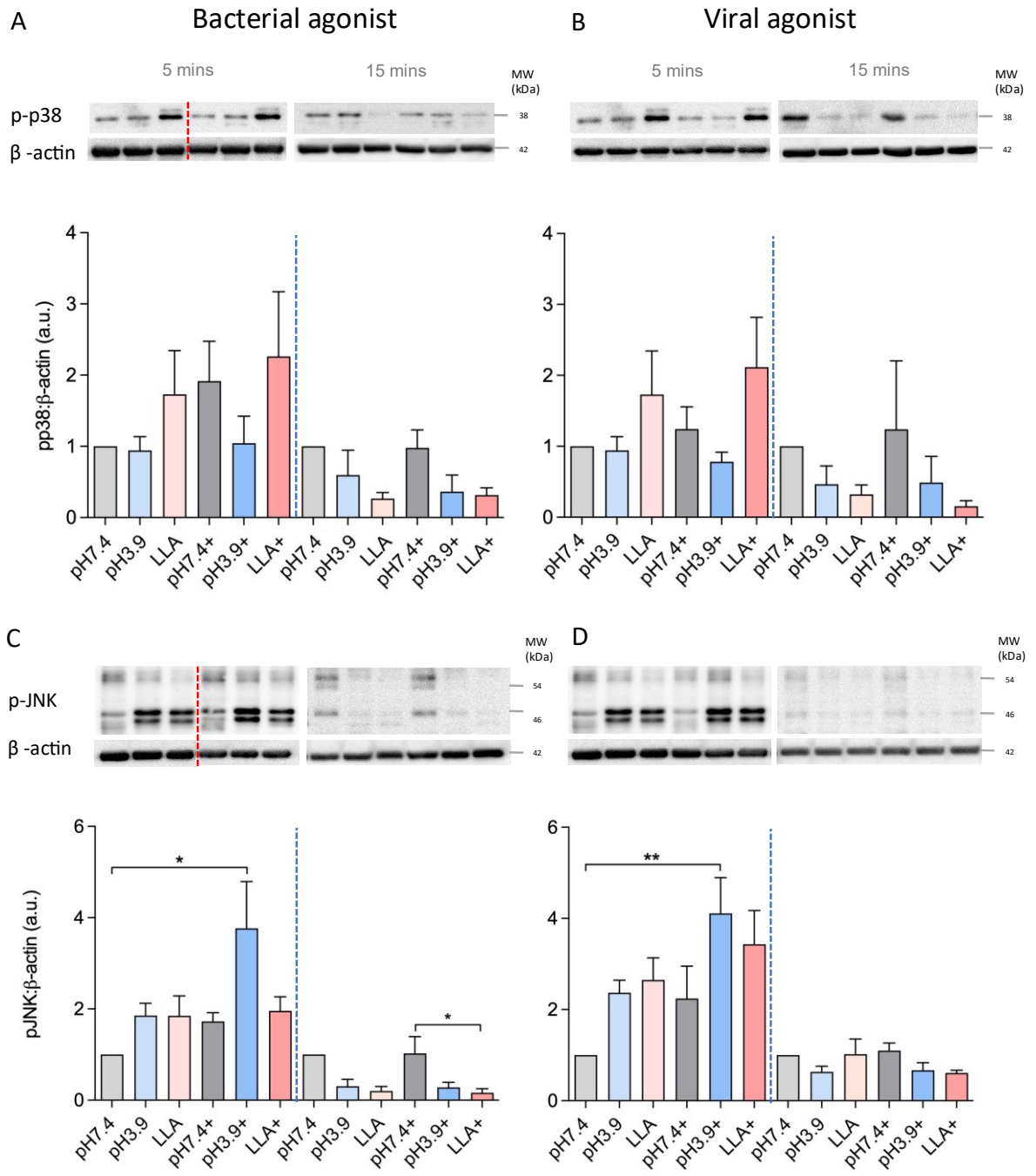

Figure 4.3 LA-mediation of p38 and JNK phosphorylation in VECs treated with FSL-1 or PIC.

Multilayered VECs, acclimatised for 2 hours in medium at pH 7.4 or acidified to pH 3.9 in the presence or absence of 30 mM L-LA, were stimulated with bacterial agonist FSL-1 (1.0 µg ml^{-1}) or viral agonist PIC (20 µg ml^{-1}) for 5 mins and 15 mins in the presence or absence of 30 mM L-LA (pH 3.9), or media alone (pH 7.4) as indicated. Whole cell protein extracts were probed for **(A)** and **(B)** p-p38 and **(C)** and **(D)** p-JNK. Cutting point of blots to remove blots where cells were treated with the viral agonist is indicated by the red line. Graphs show mean ±SD from at least three independent experiments (n = 3). Statistically significant differences between the different conditions and treatments were tested using one-way ANOVA and Tukey's post

hoc test. * and ** denote $P < 0.05$ and 0.01, respectively. All data were standardised to untreated cells at pH 7.4.

Later timepoints were also investigated and LA suppression of p38 activation induced by both bacterial and viral agonists became significant by 30 minutes ($P < 0.05$ and 0.01, respectively) (Supplementary 9.5; Figure 9.2).

4.2.1.4 LA mediation of ERK activation

Culture of VECs in media acidified by either HCl or LA led to a rapid and significant increase in phosphorylation of ERK as early as 5 minutes ($P < 0.001$ and 0.0001, respectively). Activation of ERK was maintained up to 4 hours (2 hours acclimatisation and 2 hours exposure with or without TLR agonist) following exposure to LA, whereas the activation of ERK by acidity was more transient. By 30 minutes ERK activation by acidity had halved compared with LA and after 2 hours it was reduced to about 20% of LA-induced activation (Supplementary 9.6; Figure 9.3). Neither agonist FSL-1 or PIC activated ERK (Figure 4.4).

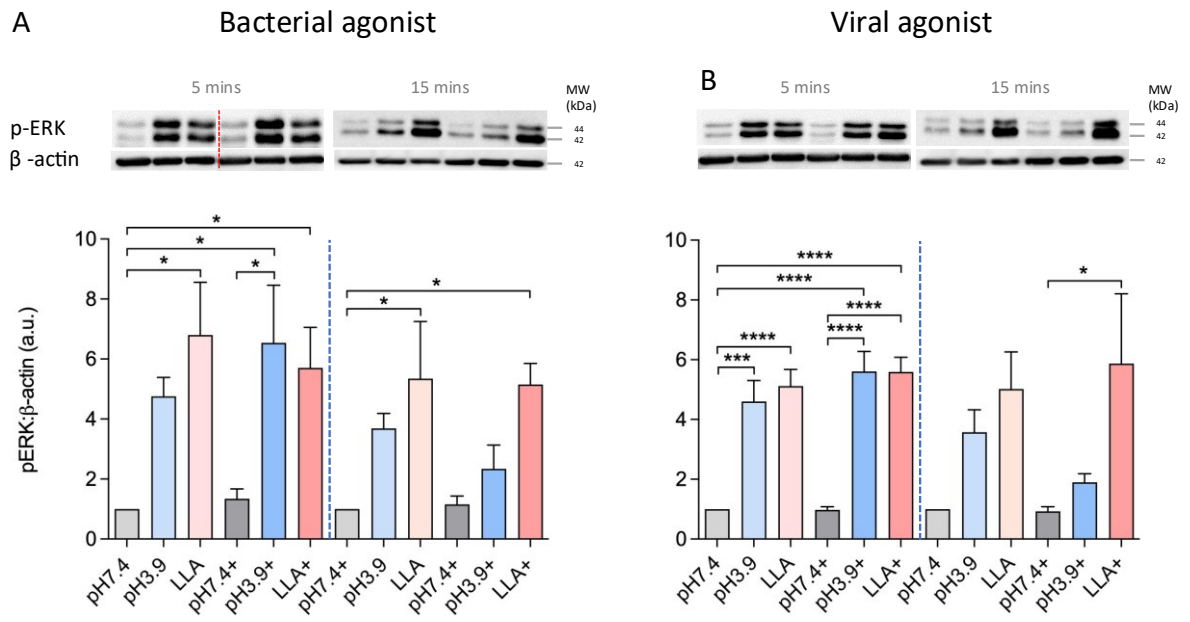

Figure 4.4 ERK is rapidly and strongly activated by LA.

Multilayered VECs acclimatised for 2 hours in medium at pH 7.4 or acidified to pH 3.9 in the presence or absence of 30 mM L-LA were stimulated with **(A)** bacterial agonist FSL-1 (1.0 µg ml^{-1}) or **(B)** viral agonist PIC (20 µg ml^{-1}) for 5 mins or 15 mins. Whole cell protein extracts were probed for p-ERK. Cutting point of blots to remove blots where cells were treated with the viral agonist is indicated by the red line. Graphs show mean ±SD from five independent experiments (n = 5). Statistically significant differences between the different conditions and treatments were tested using one-way ANOVA and Tukey's post hoc test. *, **, *** and **** denote $P < 0.05$, 0.01, 0.001 and 0.0001, respectively. All data were standardised to untreated cells at pH 7.4.

4.2.2 Inhibition of ERK activation

Given that ERK is upstream of AP-1 and NF-κB, the VEC model was used to investigate whether LA inhibition of AP-1 and NF-κB is dependent on ERK phosphorylation. The inhibitor U0126, which is highly selective for both MEK1 and MEK2, the two kinases that phosphorylate ERK1/2, was used to treat a multilayered VK2 cell culture at pH 7.4 and pH 3.9 in the presence or absence of L-LA. ERK was suppressed in presence of the MEK inhibitor which confirmed the efficacy of U0126 as an inhibitor of ERK activation (Figure 4.5).

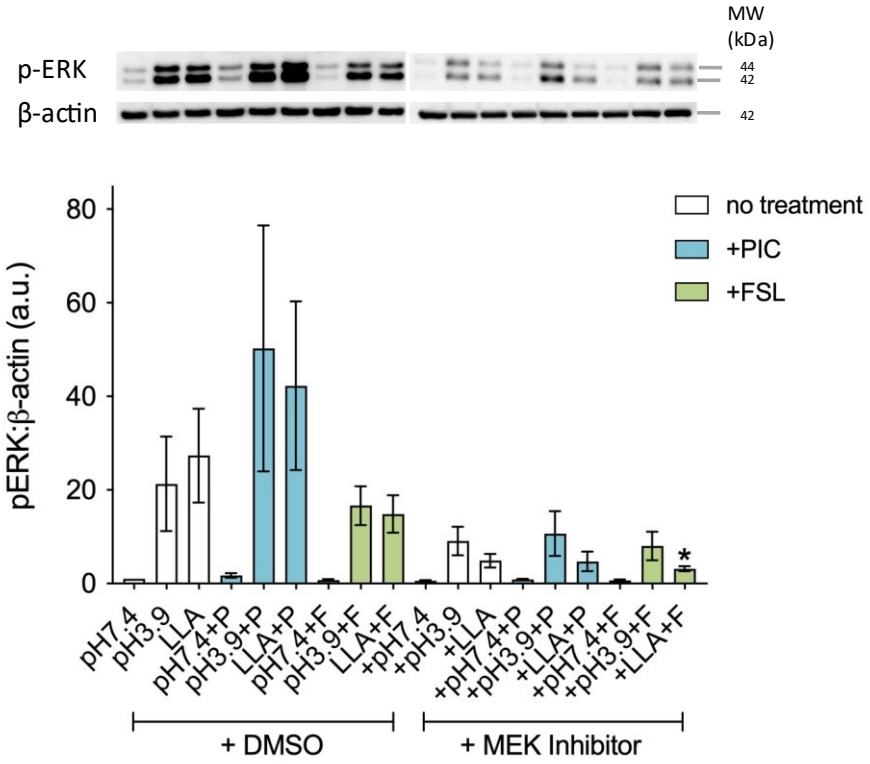

Figure 4.5 ERK activation by LA is suppressed by MEK inhibitor U0126.

Multilayered VECs were treated with 10 µM MEK inhibitor U0126 resuspended in DMSO for 30 mins before being acclimatised for 2 hours in medium at pH 7.4 or acidified to pH 3.9 in the presence or absence of 30 mM L-LA. The cells were stimulated apically with bacterial agonist FSL-1 (1.0 µg ml^{-1}) or viral agonist PIC (20 µg ml^{-1}) for 30mins. Whole cell protein extracts were probed for p-ERK. Graphs show mean ±SD from four independent experiments (n = 4). Statistical significance was tested using the Mann-Whitney U-test with * indicating $P < 0.05$. All data were standardised to untreated cells at pH 7.4.

4.2.3 Effect of MEK inhibition on NF-κB and AP-1

Having shown that the MEK inhibitor effectively inhibits ERK, the phosphorylation status of NF-κB and AP-1 was assessed in the samples. Initial examination of the results indicated that inhibition of ERK did not alter FSL-1-induced phosphorylation NF-κB in VECs cultured in either pH 7.4 or acidified media (Figure 4.6A). However, NF-κB phosphorylation was not suppressed in vehicle-treated cells grown in acidified media indicating that DMSO may be impacting inflammatory pathway signalling in VECs. AP-1 activation by bacterial and viral agonists

remained unchanged in the presence of MEK inhibitor (Figure 4.6B) with LA maintaining its capacity to suppress AP-1 activation in the presence of the MEK Inhibitor.

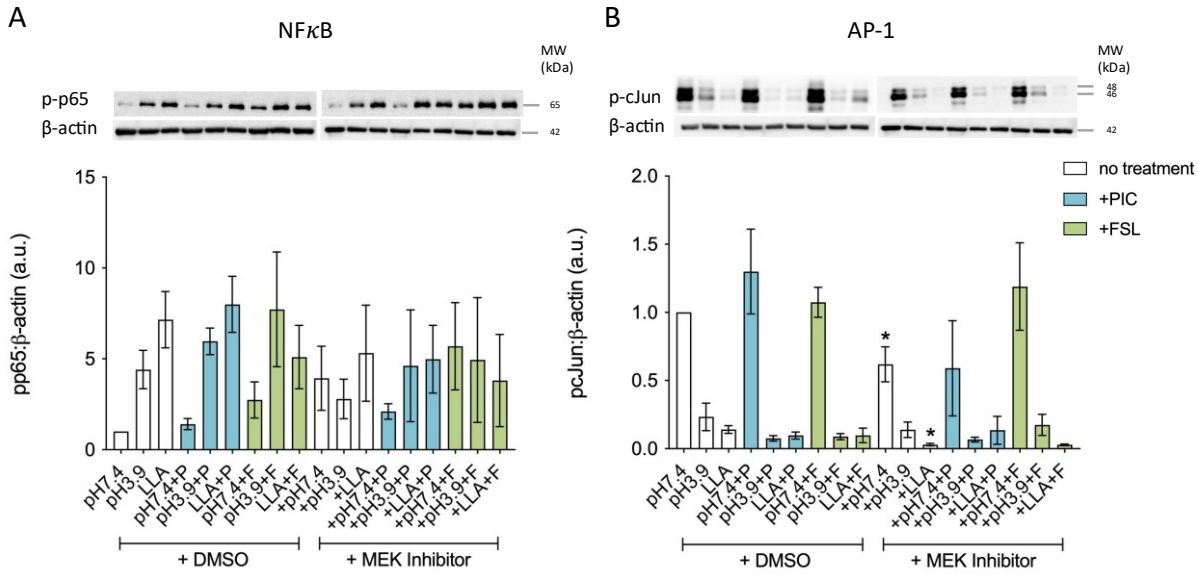

Figure 4.6 NF-κB and AP-1 activation are independent of ERK activation by LA.

Multilayered VECs were treated with 10 µM MEK inhibitor U0126 suspended in DMSO for 30 mins before being acclimatised for 2 hours in medium at pH 7.4 or acidified to pH 3.9 in the presence or absence of 30 mM L-LA. The cells were stimulated apically with bacterial agonist FSL-1 (1.0 µg ml^{-1}) or viral agonist PIC (20 µg ml^{-1}) for 30 mins. Whole cell protein extracts were probed for **(A)** p-p65 and **(B)** p-cJun. Graphs show mean ±SD from four independent experiments (n = 4). Statistical significance was assessed using the Mann-Whitney U-test with * indicating $P < 0.05$. All data were standardised to untreated cells at pH 7.4.

4.2.3.1 Assessment of alternative solvents for U0126

Given that DMSO appeared to be modulate LA-mediated suppression of NF-κB phosphorylation, alternative solvents for U0126 were tested. The manufacturer of the MEK inhibitor U0126 recommended methanol as a substitute for DMSO, prompting an assessment of methanol's effect on NF-κB phosphorylation in VECs without the MEK inhibitor. Similar to DMSO, methanol activated NF-κB in acidic conditions and in the presence of L-LA. Furthermore, in the presence of methanol, FSL-1 treatment did not lead to increased NF-κB phosphorylation at either pH 7.4 or pH 3.9 (Figure 4.7).

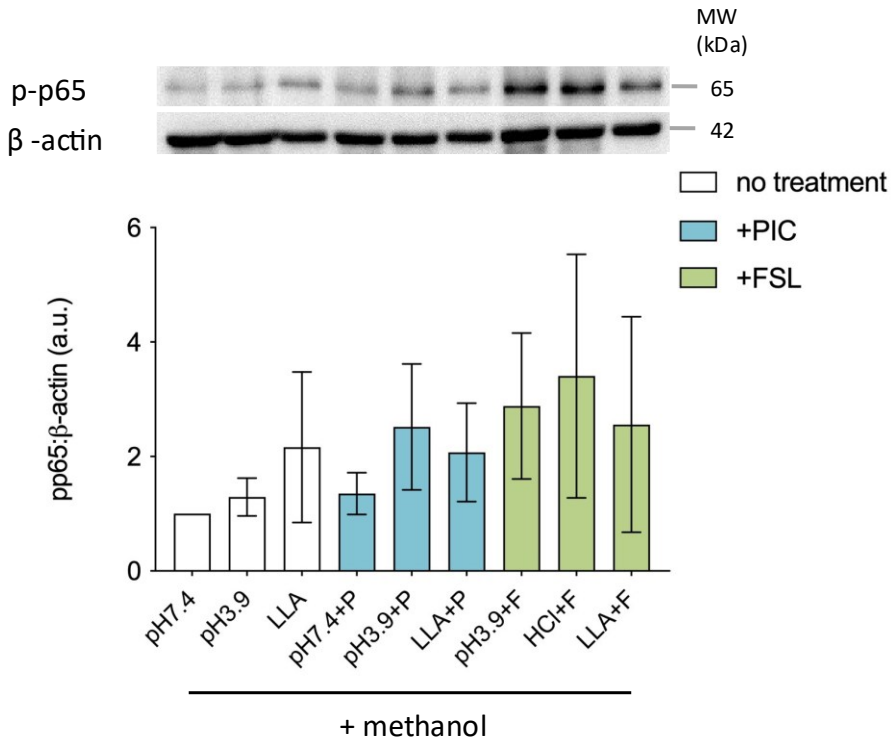

Figure 4.7 Methanol activates NF-κB in acidic conditions.

An alternative solvent for U0126, methanol, was suggested by the manufacturer of U0126. VECs grown as a multilayer were exposed to methanol for 30 mins before being acclimatised for 2 hours in medium at pH 7.4 or acidified to pH 3.9 in the presence or absence of 30 mM L-LA. The cells were stimulated apically with bacterial agonist FSL-1 (1.0 µg ml^{-1}) or viral agonist PIC (20 µg ml^{-1}) for 30 mins. Whole cell protein extracts were probed for p-p65 and p-cJun. Graphs show mean ±SD from three independent experiments (n = 3). Statistical significance was assessed using one-way ANOVA and Tukey's *post hoc* test. All data were standardised to untreated cells at pH 7.4.

A comprehensive search of the literature identified Cyrene™ as a potential alternative solvent for U0126 (352). To evaluate its suitability, multilayered VECs were pre-treated for 30 minutes with 10 µM MEK inhibitor U0126 dissolved in Cyrene™. Following a 2-hour acclimatisation period, the cells were stimulated with either a bacterial or a viral agonist. Western blot analysis of ERK activation demonstrated that U0126 prepared in Cyrene™ effectively inhibited ERK activation (Figure 4.8).

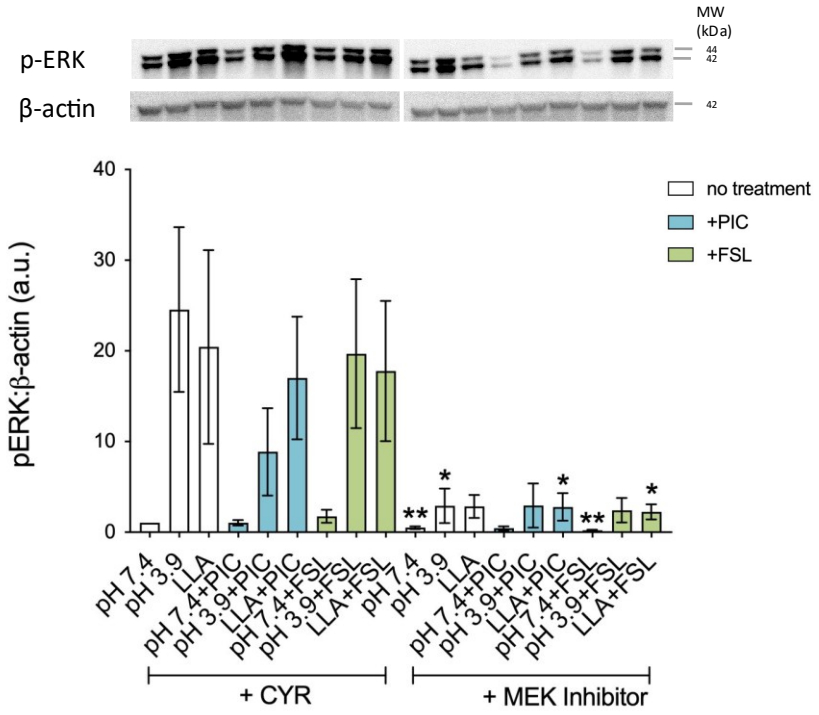

Figure 4.8 ERK activation by LA is suppressed by MEK inhibitor U0126 solubilised in Cyrene™.

Multilayered VECs grown in Transwells® were treated with 10 µM MEK inhibitor U0126 suspended in Cyrene™ for 30 mins before being acclimatised for 2 hours in medium at pH 7.4 or acidified to pH 3.9 in the presence or absence of 30 mM L-LA. The cells were stimulated apically with bacterial agonist FSL-1 (1.0 µg ml^{-1}) or viral agonist PIC (20 µg ml^{-1}) for 30 mins. Whole cell protein extracts were probed for p-ERK. Graphs show mean ±SD from four independent experiments (n = 4). Statistical significance was assessed by the Mann-Whitney U-test with * and ** denoting $P < 0.05$ and $P < 0.01$. All data were standardised to untreated cells at pH 7.4.

The morphology of the cells was examined and compared across the three solvents - DMSO, methanol and to the other two solvents, DMSO and methanol, and Cyrene™ - as well as a control condition without solvents at pH 7.4 (Figure 4.9). The VEC monolayer in the negative control (KSF medium) and in the presence of Cyrene™ reached 80-90% confluence after 36 hours of growth, with the VECs retaining their characteristic cuboid shape, typically observed as confluence increases. In contrast, VECs grown in the presence of DMSO or methanol reached only 30-50% confluence during the same period. These cells appeared more elongated compared to their initial morphology at seeding and exhibited increased cellular debris, indicative of cellular stress.

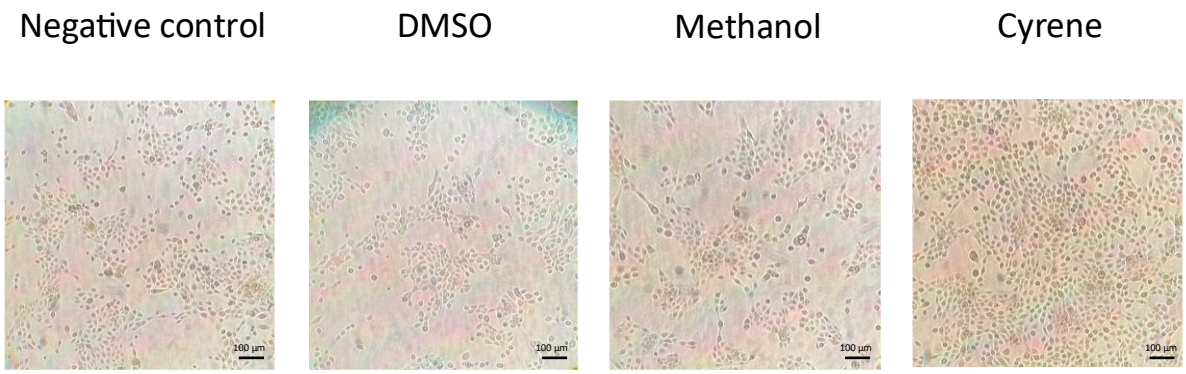

Figure 4.9 Cyrene and KSF medium have less impact on the confluence of the VEC monolayer treated with MEK inhibitor U0126.

Representative images of VK2/E6E7 cells exposed to solvents DMSO, methanol and Cyrene™ for 30 mins followed by a 2-hour acclimatisation at pH 7.4. Images were taken using white light confocal microscopy (10 x magnification; scale bar = 100 µm).

4.2.3.2 Effect of MEK inhibition on NF-κB and AP-1, using Cyrene™ as a MEK inhibitor solvent

Having shown that the MEK inhibitor in Cyrene™ effectively inhibits ERK, the samples were probed for NF-κB and AP-1. In the controls, NF-κB was activated by FSL-1 at pH 7.4 and pH 3.9 and suppressed by LA as seen previously in Chapter 3. The inhibition of ERK did not prevent activation of NF-κB by FSL-1 at either pH 7.4 and pH 3.9 and LA retained its suppressive effect of NF-κB in VECs treated with FSL-1 even when ERK was suppressed (Figure 4.10A). Similarly, AP-1 activation by both bacterial and viral agonists remained unchanged in presence of the MEK inhibitor (Figure 4.10B). In addition, LA continued to suppress AP-1 activation despite ERK inhibition.

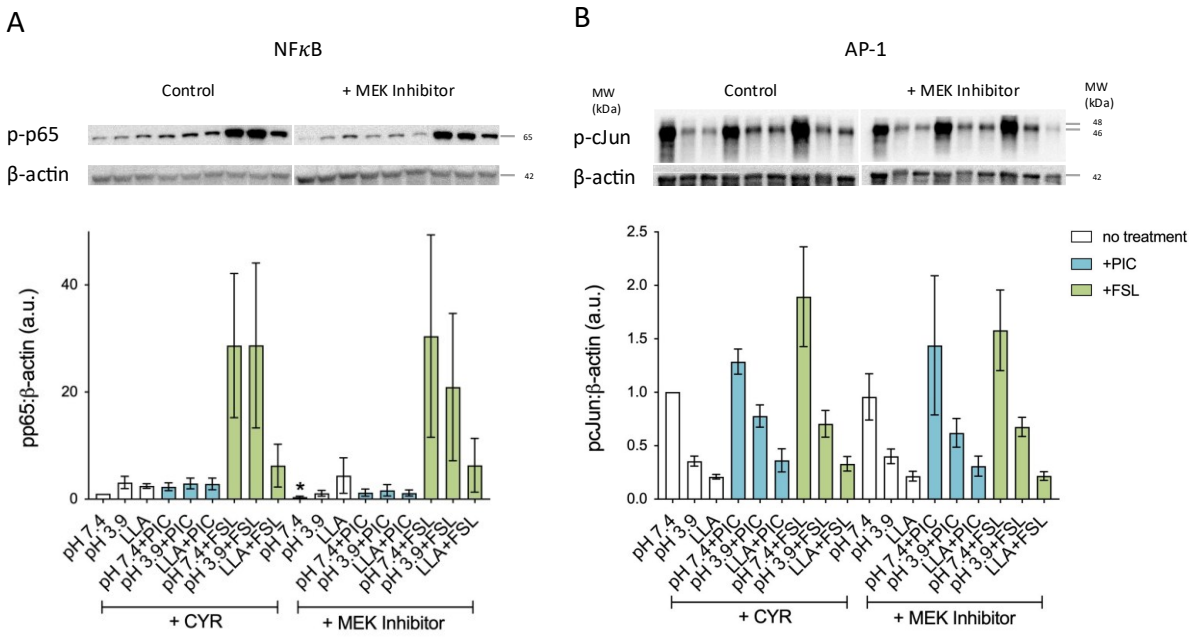

Figure 4.10 NF-κB and AP-1 activation and inhibition are independent of ERK activation.

ERK phosphorylation was suppressed with 10 µM MEK Inhibitor U0126 suspended in Cyrene™ and its effect on expression of transcription factors NF-κB and AP-1 was examined. Protein levels of **(A)** p-p65 and **(B)** p-cJun in VECs stimulated apically with bacterial agonist FSL-1 (1.0 µg ml^{-1}) or viral agonist PIC (20 µg ml^{-1}) for 30 mins in low pH medium (pH 3.9), in the presence or absence of 30 mM L-LA or medium alone (pH 7.4) were assessed by Western blot analysis. Graphs were generated from at least four independent experiments (p-p65, n = 4; p-cJun, n = 5). Statistical significance was assessed by the Mann-Whitney U-test; * and ** denote $P < 0.05$ and 0.01, respectively. All data were standardised to untreated cells at pH 7.4.

4.2.4 Effect of MEK inhibition on vaginal epithelial cell barrier integrity

Tight junctions between the epithelial cells decrease the permeability of the epithelial cell barrier. This barrier is crucial in protecting the host from external pathogens (422). The integrity of the cell barrier can be quantified using transepithelial electrical resistance (TEER) (355). A recent study implicated bacterial metabolites in the mediation of epithelial barrier function in the lower female reproductive tract. Delgado-Diaz *et al.* showed that both D-LA and L-LA upregulate the gene expression of tight junction proteins and increase the epithelial cell barrier integrity, but the mechanism was not investigated (383). Therefore, it was hypothesised that LA may increase VEC barrier integrity via a MAPK-dependent mechanism. To test this, the effect of L-LA on cell barrier resistance was measured in VECs treated with MEK inhibitor, U0126, and untreated cells.

Apical treatment of cells with 30 mM L-LA at pH 3.9 elicited a significant enhancement of barrier integrity compared to cells treated with medium acidified to pH 3.9 with HCl (Figure 4.11A). Cells maintained in medium at pH 7.4 demonstrated no change in resistance. The cells were then pre-treated with a MEK inhibitor U0126 to investigate whether inhibiting MEK influenced barrier integrity (Figure 4.11B). MEK inhibition had no effect on barrier integrity at pH 3.9-HCl but there was a trend decrease in TEER at pH 3.9 when L-LA was present. Inhibiting MEK at pH 7.4 had the unexpected temporary effect of increasing TEER readings at 2 hours.

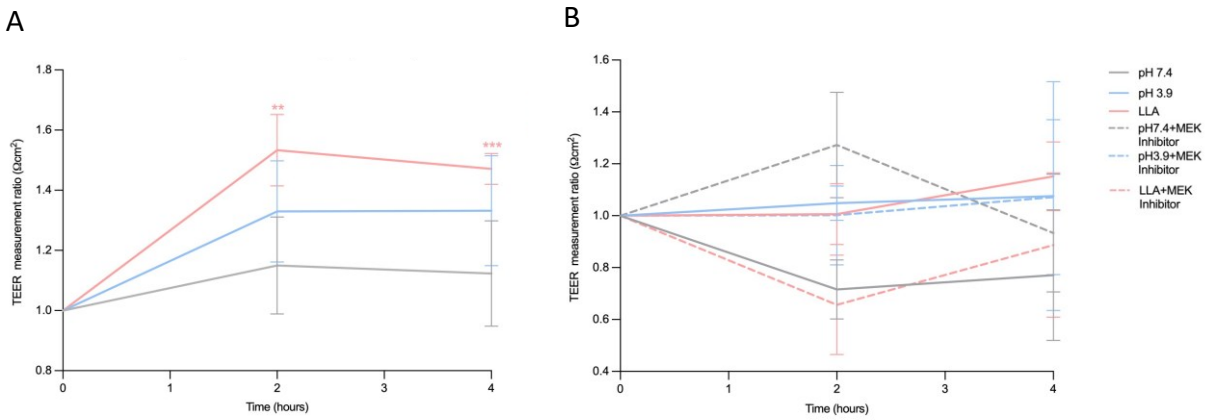

Figure 4.11 L-LA attenuates barrier disruption by a MAPK-dependent mechanism in vaginal epithelial cells.

(A) VECs multilayers were acclimatised at pH 7.4 or pH 3.9 with or without 30 mM L-LA and exposed for a further 2 hours (treatment time of previous control experiments) as indicated. **(B)** VEC multilayers were pre-incubated with MEK inhibitor U0126, acclimatised at pH 7.4 or pH 3.9 with or without 30 mM L-LA and exposed for a further 2 hours (treatment time of previous control experiments) as indicated. Epithelial barrier integrity was assessed by transepithelial electrical resistance (TEER) measured at time points 0 hours, 2 hours and 4 hours. Graphs show mean ±SD from at least three independent experiments (n = 3). Statistically significant differences were tested using one-way ANOVA and Dunnett's *post hoc* test. ** and *** denote $P < 0.01$ and 0.001, respectively.

4.3 Discussion

Understanding the intricate interplay between signalling pathways and inflammatory responses is crucial for deciphering the complex mechanisms underlying immune mediator regulation in VECs. This chapter investigated the dynamic interplay between upstream kinases, the transcription factors NF-κB, AP-1 and IRF3, and LA in response to different agonists in VECs.

Treatment of VECs with the bacterial TLR2/6 agonist FSL-1 led to rapid activation of the kinases IKK and TBK1. IκB kinase (IKK) activity, significantly increased within 5 minutes of stimulation, is essential for NF-κB activation. Oeckinghaus *et al.* showed that it is the IKKβ subunit of the IKK complex that phosphorylates Iκ$B, leading to its degradation and nuclear translocation of the NF-kB dimer (139). Consistent with this, pharmacological inhibition of IKKs prevents nuclear translocation of the NF-κB p65 subunit and inhibits pro-inflammatory cytokine

transcription (423-425). Phosphorylation and activation of IKKα/β were significantly inhibited by LA, likely accounting for the reduced NF-κB activation observed in Chapter 3.

Surprisingly, TBK1 was significantly activated by the bacterial agonist FSL-1 ($P < 0.01$) but not by the viral agonist, PIC, even though IRF3, a known TBK1 substrate, was significantly activated by PIC in earlier experiments. One possible explanation is that TBK1 can also be activated by TRIF when TLR4 signalling switches from MyD88 to TRIF as TLR4 relocates to endosomes (426). Evidence from cancer cell lines suggests that NF-κB signalling can also be mediated by TBK1; downregulation of TBK1 suppresses NF-κB target genes such as *IL8* (427). Additionally, NF-κB-independent regulation IRF3, HIF-2α, and MAPK activation by NEMO (IKKγ) has been reported (428). The kinase IKKε has been implicated in phosphorylating p65, which can transactivate p50 and p52 to drive NF-κB gene expression (429, 430). When TBK1 is phosphorylated by TRAF3, it forms a heterodimer with IKKε, potentially leading to IRF3 activation in VECs, as both kinases can phosphorylate IRF3 (431-433). Further research in VECs is needed to determine whether IKKε rather than TBK1 phosphorylates IRF3. Moreover, TBK1 itself can be phosphorylated by IKKβ, suggesting crosstalk within the IKK family of proteins (434). Finally, TBK1 has also been implicated in mTORC1 regulation downstream of growth factors such as epidermal growth factor (EGF) (435), warranting further investigation in the context of inflammation in VECs.

LA rapidly and significantly suppressed phosphorylation of both IKKα/β and TBK1 in response to FSL-1, contrasting with the absence of MAPK activation by this agonist. This raises questions about how AP-1 signalling is activated, given that the canonical TLR2/6 -> TRAF6 -> TAK1 -> JNK pathway does not seem to operate here (165). One possibility is a coordinated regulation of NF-κB and AP-1, as Fujioka *et al.* observed in human pancreatic cancer cells, where both transcription factors appear to be simultaneously activated by the same stimuli and regulated by the same signal transduction cascades (393). NF-κB was shown to modulate Elk-1, which is activated by MAPKs to induce AP-1 activity.

Early activation of p38 and JNK by acidity was observed at 5 minutes but not sustained at 15 minutes, and both were suppressed by acidity and, in particular, LA even though FSL-1 itself

did not activate them. Previous work by Pirianov *et al.* demonstrated that inhibiting JNK could mitigate infection- and inflammation-induced preterm labour and prevent associated detrimental effects to the neonatal brain (436). Collectively, these results support the idea that a vaginal microbiome dominated by LA-producing bacteria fosters an anti-inflammatory environment, potentially contributing to improved pregnancy outcomes and reduced risk of infections, including HPV and HIV (42, 224, 437, 438). Importantly, the current findings suggest that LA, not simply acidity, suppresses key pro- inflammatory kinases. The potential therapeutic benefits of LA have already been exploited in several LA-containing vaginal products that are currently available. However, some have shown high cytotoxicity (> 90%) and impaired epithelial barrier integrity in primary VEC models (439), underlining the need to understand LA's mechanisms more fully to design safer interventions.

The differential kinase activation observed in response to viral and bacterial agonists highlights the selectivity of inflammatory cascades in VECs. Given the bacterial dominance of the vaginal niche (440-442), VECs may have evolved to respond to bacterial MAMPs while maintaining tolerance. The strong suppression of IKK, JNK and p38 by LA may reflect an evolutionary adaptation of *Lactobacillus* species to dampen host inflammation. Of the kinases itested only IKK was significantly activated by PIC ($P < 0.01$; Supplementary 9.4 Figure 9.1) and significantly suppressed by LA ($P < 0.001$). These findings align with reports that *Lactobacillus*-dominant microbiomes are associated with lower HPV acquisition risk (443, 444), and they suggest that LA may help suppress NF-κB-driven responses to viral stimuli. The potential role of IKKε in IRF3 activation warrants future investigation.

While these results highlight LA's anti-inflammatory effects, they also show robust activation of ERK signalling, typically associated with cell proliferation and inflammation, in response to LA. In other systems, ERK activation has been linked to NF-κB and AP-1 activation (445, 446), yet in VECs, LA-induced ERK activation coincides with inhibition of these transcription factors. ERK activation by LA has been described in human CHO-K1 cells, where lactate receptor HCAR1 mediates this activation through either a PKC-dependent pathway or an IGF-IR transactivation-dependent pathway (447). In a cervical cancer cell line, D-LA has been shown to induce higher levels of ERK activation compared to L-LA (448). Particularly relevant to the

findings of this thesis, ERK also contributes to reducing inflammation in endothelial cells by inhibiting the activation of NF-kB-dependent inflammatory genes via IKK (449). However, inhibition of ERK with the MEK inhibitor U0126 did not prevent FSL-1-induced NF-κB or AP-1 activation or their inhibition LA, suggesting these pathways operate independently of ERK. As the MEK inhibitor is not entirely specific to ERK1/2 off-target effects cannot be excluded, and the precise role of ERK in VECs remains unclear.

Scaffolding proteins localise ERK1/2 to specific membrane domains to compartmentalise its activity to specific pathways. Several proteins have been identified such as paxillin, FHL1, GIT1 at focal adhesions (408), CAVIN4, β -arrestin and MORG1 at GPCRs (450, 451) and IQGAPs at the plasma membrane (452). The mechanisms underlying ERK1/2 recruitment to these scaffolds and their exact function in ERK signalling remain incompletely characterised, especially in VECs (404). The complexity and pleiotropism of ERK signalling are in part due to the large number of effector substrates. Signals at the plasma membrane initiate the small Ras GTPases to trigger a phosphorylation cascade down to the ERK proteins (453). Only a small number of these effectors have been characterised indicating that this is an area for further research particularly in VECs. Emerging evidence suggests ERK may regulate actin polymerisation and adhesion, which could influence barrier function (454).

Additionally, the nuclear translocation of activated ERK is not fully understood but is known to be important for ERK to activate its nuclear targets. Cytoplasmic targets of ERK activation include ribosomal protein S6 kinase (RSK), mitogen- and stress-activated protein kinase (MSK) and MAPK-interacting kinase (MNK) (166, 455, 456). The subcellular localisation of activated ERK in VECs, whether nuclear or cytoplasmic, was not determined in this study but could explain why the high ERK phosphorylation does not drive inflammatory gene expression.

The role of ERK in modulating tight junction proteins and maintaining barrier integrity has been demonstrated across various cellular systems. Tight junction proteins are important structural components that play a critical role in epithelial barrier function. Activation of ERK can either upregulate or downregulate these proteins, depending on the specific cell type and the junctional protein examined (151, 457, 458). For example, Aggarwal *et al.* reported that

inhibiting ERK enhanced tight junction integrity while reducing the disruption caused by epidermal growth factor (EGFR) activation (151). Similarly, in the mouse proximal epididymis, Kim *et al.* showed that MEK inhibition, which reduces ERK phosphorylation, decreased the expression of tight junction proteins claudin-1 (CLDN-1), claudin-4 (CLDN-4) and zonula-occludens-1 (ZO-1), while increasing the levels of ZO-3 and occludin. In the gut, certain microbes disrupt the epithelium via the ERK pathway, for example *Helicobacter pylori* activates ERK, leading to the breakdown of cell-cell junctions in the gut epithelium (459). Using an *in vitro* model of the vaginal niche, Anton *et al.* recently demonstrated that *G. vaginalis,* which is commonly associated with adverse reproductive health outcomes, causes the epithelial barrier breakdown and cell death through a TLR2/6 and NF-κB pathway (370). Further investigation is needed into the interplay between LA, ERK and epithelial barrier integrity in VECs.

Overall, these findings offer new insights into how LA modulates upstream kinases to regulate inflammatory transcription factors in VECs. LA exerts both inhibitory and activating effects on key signalling molecules, contributing to an anti-inflammatory environment while maintaining ERK activation through pathways apparently independent of NF-κB and AP-1. These results lay the groundwork for future investigations into LA's mechanisms of action and its potential for developing targeted interventions to improve adverse female reproductive outcomes.

Chapter 5: Mediation of VEC Inflammatory Pathways by Succinate

5.1 Introduction

Microbial-derived short-chain fatty acids (SCFAs), produced by fermentation of dietary fibre in the gut, play a pivotal role in protecting the intestinal epithelial barrier, regulating immune function, inflammation and influencing metabolic processes throughout the body (297-299, 460). Levels of SCFAs in the gut are influenced by both the nutrients ingested by the host as well as the bacteria found in the gut (321, 461, 462). The SCFAs acetate, propionate, butyrate as well as the dicarboxylic acid, succinate, have an anti-inflammatory role in the gut where they were shown to suppress NFκB and the production of pro-inflammatory cytokines (272, 299, 463, 464). The role of SCFAs and succinate in the lower FRT has not been as extensively studied.

SCFAs and succinate in the vaginal mucosa have been associated with a non-optimal bacterial community dominated by anaerobes and a depletion of beneficial *Lactobacilli* (273, 274, 293, 465). In the vaginal mucosa of women with symptomatic BV there is an increase in SCFAs and their metabolic precursors which includes acetate, butyrate, propionate, succinate, formate, valerate and caproate (294, 466-471). A high succinate:lactate ratio has been associated with BV and this metabolite has not been extensively studied in the vaginal niche (293). *In vitro*, many BV-associated bacteria were shown to produce SCFAs; for example, acetate is produced by *Peptococcus* and *G. vaginalis*, propionate by *Clostridium* and *Dialister*, and succinate by *Bacteroides* and *G. vaginalis*. Unlike LA, which is produced by both VECs and microbiota, SCFAs and succinate in vaginal mucosa are almost entirely derived from microbes (245). Succinate, which can be metabolised by both BV-associated bacteria and certain *Lactobacillus* species, particularly *L. crispatus* and *L. gasseri*, was selected for further investigation into its role in inflammatory pathways.

In the absence of *Lactobacilli*, the vaginal pH increases due to the presence of SCFAs as well as the production of biogenic amines, making it favourable for the growth of anaerobic bacteria that produce virulence factors that can degrade mucin, disrupt the epithelial cell barrier and increase the risk of infection (272, 273, 465, 472). Recent studies have correlated vaginal levels of SCFAs and succinate to adverse reproductive health outcomes, such as

preterm birth, but their relationship with bacterial composition remains underexplored (305, 473, 474). In certain cell types, such as macrophages, succinate can exhibit an anti-inflammatory role (475-477). Recent evidence highlights succinate's dual role as a signalling molecule in inflammation. Elevated levels of intracellular succinate are increasingly recognised as pro-inflammatory (478), whereas extracellular succinate, acting through succinate receptor 1 (SUCNR1 or GPR91), has an anti-inflammatory functionality associated with SUCNR1 (479). Despite its established link to reproductive health and disease, the mechanisms through which succinate modulates inflammatory pathways in the vaginal niche remain poorly understood. This chapter investigates the hypothesis that succinate functions as a pro-inflammatory metabolite within the vaginal niche, activating NFκB and AP-1 in VECs. To address this, metabolomic data from the VMET1 study was analysed to compare vaginal succinate concentrations during pregnancy in women with *Lactobacillus*-dominant versus *Lactobacillus*-deplete microbiota compositions. Additionally, the impact of succinate on NFκB, AP-1 and the MAP kinase ERK inflammatory pathways was examined using a multilayer VEC *in vitro* model. Finally, vaginal succinate concentrations were evaluated following therapeutic modulation of the microbiota toward a *Lactobacillus*-dominant composition using Lactin-V.

5.2 Results

5.2.1 Cervicovaginal microbial composition associates with succinate levels in CVF of pregnant women

Using the data generated from the VMET1 study, which investigated the metabolic profiles of CVF in pregnant women to understand microbial and metabolite associations with reproductive health (outlined in Chapter 3), the levels of succinate in the CVF were assessed. A total of 165 pregnant women were sampled longitudinally through their pregnancy (n = 455 swabs). Succinate concentrations were significantly higher in *Lactobacillus*-deplete samples compared to those dominated by *Lactobacillus* species (P = 4.65e-06; Figure 5.1A). Conversely, LA levels were significantly higher in *Lactobacillus*-dominated samples. When samples were stratified by CST, succinate levels were found to be significantly elevated in women with CST

IV microbiota compared to those with CST I (*L. crispatus*; $P < 0.01$), CST III (*L. iners*; $P < 0.0001$) or CST V (*L. jensenii*; $P < 0.0001$) (Figure 5.1B).

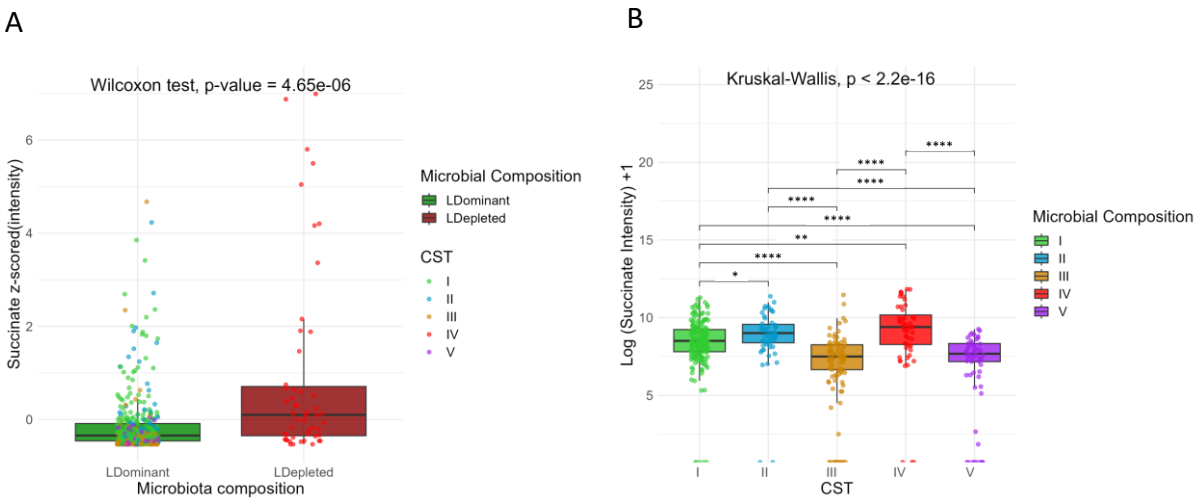

Figure 5.1 Assessment of CVF succinate concentration during pregnancy using direct on-swab desorption electrospray ionisation mass spectrometry (DESI-MS).

(A) Levels of succinate (calculated z-score) in women with *Lactobacillus*-dominant (green, n = 404) were significantly lower than women with *Lactobacillus*-deplete (red, n = 51) vaginal microbiota ($P < 0.0001$; Wilcoxon rank-sum test). **(B)** Levels of succinate (calculated z-score) in women with a CST II-dominant (blue, n = 53; $P < 0.05$) and CST IV-dominant (red, n = 51; $P < 0.01$) vaginal microbiota were significantly higher compared to women with a CST I-dominant (green, n = 188) vaginal microbiota. Whereas women with a CST III-dominant (mustard, n = 102) and CST V-dominant (purple, n = 55) vaginal microbial composition had significantly lower levels of succinate ($P < 0.0001$) compared to the CST I group. Statistical significance was tested using one-way ANOVA Kruskal-Wallis, with Dunn's *post hoc* test. *, ** and **** denote $P < 0.05$, 0.01 and 0.0001, respectively.

5.2.2 Effect of succinate on transcription factor activation in VECs treated with bacterial agonist

Next, FSL-induced phosphorylation of NFκB (p-p65), and AP-1 (p-cJun), following succinate treatment, was assessed in VECs cultured in KSF pH 7.4, KSF pH 3.9-HCl or KSF (20 mM succinate; pH 4.86). Succinate acid is a dicarboxylic acid with two pKa values of 4.2 and 5.6 and so at pH 4.86 it will be partially protonated. A trend increase in bacterial agonist activation of NFκB at 30 minutes was seen in VECs. This was suppressed by succinate to a level greater than acidity alone. This effect was more pronounced at 1 hour following TLR stimulation

(Figure 5.2A). Consistent with results presented in Chapter 3, AP-1 was significantly activated at 30 minutes by FSL-1 at both pH 7.4 ($P < 0.05$) and in cells exposed to acidified media pH 3.9-HCl. This activation was suppressed by succinate ($P < 0.01$) and continued to be suppressed at 1 hour ($P < 0.001$) and 2 hours ($P < 0.0001$) after FSL-1 treatment (Figure 5.2B).

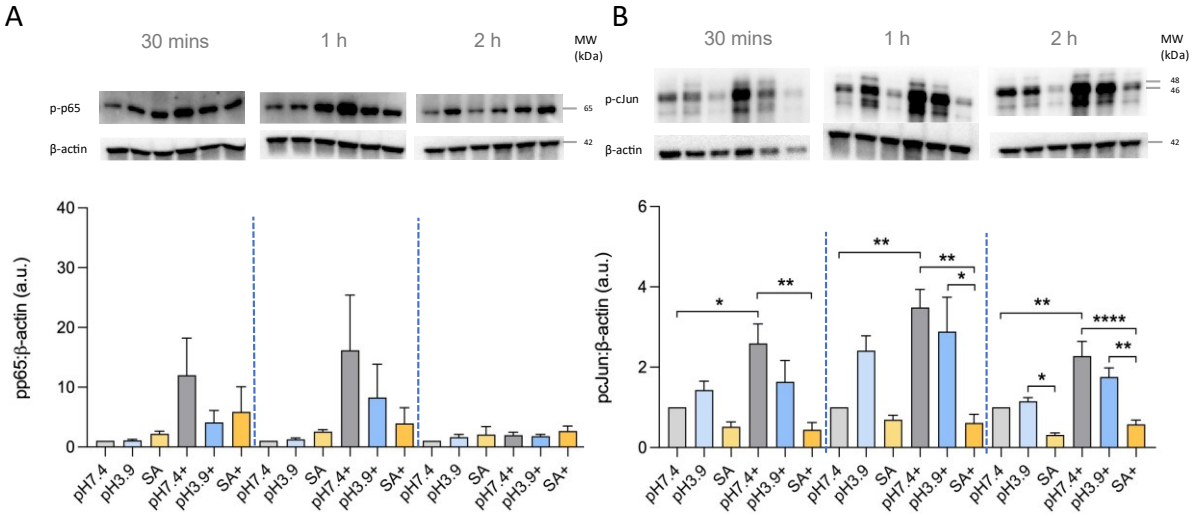

Figure 5.2 Succinate suppresses bacterial agonist-induced activation of transcription factors NFκB and AP-1.

VECs acclimatised for 2 hours in KSF medium at pH 7.4 or acidified to pH 3.9 with HCl or 20 mM succinate (SA; pH 4.86) were stimulated with bacterial agonist FSL-1 (1.0 µg ml^{-1}) for 30 mins, 1 hour and 2 hours as indicated. Whole cell protein extracts were probed for **(A)** p-p65 and **(B)** p-cJun. β-actin was used as a loading control. Graphs show SD from at least three independent experiments (n = 3). Statistically significant differences between the different conditions and treatments were tested using one-way ANOVA and Tukey's *post hoc* test. *, ** and *** denotes $P < 0.05$, 0.01, and 0.0001, respectively. All data were standardised to untreated cells at pH 7.4 for each timepoint.

5.2.3 Effect of succinate on MAP kinase ERK activation in VECs treated with bacterial agonist

Examination of phosphorylation status by Western blotting indicated that both acidity (pH 3.9) and succinate (pH 4.86) led to activation of ERK in VECs. This reached statistical significance after 1 hour ($P < 0.05$) of exposure and was maintained at 2 hours (Figure 5.3). Treatment of VECs with the bacterial agonist FSL-1, did not change ERK phosphorylation.

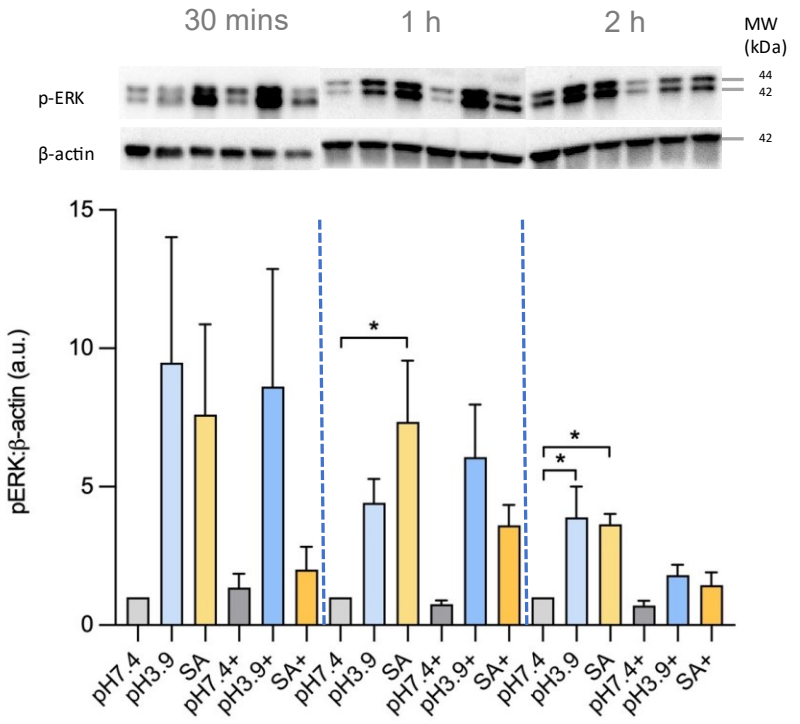

Figure 5.3 ERK activation by succinate is reduced when the VECs have been exposed to a bacterial agonist.

VEC multilayers acclimatised at pH 7.4 or pH 3.9, 20 mM succinate (pH 4.86) for 2 hours were stimulated with bacterial agonist FSL-1 (1.0 µg ml^{-1}) for 30 mins, 1 hour and 2 hours as indicated. Whole cell protein extracts were probed for p-ERK. β-actin was used as a loading control. Graphs show SD from at least three independent experiments (n = 3). Statistically significant differences between the different conditions and treatments were tested using one-way ANOVA and Tukey's *post hoc* test. * denotes $P < 0.05$.

5.2.4 The effect of *L. crispatus* colonisation in pregnant women on CVF succinate concentration and inflammation

The FLIP-1 study data were interrogated to determine if vaginal CST transition from a *L. crispatus*-deplete microbial community to *L. crispatus*-dominant state was associated with a change in succinate levels. Prior to treatment with Lactin-V, succinate levels were similar between the *Lactobacillus*-dominant and the *Lactobacillus*-deplete samples. Concentrations of succinate remained similar in women who shifted from CST IV to CST I post-treatment at timepoint 4, 8 weeks following the last dose of Lactin-V. In the two women whose microbial

composition did not transition from CST IV despite treatment, high levels of succinate were observed (Figure 5.4A).

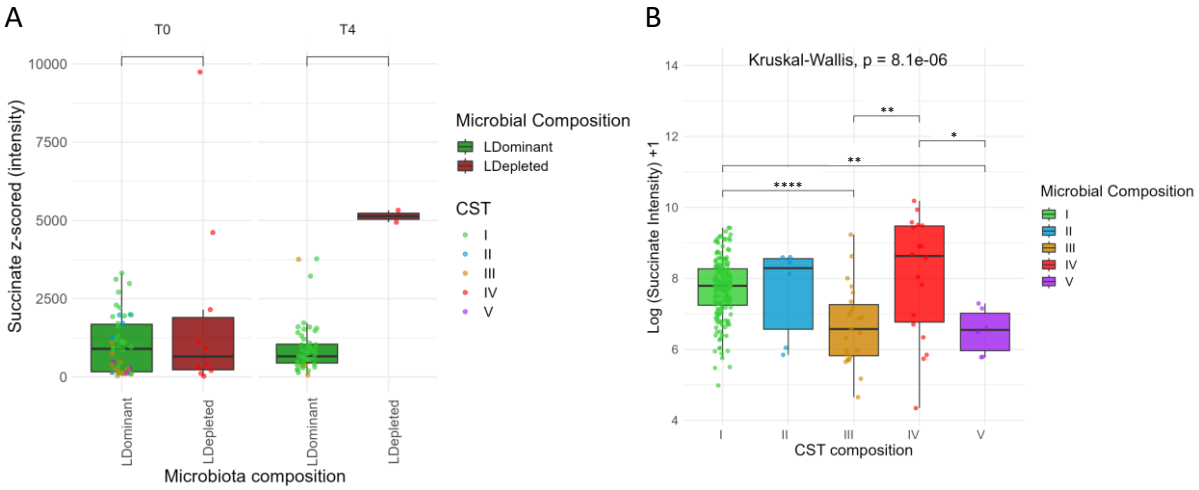

Figure 5.4 Following treatment with Lactin-V levels of succinate increase in cervicovaginal fluid samples that are Lactobacillus-deplete.

(A) Levels of succinate (calculated z-score) are similar between *Lactobacillus*-dominant (green, n = 333) states with *Lactobacillus*-deplete (red, n = 29) at T0. At T4 succinate levels remain low in all but two patients. Statistical significance was tested using Wilcoxon rank-sum test. **(B)** Boxplots showing levels of succinate (calculated z-score) in CST I (green, n = 292), CST II (blue, n = 6), CST III (mustard, n = 29), CST IV (red, n = 29) and CST V (purple, n = 6). Statistical significance was tested using one-way ANOVA Kruskal-Wallis test, with Dunn's *post hoc* test. *, ** and **** denote $P < 0.05$, 0.01 and 0.0001, respectively.

When samples were stratified by CST, succinate levels were higher in women with a CST IV-dominant microbiota composition compared to CST I, CST II, CST III and CST V. These differences reached statistical significance for comparisons with CST III ($P < 0.01$) and CST V ($P < 0.05$). In addition, elevated succinate levels were also observed in women with *L. crispatus* (CST I) or *L. gasseri* (CST II) dominance in their CVF. In contrast, succinate levels were significantly lower in microbiota dominated by *L. iners*- (CST III) or *L. jensenii*-dominant (CST V) compared to CST I ($P < 0.0001$ and $P < 0.01$ respectively) (Figure 5.4B).

Despite these findings, the analysis of paired samples revealed that succinate levels increased in 20 out of 28 participants (71.4%) between baseline (T0) and T4 during the trial. Two patients (F035 and F039) did not transition and, whilst retaining a CST IV-dominant microbiota composition, exhibited higher succinate levels. In cases where succinate levels of decreased,

one participant transitioned to CST III (F049) and six participants transitioned to CST I (F001, F034, F059, F063, F067 and F071) (Figure 5.5).

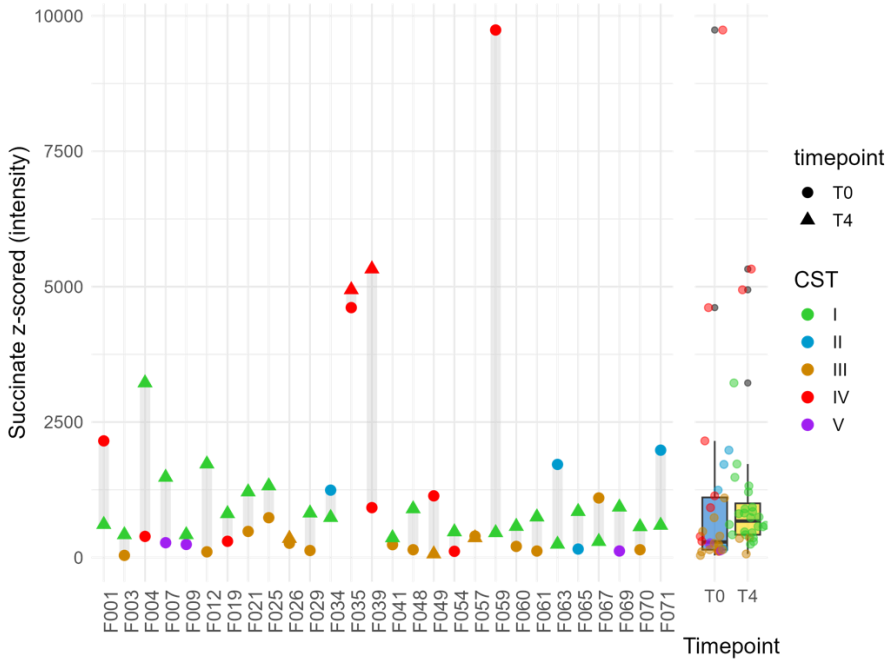

Figure 5.5 Succinate levels show an upward trend in the paired samples following Lactin-V treatment.

Levels of succinate were measured using DESI-MS in paired samples (n = 28) following treatment with *L. crispatus* biotherapeutic Lactin-V. from time point zero (T0 = 14 weeks' gestation) to time point 4 (T4 = 28 weeks' gestation).

A sub analysis of women who transitioned from CST IV to CST I showed a variable change in CVF succinate levels. In patient F059, transition from CST IV to CST I was associated with a dramatic decrease in succinate levels. A moderate decrease in succinate levels was observed for patient F001. However, in the remaining three patients, transition to CST I was associated with a relatively small increase in succinate levels at T4 (Figure 5.6).

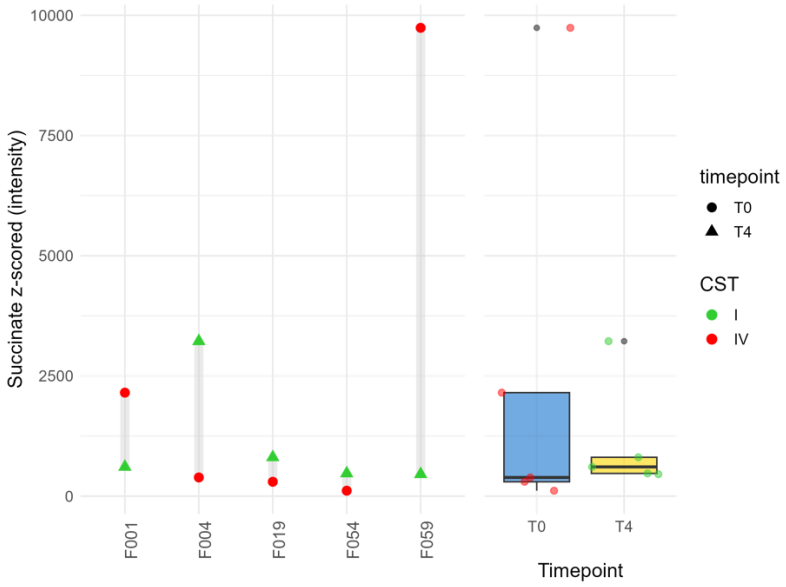

Figure 5.6 Succinate levels change when CVF microbial community transitions from CST IV to CST I following Lactin-V treatment.

Levels of succinate were measured from time point zero (T0 = 14 weeks' gestation) to time point 4 (T4 = 28 weeks' gestation) using DESI-MS in paired samples (n = 28) following treatment with *L. crispatus* biotherapeutic Lactin-V.

As presented in Chapter 3, composition analysis of these patients indicated that changes in succinate levels were closely linked to bacterial composition. In the two patients where succinate levels decreased following transition to CST I initial colonisation at T0 was dominated by *G. vaginalis* (66.0%) and *L. iners* (16.9%) (F001), and by *P. amnii* (33.3%), *G. vaginalis* (12.8%) and an uncultured bacterium (34.5%) (F059). In both cases, lactate levels increased and IL-1β levels decreased following treatment with Lactin-V (Figure 3.17; Chapter 3). In patient F004 where succinate levels increased nearly fourfold, initial colonisation was dominated by the LA-producing bacterium *Bifidobacterium* (96.1%) and this corresponded to a decrease in IL-1β levels. In two patients (F019 and F054), succinate levels showed only a slight increase following transition to CST I. Both were colonised by *G. vaginalis* (46.6% and 96.0% respectively) at the start of the study. Patient F019, who was also colonised by *L. acidophilus* (48.3%), exhibited high levels of lactate at T0, while patient F054 had low lactate levels. Minimal changes were observed in the IL-1β levels in both patients.

In women who did not transition to CST I following treatment with Lactin-V, succinate levels in CVF were observed to vary (Figure 5.7). In three patients (F026, F049 and F057), maintenance of *L. iners* dominance (F026 and F057) or a shift from CST IV to *L. iners* (F049) resulted in minimal changes in succinate concentrations. In patient F035, initial colonisation at T0 was dominated by *S. amnii* (46.81%), *G. vaginalis* (19.52%) and *S. sanguinegens* (15.48%). This patient transitioned to *G. vaginalis* (74.21%) dominance at T4, maintaining relatively high levels of succinate across both timepoints. Lactate levels remained low, and IL-1β levels stayed relatively high (Figure 3.18; Chapter 3). Patient F039 exhibited a substantial increase in succinate levels between T0 and T4, coinciding with a shift in dominance from *G. vaginalis* (67.82%) and *L. iners* (18.40%) to *G. vaginalis* (82.34%).

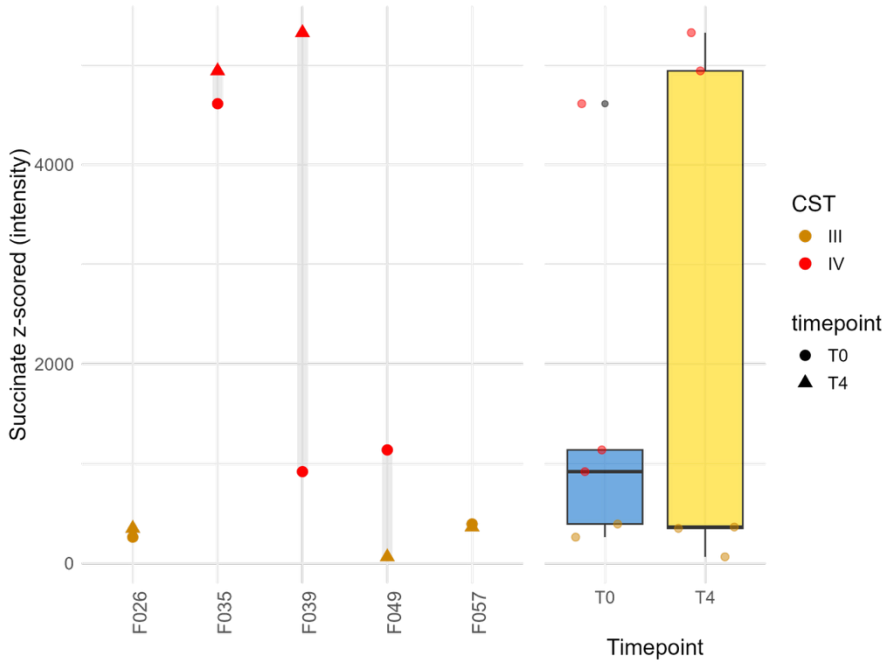

Figure 5.7 Failure to transition to CST I following Lactin-V treatment leads to changes in succinate levels.

Using DESI-MS levels of succinate were measured in paired samples that did not transition to CST I (n = 5) following treatment with *L. crispatus* biotherapeutic Lactin-V (n = 5).

5.3 Discussion

As shown in Chapters 3 and 4, LA plays a protective role by suppressing key kinases involved in inflammatory pathways and their associated transcription factors. Whilst LA is the main bacterial metabolite when *Lactobacillus* species dominate the lower FRT, acetic acid and succinic acid are also present and to a lesser extent propionic and butyric acid (200, 293, 294, 465). Depletion of *Lactobacillus* species in the vaginal microbiota, often observed in BV, is associated with decreased vaginal LA concentrations and increased levels of SCFAs such as acetate, propionate and butyrate, alongside fatty acid metabolism intermediates like succinate (1, 217, 295). This shift in the CVF metabolome is often linked to increased pH and inflammation (199, 200).

In this chapter, the immunomodulatory role of succinate was investigated as a representative bacterial metabolite linked to a pro-inflammatory vaginal environment. CST IV bacteria *Prevotella*, *Bacteroides* species and *G. vaginalis* are often implicated where vaginal succinate levels are high (245). Building on findings in non-pregnant women reported in the literature, it was hypothesised that during pregnancy, depletion of *Lactobacillus* species in the vaginal niche would correlate with elevated succinate levels. Consistent with this hypothesis, the highest succinate concentrations were observed in women with CST IV microbiota. However, relatively high levels of succinate were also observed in women with CST I and CST II vaginal microbiota compositions. A recent study using NMR-based metabolic profiling measured and compared succinate levels in the CVF of women delivering term and preterm and made similar observations (305). These findings align with *in vitro* data showing that *L. crispatus* and *L. gasseri* can produce succinate, potentially accounting for the elevated levels in the CVF of women with CST I and II microbiota compositions (248, 306).

Like LA, succinate can function as an immunomodulatory signalling molecule (480). For example, in macrophages, extracellular succinate activates the succinate receptor 1 (SUCNR1 or GPR91) initiating G protein-mediated phosphoinositide-specific phospholipase C (PLC) signalling. This leads to increased transcription of anti-inflammatory genes, including Arg1, Mrc1, and Fizz1, as well as genes associated with fatty acid oxidation (475, 477, 481, 482).

However, mice studies suggest that microbially derived succinate may exert pro-inflammatory effects in gut mucosal macrophages (483). In a reproductive context, Stafford *et al.* reported significantly lower succinate levels (approximately twofold) in women who delivered preterm compared to those delivering at term (305). Evidence from the MacIntyre and Bennett laboratory at Imperial College and others shows that preterm birth is associated with reduced *Lactobacillus* species and increased bacterial diversity (231-233, 484, 485). The findings from Stafford *et al.* may reflect a reduced prevalence or absence of CST I and CST II vaginal microbial communities, which are typically associated with higher levels succinate production (305). This study extends those previous observations by integrating a substantially larger longitudinal pregnancy cohort (165 women sampled at five timepoints versus 78 women at two timepoints), incorporating CST profiling that included CST IV, applying on-swab DESI-MS metabolomics rather than the less sensitive ^{1}H-NMR analysis, and adding a randomised biotherapeutic intervention. For the first time it has been demonstrated that succinate levels are highest in in pregnant women with a CST IV-enriched vaginal microbiota rather than CST I or CST II, revealed distinct *Lactobacillus* species-specific succinate profiles, and linked these to concurrent inflammatory cytokine responses. Unlike prior work, observational and interventional datasets were combined to show how microbiota shifts following *L. crispatus* administration alter succinate trajectories in a CST- and woman-specific manner. Furthermore, the vaginal epithelial cell assays provide mechanistic evidence that succinate can directly modulate innate immune signalling in a pH-dependent manner, suppressing NFκB and AP-1 activation while activating ERK. Together these findings move beyond association to elucidate potential causal pathways linking vaginal microbiota composition, metabolite production, and regulation of local innate immune activity during pregnancy, with implications for mitigating the risk of adverse pregnancy outcomes such as preterm birth (137).

Although SUCNR1 has been identified in various cell types, data from the Human Protein Atlas Project (SUCNR1 gene data available from v23.0.proteinatlas.org) indicate that it is not expressed in vaginal tissues. However, it is found in other reproductive tissues, including the cervix, placenta and endometrium (486). This raises the possibility that other, as yet unidentified, receptors may be involved in succinate signalling. When succinate binds to SUCNR1, it activates secondary messengers like cAMP, Ca^{2+} and inositol 1,4,5-trisphosphate

(IP3), as well as downstream effectors which mediate cell-specific responses. In dendritic cells, succinate triggers intracellular calcium mobilisation, induces migratory responses and acts in synergy with TLR ligands to produce pro-inflammatory cytokines (487). Conversely, in macrophages, succinate activates anti-inflammatory signalling via PKA and CREB (477). This effect is specific to succinate and independent of acidity. In VECs, succinate did not strongly activate the NFκB and AP-1 signalling pathways. Instead, AP-1 activation was inhibited by succinate to a greater extent than acidity alone. Similar results were observed when VECs were treated with FSL-1, mirroring the effects of LA reported in Chapter 3. Delgado-Diaz *et al.* similarly demonstrated in a VEC monolayer model cultured at pH 7, that succinate did not increase in pro-inflammatory immune mediators such as IL-6, IL-8, IL-1β, RANTES and TNFα (308). The findings in this chapter suggest that succinate is an important modulator of inflammatory pathways in VECs. Whether SUCNR1 or an alternative succinate receptor is expressed by VECs requires further investigation.

In human dendritic cells, cardiomyocytes and embryonic kidney cells, succinate activates the ERK1/2 pathway (487-489). Similarly, succinate activated ERK in VECs, albeit not to the same extent as LA. There did not appear to be as marked a difference in activation between acidity and succinate. However, the physiological role of ERK activation by succinate in VECs remains unclear. Furthermore, this chapter's focus on ERK precluded investigation of other upstream kinases explored in Chapter 4. Evidence from a retinal rat cell line suggests succinate may also activate JNK and p38 (490). Further studies should address upstream mechanisms underlying succinate-mediated inhibition of NFκB and AP-1.

The functional role of succinate in modulating inflammatory pathways is highly tissue and cell-type dependent. While succinate drives IL-1β production in murine macrophages, it exhibits anti-inflammatory properties in VECs (491). Supporting this anti-inflammatory role in the vaginal niche, the FLIP-1 study *in vivo* data showed that transitioning vaginal microbiota to *L. crispatus* dominance increased succinate levels in 78% of participants. Instances where succinate levels did not increase were potentially influenced by changes in microbiota composition. For example, one participant (F059), with two bacterial species dominant at baseline: *Prevotella* (33.3%) which is a succinate-producer and an unknown species,

transitioned to CST I, and succinate levels decreased. It is feasible that the unassigned species observed at baseline was an active succinate producer and that the shift towards *L. crispatus* dominance led to an overall reduction in succinate production. Another participant, initially dominated by *S. amni* (46.8%), *G. vaginalis* (19.5%) and *S. sanguinegens* (15.5%) maintained high levels of succinate after transitioning to *G. vaginalis* (74.2%) dominance, consistent with earlier reports associating *G. vaginalis* with high vaginal levels of succinate (492-495).

Further research should investigate succinate's upstream signalling pathways in the vaginal environment and assess other SCFAs, such as acetate, propionate and butyrate. Identifying SCFA receptors in VECs, including SUCNR1, is critical to understanding the signalling role of these metabolites. (496).

This work offers a new perspective on succinate's role in modulating inflammation in the cervicovaginal niche. Elevated levels of succinate, previously associated with pro-inflammatory states, exhibited anti-inflammatory effects in VECs by inhibiting transcription factors like NF-κB and AP-1. Transitioning a woman's vaginal microbiota to CST I through *L. crispatus* biotherapeutic intervention increased succinate levels and correspondingly reduced inflammation, as shown by a 65% decrease in IL-1β levels. These findings are important clinically as they highlight that succinate levels in the cervicovaginal niche may support reproductive health rather than indicate adverse outcomes.

Chapter 6: Preliminary Investigation into Lactate Receptors

6.1 Introduction

Having demonstrated that LA suppresses the transcription of immune mediators in VECs by inhibiting both transcription factor activation and upstream kinase activation, the next step was to investigate how LA initiates these signalling cascades. Recent studies have proposed several pathways for lactate signalling, as summarised in Figure 6.1 (339). The immunomodulatory effects of LA are highly dependent on cell-type and can be either pro- or anti-inflammatory (497-499). Functional differences in these effects appear to be linked to how and where LA is generated and metabolised. Regardless, LA mediates its effects either directly through GPCRs sensitive to lactate or indirectly via its influence on extracellular acidification (331, 332, 334, 335, 339, 342).

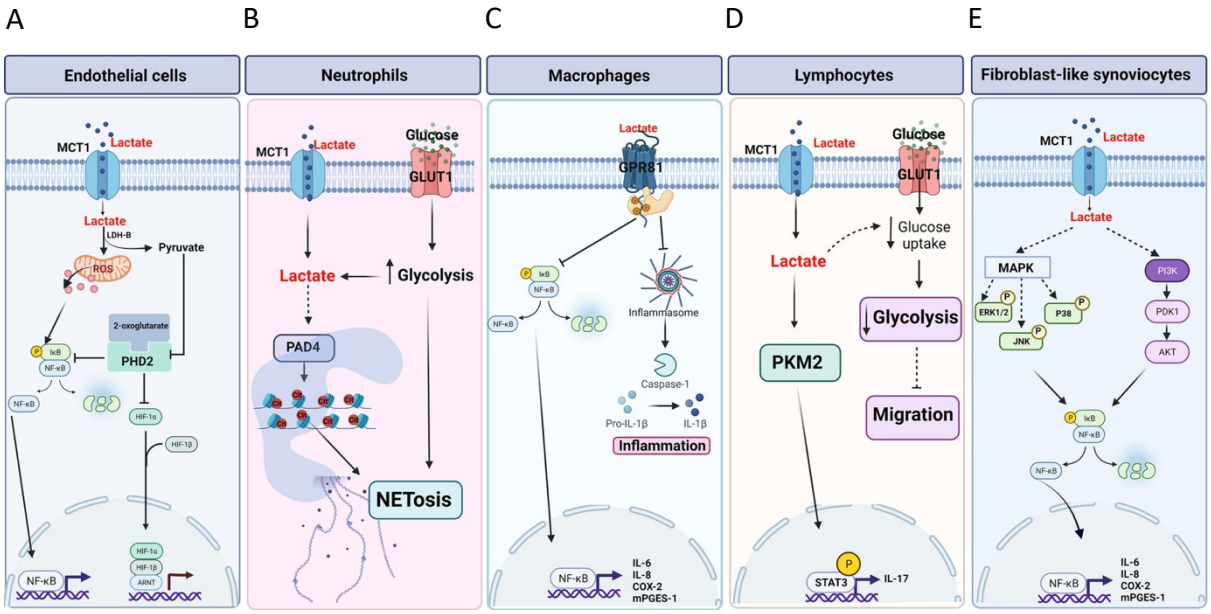

Figure 6.1 Overview of receptor- and channel-mediated mechanisms regulating LA signalling pathways in different cellular systems.

(A) In endothelial cells LA enters the cell through MCT1 transporters and activates the NF-κB pathway through the formation of reactive oxygen species (ROS) (499). **(B)** In neutrophils MCT-1-dependent peptidyl-arginine deiminase-4 (PAD4) activation and glycolysis by LA induces NETosis (Neutrophil Extracellular Traps) (497). **(C)** Both MCT1 and HCAR1 are expressed on macrophages. When LA signals through HCAR1 it reduces the activity of NF-κB and the expression of pro-inflammatory cytokines (341, 498). **(D)** In lymphocytes LA increases the production of pro-inflammatory cytokine IL-17 through MCT1 (500). **(E)** Pro-inflammatory cytokines are produced in fibroblast-like synoviocytes through activation by LA of MAPK and

NF-κB pathways (501) (339). Figure adapted from Manosalva *et al*. (339). *Created with BioRender.com.*

Lactate is transported across the cellular plasma membrane in a stereospecific manner, facilitated by both proton-dependent monocarboxylate transporters: MCT1 (SLC16A1), MCT2 (SLC16A7), MCT3 (SLC16A8), and MCT4 (SLC16A3), as well as sodium-dependent transporters SMCT1 (SLC5A8) and SMCT2 (SLC5A12) (502, 503). While each transporter preferentially facilitates lactate transport in a specific direction, for instance MCT4 favours efflux and MCT1 favours influx, the actual directionality depends on the lactate gradient. Additionally, the undissociated form of lactic acid can diffuse passively across the plasma membrane, although this process is limited. Under acidic conditions lactate exists predominantly in its protonated form LA ($pK_a = 3.86$), whereas at neutral pH, it primarily exists as the charged unprotonated lactate anion (273).

Recent research has revealed that metabolism-derived small molecules, such as LA and succinate, can initiate signalling pathways by activating GPCRs (322). HCAR1 was first receptor identified as a lactate sensor, initially described in adipocytes (309). This receptor is expressed in various cell types, including the brain, skeletal muscle, kidney, adipose, liver and macrophages, and its expression is influenced by the tissue microenvironment (310, 323-325, 342). Liu *et al.* demonstrated that HCAR1 expression increases as preadipocytes differentiate into adipocytes (310). Binding of LA to HCAR1 induces a conformational change in the receptor, activating the $G\alpha_i$ protein, which subsequently inhibits adenylate cyclase activity and decreases intracellular cAMP levels (310, 324). The reduction in cAMP modulates several key signalling pathways involved in regulating cellular metabolism and survival. These findings suggest that HCAR1 activation plays a significant role in maintaining health and mediating the body's response to disease (323).

Several experimental strategies are available to investigate the molecular mechanisms of GPCR signal transduction. Measuring cAMP levels is a common method to assess the activity of GPCRs as activation of these receptor can trigger a cascade of events that lead to changes in intracellular cAMP levels (504). For example, pertussis toxin (PTX), a bacterial toxin isolated from *Bordetella pertussis*, inhibits G protein coupling to their cognate GPCRs by catalysing

ADP-ribosylation of membrane-bound α subunit of the heterotrimeric $G\alpha_{i/o}$ protein family ($G\alpha_i$, $G\alpha_o$ and $G\alpha_t$ but not $G\alpha_z$) (505, 506). This modification "locks" the $G\alpha_{i/o}$ protein in its GDP-bound state, preventing inhibition of adenylate cyclase and resulting in increased intracellular cAMP levels. The elevated cAMP levels mediate downstream signalling events including activation of cAMP-dependent PKA and exchange protein activated by cAMP (EPAC)production and mediation of downstream transcription factor activation. Activated PKA suppresses the expression of NF-κB-induced pro-inflammatory cytokines and chemokines, while EPAC reduces NF-κB activation and can activate c-Jun via Ras-related protein 1 (Rap1) signalling (Figure 6.2) (507).

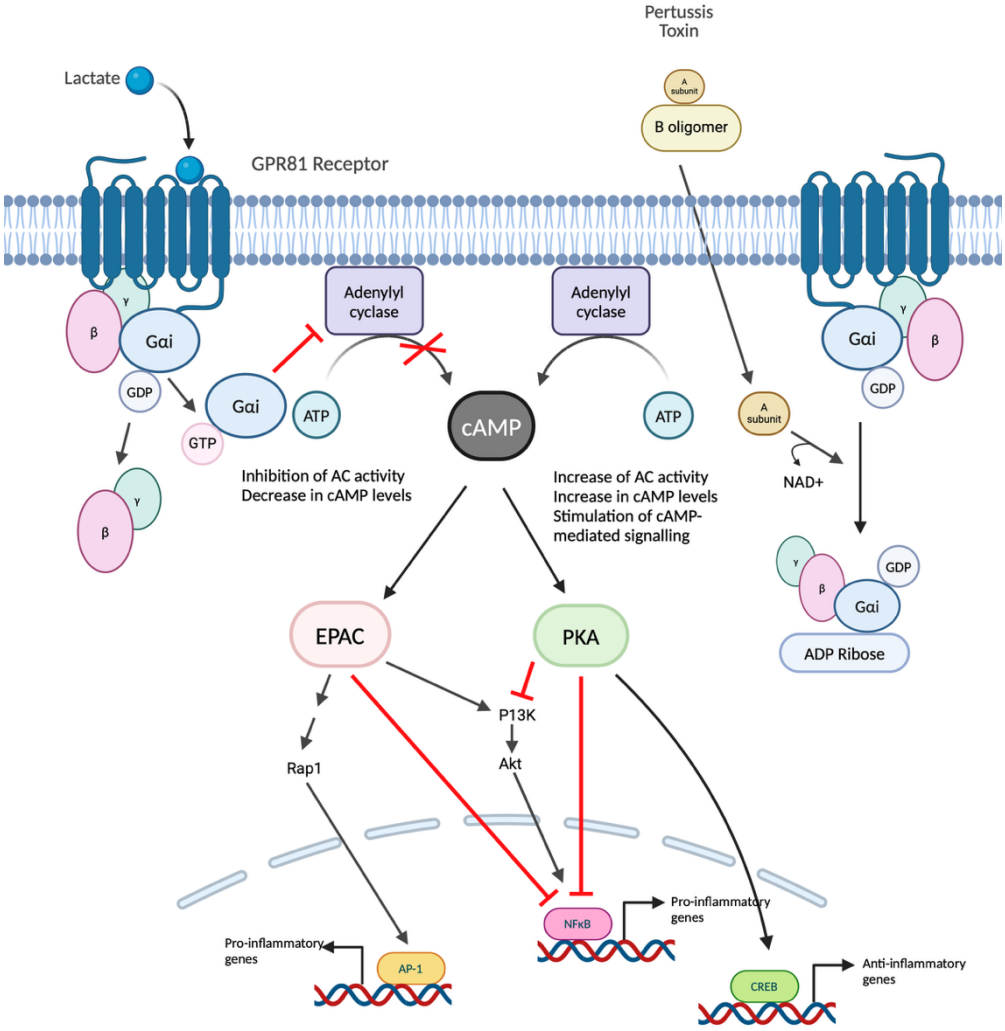

Figure 6.2 LA ligand inhibits cAMP signalling pathways via HCAR1 receptor.

LA binding of HCAR1 leads to the dissociation of the heterotrimeric G protein complex into $G\alpha_{i/o}$ and Gβγ subunits. The resulting activated $G\alpha_{i/o}$ protein then inhibits adenylate cyclase

activity and there is a decrease in intracellular levels of cAMP, a secondary signalling messenger molecule. When the cells are treated with PTX, the A protomer of PTX enters the cells where it catalyses the ADP-ribosylation of $G\alpha_{i/o}$ preventing it from inhibiting adenylate cyclase and resulting in an increase in cAMP levels. The downstream effectors of cAMP include cAMP-dependent protein kinase (PKA), exchange protein activated by cAMP (EPAC) and ion channels. PKA inhibits NF-κB and the PI3K/AKT pathway decreasing the transcription of pro-inflammatory cytokines. In addition, PKA activates the transcription factor CREB. EPAC also inhibits the NF-κB pathway and activates Ras-related protein 1 (Rap1) signalling which leads to the phosphorylation of c-Jun. Adapted from Tavares *et al.* (508). *Created with BioRender.com.*

Lactate receptors or transporters have not yet been identified in VECs. Earlier studies hypothesised that protonated lactate can freely diffuse across the plasma membrane of VECs without requiring monocarboxylate transporters or the HCAR1 receptor (509, 510). In bacterial cells, the entry of LA into the cytosol leads to acidification, which inhibits cellular functions and ultimately results in cell death (277). However, *Lactobacilli* can tolerate a cytoplasmic pH as low as 3.5, and multilayered VECs remain viable when cultured at a pH below 3 (250, 511, 512). This indicates the potential co-evolution of mechanisms in both host and microbial cell types to tolerate acidic conditions. Based on this, it was hypothesised that in VECs, LA acts as a signal transduction molecule by activating transmembrane receptors, which undergo conformational changes to relay the signals to the intracellular environment. To test this hypothesis, a comprehensive literature review was conducted to identify potential receptors and channels, followed by examining the expression of top candidates in VECs. Additionally, the potential involvement of GPCRs in mediating LA-induced activation of intracellular signalling pathways in VECs was investigated.

6.2 Results

6.2.1 Identification of putative LA receptors and channels in VECs

Fourteen potential LA and SCFA receptors and transporters were identified using a BLAST search and a detailed review of the literature (Table 6.1). These included SCFA receptors FFAR3/GPR41 and FFAR2/GPR43, as well as the succinate receptor SUCNR1/GPR91.

Qualitative prospect ranking of each receptor, based on its affinity for lactate in other cellular systems and tissues, led to the selection of five category A candidates for further investigation: MCT1, MCT4, GPR81, SMCT1, and SMCT2.

Table 6.1 Potential receptors for LA identified by BLAST search and literature review.

RECEPTOR	FUNCTION	TISSUE TYPE	PROSPECT RANK
MCT1/SLC16A1	Proton-linked monocarboxylate transporter	Ubiquitous distribution including brain, muscle, liver, kidney and heart (316, 503, 513)	A
MCT4/SLC16A3	Proton-linked monocarboxylate transporter	Commonly found in tissues exporting LA derived from glycolysis eg skeletal muscle, heart, lung, astrocytes, white blood cells, and chondrocytes (316, 503, 513)	A
HCAR1/GPR81	G_i protein-coupled hydroxycarboxylic acid receptor with high affinity for lactic acid	Adipose tissue, intestine, brain, kidney, breast, cervix, uterus (314, 315)	A
SMCT1/SLC5A8	Sodium-coupled monocarboxylate and short-chain fatty acid transporter	Thyroid, kidney, intestine, brain, retina (318, 320, 514)	A
SMCT2/SLC5A12	Sodium-coupled monocarboxylate and short-chain fatty acid transporter	Thyroid, kidney, intestine, brain, retina (318, 320, 514)	A
MCT2/SLC16A17	Proton-linked monocarboxylate transporter	Neurons, liver, parenchymal cells, kidney testes (503)	B
MCT3/SLC16A8	Proton-linked monocarboxylate transporter	Retinal pigment epithelium, chronic plexus epithelium (503)	B
MCT5/SLC16A4	Proton-linked monocarboxylate transporter	Brain, muscle, heart, intestine, liver, kidney, lung, ovary, placenta (503)	B
HCAR2/GPR109A	G_i protein-coupled hydroxycarboxylic acid receptor with high affinity for nicotinic acid	Bone marrow, lymph nodes, brain, intestine, vagina, uterus, ovary, skin (509)	C
HCAR3/GPR109B	G_i protein-coupled hydroxycarboxylic acid receptor with high affinity for nicotinic acid	Bone marrow, lymph nodes, brain, intestine, vagina, uterus, ovary, skin (509, 515)	C
FFAR3/GPR41	G_i protein-coupled free fatty acid receptor	Thyroid, intestine, peripheral nervous system, vagina, uterus, endometrium, placenta (516)	C
FFAR2/GPR43	G_i protein-coupled free fatty acid receptor	Spleen, adipose tissue, immune cells, intestine, endometrium, ovary (300, 516)	C
SUCNR1/GPR91	G_i protein-coupled succinate receptor	Kidney, thyroid, spleen, stomach, uterus (low concentration) (488, 517, 518)	C

The expression of MCT1, MCT4, GPR81, SMCT1, and SMCT2 was measured using qRT-PCR in multilayered VECs cultured at pH 7.4 or pH 3.9 +/- 30 mM L-LA for 2 hours following a 2-hour acclimatisation. mRNA from brain extract was used as a positive control (Figure 6.3).

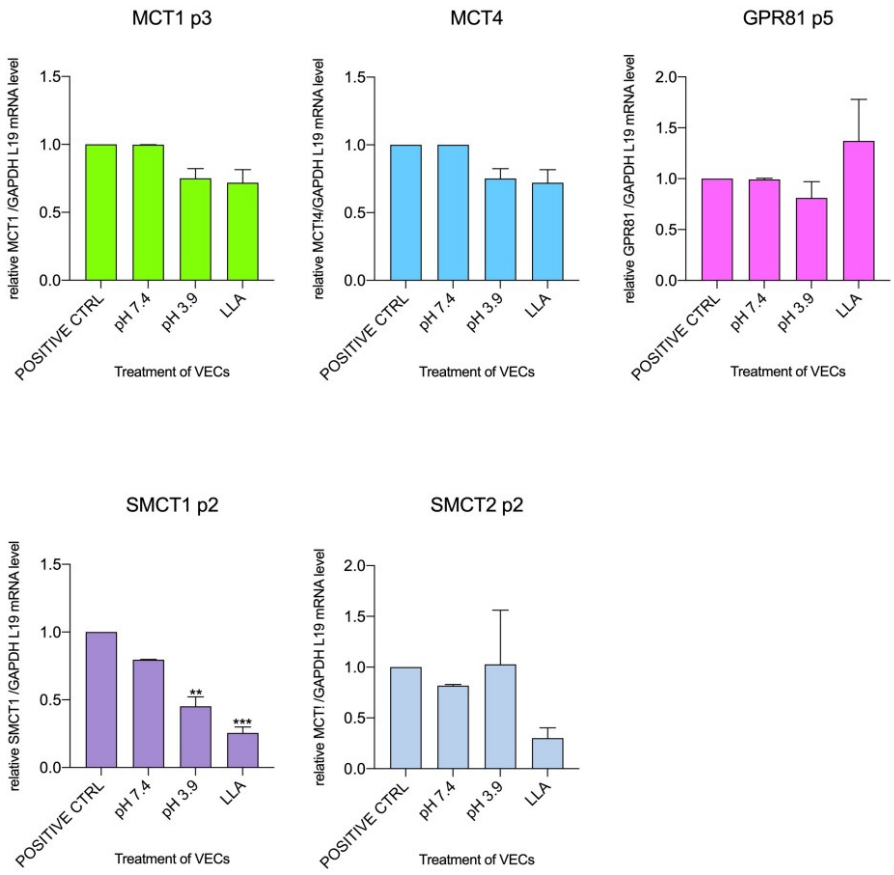

Figure 6.3 mRNA gene expression levels of lactate receptor GPR81 (HCAR1) are increased in the presence of L-LA levels.

Multilayer VECs grown on Transwells® were acclimatised in media at pH 7.4 and pH 3.9 in the absence or presence of 30 mM L-LA for 4 hours. mRNA was isolated from the cells and expression of **(A)** *MCT1* **(B)** *MCT4* **(C)** *GPR81* **(D)** *SMCT1* and **(E)** *SMCT2* genes was measured by quantitative RT-PCR. Gene expression was standardised to the housekeeping genes *L19* and *Gapdh* expressed as a fold change using the $\Delta\Delta C_T$ method. Brain mRNA was used as a positive control. Graphs show SD from at least three independent experiments. Statistically significant differences were tested using one-way ANOVA and Tukey's *post hoc* test. ** and *** denote $P < 0.01$ and 0.001, respectively.

qRT-PCR offers a more sensitive and specific approach to identifying the presence or absence of a particular receptor genes as well as being more cost-effective than proteomics. All five receptors and channels were found to be expressed in VECs, and similar results were obtained before the data were normalised.

The expression of proton-linked monocarboxylate transporters, MCT1 and MCT4, did not increase following acclimatisation in medium at pH 3.9 +/- 30 mM L-LA. Although it did not

reach statistical significance, expression of GPR81/HCAR1 was increased in the presence of 30 mM L-LA but not in media acidified with HCl. SMCT1 expression was significantly decreased by acidity and L-LA ($P < 0.01$ and 0.001, respectively). In contrast, SMCT2 expression decreased in the presence of L-LA but not acidity.

6.2.2 Effect of L-lactate on $G\alpha_i$ signalling of HCAR1

As HCAR1 exhibited the highest relative expression of the examined receptors and MCTs in VECs, and in consideration of its well-described role in regulating LA function in gut epithelial cells, it was hypothesised that in VECs LA signalling is mediated via a GPCR and specifically, $G\alpha_i$ activation. And in addition, that inhibition of HCAR1 would lead to LA-mediated inhibition of cAMP accumulation in VECs.

Examination of cAMP levels in VECs was undertaken in multilayered VEC cultures exposed to 30 mM LA at pH 7.4. As the levels of cAMP in VECs were unknown, the experiment was performed with and without forskolin, a cell-permeable diterpene used to increase cAMP levels through direct activation of adenylate cyclase. Further, as the effect of low pH on cAMP or forskolin was unknown, cell culture conditions were maintained at pH 7.4. Forskolin treatment effectively increased the levels of cAMP in VECs at pH 7.4 ($P < 0.0001$) compared to untreated cells, including in the presence of LA ($P < 0.0001$). However, in forskolin-treated VECs, cAMP levels were significantly reduced by LA ($P < 0.01$) when compared to forskolin-treated VECs without LA present (Figure 6.4).

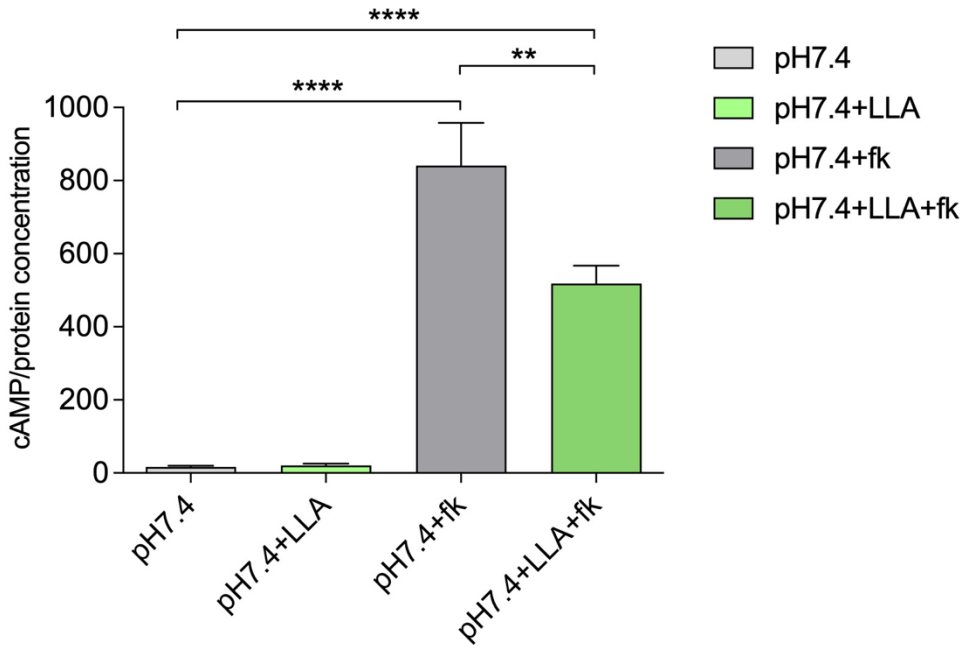

Figure 6.4 L-LA decreases forskolin-induced intracellular cAMP levels at pH 7.4.

Multilayered VECs were treated with IBMX (15 mins, 0.5 mM) before stimulation with or without forskolin (5 mins, 3 µM) at pH 7.4 +/- L-LA (30 mM). The cAMP concentrations (nM) were compared to the protein concentration (µg μl^{-1}). Graphs show ± SD from 3 independent experiments (n = 3). Statistically significant differences were tested using one-way ANOVA and Tukey's *post hoc* test. ** and **** denote $P < 0.01$ and 0.0001, respectively.

Next, VECs were exposed to the physiologically relevant pH of 3.9, acidified either with HCl or 30 mM L-LA (Figure 6.5). Forskolin treatment in the acidified media failed to increase cAMP levels as expected, suggesting that low pH may inhibit forskolin activity.

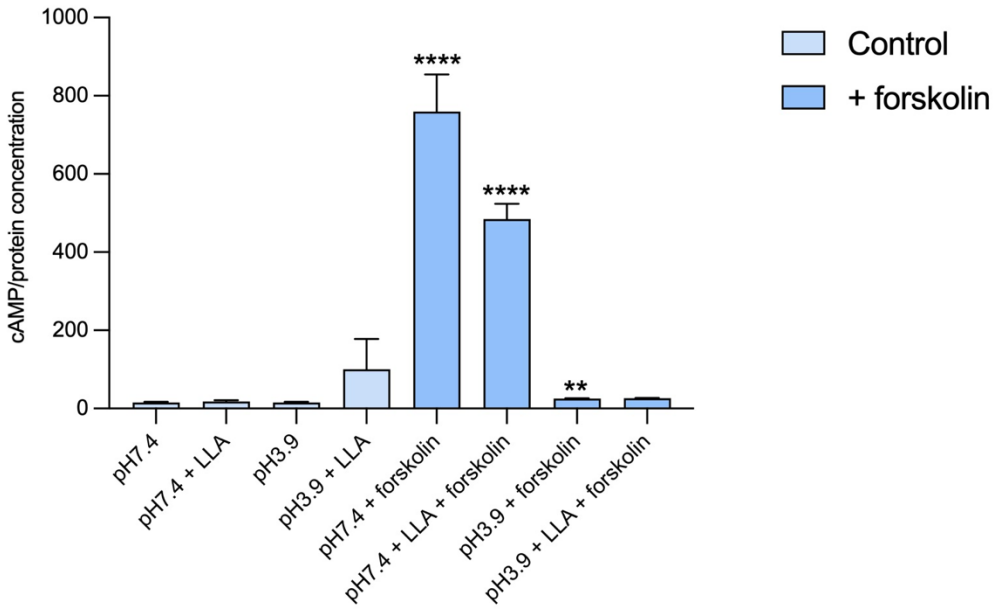

Figure 6.5 Intracellular cAMP levels are affected by low pH.

Multilayered VECs were treated with IBMX (15 mins, 0.5 mM) before stimulation with or without forskolin (5 mins, 3 µM) at pH 7.4 or pH 3.9 +/- 30 mM L-LA. The cAMP concentrations (nM) were compared to the protein concentration (µg μl^{-1}). Data represent mean ± SEM from 4 independent experiments (n = 4). Statistically significant differences were tested using an unpaired t-test. **, *** and **** denote $P < 0.01$, 0.001 and 0.0001, respectively.

6.2.3 Effect of pertussis toxin (PTX) on GPCR signalling in VECs

It was hypothesised that the suppressive effect of cAMP levels by L-LA could be inhibited by treating the cells with PTX which prevents the $G\alpha_i$ protein from inhibiting adenylyl cyclase. VECs were pre-treated with PTX (200 ng ml^{-1}), and cAMP levels were assessed following stimulation with or without forskolin (5 minutes, 3 µM) at pH 7.4 +/- L-LA (30 mM) or pH 3.9 +/- L-LA (30 mM) (Figure 6.6). First it was observed that cAMP levels in VECs unexpectedly decreased when the cells were pre-treated with PTX. This reduction was significant in all the conditions measured ($P < 0.05$) except for pH 3.9-HCl.

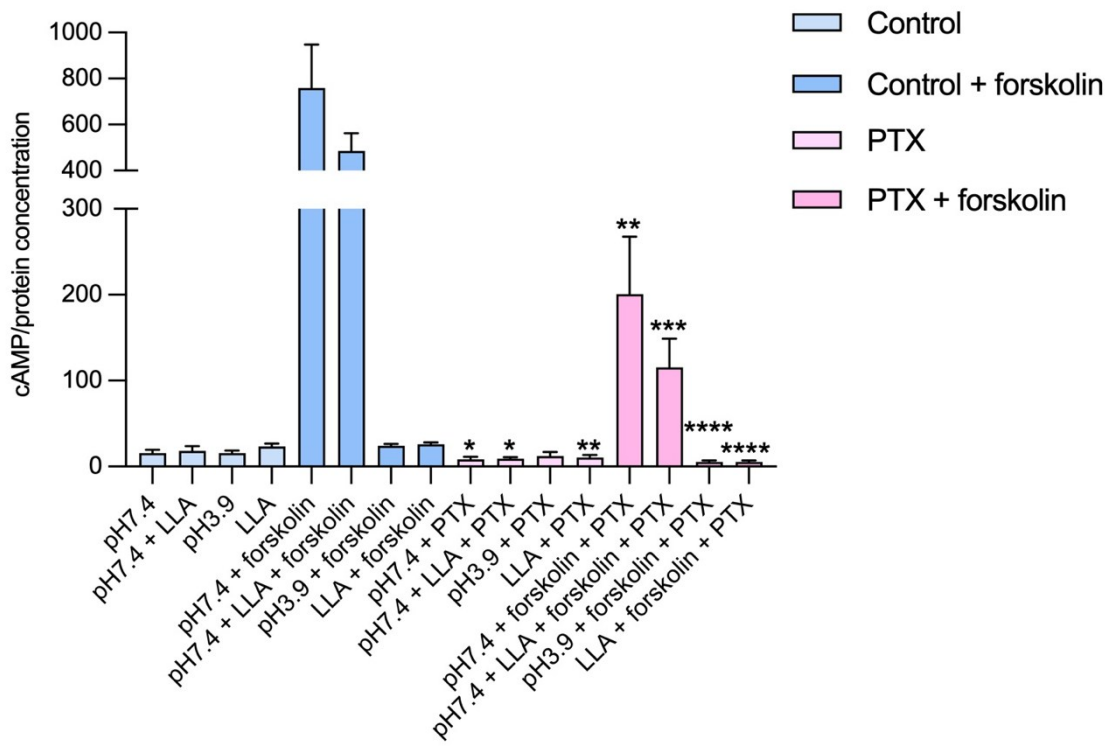

Figure 6.6 Pertussis toxin (PTX) significantly decreases concentrations of intracellular cAMP at pH 7.4.

Multilayered VECs were pre-treated with PTX (200 ng ml^{-1}) for 24 hours before treatment with IBMX (15 mins, 0.5 mM) and stimulation with or without forskolin (5 mins, 3 µM) at pH 7.4 +/- L-LA (30 mM) or pH 3.9 +/- 30 mM L-LA. The cAMP concentrations (nM) were compared to the protein concentration (µg/$µl^{-1}$). Data represent mean ± SEM from 4 independent experiments (n = 4). Statistically significant differences were tested using an unpaired t-test. *, **, *** and **** denote $P < 0.05$, 0.01, 0.001 and 0.0001, respectively.

Next the effect of forskolin on the L-LA-induced suppression of cAMP in VECs was compared to the treatments with and without PTX pre-treatment (Figure 6.7).

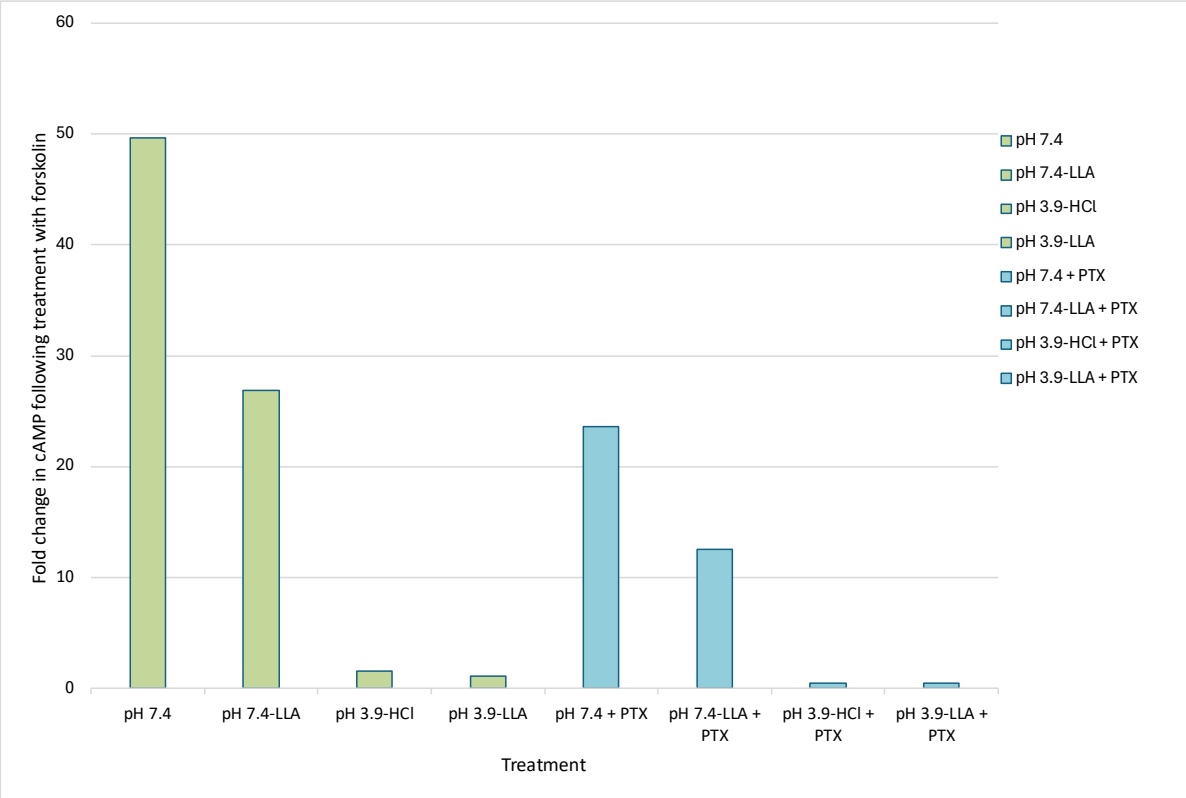

Figure 6.7 Effect of forskolin on cAMP levels in VECs.

Multilayered VECs were treated with IBMX (15 mins, 0.5 mM) before stimulation with or without forskolin (5 mins, 3 µM) at pH 7.4 or pH 3.9 +/- 30 mM L-LA. The cAMP concentrations (nM) were compared to the protein concentration (µg μl^{-1}). The fold change in cAMP levels when forskolin was present was calculated relative to VECs not exposed to forskolin. Data are mean ± SEM from 4 independent experiments (n = 4).

At pH 7.4, forskolin treatment of VECs led to a 49.6-fold increase in cAMP and when L-LA was present the increase was 26.9-fold. Whereas when PTX was present at pH 7.4 the increases in cAMP levels were much lower: 23.6- and 12.6-times higher, respectively. No effect was observed when the pH was lowered to 3.9.

6.2.4 Effect of pertussis toxin on inflammatory transcription factors NFκB and AP-1, and MAP kinase ERK

One of the major cellular effectors activated by GPCRs is the MAPK pathway, including phosphorylation of ERK1/2, resulting in its nuclear translocation (519). As L-LA strongly

activates ERK in VECs, the effect of treating VECs with PTX on ERK and transcription factors NF-κB and AP-1 was investigated (Figure 6.7). Activation of NF-κB was significantly suppressed by PTX at pH 3.9-HCl ($P < 0.05$) and pH 3.9-LLA ($P < 0.01$) (Figure 6.7A). Both AP-1 and ERK were suppressed when cells had been pre-treated with PTX, but this did not reach statistical significance (Figure 6.7B and C).

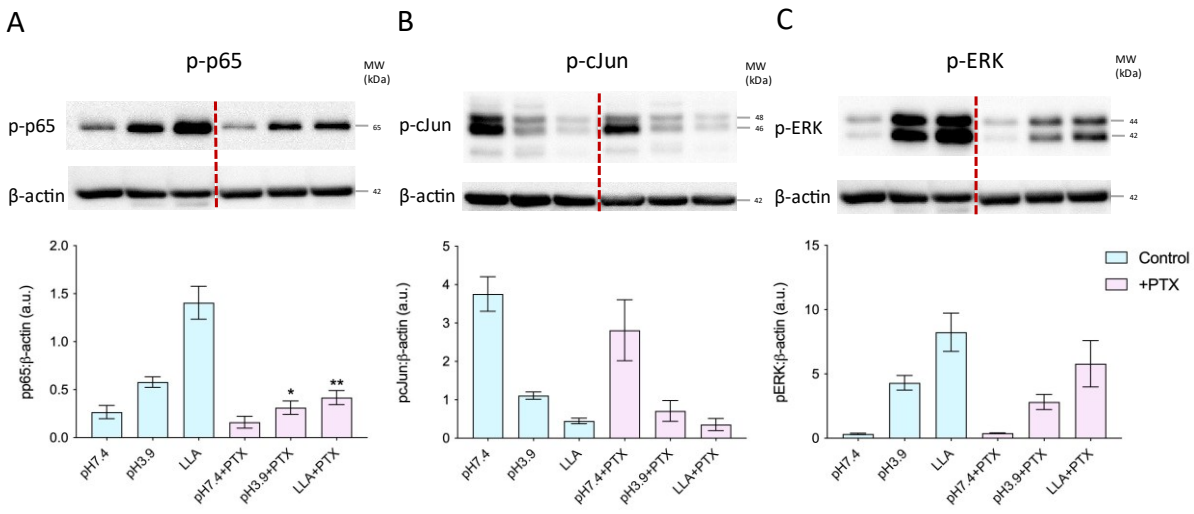

Figure 6.8 Pertussis toxin suppresses phosphorylation of p65, c-Jun and ERK in VECs.

VECs grown in multilayers were pre-treated with PTX (200 ng ml^{-1}) for 24 hours, acclimatised for 2 hours in the presence or absence of 30 mM L-LA (pH 3.9), or media at pH 7.4 and incubated for an additional 30 mins. Whole cell protein extracts were probed for **(A)** p-p65, **(B)** p-cJun and **(C)** p-ERK. Cutting point of blots to remove blots where cells were treated with the viral agonist is indicated by the red line. Data represent mean ± SEM from 4 independent experiments (n = 4). Statistically significant differences were tested using an unpaired t-test. * and ** denote $P < 0.05$ and 0.01, respectively.

As demonstrated in Chapters 3 and 4, LA suppresses FSL-1-induced MAPK and pro-inflammatory transcription activation in VECs, while concurrently increasing activation of ERK. If LA signalling in VECs is mediated via a GPCR/$G\alpha_i$-coupled mechanism, then inhibition with PTX would be expected to inhibit the capacity of LA to suppress transcription factor and MAPK activation.

Treatment of VECs with PTX for 24 hours prevented FSL-1-induced activation of NF-κB and neither HCl nor LA suppressed NF-κB beyond baseline (Figure 6.8D). AP-1 was significantly activated by FSL-1 in cells treated with PTX ($P < 0.0001$) (Figure 6.8E) and this activation was

still suppressed by either HCl or LA ($P < 0.0001$). ERK activation by both HCl and LA acidification, was tapered by PTX treatment. However, ERK phosphorylation was still significantly increased with LA after 30 minutes of exposure in the presence of PTX ($P < 0.01$) (Figure 6.8F).

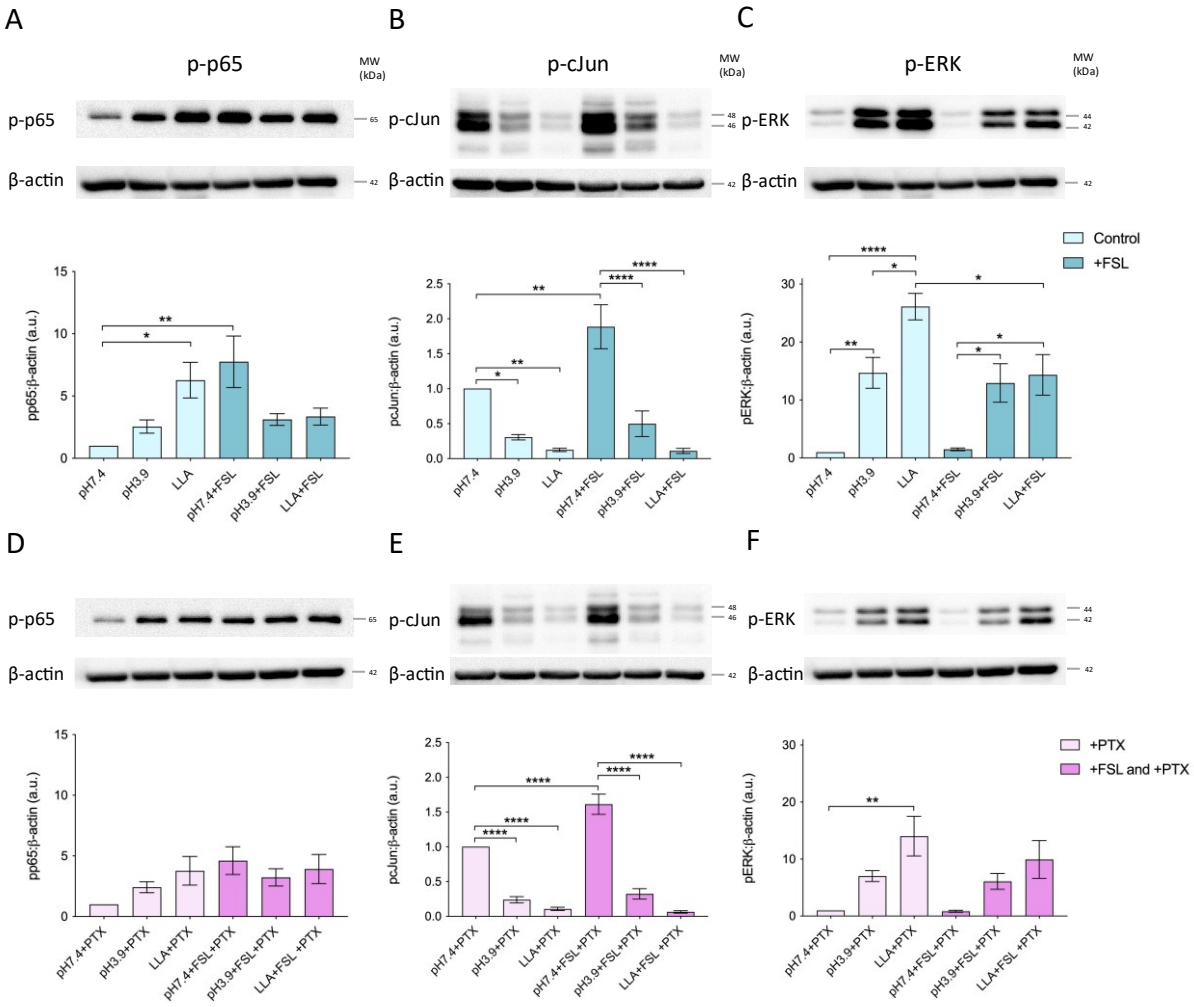

Figure 6.9 L-LA activation of ERK is reduced but not absent when VECs have been pre-treated with pertussis toxin.

VECs grown in multilayers were pre-treated with PTX (200 ng ml^{-1}) for 24 hours **(D, E, F)** or left untreated with PTX **(A, B, C)**, acclimatised for 2 hours in the presence or absence of 30 mM L-LA (pH 3.9), or media at pH 7.4 before 30 mins treatment with bacterial agonist FSL-1 (1.0 µg ml^{-1}). Whole cell protein extracts were probed for p-p65 **(A, D)**, p-cJun **(B, E)** and p-ERK **(C, F)**. Data represent mean ± SEM from 4 independent experiments (n = 4). Statistically significant differences were tested using one-way ANOVA and Tukey's *post hoc* test. *, ** and **** denote $P < 0.05$, 0.01 and 0.0001, respectively.

To determine the effect of PTX on VECs as well as the response of treating the cells with a bacterial agonist, a 2-way ANOVA statistical analysis was carried out. To facilitate visualisation of these comparisons, the data has been replotted in Figure 6.9.

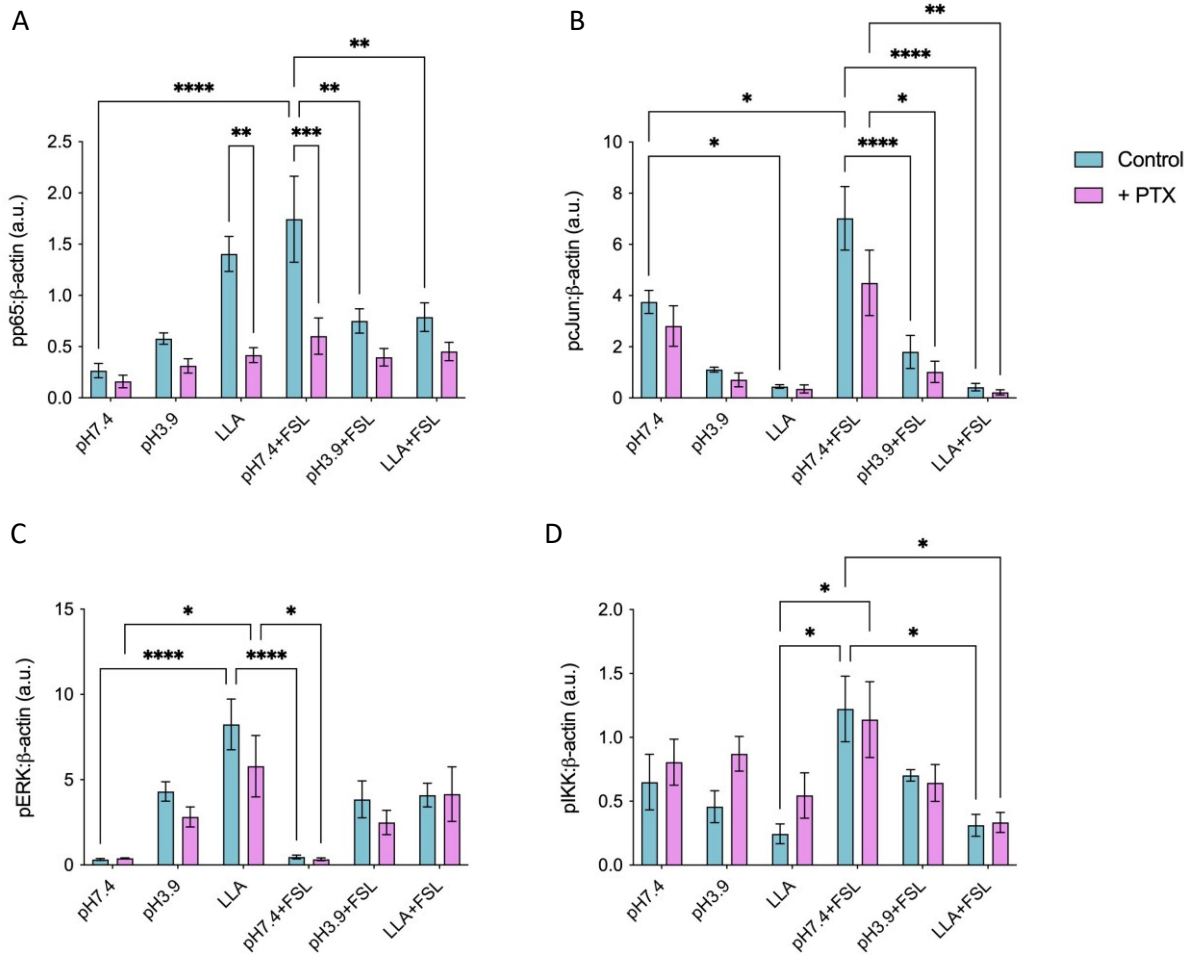

Figure 6.10 Differential effects of cAMP regulation of inflammatory pathways.

VECs grown in multilayers were pre-treated with PTX (200 ng ml^{-1}) for 24 hours or left untreated with PTX, acclimatised for 2 hours in the presence or absence of 30 mM L-LA (pH 3.9), or media at pH 7.4 before 30 mins treatment with bacterial agonist FSL-1 (1.0 µg ml^{-1}). Whole cell protein extracts were probed for **(A)** p-p65, **(B)** p-cJun, **(C)** p-ERK and **(D)** p-IKK. Data represent mean ± SEM from 4 independent experiments (n = 4). Statistically significant differences were tested using two-way ANOVA and Tukey's *post hoc* test. *, **, *** and **** denote $P < 0.05$, 0.01, 0.001 and 0.0001, respectively.

This set of experiments demonstrated an increase in NF-κB in the presence of L-LA, a result not observed in Chapter 3. This may be attributed to the acidification effect previously described, which had not yet returned to basal levels in this set of cells. Nevertheless, NF-κB was significantly upregulated by FSL-1 at pH 7.4 ($P < 0.0001$), although the increase was less

pronounced than initially observed. This activation was significantly suppressed by both acidity ($P < 0.01$) and L-LA ($P < 0.01$). When PTX was introduced, NF-κB activation was suppressed across all conditions, with significant suppression observed in cells treated with L-LA ($P < 0.01$) and in FSL-1-treated cells at pH 7.4 ($P < 0.001$) (Figure 6.9A). In contrast, AP-1 activation was not significantly suppressed by PTX. Importantly, L-LA retained its ability to suppress FSL-1-induced AP-1 activation even in the presence of PTX ($P < 0.01$) (Figure 6.9B).

The effect of PTX on two upstream regulators discussed in Chapter 4 was also examined. Consistent with previous observations, FSL-1 did not activate ERK, even in the presence of PTX. However, the significant basal activation of ERK by L-LA ($P < 0.0001$) was also observed when PTX was present ($P < 0.05$) (Figure 6.9C). As PTX is known to influence NF-κB, its effect on IKK, a kinase upstream of NF-κB, was examined. PTX notably increased IKK expression at basal levels under all three conditions: pH 7.4, pH 3.9-HCl and pH 3.9-LLA, though these increases did not reach statistical significance (Figure 6.9D). When VECs were treated with the TLR2/6 agonist FSL-1, PTX-induced IKK activation by was not observed. Additionally, L-LA's suppression of FSL-1-induced IKK remained unaffected by PTX and approached statistical significance ($P = 0.0658$).

6.3 Discussion

This chapter has focused on the transporters and receptors involved in lactate signalling in VECs. The results show the mRNA expression of proton-linked monocarboxylate transporters MCT1 and MCT4 as well as the lactate G_i-type G protein-coupled receptor HCAR1 (GPR81) in VECs. Expression of the sodium-linked monocarboxylate transporters SMCT1 and SMCT2 was suppressed by acidity with SMCT2 being suppressed specifically by LA. The main function of MCTs and SMCTs is to remove LA from the cell to prevent excess intracellular accumulation of LA due to increased glycolytic activity. As the focus of this thesis was the signalling properties of LA, only HCAR1 was investigated further.

GPCRs are involved in the transduction of a variety of extracellular signals, modulating cell metabolism and function, and activating intracellular cascades leading to different responses. Lactate was first identified as the endogenous ligand for HCAR1 in adipocytes and this receptor has since been identified in many other types of cells but not VECs (310, 520). As HCAR1 is coupled to an inhibitory G-protein, lactate binding would be expected to reduce intracellular cAMP levels (310, 509). Additionally, cAMP can activate downstream effectors such as PKA and EPAC which can lead to suppression of NF-κB. PKA inhibits NF-κB through different mechanisms such as preventing nuclear translocation by inhibiting IκB degradation or by inhibiting upstream signalling pathways like PI3K/AKT (521-523).

For the first time in VECs, these experiments demonstrated that at pH 7.4, L-LA mediated a lactate receptor/cAMP-coupled response. When VECs were treated with 30 mM L-LA, cAMP levels decreased by approximately 30%, suggesting that the $G\alpha_i$ subunit had decoupled from the G protein in the HCAR1 receptor, indicating a potential $G\alpha_i$ response. However, at pH 3.9, the low pH markedly reduced the ability of forskolin to increase cAMP levels, making it impossible to evaluate the effects of L-LA or acidity on cAMP. The data allude to the possibility that forskolin's functionality in VECs is affected by pH. Low pH could be inhibiting forskolin's action on adenylate cyclase, or having an impact on adenylate cyclase activity, indicating that the tools chosen to study GPCR signalling in VECs may not be optimal for low pH environments (524). A kinetic study of the degradation of forskolin in aqueous systems found that forskolin's activity is susceptible to pH changes, being relatively stable in the pH range of 3.5-6.5, but less stable outside this range (525). These findings suggest that forskolin may be degrade at pH 3.9 or that its capacity to interact with cAMP is diminished under low pH conditions in VECs.

The robust response to forskolin at pH 7.4 and inhibition by L-LA of intracellular cAMP levels observed were unexpectedly decreased when the VECs were pre-treated with PTX. When cells are treated with PTX, adenylyl cyclase is no longer inhibited and so cAMP levels will increase. Additionally, these findings showed that PTX does not affect the L-LA-induced inhibition of cAMP at pH 7.4. Although PTX is useful for interrogating inhibitory G protein signalling as it inhibits activation of the G proteins by ligand-bound GPCRs by modifying a cysteine residue

near the C terminus of the Gα subunit, in VECs PTX is decreasing intracellular cAMP levels by 47.6% at pH 7.4 and 46.8% when L-LA is present at pH 7.4 (526, 527).

Again, cAMP levels did not increase when forskolin was added to the PTX pre-treated samples at low pH. A study by Locht *et al.* suggested that PTX action is pH sensitive and can be affected by the addition of ammonium chloride or chloroquine which raises the pH in intracellular compartments (528-530). An earlier study, by Hausman and Burns, investigated whether an acidic environment was required for PTX action and found that unlike many other bacterial toxins PTX does not require a low pH (531).

When LA activates HCAR1, the subsequent reduction in intracellular cAMP levels typically inhibits the activity of key cAMP-dependent pathways, including PKA and EPAC. These pathways play crucial roles in regulating inflammatory responses, often through mechanisms that prevent inhibition of NF-κB. However, in VECs, this was not observed, suggesting that LA's anti-inflammatory effects may involve additional or alternative signalling mechanisms independent of cAMP. One such alternative pathway involves the PI3K/AKT signalling axis which is also regulated by cAMP. This pathway has been shown to influence NF-κB activation through the phosphorylation and degradation of IκB, releasing NF-κB for nuclear translocation ad transcriptional activity. Recently PI3K/AKT signalling has been implicated in mediating vaginal epithelial dysfunction, including inflammation and barrier disruption, in response to microbial metabolites and environmental stress (175, 532). The observation that LA suppresses NF-κB activation in VECs despite reduced cAMP levels raises the possibility that LA might directly modulate PI3K/AKT signalling, either through HCAR1-dependent mechanisms or via other receptors or pathways. Further investigation into how LA interacts with the PI3K/AKT pathway in the vaginal epithelial environment could provide valuable insights into its role in maintaining mucosal homeostasis.

To determine whether L-LA-induced suppression of NF-κB and AP-1 activation following VEC treatment with FSL-1, as described in Chapter 3, is mediated by a GPCR event, cells were pre-treated with PTX. NF-κB activation was significantly suppressed when PTX was present, with a corresponding increase in cAMP levels. This effect reached statistical significance at

physiological vaginal acidity (pH 3.9 with LLA) ($P < 0.01$) and following FSL-1 treatment at pH 7.4 ($P < 0.001$; Figure 6.9A). PTX had a pronounced effect on NF-κB activation by FSL-1. Consistent with observations from Chapter 3, L-LA significantly suppressed FSL-1-induced activation of NF-κB ($P < 0.01$). However, this suppression was not seen in the presence of PTX, suggesting that inactivating the $G\alpha_i$ subunit of HCAR1 interferes with L-LA's ability to suppress NF-κB. Since cAMP/PKA activation can prevent IκB degradation, the effect of PTX on the upstream kinase IKK was investigated to determine whether PTX also inhibits IKK in VECs. In fact, the opposite was observed, with IKK activation occurring when PTX was present. A recent review highlights the crosstalk between the PI3K/AKT pathway and NF-κB signalling, where AKT phosphorylates IκB to activate NF-κB (533, 534). In contrast, AP-1 was not significantly affected by PTX, indicating that PTX is not mediating pathways involved in bacterial agonist activation or L-LA-mediated inhibition of FSL-1-induced AP-1 activation. These findings suggest that the AP-1 inflammatory signalling pathway operates independently of cAMP signalling.

ERK is strongly activated by L-LA, and a previous study showed that in CHO-K1 cells ERK1/2 was rapidly activated by LA via HCAR1 and significantly blocked by PTX, prompting an investigation of the impact of PTX in VECs (Figure 6.9C) (447). This effect was not seen in VECs indicating that the $G\alpha_i$ protein is not involved in ERK phosphorylation. The study by Li *et al.* concluded that ERK activation is via two distinct pathways: the PKC-dependent and the IGF-IR transactivation pathways, with PI3K playing an important role in HCAR1-mediated activation of ERK via the $G\beta\gamma_i$ subunit.

Subsequent studies have shown that this mechanism is much more nuanced. In human lung cancer cells, lactate-induced reduction of cAMP and inhibition of PKA signalling occur via TAZ-dependent upregulation of programmed death-ligand 1 (PD-L1) (326). However, contrasting observations have been reported; in brain tissue LA reduces cAMP levels, whereas in astrocytes and the locus coeruleus LA increases cAMP levels, suggesting differences in lactate signalling patterns (323, 535-537).

Both the $G\alpha_i$ and $G\beta\gamma_i$ subunits of the HCAR1-associated G protein can exert downstream effects on signalling when lactate binds to the receptor. HCAR1 activation enhances ERK1/2 phosphorylation to modulate metabolism in various cells and tissues such as the brain, muscle and osteoblasts (447, 538-540). For the first time, our results demonstrate this in VECs. Lactate stimulates the G_i protein by dissociating $G\alpha_i$ and $G\beta\gamma_i$ subunits. The $G\alpha_i$ subunit can then activate ERK by inhibiting adenylate cyclase and activating the small GTPase protein Ras (507). The Ras/Raf/MEK/ERK pathway is well characterised and could be a possible mechanism for ERK1/2 activation by lactate in VECs. In most cells where Raf-1 is the predominant Raf isoform, cAMP inhibits the MAPK pathway (541). The $G\beta\gamma_i$ subunits also play a critical role in signal transduction, interacting with effector proteins such as phospholipases, ion channels, Src-dependent phosphorylation of the epidermal growth factor receptor (EGFR) and G protein-coupled receptor kinases (GRK). Inhibition of $G\beta\gamma_i$ impairs effector signalling (542). The $G\beta\gamma_i$ subunits can also stimulate the MAPK ERK1/2 by mechanisms involving Ras and the tyrosine kinase class of growth receptors (542-545). Although this was beyond the scope of this study it would be an area for future investigation.

Lactate binding to HCAR1 can also signal via the GPCR adaptor proteins, β-arrestins. β-arrestins regulate many receptors and signalling pathways including GPCR desensitisation, receptor trafficking and internalisation, and activation of downstream signalling (546-548). Hoque *et al.* found that lactate-induced suppression of TLR- and NLPR3-mediated pro-inflammatory responses was independent of cAMP signalling and required β-arrestin-2 (ARRB2) interacting directly with HCAR1 leading to reduced activation of NF-κB and IL-1β (325, 342, 549, 550). Lactate reduces glutamate damage in astrocytes through the HCAR1-β-arrestin2 pathway in astrocytes rather than the G_i protein (551). In macrophages, ARRB2 antagonises both TLR and NLRP3 signalling pathways (552, 553). The β-arrestin signalling pathway can activate MAP kinases as well as other kinases such as protein kinase B (AKT). So, while the cAMP measurement in this thesis was used as a readout of HCAR1 activity and to assess if the PTX conditions were working, further work could investigate β-arrestin effectors and signalling pathways in VECs (517). A recent study in 2023 showed that β-arrestins enhance ERK2 phosphorylation in a MEK1/2 independent manner in HEK293 cells, an immortalised human embryonic kidney cell line (554). Another study reported that specific receptor

phosphorylation site clusters determine whether β-arrestin promotes or inhibits receptor activation of ERK (555).

Wu *et al.* proposed that other receptors may be involved, such as GPR132 which senses extracellular pH, rather than lactate specifically, to increase levels of cAMP. GPR132 is expressed in various tissues including the lungs, gut, and in immune cells and studies of lactate signalling through GPR132 have been limited (327, 556). GPR132 also works with Olfr78, an olfactory receptor found in many different tissue types and known to sense lactate by forming a heterodimer (557-559). Three other proton-sensing GPCRs, GPR4, GPR65 and GPR68 have been described in the tumour microenvironment (560). These receptors have not yet been identified in VECs but could be included in future work.

GPCR signalling is an essential part of cellular function, but overstimulation can be harmful. So, cells have evolved to limit or desensitise GPCR signalling; rapid desensitisation is affected by G protein-coupled receptor kinases and β-arrestins which prevent the G protein from associating with the receptor whereas longer-term desensitisation involves additional mechanisms that include ubiquitin-dependent regulation of GPCRs and β-arrestins. Treating the VECs with PTX for 24 hours could be leading to desensitisation of the receptor. The use of PTX in multilayered VECs has not been previously reported although Li *et al.* treated a cell line isolated from the ovary of an adult female hamster grown as a monolayer with 100 ng ml^{-1} PTX overnight (447). In addition, PTX is not a specific inhibitor of HCAR1 and may be inhibiting other receptors on VECs and affecting other signalling pathways. This could help explain why TLR agonist FSL-1 did not continue to activate NF-κB but further experiments looking at additional timepoints and concentrations of PTX would be needed to confirm this.

To study the lactate specific effects on HCAR1 an alternative ligand would be useful. Some studies suggested using 3-hydroxy-butyric acid (3-OBA) as a HCAR1 antagonist. However, Nezhady *et al.* demonstrated that although 3-OBA exhibits some effects consistent with HCAR1 knockdown experiments, it is in fact an agonist ligand for HCAR2/GPR109A not HCAR1 (561-563). Despite the lack of specific inhibitors, GPR81 modulation through genetic deletion

or pharmacological approaches is an area of active research, particularly in the context of inflammation, cancer and metabolic disorders (564).

GPCR signalling can be investigated using a variety of fluorescent and bioluminescent biosensors. In this study cAMP concentration was measured using a fluorescent biosensor (FRET). Other secondary messenger molecules such as PKA, DAG, IP3, PKC and Ca^{2+} as well as β-arrestin biosensors, can also be measured. Receptor activation is now known to have multiple layers of complexity rather than being a simple binary “on and off” switch.

This preliminary investigation into the lactate receptors and their signalling pathways indicates that GPCR signalling is involved in activation of NF-κB but not AP-1. L-LA binding at pH 7.4 significantly reduces cAMP levels, but it remains unclear whether this cAMP reduction is directly mediated by LA or is due to low pH. Future research into receptor signalling in VECs should include $G\beta\gamma_i$ signalling pathways and the role of β-arrestin proteins.

Chapter 7: Proteomic-based Characterisation of VEC response to Lactic Acid

7.1 Introduction

The results of the previous chapters demonstrate major alterations in VEC transcriptional signalling pathways in response to LA exposure. While previous work was targeted towards characterising hypothesis-driven inflammatory changes in VECs, it is likely that other key functional responses are instigated by LA exposure. Moreover, the key phenotypic changes that VECs undergo will be underpinned by effector molecules of function, i.e. proteins.

Recent advancements in -omics technologies facilitate large-scale identification and quantification of functional biomolecules, including proteins. Proteomics approaches give insight into the mechanisms of biological processes by characterising the entire protein content present in a cell, tissue or bodily fluid at a given time point. This information can be then used to measure changes between different conditions and to determine the functional linkages within larger protein complexes or pathways (565). The typical workflow of a proteomics experiment involves separation of proteins based on their chemical and physical properties, followed by mass spectrometry (MS), which provides structural information required for identification, and quantification (566). Downstream bioinformatics analysis methods can then be applied to investigate relationships between protein regulatory mechanisms at a molecular level and phenotypic behaviour, such as disease developments and progression. There are two broad approaches used for MS-based proteomics: bottom-up and top-down (567). The more common approach is bottom-up where the protein samples are proteolytically digested into peptides before being analysed in a mass spectrometer (568). In top-down proteomics, intact proteins are directly analysed by MS but this approach can be challenging both experimentally and computationally (569). An example workflow for high-throughput, high-dimensionality proteomics is provided below (Figure 7.1).

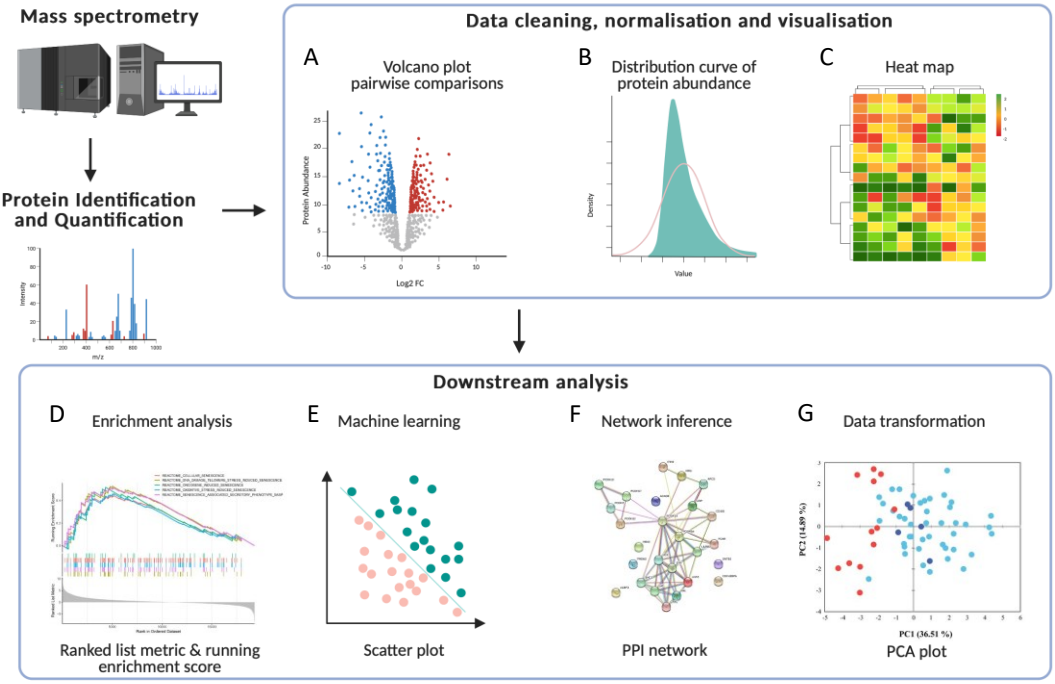

Figure 7.1 General workflow of analysis using bioinformatics in MS-based proteomics.

(A) Volcano plot describing pairwise comparisons between experiments or conditions using protein abundance and log2 fold change data. **(B)** Distribution of protein abundance data before and after normalisation. **(C)** Heatmap analysis to visualise and understand protein abundance with clustering across different samples and conditions. **(D)** Protein set enrichment analysis using ranked list metric (above) or running enrichment score (below). **(E)** Scatter plots generated using different types of intensity and samples. **(F)** Mapping proteins to a protein-protein interaction (PPI) network. **(G)** Principal component analysis (PCA) plot helping to identify clusters. Figure adapted from Chen 2020 (570). *Created with BioRender.com.*

The work in this chapter set out to apply a proteomic-based approach to assess global changes in VEC protein abundance in response to acidity and in particular LA exposure. Specifically, a liquid chromatography-mass spectrometry (LC-MS)-based approach was used to identify differentially expressed proteins (DEPs) between VECs treated at the physiologically relevant pH 3.9 with or without 30 mM LA or at pH 7.4. It was hypothesised that exposure of VECs to LA would inhibit changes in the abundance of proteins associated with inflammatory pathways. Additionally, it was postulated that a distinct set of proteins would be regulated through LA-induced activation of the MEK/ERK signalling pathway. A further objective was to characterise downstream alterations in VEC protein abundance driven by LA-induced

MEK/ERK activation. In doing so, novel pathways and mechanisms involved in LA-mediated VEC function could be identified for further investigation.

7.2 Results

A total of six different treatment groups (n = 5 for each) were investigated in this study (Table 7.1).

Table 7.1 Different VEC treatments used for proteomics study

Apical Treatment of VECs	Graph ID
pH 7.4	pH7.4
pH 7.4 + MEK Inhibitor	pH7.4MEK
pH 3.9	pH3.9
pH 3.9 + MEK Inhibitor	pH3.9MEK
pH 3.9 + L-LA	LLA
pH 3.9 L-LA + MEK Inhibitor	LLAMEK

Cells were treated apically with the different treatments for 6 hours before proteins were extracted, enzymatically digested into smaller peptides, separated by liquid chromatography and subsequently analysed by mass spectrometry.

7.2.1 Generation of proteomics data

MS analysis of the VEC extracts identified 39,546 individual peptides. Between 70-80% of the peptides had a coefficient of variation < 30% indicating a low level of variability between the multiple measurements from different replicates. The highest amount of variability was observed for the pH 3.9 + MEK Inhibitor (pH3.9MEK) treatment group (Figure 7.2A). The number of peptides identified was generally consistent across all treatment groups and

repeats (n = 5) (Figure 7.2B), as was the number of proteins that were assigned from these peptides (Figure 7.2C).

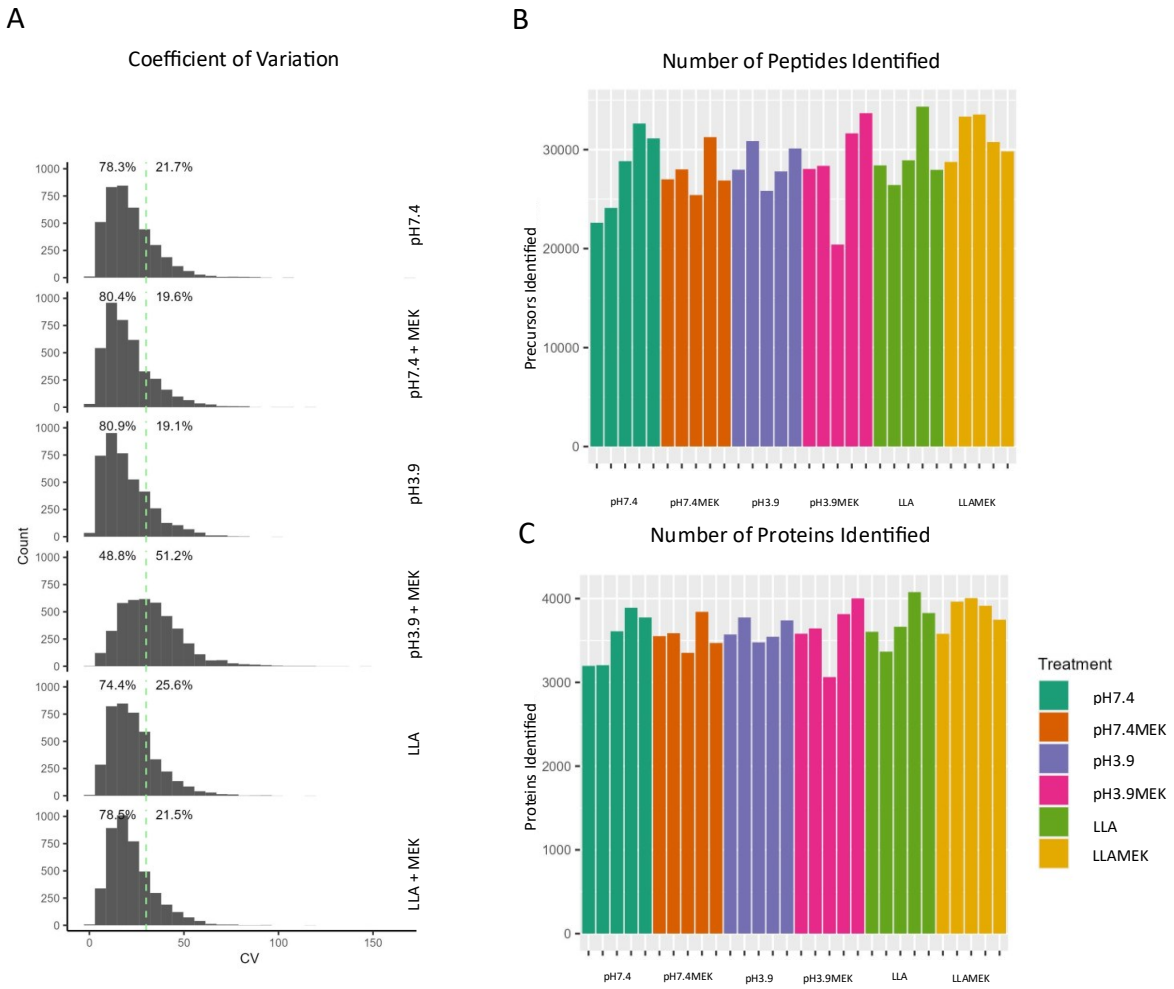

Figure 7.2 Examination of data quality and robustness generated by LC-MS for different VEC treatments.

(A) The coefficient of variation for each of the six treatments, and the number of **(B)** peptides and **(C)** proteins across each of the treatments for each repeat identified by LC-MS.

Further assessment of data quality revealed that over 70% of all proteins were consistently identified across all five replicates within each treatment condition (Figure 7.3).

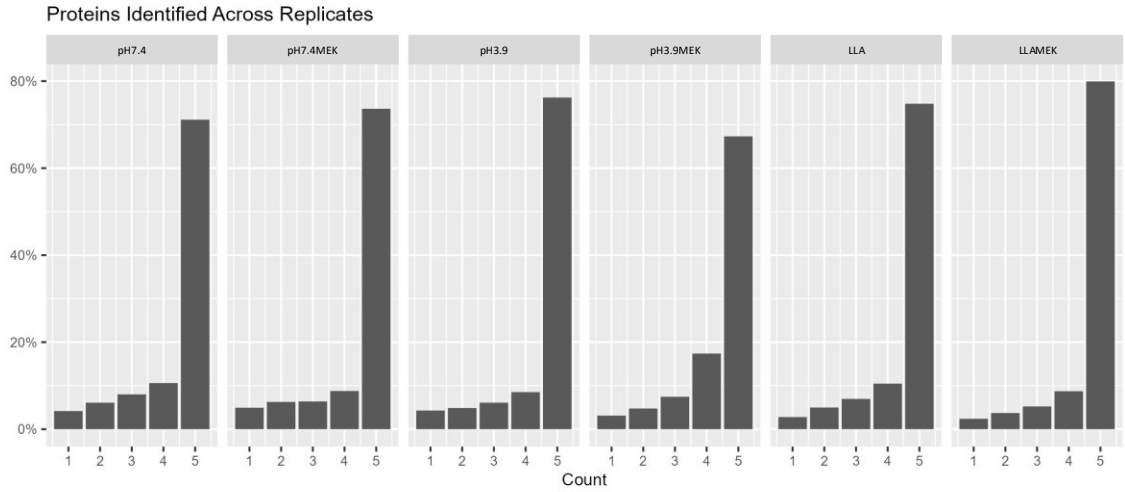

Figure 7.3 Protein abundance quantification across replicates.

Over 70% of the proteins identified were seen across the five replicates for each treatment.

An initial comparison of the protein profiles for VECs cultured at pH 7.4, pH 3.9 and pH 3.9-LLA with or without MEK inhibitor identified a total of 4601 DEPs. Subsequent analyses focused on the 4461 DEPs identified in at least 3 replicates per treatment. Comparison of the DEPs across the samples revealed that the protein profile of one of the L-LA repeats was more similar to samples cultured at pH 7.4. This similarity suggested either a lack of response to pH 3.9 exposure, or a potential mislabelling issue during the experiment. Consequently, this sample was excluded from further downstream analyses (Figure 7.4). Although the final data set comprised 4461 proteins, only 2555 were quantifiable using the Amica proteomics platform. This is reduction is consistent with typical proteomics workflows, where not all identified proteins are quantified for downstream analyses due to biological and technical factors. For instance, filtering criteria in Amica such as log2 fold change thresholds or adjusted *P*-values, often lead to the exclusion of some proteins.

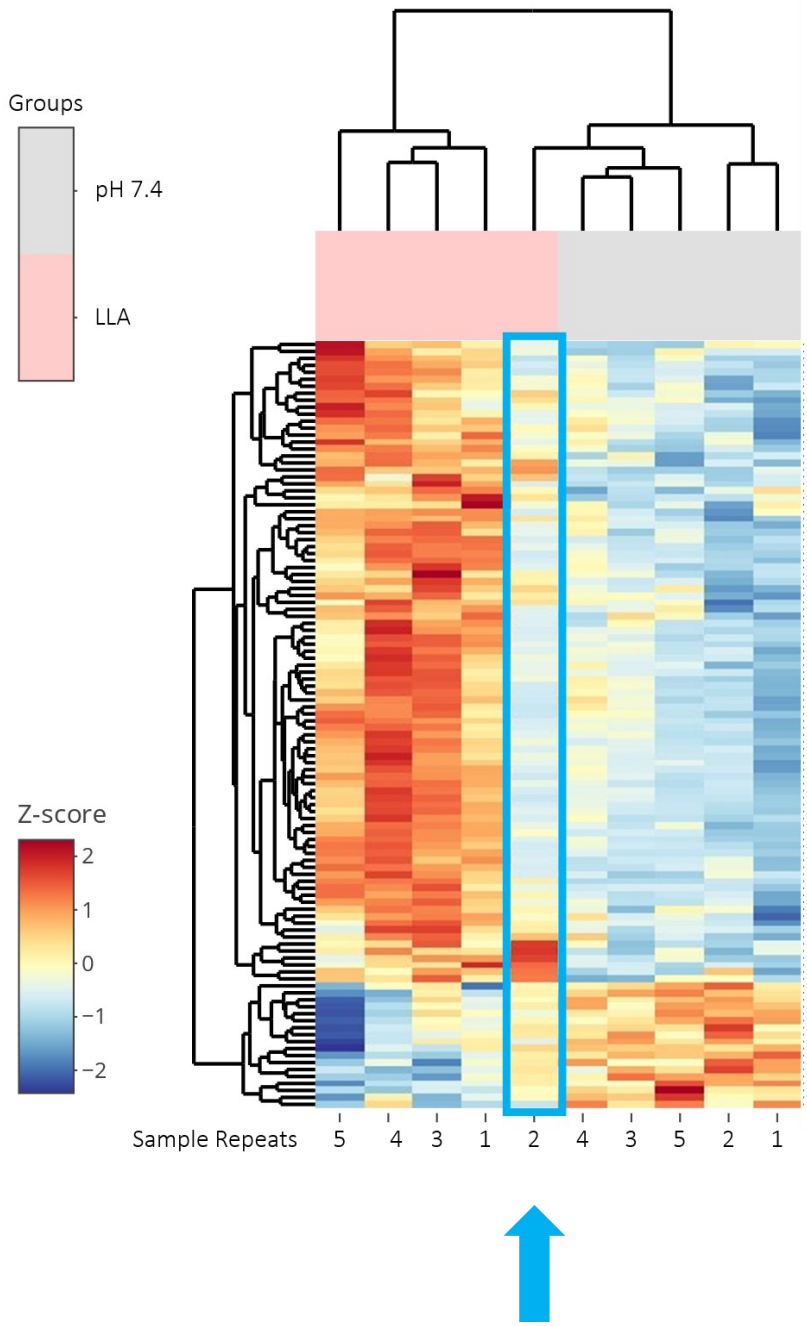

Figure 7.4 Sample LLA.2 was excluded from the final data set used for analysis based on the different protein abundance patterns compared to the other replicates.

Heatmap showing differential abundance of proteins in VECs at pH 7.4 or pH 3.9 with 30 mM L-LA present and highlighting sample LLA.2 which was removed from further analyses.

Eight different pairwise comparisons were undertaken: pH 7.4 vs L-LA, pH 3.9 vs L-LA, pH 7.4 vs pH 3.9, pH 7.4 vs pH7.4MEK, pH3.9 vs pH3.9MEK, L-LA vs L-LAMEK, pH 7.4 vs L-LAMEK and pH 3.9 vs L-LAMEK. The log2 fold change threshold was set at 0.5 and the threshold on the *P*-

value was set at 0.05. These thresholds could then be applied to single or multiple pairwise group comparisons.

7.2.2 Impact of acidification on protein abundance in VECs

A total of 324 VEC proteins were found to change in response to acidification (Figure 7.5A). A substantial number of these DEPs were consistently altered in both pH 3.9 and LLA treatments. Hierarchical clustering of the DEPs showed that L-LA treatment was associated with a higher proportion of upregulated proteins (n = 207, 63.8%).

A Euler plot comparing DEPs across the three groups showed that there was a total of 182 unique DEPs up- or downregulated uniquely by L-LA compared to pH 7.4 or pH 3.9 (Figure 7.5B). Figure 7.5C shows the data as an Upset plot which visualises the intersecting data set as a matrix. It shows an additional three DEPs that were unique to pH 3.9 and L-LA which were not visualised in the Euler plot (Figure 7.5C).

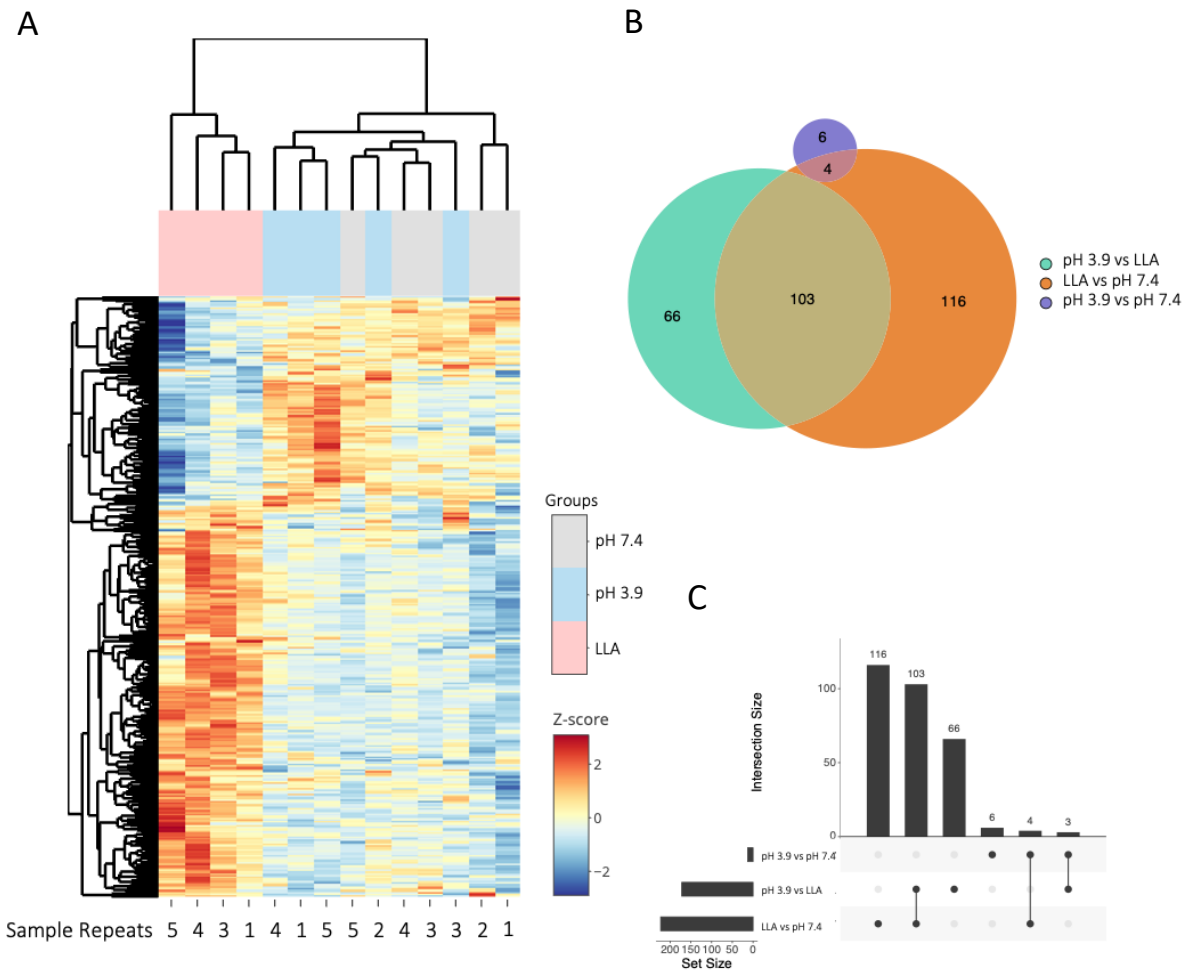

Figure 7.5 Proteomic differences in VECs exposed to different pH conditions with or without L-LA.

(A) Heatmap showing differently abundant proteins (324; 1% FDR) between VECs in medium at pH 7.4 or pH 3.9 with or without 30 mM L-LA present. **(B)** Euler diagram representing overlapping proteins that change in abundance with the different treatments (n = 295) **(C)** Upset plot to visualise intersecting data.

Annotation of DEPs using PANTHER and gene ontology (GO) enabled DEPs to be mapped to molecular function, biological processes, protein classes and pathways (362). Proteins affected by acidity were predominantly enzymes, cytoskeletal and scaffold/adaptor proteins, and membrane traffic proteins (Figure 7.6A). These proteins could be mapped to the integrin signalling pathway, cytoskeletal regulation and the Ras pathway as well as inflammatory signalling pathways such as chemokine and cytokine signalling, growth factor signalling and TLR signalling (Figure 7.6B).

A

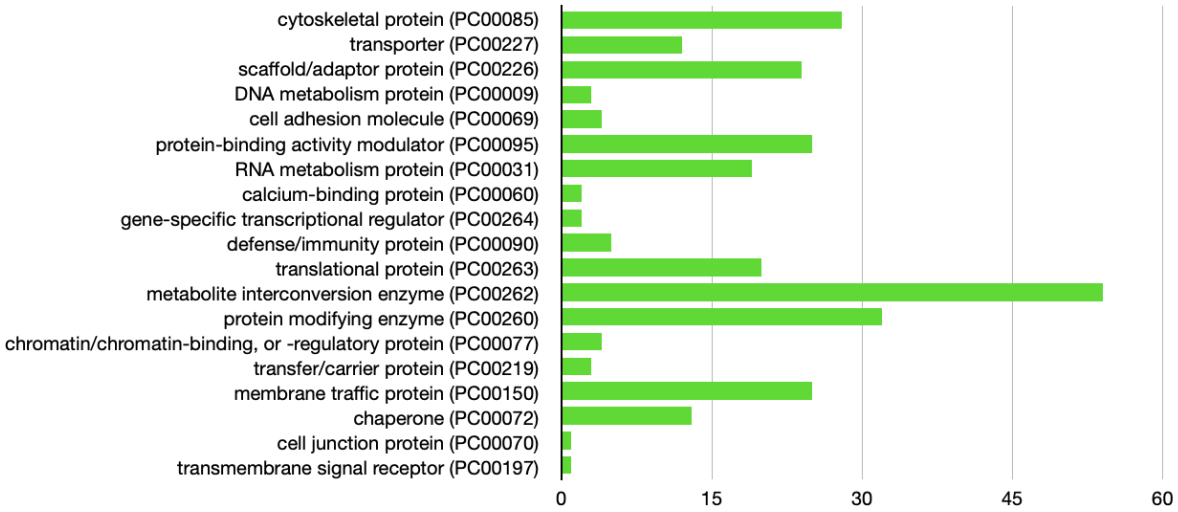

B

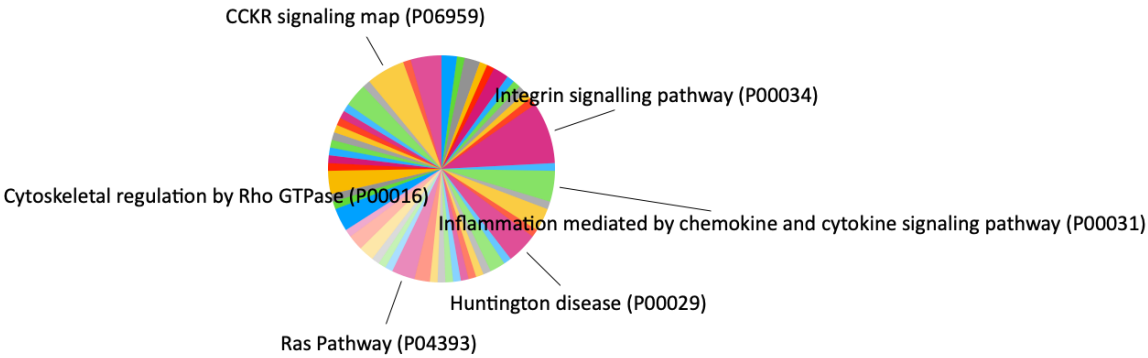

Figure 7.6 Differentially expressed proteins in VECs exposed to acidity were predominantly enzymes or involved in cellular structure and mapped to cytoskeletal regulation pathways as well as inflammatory signalling pathways.

(A) GO enrichment analysis of protein classes for DEPs when VECs are exposed to pH 3.9. **(B)** Using data generated by PANTHER, key signalling pathways were identified to which DEPs were mapped (324 proteins).

7.2.2.1 Impact of acidification using HCl on protein abundance in VECs (pH 7.4 vs pH 3.9)

A sub-analysis was performed comparing the relative abundance of the DEPs when VECs are exposed to an acidic medium pH 3.9 to pH 7.4 and only thirteen DEPs were identified (Figure 7.7A). Twelve of these proteins increased in abundance and one, Ran-Binding Protein 9 (RanB9) decreased significantly. A GO enrichment analysis of the key pathways found these proteins were involved in integrin signalling, cytoskeletal regulation by Rho GTPases, the Ras pathway, platelet-derived growth factor (PDGF) signalling and the Huntington disease pathway (Figure 7.7B).

A

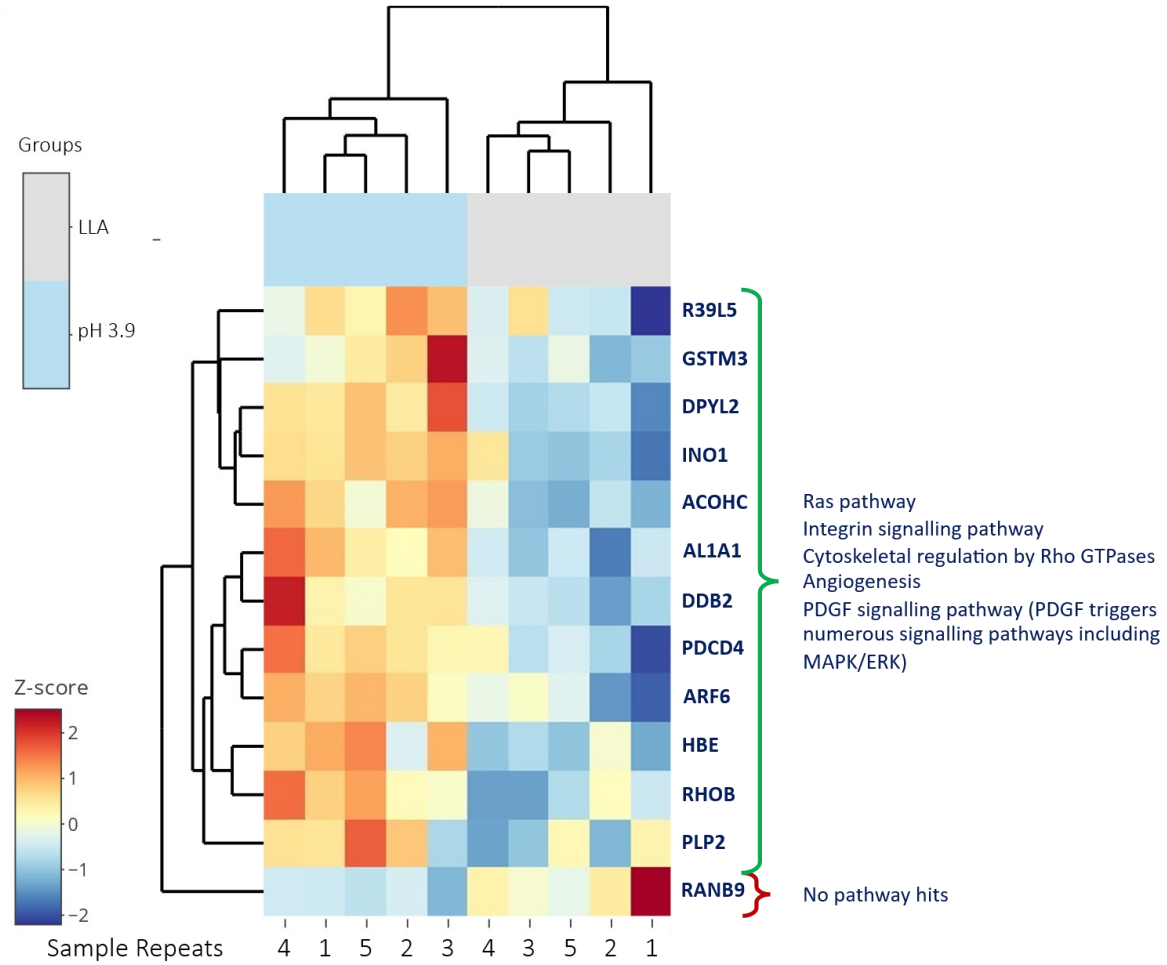

B

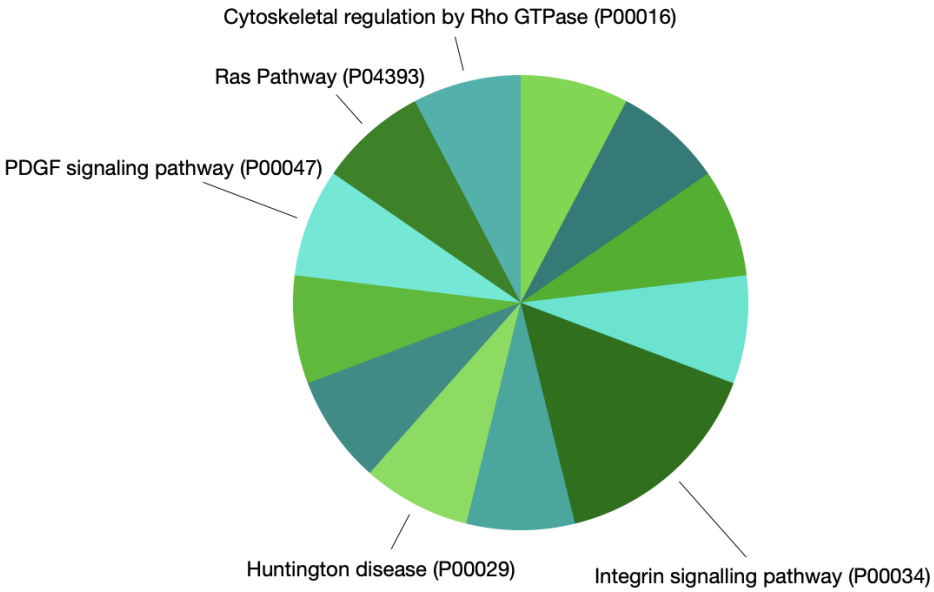

Figure 7.7 Exposure of VECs to acidity altered the abundance of relatively few proteins.

(A) Heatmap showing the 13 DEPs identified between VECs cultured at pH 7.4 and pH 3.9 for 6 hours. The DEPs are annotated with their most commonly associated biological pathways. **(B)** GO enrichment analysis revealed that proteins with significantly altered abundance under pH 3.9 conditions were predominantly involved in cellular signalling pathways and cytoskeletal regulation.

7.2.2.2 Impact of acidification with L-LA on protein abundance in VECs

In contrast to the comparison of pH 7.4 versus pH 3.9-treated samples, a substantially larger number of DEPs were observed in VECs exposed to L-LA acidification (LLA). In total 223 DEPs were identified, indicating that L-LA drives proteome changes in VECs substantially more than acidification alone in this niche (Figure 7.8). GO enrichment analysis indicated that these proteins were involved in integrin signalling, cytoskeletal regulation, Ras and TLR signalling as well as MAPK pathways.

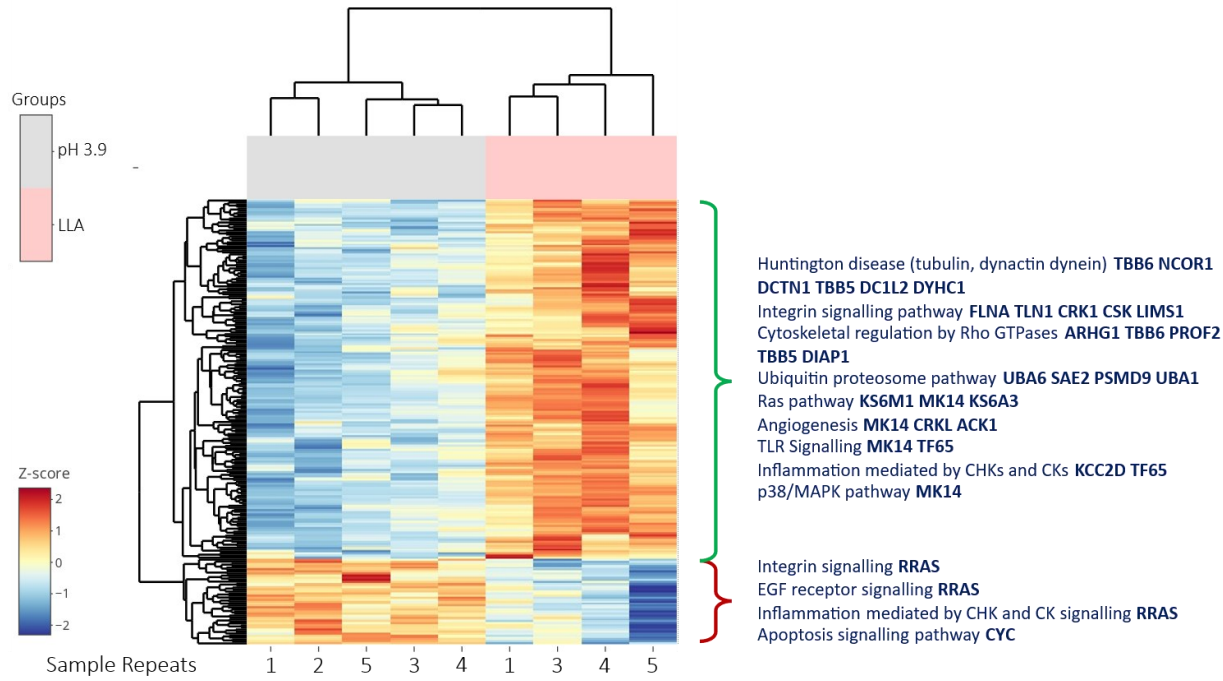

Figure 7.8 Differences in protein abundance in VECs exposed to pH 7.4 or LLA.

Heatmap showing differentially abundant proteins (223 proteins) between VECs exposed to pH 7.4 for 6 hours and VECs exposed to L-LA and the most common pathways to which they map using GO enrichment analysis. The presence of L-LA leads to a significant increase in abundance of proteins involved in cytoskeletal regulation and inflammatory signalling pathways.

Proteins differentially regulated by L-LA were analysed using the STRING database to construct a PPI network, which can provide insights into potential protein functions and pathways. The analysis revealed a highly complex network of interactions comprising 221 nodes and with a PPI enrichment *P* value < 1.0e-16, indicating a significantly higher number of interactions than would be expected by chance (Figure 7.9).

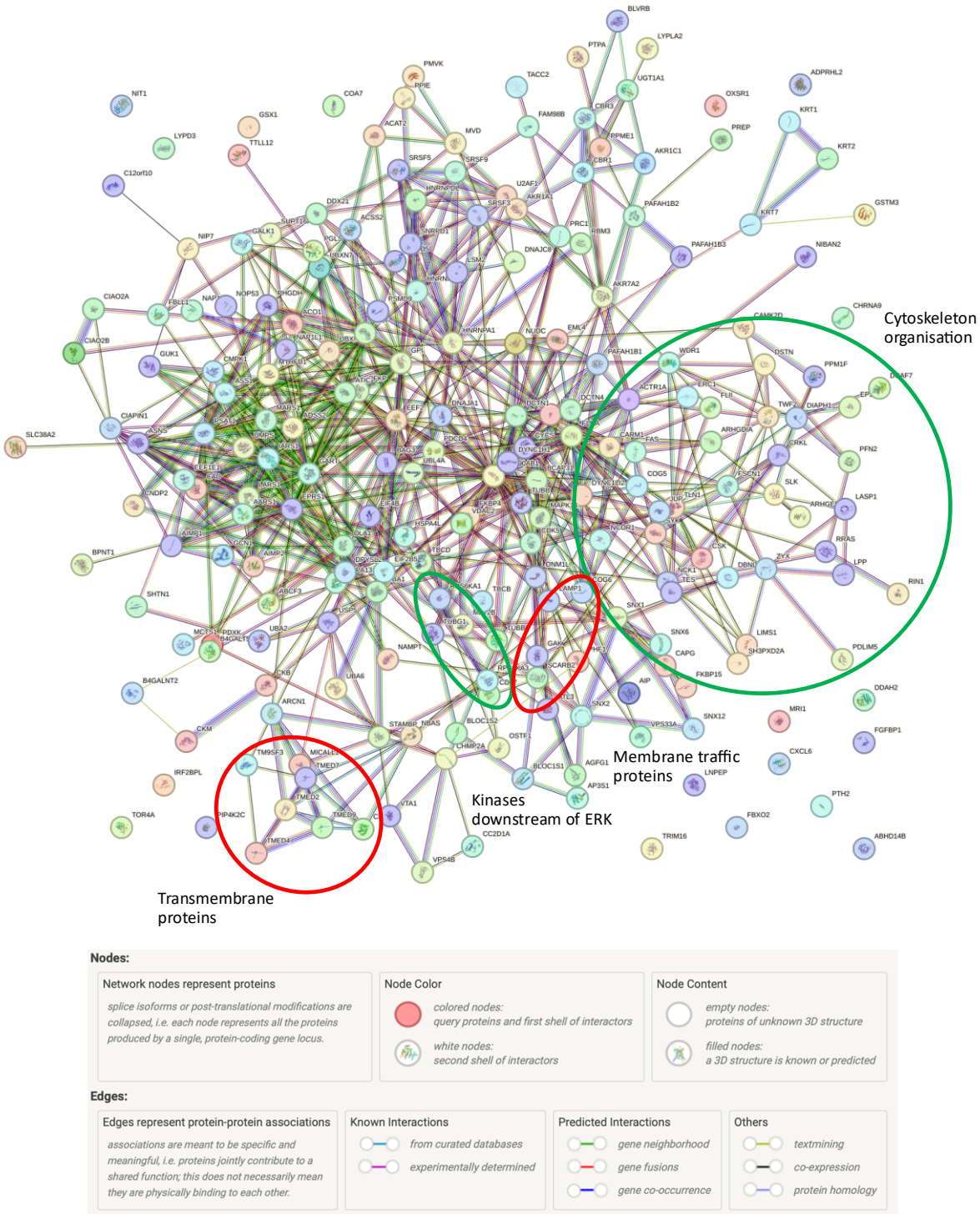

Figure 7.9 STRING protein-protein interaction (PPI) network of the differentially expressed proteins that changed in abundance when VECs were treated with L-LA.

The PPI network enabled visualisation of clustering of protein-protein interactions. The proteins that changed in abundance with L-LA mapped to 221 nodes. The line colour indicates the type of interaction evidence, and the line thickness indicates the strength of data support. Some key groupings of upregulated DEPs (green) and downregulated DEPs (red) are highlighted.

In the presence of L-LA, 180 proteins were found to significantly increase in abundance. These were predominantly cytoskeletal proteins, scaffold/adaptor proteins, chaperones, membrane traffic proteins and cell junction proteins (Figure 7.10A) and could be mapped to the integrin signalling pathway, cytoskeletal remodelling and the Ras pathway as well as inflammatory signalling pathways such as chemokine and cytokine signalling, growth factor signalling and TLR signalling (Figure 7.10B).

A

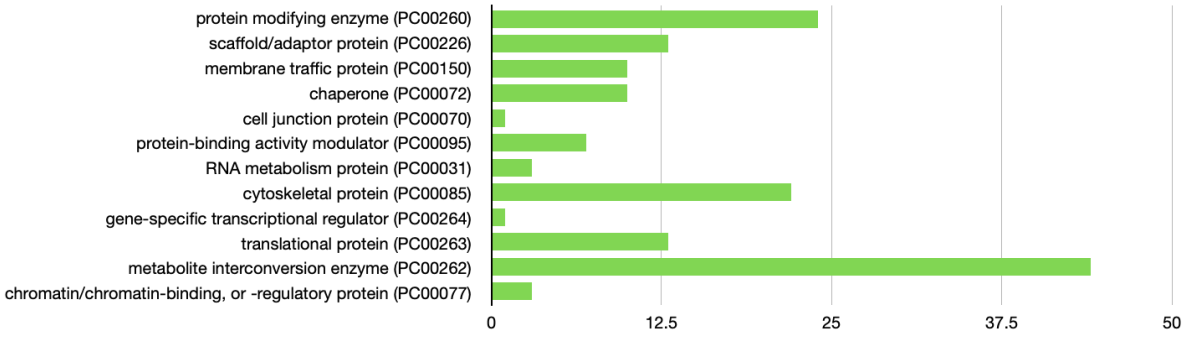

B

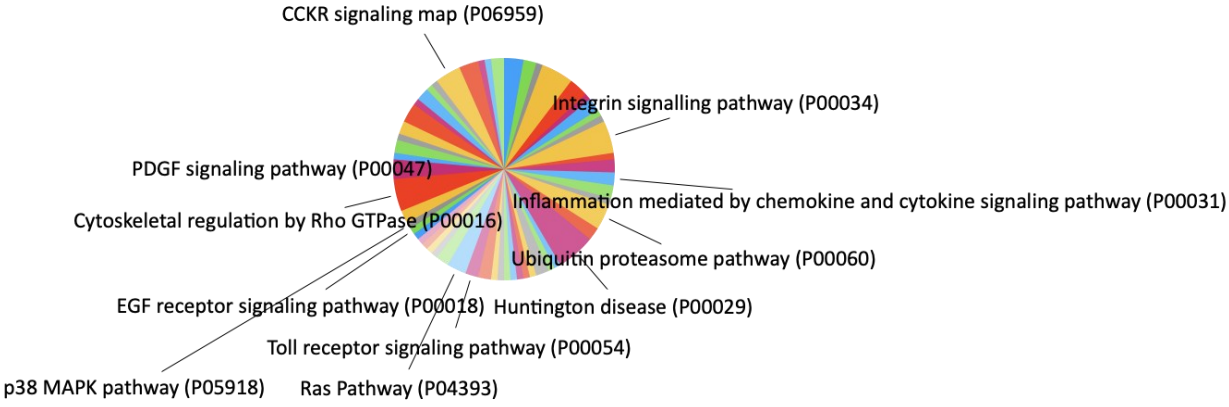

Figure 7.10 Proteins upregulated by L-LA are predominantly enzymes or involved in cellular structure and map to cytoskeletal regulation pathways as well as inflammatory signalling pathways.

(A) GO enrichment analysis of protein classes for DEPs that are upregulated when VECs are exposed to L-LA relative to pH 7.4. **(B)** Using data generated by PANTHER, key signalling pathways were identified in which proteins were upregulated by L-LA relative to pH 7.4 (180 proteins).

A PPI network was generated for this set of upregulated proteins to enable a more focused assessment of potential interactions between proteins upregulated in response to L-LA (Figure 7.11).

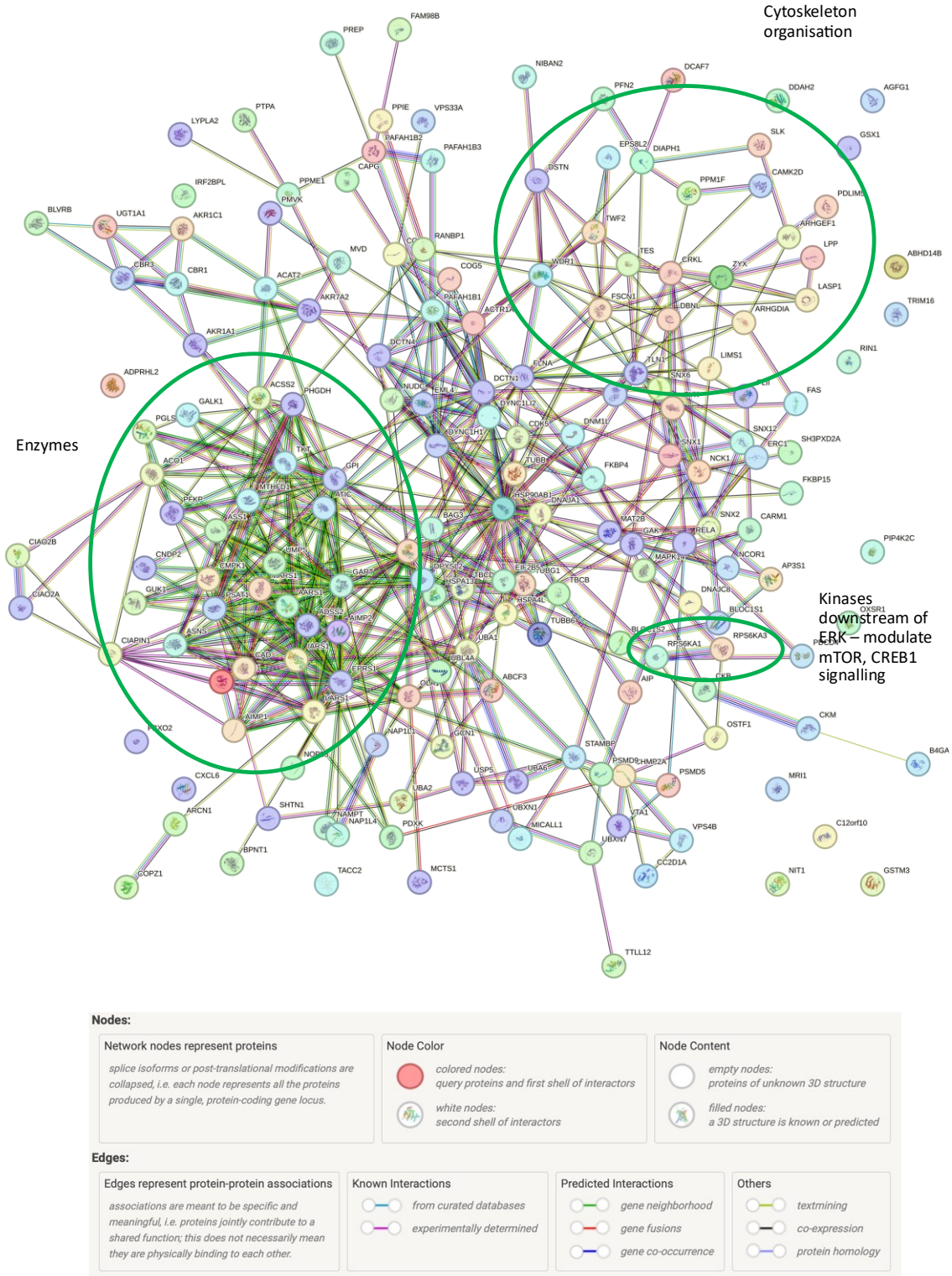

Figure 7.11 Protein-protein interaction network of the differentially expressed proteins that increase in abundance relative to pH 7.4 when VECs were treated with L-LA.

PPI clusters map to 180 nodes and several clusters can be visualised (circled in green). The line colour indicates the type of interaction evidence, and the line thickness indicates the strength of data support.

One of the resulting clusters observed in the PPI analysis was enriched for proteins involved in cytoskeletal organisation. As described in Chapter 4, cell barrier integrity is mediated by ERK in other cell types. Thus, this cluster was chosen for further exploration, which is described later in this chapter (Section 7.2.5).

A total of 43 proteins were found to be downregulated by L-LA (Figure 7.12A). Notably these proteins were shown to be involved in inflammatory cytokine and chemokine signalling pathways, EGF receptor signalling and apoptosis signalling (Figure 7.12B).

A

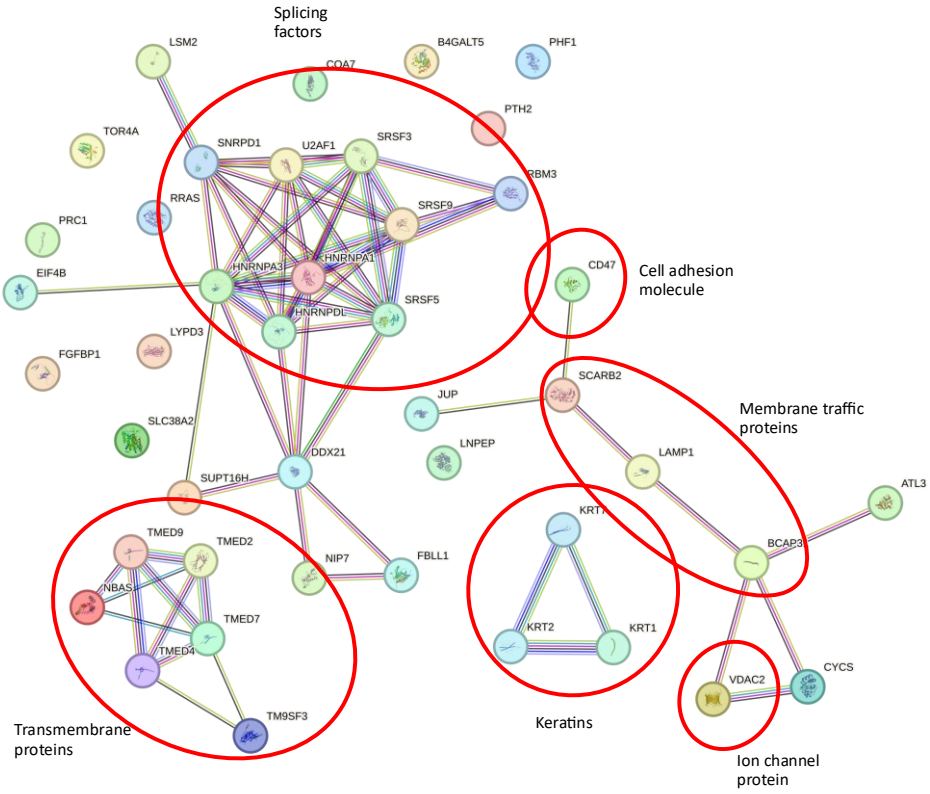

B

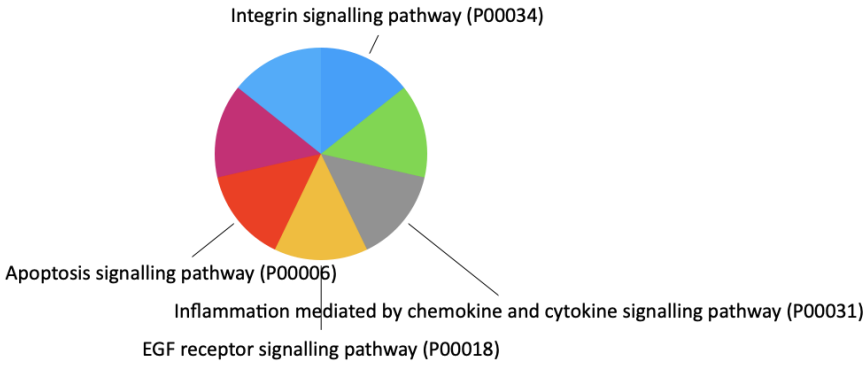

Figure 7.12 Protein-protein interaction network showing key protein clusters and important pathways for differentially expressed proteins significantly decreased by L-LA. relative to pH 7.4.

(A) The abundance of 43 proteins decreases when L-LA was present relative to pH 7.4 and distinct clusters were seen (circled in red). **(B)** Using data generated by PANTHER, key signalling pathways were identified in which proteins were downregulated by L-LA relative to pH 7.4 (43 proteins). Chart was created using GO enrichment data for pathways.

To better understand the effect L-LA has on protein abundance in VECs, a comparison was made between the proteome profiles of VECs exposed to pH 3.9 and L-LA. A total of 176 DEPs

were identified between the two groups. Of these, 105 proteins were upregulated, and 71 proteins were downregulated by L-LA (Figure 7.13).

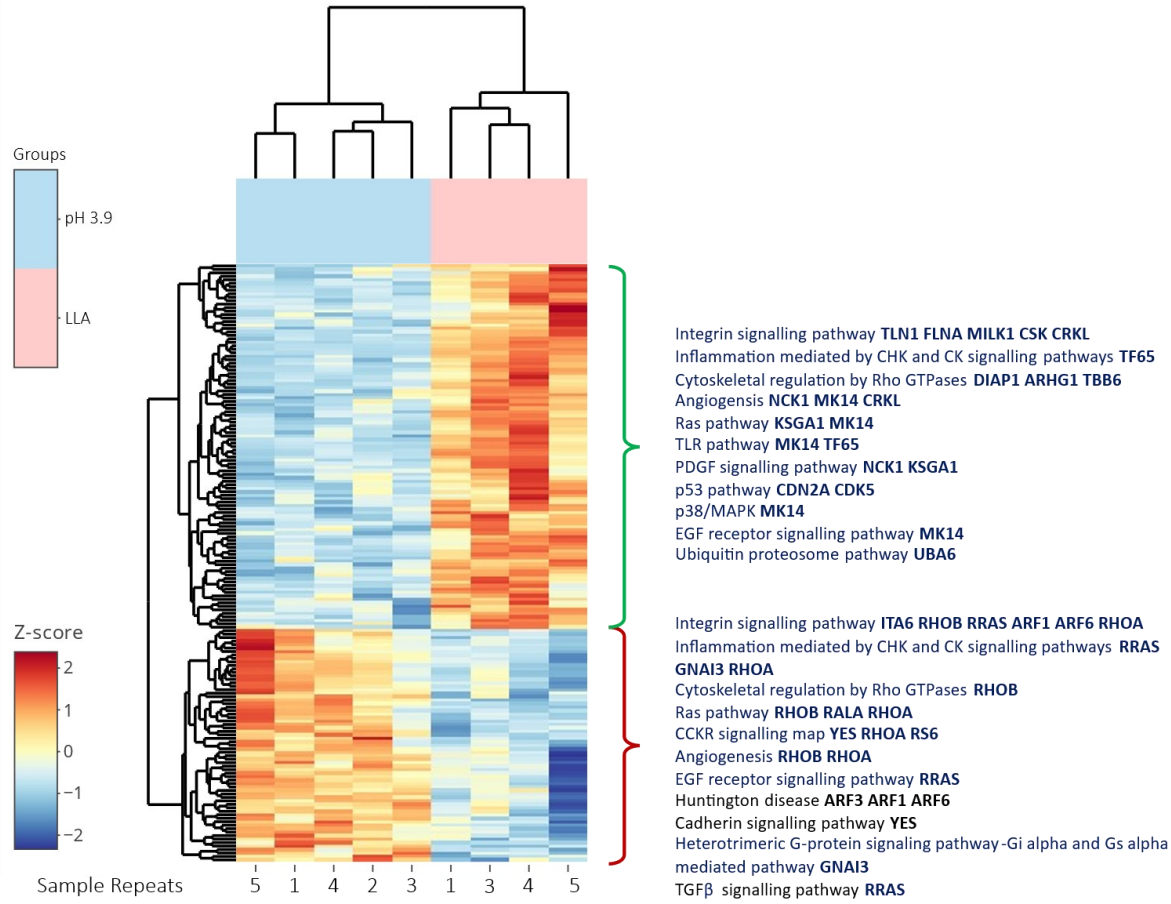

Figure 7.13 Protein abundance differences in VECs exposed to pH 3.9 or L-LA.

Heatmap showing DEPs between VECs exposed to pH 3.9 or L-LA (176 proteins).

Using GO enrichment analysis, 85/105 (81.0%) upregulated DEPs could be assigned to different protein classes. The majority of these proteins were enzymes involved in protein modifications or metabolite interconversion (49.4%) and cytoskeletal or scaffold and adaptor proteins (22.4%) or protein-binding activation modifiers (10.6%) (Figure 7.14A). These proteins were involved in the integrin signalling pathway, cytoskeletal regulation as well as inflammatory signalling pathways (Figure 7.14B).

A

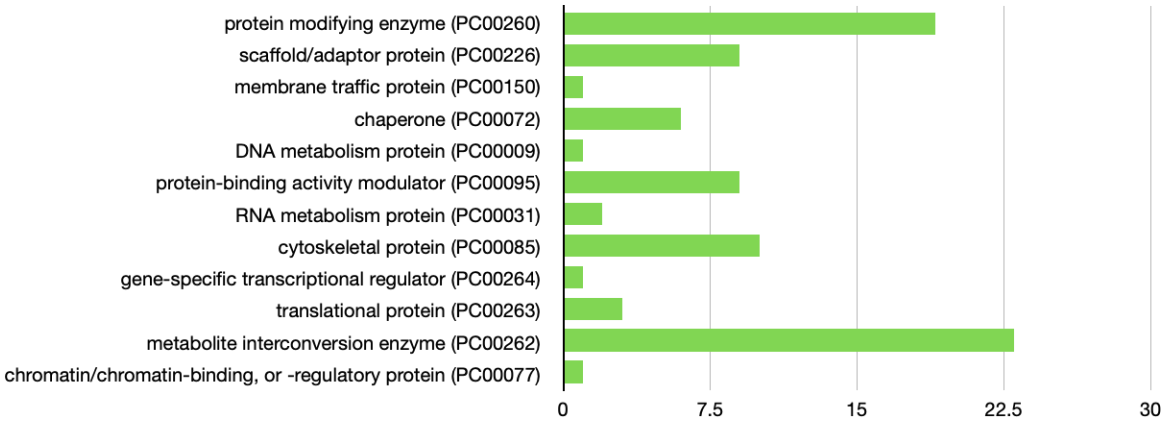

B

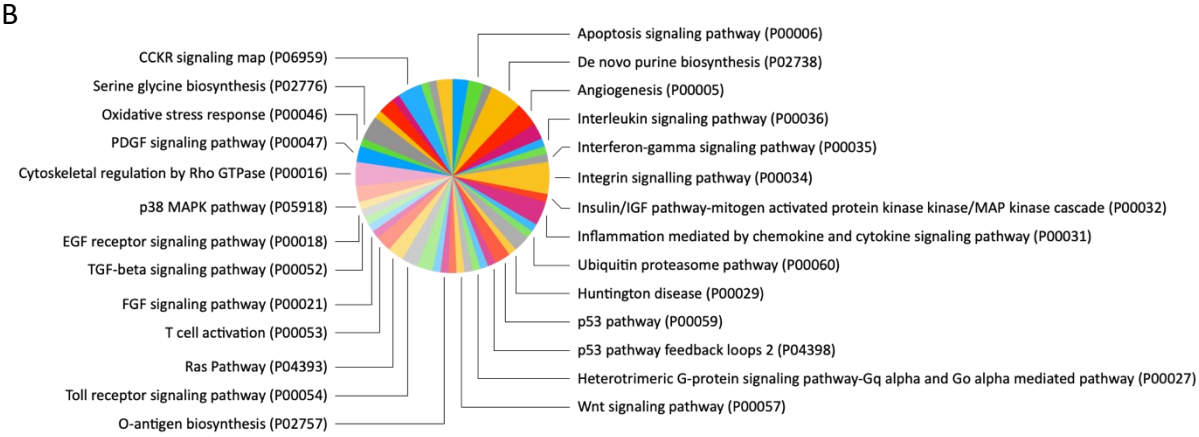

Figure 7.14 L-LA upregulated 105 proteins that did not increase in abundance with acidity alone.

(A) GO enrichment analysis of protein classes revealed that DEPs upregulated specifically in response to L-LA (and not pH 3.9 alone) were predominantly enzymes or structural proteins. **(B)** Functional analysis showed that these proteins were primarily associated with cytoskeletal regulatory pathways and inflammatory signalling pathways (n = 105).

Potential interactions between proteins upregulated in response to L-LA were investigated using a PPI network (Figure 7.15).

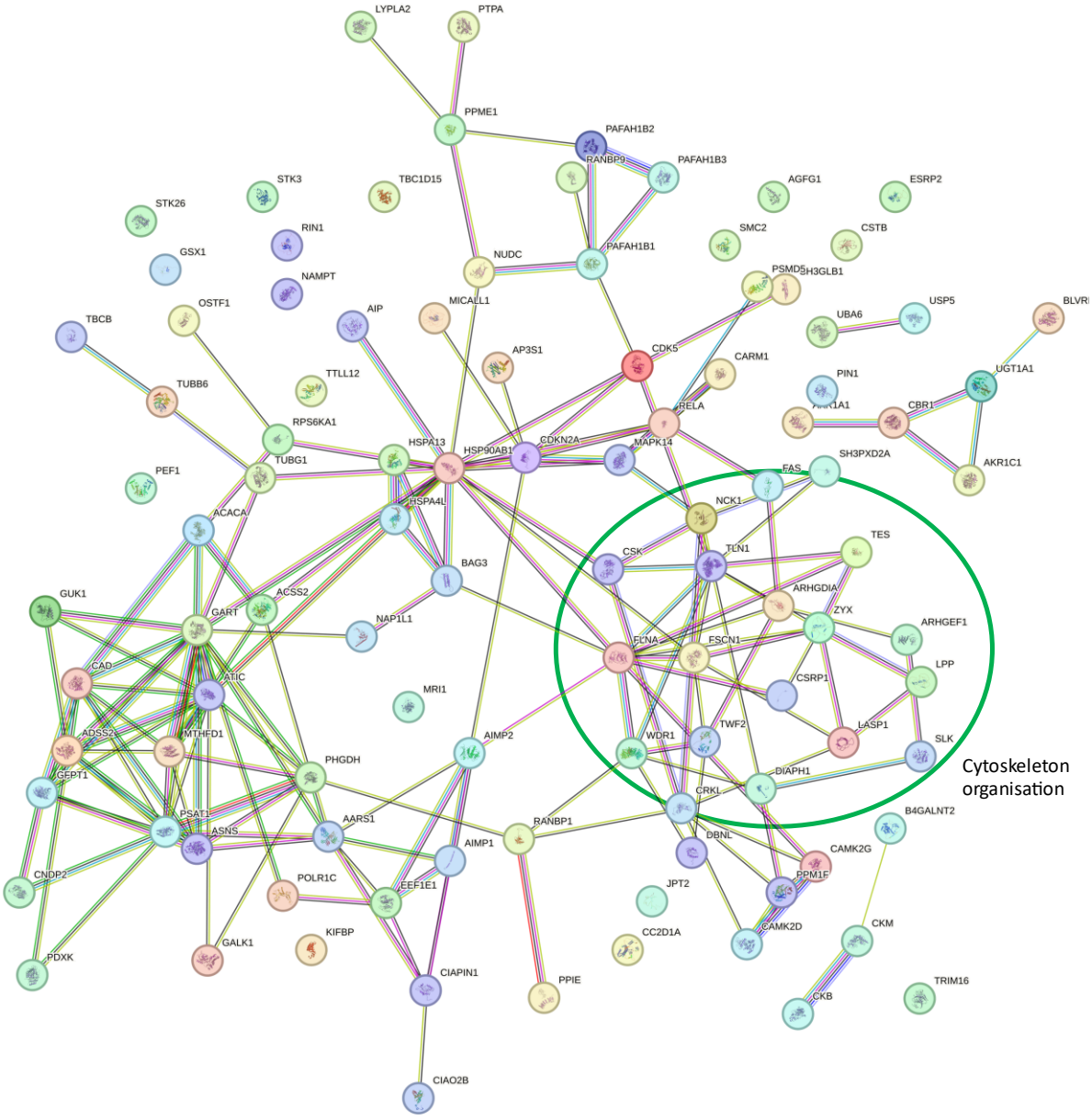

Figure 7.15 L-LA upregulated proteins associated with cytoskeletal regulation.

The PPI network of DEPs that increased in abundance specifically with L-LA treatment highlighted a cluster of proteins involved in cytoskeletal regulation (circled in green) (n = 105).

L-LA downregulated the abundance of 71/176 DEPs and 61 could be assigned to a protein class by the GO enrichment analysis. Over half these proteins were transporter and membrane traffic proteins (32.8%), cytoskeletal/cell adhesion proteins (8.2%) or protein-modifying/metabolite interconversion enzymes (13.1%) (Figure 7.16A). These proteins were

involved in the integrin signalling pathway, cytoskeletal regulation as well as several inflammatory signalling pathways (Figure 7.16B).

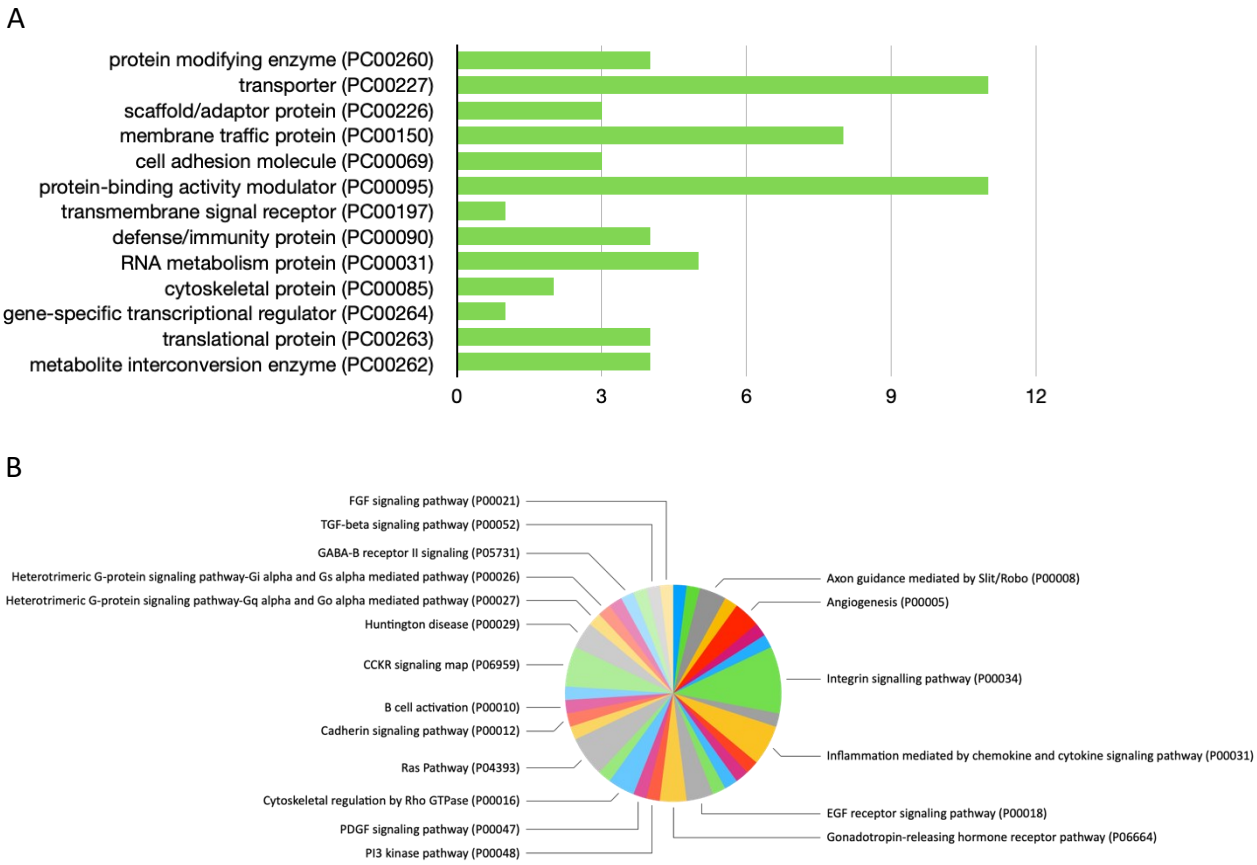

Figure 7.16 Downregulation of 71 unique proteins by L-LA exposure.

(A) GO enrichment analysis of downregulated DEPs identified in VECs exposed to L-LA (but not to acidity alone) highlighted that these proteins were primarily transporter or membrane traffic proteins, or modulators of protein binding activity. **(B)** Functional analysis showed that these proteins were involved in integrin signalling, cytoskeletal regulatory pathways, and inflammatory signalling pathways (n = 71).

Visualisation of the proteins downregulated by L-LA using a PPI network again showed clusters of protein interactions involved in cytoskeletal regulation and endolysosomal trafficking (Figure 7.17). These included proteins with well-described roles in regulating tight junction formation and cell adhesion, such as F11R and YES1.

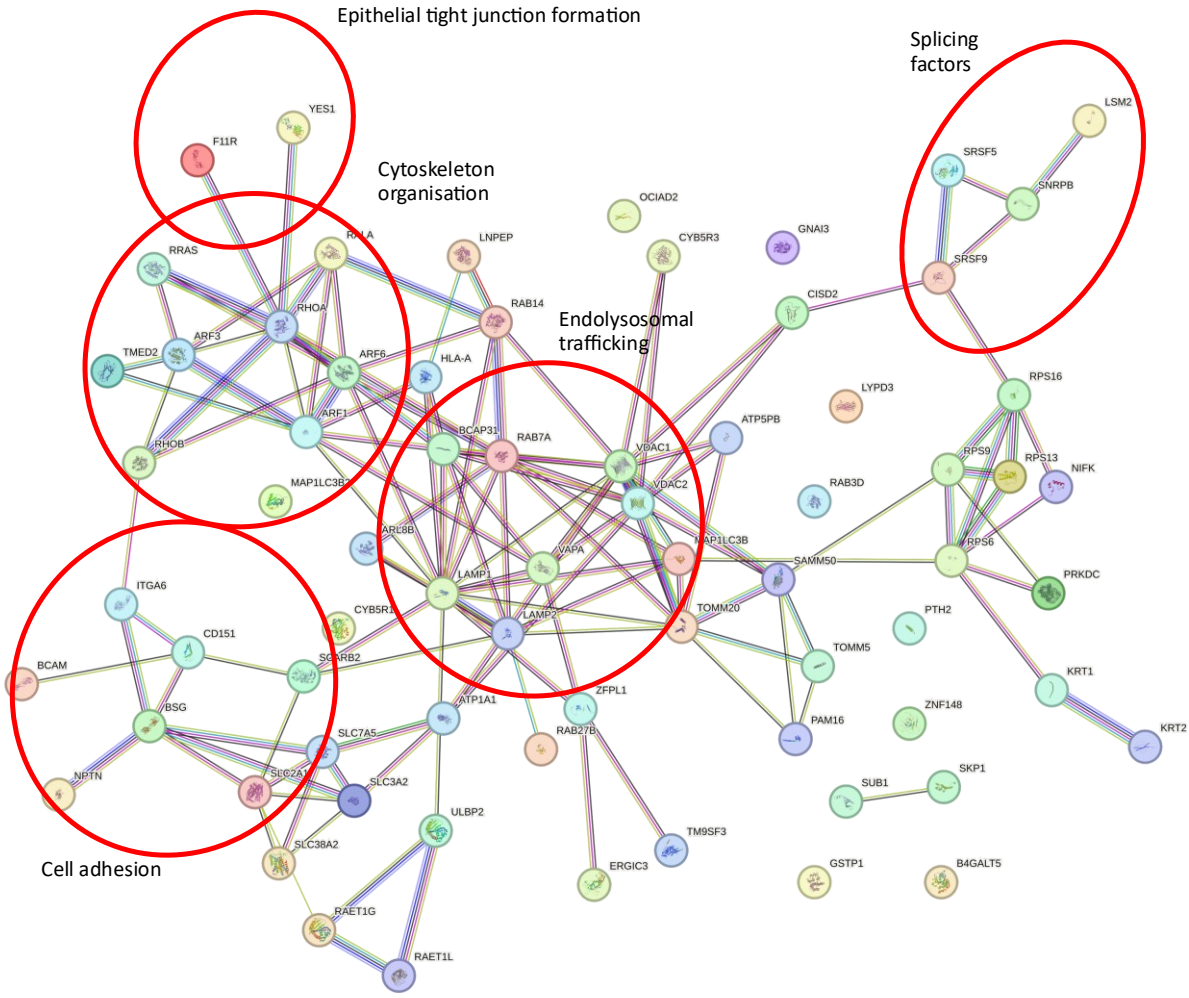

Figure 7.17 L-LA downregulated signal transduction pathway proteins at the plasma membrane.

Proteins downregulated by L-LA formed several clusters of protein interactions involved in cytoskeletal regulation, endolysosomal trafficking, cell adhesion and epithelial tight junction formation (n = 71). Clusters associated with these different functions are circled in red.

7.2.3 Effect of inhibiting MEK/ERK on protein abundance

Chapter 4 demonstrated that low pH, particularly in the presence of L-LA, significantly activated ERK. However, inhibiting ERK phosphorylation with a MEK inhibitor did not affect L-LA's ability to suppress inflammatory pathways mediated by NF-κB and AP-1. To identify other potential targets of ERK, proteomic analyses were conducted on VECs cultured at pH 7.4, pH 3.9 and L-LA, with or without MEK inhibition.

7.2.3.1 pH 7.4 vs pH 7.4 with MEK Inhibitor

First the proteome of VECs at pH 7.4 with or without the MEK inhibitor was investigated. Twenty-eight proteins changed significantly in abundance and this change was consistent across the sample repeats (Figure 7.18).

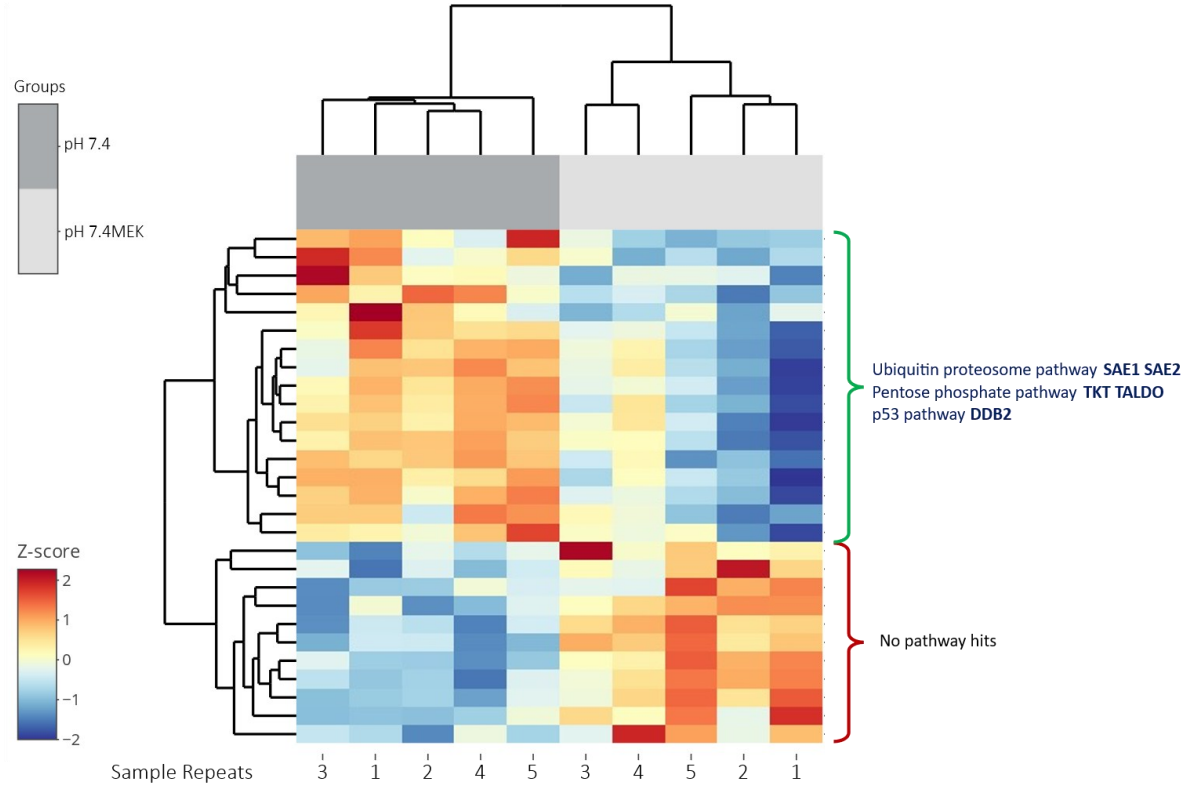

Figure 7.18 Heatmap of proteins differentially expressed following MEK inhibition at pH7.4.

The heatmap shows the differential abundance of 28 proteins significantly upregulated or downregulated in VECs following the pretreatment with the MEK inhibitor U0126 (10 µM; 30 mins) at pH 7.4. The most common biological pathways associated with these proteins are also highlighted.

Many of the proteins whose abundance was altered when MEK is inhibited do not have strong interactions with each other as shown by the PPI network (Figure.7.19).

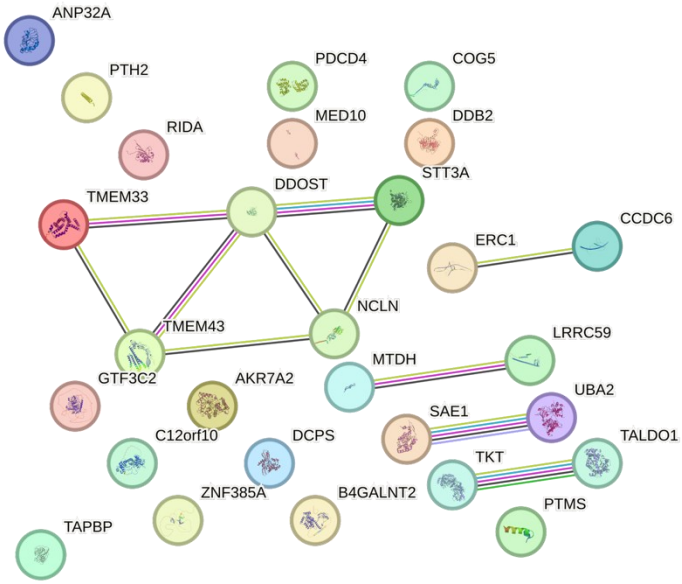

Figure 7.19 Proteins whose abundance changed when MEK was inhibited at pH 7.4 showed few interactions.

The PPI network analysis revealed that the 28 proteins with altered abundance upon MEK inhibition at pH 7.4 exhibited minimal clustering, indicating few interactions among these proteins.

Seventeen of the proteins were upregulated in the presence of MEK inhibitor. Where these proteins could be mapped to pathways, they were shown to be involved in the ubiquitin proteasome pathway, the pentose phosphate pathway or the p53 pathway (Figure 7.20).

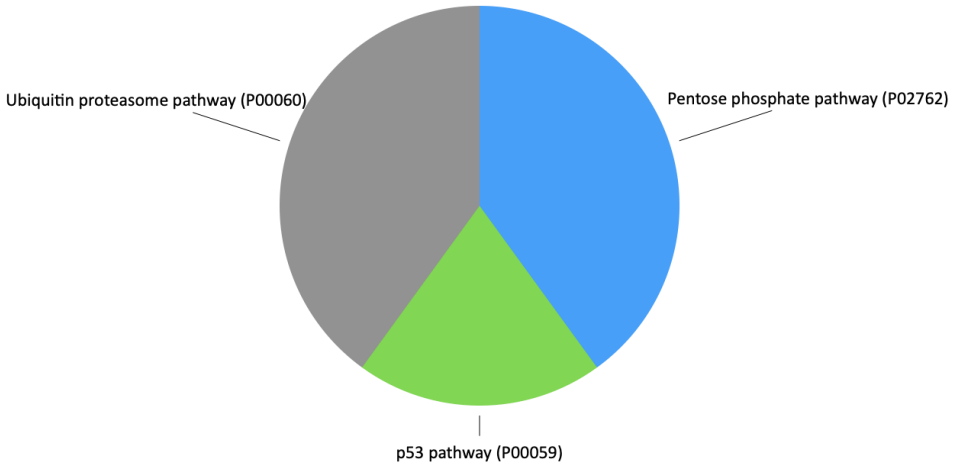

Figure 7.20 Key pathways for proteins upregulated by MEK inhibition at pH 7.4.

GO enrichment analysis (using data for pathways generated by PANTHER) identified key signalling pathways associated with the 17 differentially expressed proteins upregulated in VECs treated with a MEK inhibitor at pH 7.4.

Analysis of the protein classes upregulated by MEK inhibition revealed that the majority (35.3%) were enzymes, specifically categorised as metabolite interconversion enzymes or protein modifying enzymes.

In contrast, the 11 proteins downregulated by MEK inhibition did not map to any known pathways. However, classification using PANTHER identified these proteins as metabolite conversion enzymes (27.3%), defence/immunity proteins (9.1%), scaffold/adaptor proteins (9.1%), and RNA metabolism proteins (9.1%).

7.2.3.2 pH 3.9 vs pH 3.9 with MEK Inhibitor

The abundance of proteins at pH 3.9 was next compared in the presence and absence of MEK inhibitor. MEK inhibition at pH 3.9 resulted in nearly three times as many proteins showing significant changes in abundance compared to pH 7.4 (n = 88) (Figure 7.21A). The majority of these proteins (88.6%; n = 78) exhibited a decrease in abundance when MEK was inhibited (Figure 7.21B). Protein clusters identified in the PPI network analysis included those associated with tight junction formation and cell adhesion, such as F11R, as well as proteins involved in cytoskeletal organisation and N-glycan biosynthesis.

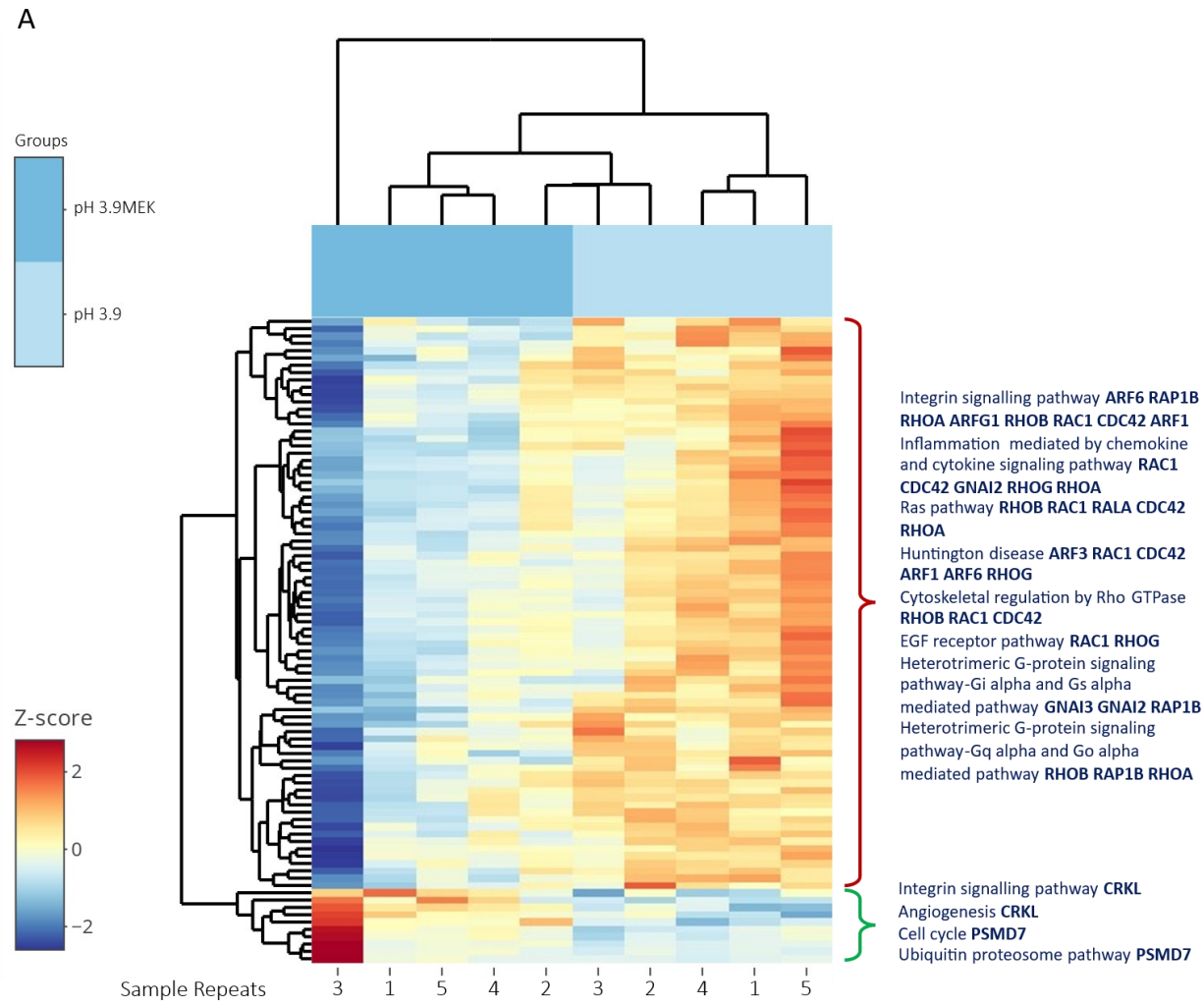
A
Groups
pH 3.9MEK
pH 3.9
Z-score
2
0
−2
Sample Repeats
3 1 5 4 2 3 2 4 1 5
Integrin signalling pathway ARF6 RAP1B RHOA ARFG1 RHOB RAC1 CDC42 ARF1
Inflammation mediated by chemokine and cytokine signaling pathway RAC1 CDC42 GNAI2 RHOG RHOA
Ras pathway RHOB RAC1 RALA CDC42 RHOA
Huntington disease ARF3 RAC1 CDC42 ARF1 ARF6 RHOG
Cytoskeletal regulation by Rho GTPase RHOB RAC1 CDC42
EGF receptor pathway RAC1 RHOG
Heterotrimeric G-protein signaling pathway-Gi alpha and Gs alpha mediated pathway GNAI3 GNAI2 RAP1B
Heterotrimeric G-protein signaling pathway-Gq alpha and Go alpha mediated pathway RHOB RAP1B RHOA
Integrin signalling pathway CRKL
Angiogenesis CRKL
Cell cycle PSMD7
Ubiquitin proteosome pathway PSMD7

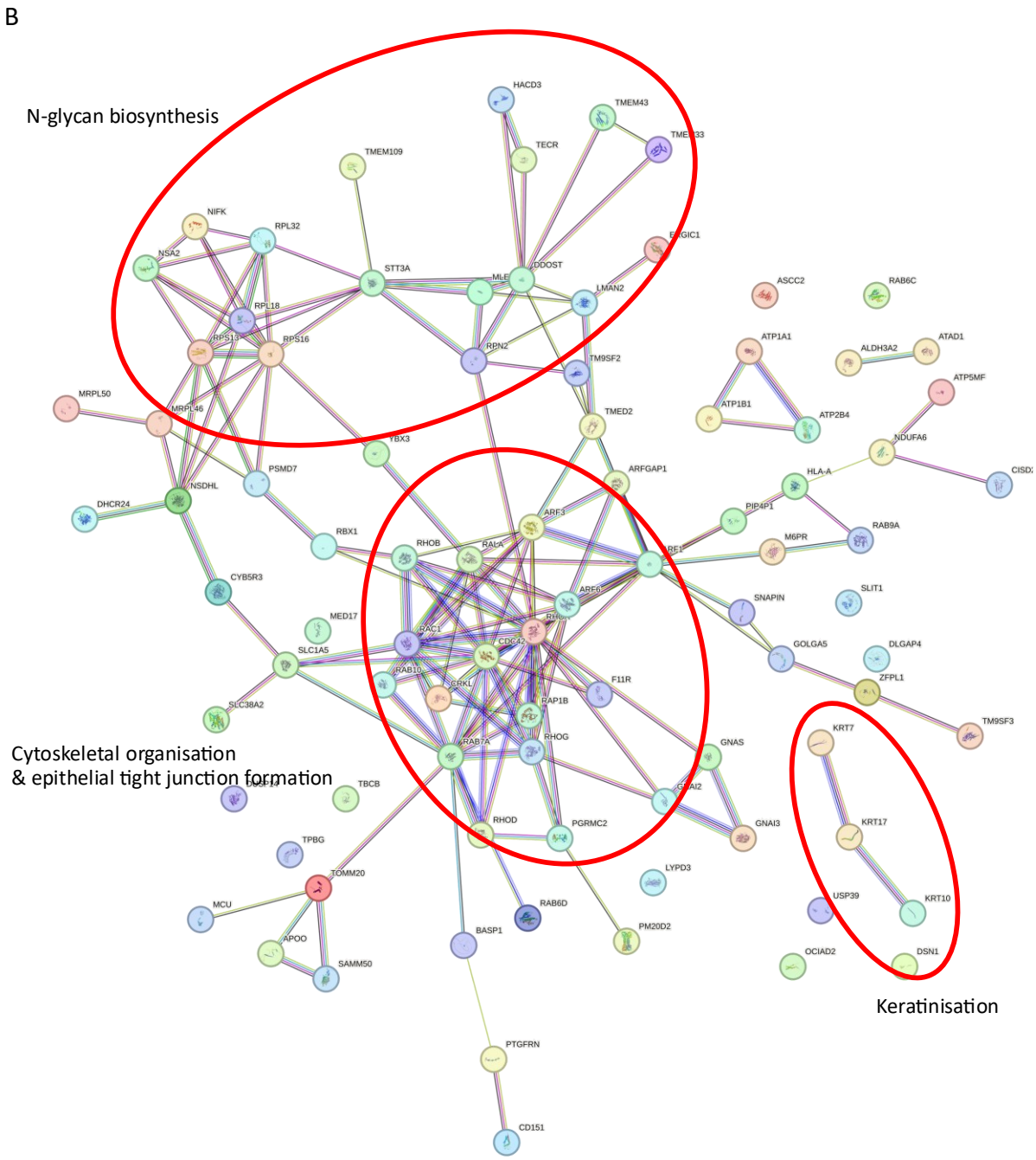

Figure 7.21 Proteomic differences in vaginal epithelial cells exposed to pH 3.9 with or without MEK inhibition.

(A) Heatmap illustrating 88 DEPs identified in VECs exposed to pH 3.9 with or without MEK inhibitor U0126 (10 µM; 30 mins pretreatment) at pH 3.9. The DEPs are annotated with their most common pathways. **(B)** PPI network of DEPs revealed that 79 proteins (circled in red) with significantly decreased abundance following MEK inhibition were involved in cytoskeletal organisation and tight junction formation, and N-glycan biosynthesis.

Only 10 proteins increased in abundance, comprising translational proteins (30%), cytoskeletal and scaffold/adaptor proteins (30%), and metabolite interconversion or protein-modifying enzymes (20%) (Figure 7.22A) with minimal protein-protein interactions observed (Figure 7.22B).

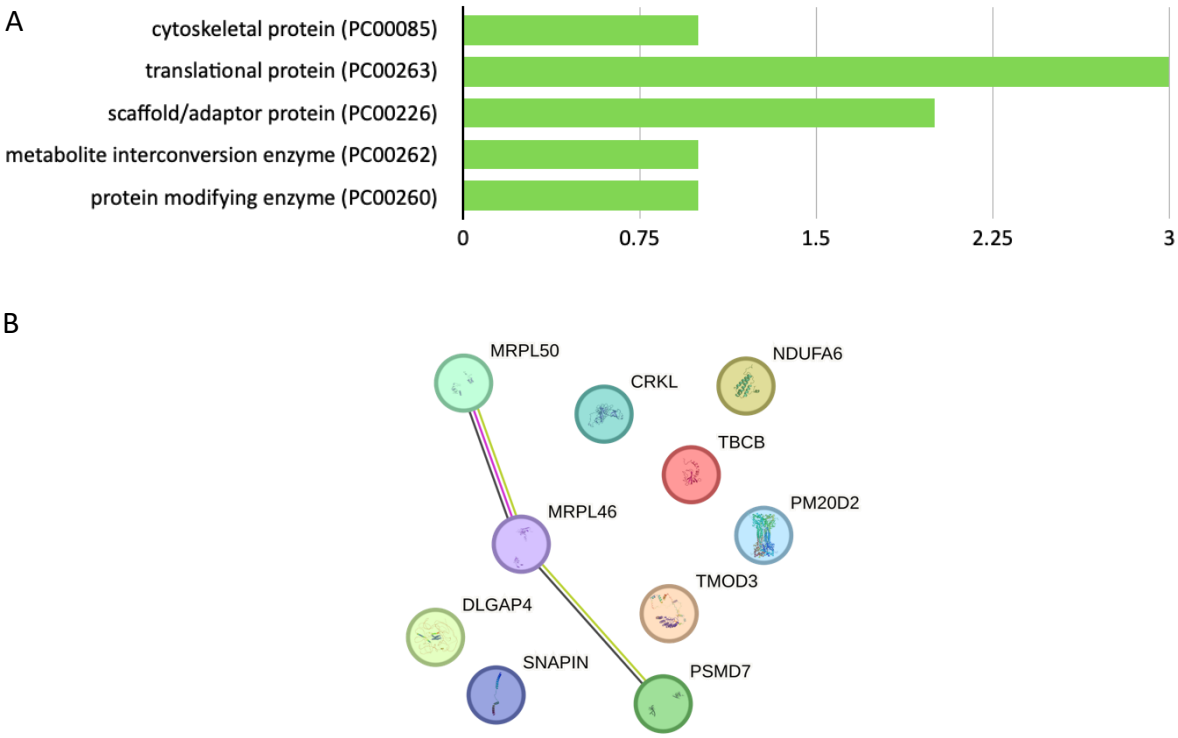

Figure 7.22 MEK Inhibition at pH 3.9 led to the upregulation of 10 proteins which showed few protein-protein interactions.

(A) GO enrichment analysis of protein classes for DEPs that were upregulated when VECs were treated with MEK inhibitor at pH 3.9. **(B)** The PPI network analysis revealed that the 10 proteins with increased abundance upon MEK inhibition at pH 3.9 exhibited minimal clustering, indicating few interactions among these proteins.

These proteins were involved in four pathways: integrin signalling, angiogenesis, cell cycle, and the ubiquitin proteasome pathway.

Proteins that decreased in abundance were involved in protein binding, transporters, membrane trafficking, cytoskeletal proteins, defence and immunity, cell adhesion, and transmembrane signal receptor. PANTHER did not assign a protein class to 32.1% of the proteins downregulated by inhibition of MEK (Figure 7.23A). Enriched pathways included

cytoskeletal modulation pathways such as the integrin signalling pathway (20.9%), inflammatory pathways (9.9%) and growth factor signalling pathways (9.9%) (Figure 7.23B).

A

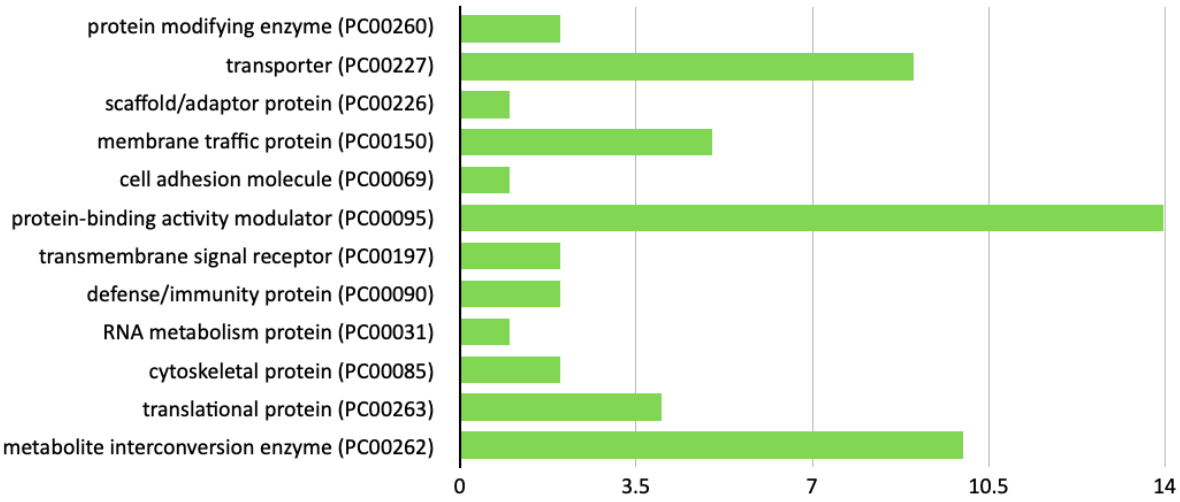

B

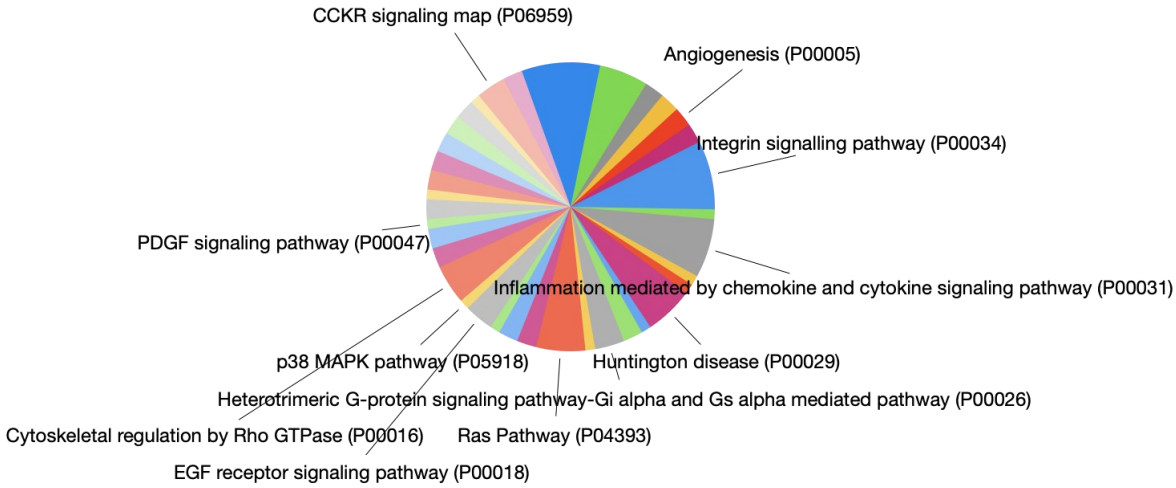

Figure 7.23 Downregulation of proteins involved in cytoskeletal regulation and inflammatory signalling pathways following MEK inhibition at pH 3.9.

(A) GO enrichment analysis of protein classes for the 78 DEPs downregulated in VECs treated with MEK inhibitor U0126 (10µM; 30 mins pretreatment) in the presence of L-LA. **(B)** These downregulated proteins were predominantly involved in cytoskeletal regulatory pathways, integrin signalling pathways and inflammatory signalling pathways.

7.2.3.3 L-LA vs L-LA with MEK Inhibitor

When MEK/ERK was inhibited in the presence of L-LA, only eight proteins showed significant changes in abundance; five were upregulated, and three were downregulated (Figure 7.24).

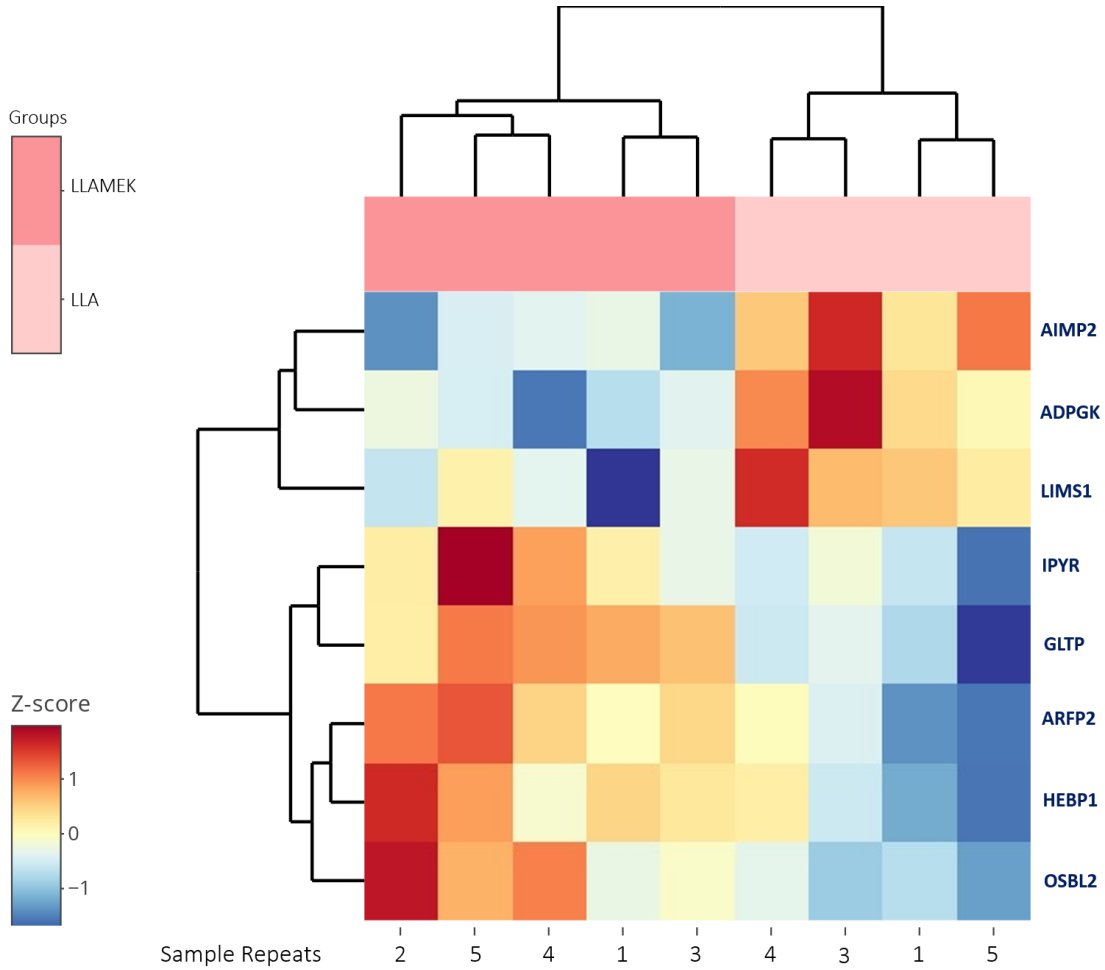

Figure 7.24 Fewer proteins changed in abundance in VECs exposed to L-LA with MEK inhibition at pH 3.9.

Heatmap illustrating the DEPs in VECs exposed to L-LA for 6 hours with MEK inhibition (8 proteins).

GO enrichment analysis identified two key pathways affected by MEK/ERK inhibition in the presence of L-LA. Proteins associated with the integrin signalling pathways were significantly downregulated, while those associated with the Huntington disease pathways were significantly upregulated.

Despite these pathway associations, the PPI network generated by STRING, which also mines the published literature, revealed no significant interactions among these proteins (Figure 7.25).

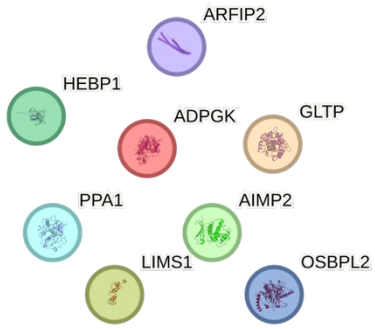

Figure 7.25 No clustering was observed in proteins that changed in abundance in VECs exposed to L-LA with MEK inhibition.

No PPIs were identified among the proteins whose abundance changed following MEK was inhibition in VECS exposed to L-LA at pH 3.9.

7.2.4 Characterisation of LA-associated proteins regulated by MEK/ERK inhibition

The next set of comparisons aimed to identify proteins that are differentially regulated by L-LA through MEK/ERK signalling. To achieve this, the following strategy was used. First, DEPs were identified between VECs cultured at pH 7.4 and VECs cultured at pH 3.9 with L-LA in the presence of MEK inhibitor (LLAMEK). Similarly, DEPs were identified between VECs cultured at pH 3.9 alone and at pH 3.9 with L-LA in the presence of MEK inhibitor. These DEPs were then compared to the original list of DEPs identified when VECs were cultured at pH 3.9 with L-LA without MEK inhibition.

A total of 156 DEPs were identified when comparing VECs cultured at pH 7.4 to those treated with L-LA and MEK Inhibitor. The majority of these proteins (141/156) showed increased abundance following MEK inhibition (Figure 7.26).

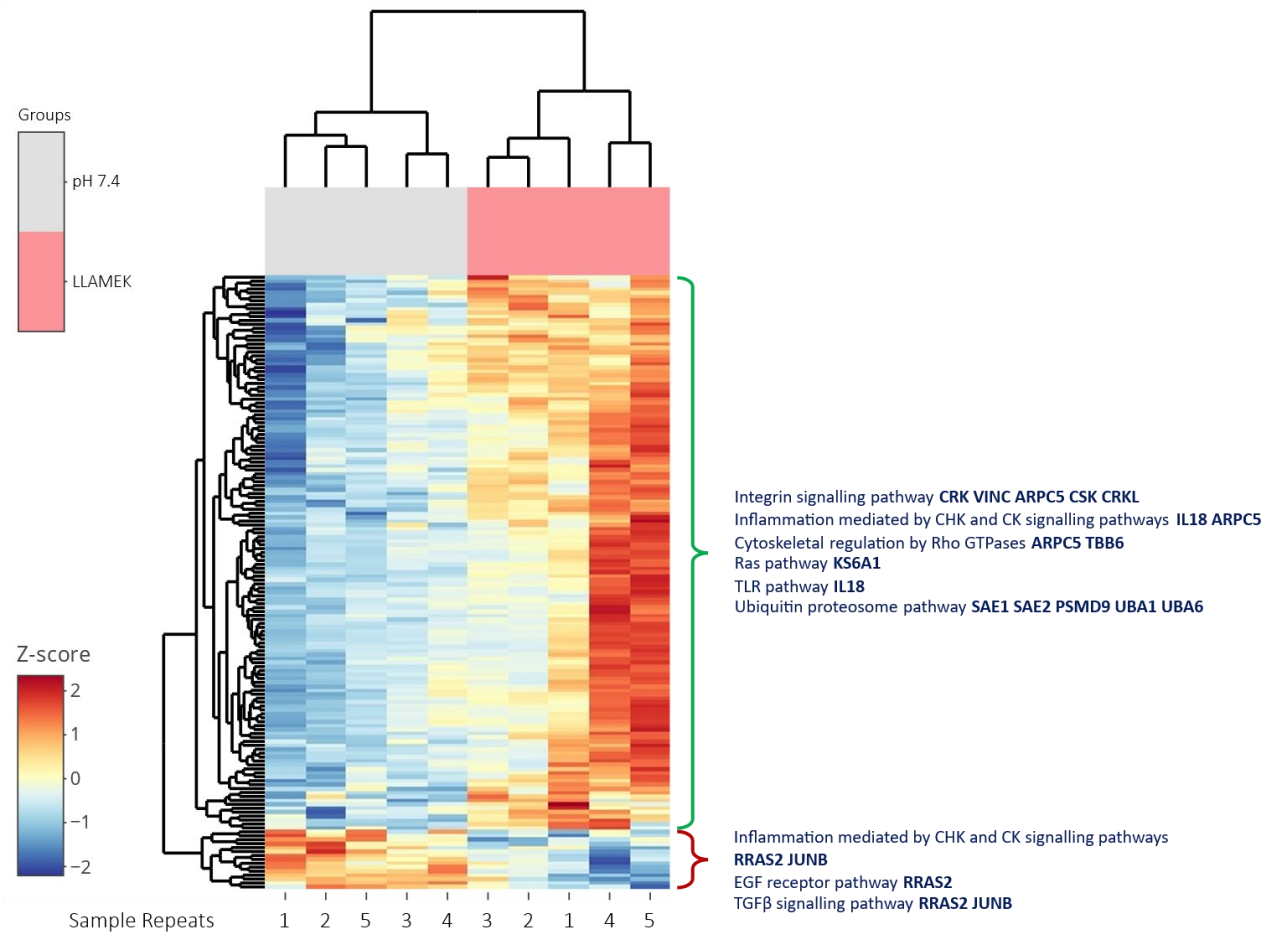

Figure 7.26 MEK inhibition in the presence of L-LA upregulated 141 proteins and downregulated 15 proteins compared to pH 7.4.

Heatmap showing 156 DEPs between VECs cultured pH 7.4 medium for 6 hours and VECs exposed to L-LA with MEK inhibitor, along with the most common pathways to which these proteins are mapped.

When comparing VECs cultured at pH 7.4 to those cultured at pH3.9 with L-LA and MEK inhibitor, a total of 68 DEPs were identified, of which 42 proteins were significantly increased and 26 significantly decreased in abundance (Figure 7.27).

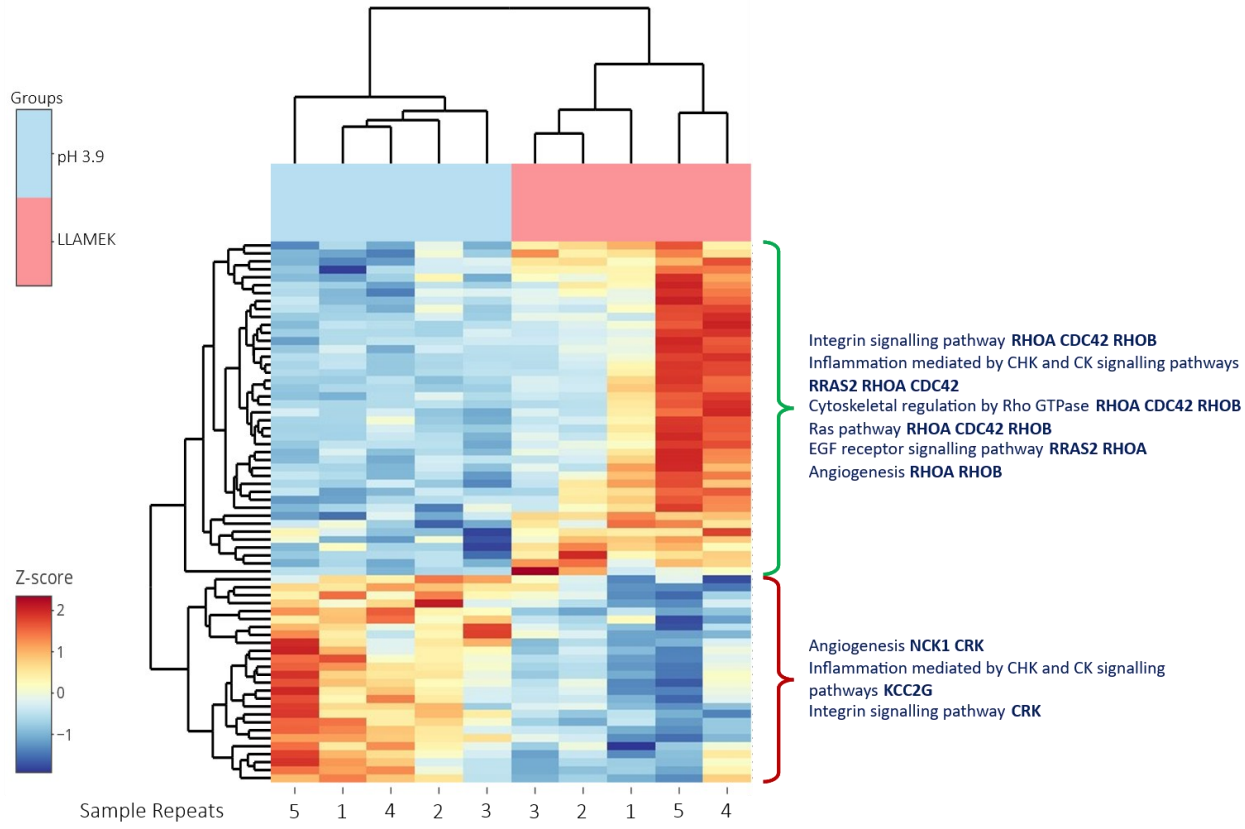

Figure 7.27 MEK inhibition in the presence of L-LA led to the upregulation of 42 proteins and downregulation of 26 proteins compared to pH 3.9.

Heatmap showing 68 DEPs in VECs exposed to MEK inhibitor at pH 3.9 with L-LA compared to VECs at pH 3.9 alone, and their most common associated pathways (68 proteins).

These DEPs were then compared them to the proteins initially identified as significantly regulated by L-LA at pH 7.4 or pH 3.9 (see Figures 7.8 and 7.13, respectively) to determine which L-LA-associated changes were likely mediated via MEK/ERK signalling.

At pH 7.4, among the 285 proteins that changed in abundance with L-LA (with or without MEK inhibitor), 129 were unique to L-LA, 62 were unique to MEK/ERK inhibition, and 94 were common to both conditions (Figure 7.28A). At pH 3.9, 205 proteins showed significant changes in abundance, 137 proteins were unique to L-LA, 29 to MEK inhibition being present and 39 were common to both conditions (Figure 7.28B).

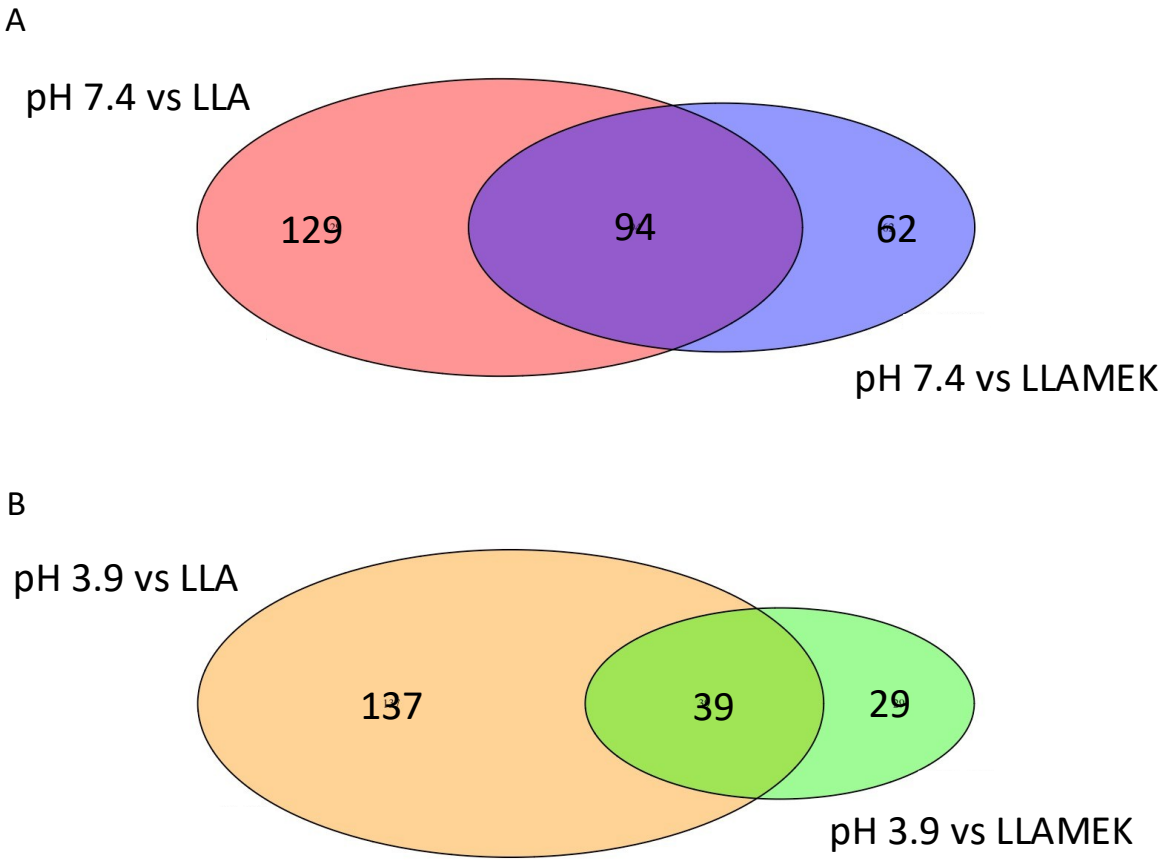

Figure 7.28 Overlap of proteins that changed in abundance in the presence of L-LA with or without MEK inhibitor at (A) pH 7.4 and (B) pH 3.9.

Table 7.2 summarises the abundance of up- or downregulated proteins at pH 7.4 and pH 3.9 under conditions where either L-LA alone or L-LA with MEK inhibitor was present. At pH 3.9, exposure of VECs to acidic conditions with L-LA resulted in 105 proteins increasing and 71 proteins decreasing in abundance. However, with MEK/ERK inhibition under the same conditions, only 42 proteins increased, and 26 proteins decreased. This represents a 2.6-fold reduction of DEPs when MEK is inhibited in acidified cells with L-LA. Specifically, MEK inhibition suppressed 67.6% of the proteins upregulated by L-LA and 85.9% of the proteins downregulated by L-LA (Table 7.2).

Table 7.2 Proteins no longer abundant when MEK is inhibited at pH 7.4 or pH 3.9 in presence of L-LA

pH	PROTEIN ABUNDANCE	L-LA	L-LA + MEK INHIBITOR	NO LONGER ABUNDANT PROTEINS	MISSING PROTEINS DUE TO MEK INHIBITION (%)
pH 7.4	Upregulated	180	141	92	51.1
	Downregulated	43	15	37	86.0
	TOTAL	223	156	129	57.8
pH 3.9	Upregulated	105	42	71	67.6
	Downregulated	71	26	61	85.9
	TOTAL	176	68	132	75.0

The data were further analysed to identify which proteins that responded to L-LA were no longer significantly altered when the MEK/ERK pathway was blocked. At pH 7.4, 129 such proteins were identified, of which 92 were upregulated and 37 downregulated by L-LA but no longer significant when MEK was inhibited. At pH 3.9, a similar number (132) of proteins were no longer significantly altered when MEK was inhibited, including 71 upregulated and 61 downregulated by L-LA. Thus, inhibition of the MEK pathway in the presence of L-LA prevents many proteins from being significantly up- or downregulated.

To explore potential functional associations, a PPI network was constructed for the proteins that were no longer abundant when MEK was inhibited. Examination of the proteins altered at pH 7.4 revealed four distinct clusters of proteins that had been regulated by L-LA but were no longer abundant with MEK inhibition (Figure 7.29A). These clusters were associated with cytoskeletal remodelling, including linking actin to the integrin signalling pathway, MAPK and NF-κB signalling, apoptosis and wound healing (Figure 7.29B).

A

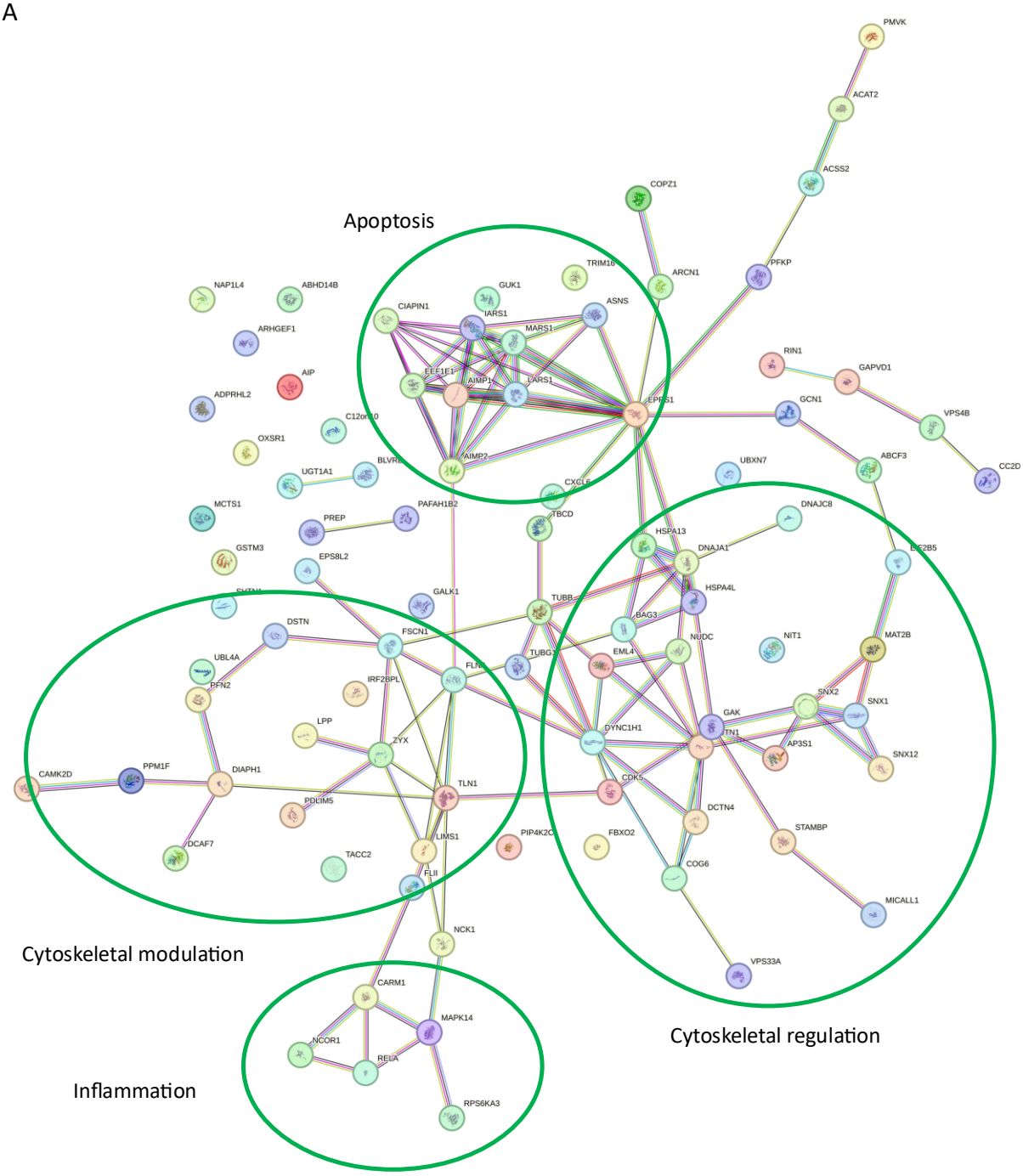
Apoptosis
Cytoskeletal modulation
Cytoskeletal regulation
Inflammation
PMVK
ACAT2
ACSS2
COPZ1
PFKP
ARCN1
TRIM16
GUK1
ASNS
CIAPIN1
IARS1
MARS1
EEF1E1
AIMP1
LARS1
EPRS1
NAP1L4
ABHD14B
ARHGEF1
AIP
ADPRHL2
C12orf10
OXSR1
BLVRB
UGT1A1
AIMP2
CXCL6
TBCD
PAFAH1B2
PREP
MCTS1
GSTM3
EPS8L2
GALK1
DSTN
FSCN1
UBL4A
PFN2
IRF2BPL
FLNA
LPP
ZYX
CAMK2D
PPM1F
DIAPH1
PDLIM5
DCAF7
TACC2
TLN1
LIMS1
FLII
NCK1
CARM1
MAPK14
NCOR1
RELA
RPS6KA3
RIN1
GAPVD1
VPS4B
CC2D
GCN1
UBXN7
ABCF3
DNAJC8
HSPA13
DNAJA1
HSPA4L
BAG3
TUBB
TUBG1
EML4
NUDC
NIT1
MAT2B
EIF2B5
SNX2
SNX1
GAK
TNI
AP3S1
SNX12
DYNC1H1
CDK5
DCTN4
STAMBP
PIP4K2C
FBXO2
COG6
MICALL1
VPS33A

B

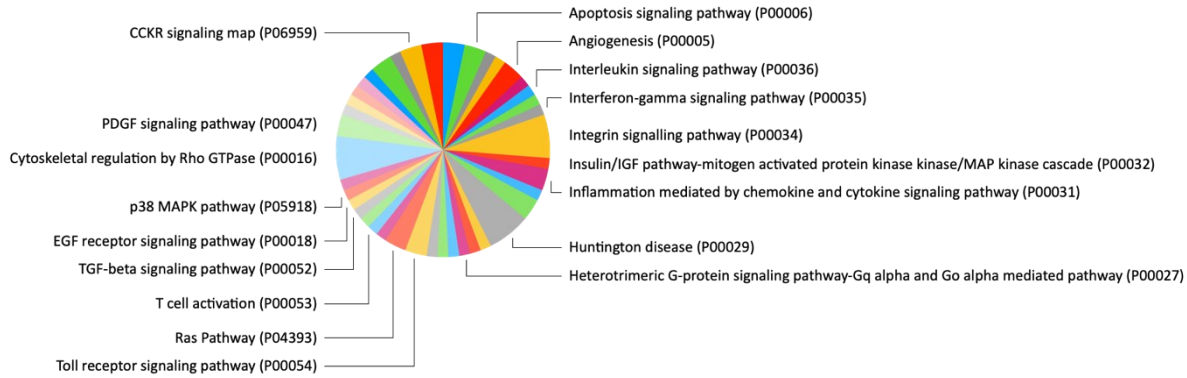

Figure 7.29 L-LA upregulated 92 proteins that failed to be upregulated when MEK was inhibited at pH 7.4.

(A) PPI network showing four clusters of proteins upregulated by L-LA but not by L-LA + MEK inhibition at pH 7.4. **(B)** These proteins were predominantly involved in cytoskeletal regulatory pathways, integrin signalling and inflammatory pathways (92 proteins).

The clusters of proteins that were downregulated by L-LA but no longer abundant when MEK was inhibited were involved in cell-cell adhesion, keratinisation and Golgi-ER transport and included a group of ribonucleoproteins involved in apoptosis and splicing (Figure 7.30).

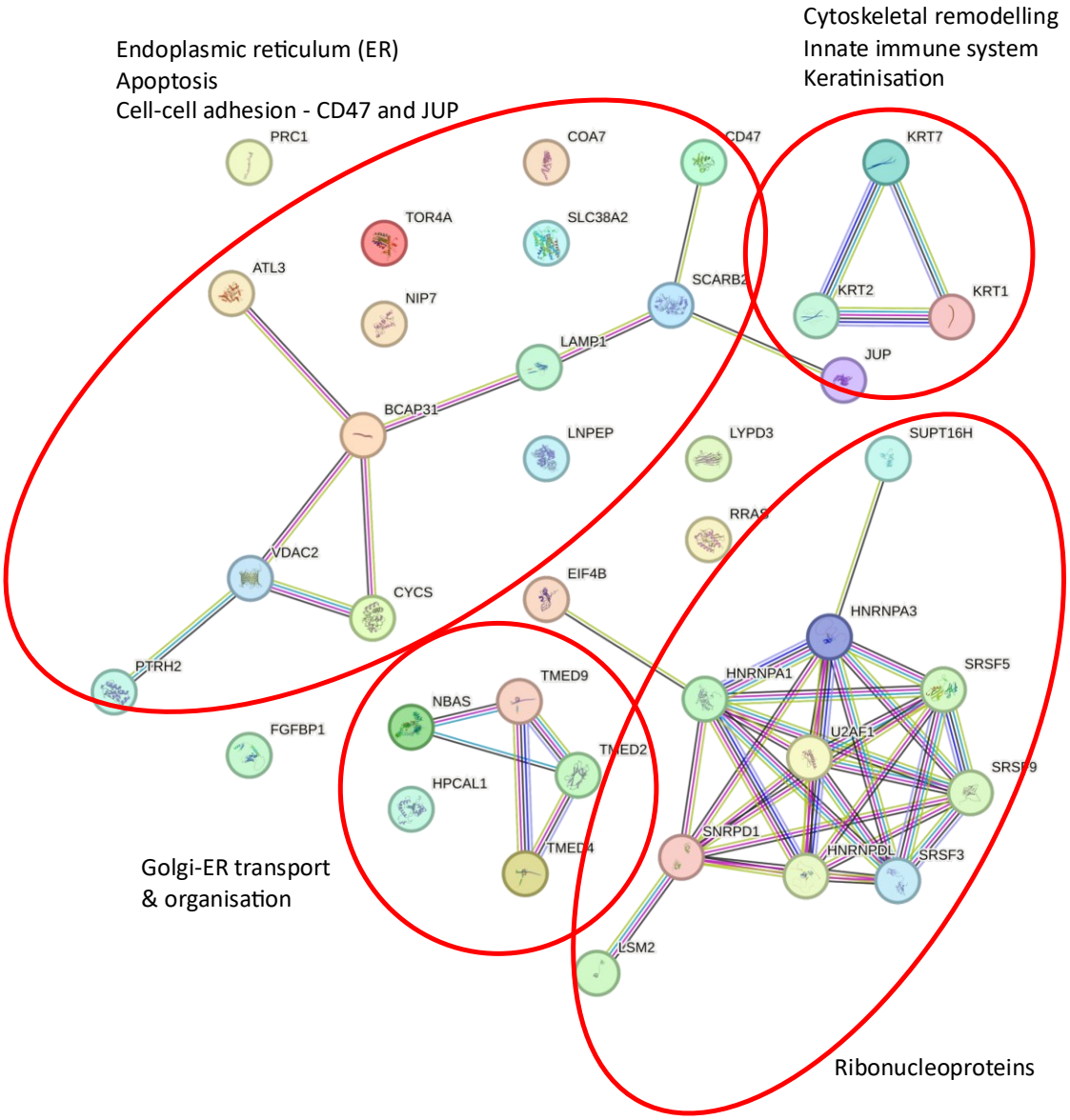

Figure 7.30 Protein-protein interaction network for 37 proteins downregulated by L-LA but no longer abundant when MEK was inhibited at pH 7.4.

PPI network showing four clusters of proteins downregulated by L-LA but not by L-LA + MEK inhibition at pH 7.4.

Next, proteins that changed in abundance at pH 3.9 with L-LA but were no longer abundant when MEK/ERK was inhibited were investigated. PPI clustering revealed an upregulation of proteins involved in cytoskeletal regulation, cell adhesion, MAPK and RIG-I inflammatory signalling, apoptosis and wound healing (n = 71) (Figure 7.31A). GO enrichment pathway analysis further highlighted inflammatory pathways, cytoskeletal remodelling and integrin signalling pathways (Figure 7.31B).

A Cytoskeletal regulation & cell adhesion

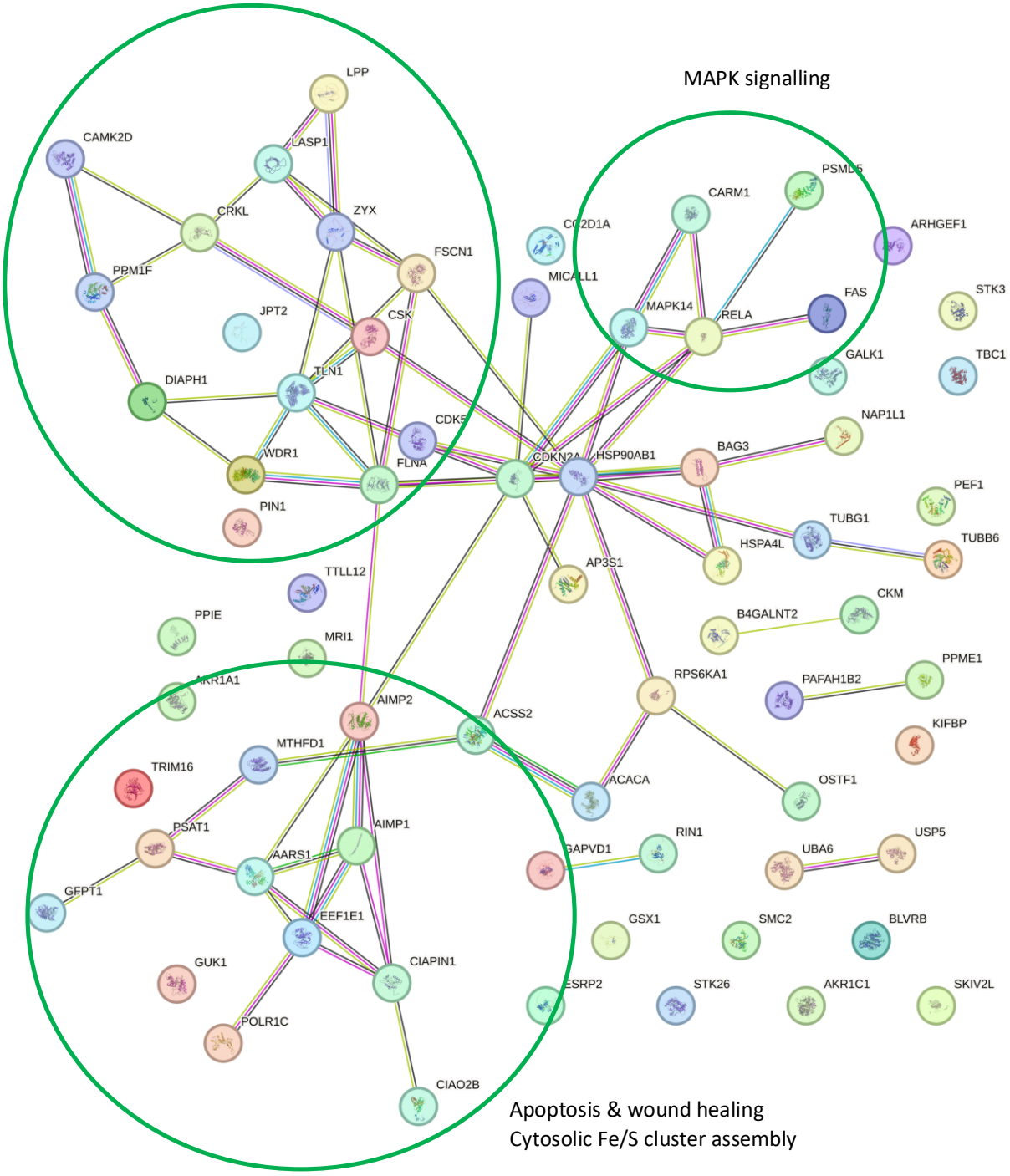

B

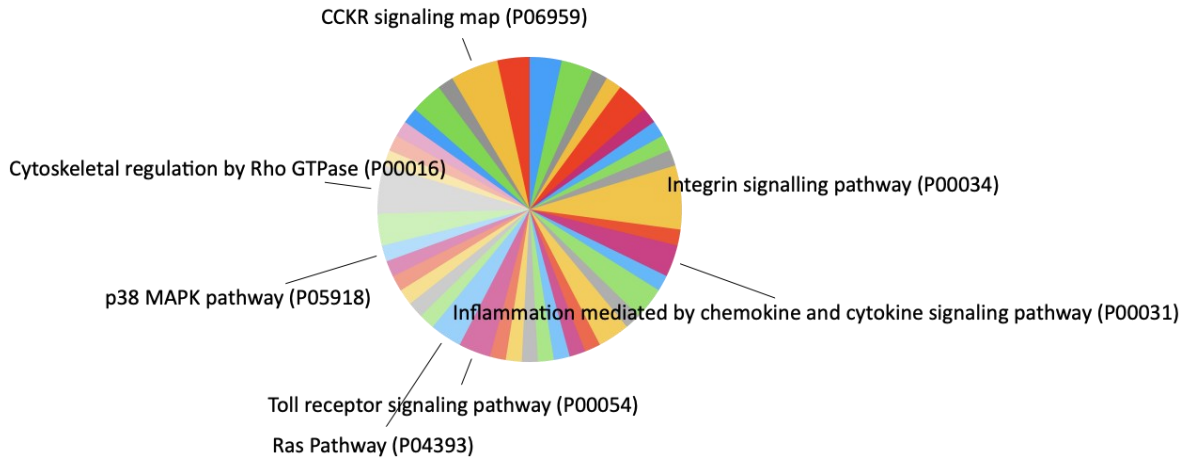

Figure 7.31 Protein-protein interaction network and key pathways for L-LA-upregulated proteins no longer detected when MEK was inhibited at pH 3.9.

(A) Three clusters were identified in the STRING PPI network for proteins upregulated by L-LA but lost with MEK inhibition at pH 3.9. **(B)** These proteins were predominantly associated with cytoskeletal regulation, apoptosis, integrin signalling and inflammatory pathways (71 proteins).

Finally, the PPI network for 61 downregulated proteins no longer detected when MEK was inhibited included proteins involved in cell surface adhesion and signalling, intracellular membrane trafficking such as reorganisation of the actin cytoskeleton, junctional remodelling and cytokine signalling (Figure 7.32A). These proteins mapped to integrin, inflammatory, cytoskeletal regulatory and cadherin signalling pathways (Figure 7.32B).

A

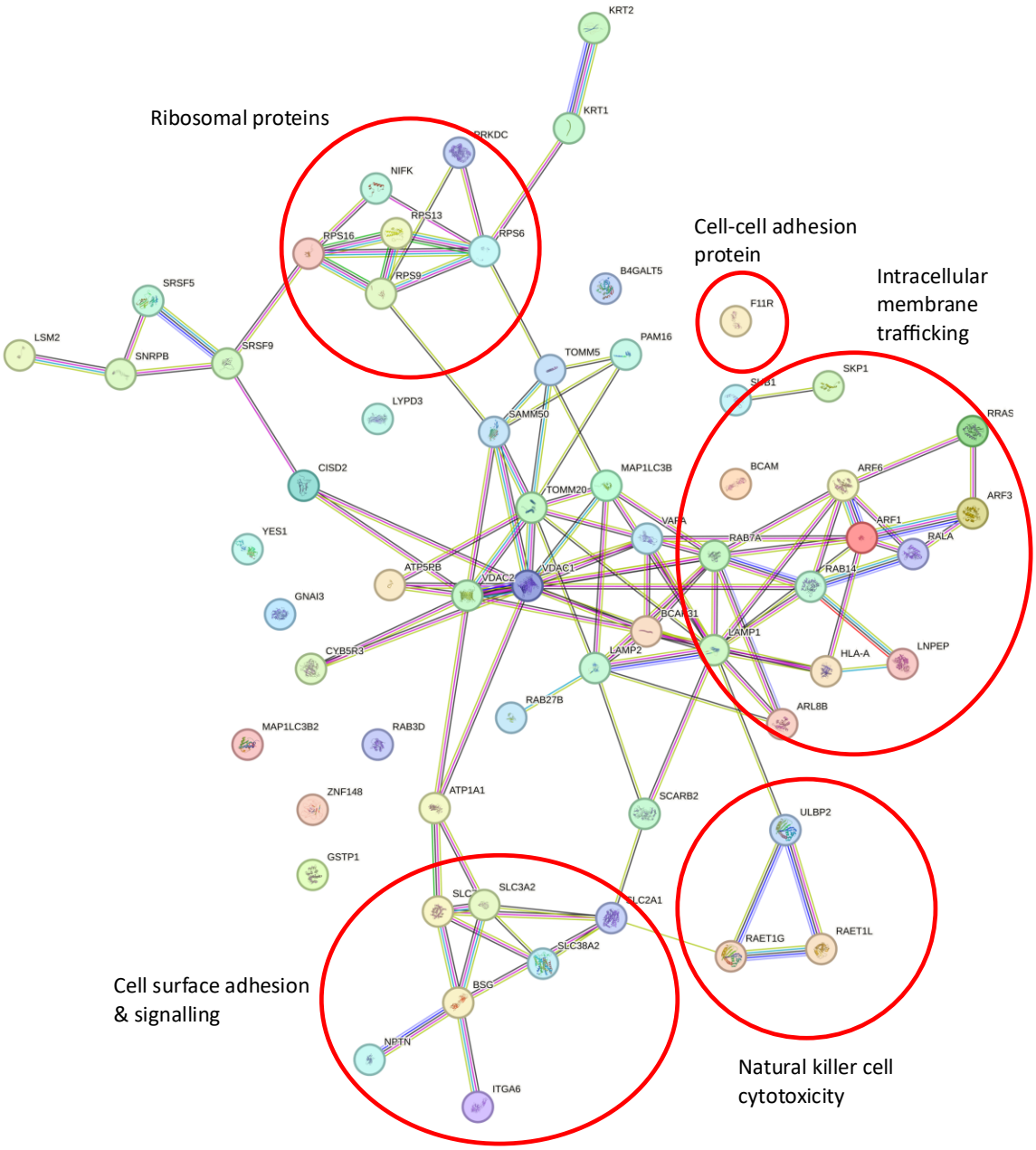
Ribosomal proteins
Cell-cell adhesion protein
Intracellular membrane trafficking
Cell surface adhesion & signalling
Natural killer cell cytotoxicity
KRT2
KRT1
PRKDC
NIFK
RPS13
RPS16
RPS6
RPS9
B4GALT5
F11R
SRSF5
LSM2
SNRPB
SRSF9
PAM16
TOMM5
SKP1
LYPD3
SAMM50
RRAS
CISD2
MAP1LC3B
BCAM
ARF6
ARF3
TOMM20
YES1
VAPA
ARF1
RAB7A
RALA
ATP5PB
VDAC2
VDAC1
RAB14
GNAI3
LAMP1
CYB5R3
LAMP2
HLA-A
LNPEP
RAB27B
ARL8B
MAP1LC3B2
RAB3D
ZNF148
ATP1A1
SCARB2
ULBP2
GSTP1
SLC3A2
SLC2A1
RAET1G
RAET1L
SLC38A2
BSG
NPTN
ITGA6

B

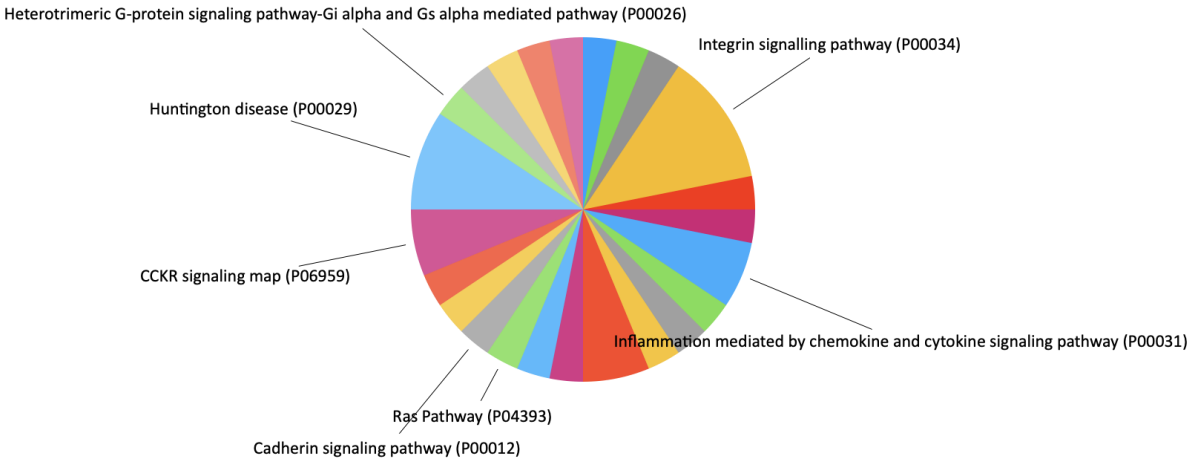

Figure 7.32 Key pathways for proteins downregulated by L-LA but no longer abundant when MEK was inhibited at pH 3.9.

(A) Protein clusters identified in the STRING protein-protein interaction network included proteins that decreased in abundance when L-LA was present but were no longer detected when MEK was inhibited at pH 3.9. **(B)** These proteins were primarily associated with intracellular membrane trafficking, cell surface and cell-cell adhesion and signalling (61 proteins).

Proteins that were differentially regulated by L-LA but not detected when MEK/ERK was inhibited at either pH 7.4 or pH 3.9 were enriched in pathways related to cytoskeletal regulation and MAPK signalling, whereas proteins involved in TLR receptor binding and signalling receptor binding were downregulated when MEK/ERK was inhibited (Figure 7.33).

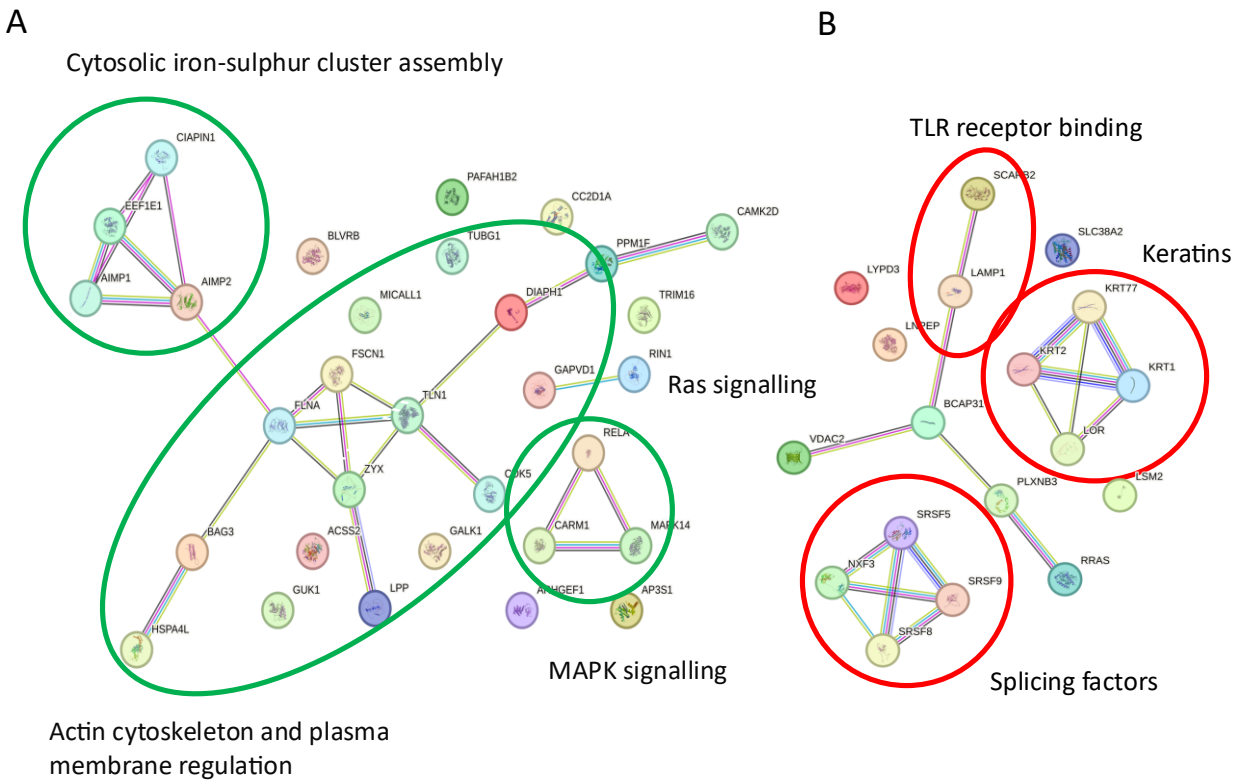

Figure 7.33 Protein clusters of L-LA-regulated proteins no longer detected when MEK was inhibited at both pH 7.4 and pH 3.9.

(A) Clusters of proteins that increased in abundance with L-LA (green) but were no longer detected when MEK was inhibited at both pH levels, identified in the STRING PPI network. **(B)** Clusters of proteins that decreased in abundance with L-LA (red) but were no longer detected when MEK was inhibited at both pH levels.

Proteins involved in cytoskeletal regulation were consistently upregulated by L-LA treatment but not when cells were treated with the MEK/ERK inhibitor. Therefore, further analyses were conducted to examine how LA influences cytoskeletal proteins in VECs.

7.2.5 Further consideration of selected pathways and proteins

7.2.5.1 Cytoskeletal proteins

Minimal change in the abundance of cytoskeletal proteins was observed in VECs cultured at pH 3.9 relative to pH 7.4. However, when cultured at pH 3.9 with L-LA, the levels of 22

cytoskeletal proteins were consistently altered. These proteins are listed in Table 7.3 along with their gene names and protein binding targets.

Table 7.3 Differentially expressed cytoskeletal proteins when L-LA is present

Gene Name	Protein Name	Type of Cytoskeletal Protein
ARPC5	Actin-related protein 2/3 complex subunit 5	Actin-binding Protein
CAPG	Macrophage-capping protein	Actin-binding Protein
CSRP1	Cysteine and glycine-rich protein 1	Actin-binding Protein
DCTN1	Dynactin subunit 1	Tubulin-binding Protein
DNM1L	Dynamin-1-like protein	Tubulin-binding Protein
DSTN	Destrin	Actin-binding Protein
EML4	Echinoderm microtubule-associated protein-like 4	Tubulin-binding Protein
EPS8L2	Epidermal growth factor receptor kinase substrate 8-like protein 2	Actin-binding Protein
FLII	Flightless-I homolog	Actin-binding Protein
FSCN1	Fascin	Actin-binding Protein
GSN	Gelsolin	Actin-binding Protein
LASP1	LIM and SH3 domain protein 1	Actin-binding Protein
MAP1LC3B	Microtubule-associated proteins 1A/1B light chain 3B	Tubulin-binding Protein
PDLIM5	PDZ and LIM domain protein 5	Actin-binding Protein
PFN2	Profilin 2	Actin-binding Protein
PRC1	Protein regulator of cytokinesis 1	Tubulin-binding Protein
RAB3D	Ras-related protein Rab-3D	Myosin-binding Protein
TAGLN2	Transgelin-2	Actin-binding Protein
TBCD	Tubulin-specific chaperone D	Tubulin-binding Protein
TUBGCP2	Gamma-tubulin complex component 2	Tubulin-binding Protein
TWF2	Twinfilin-2	Actin-binding Protein
WDR1	Actin-interacting protein 1 (AIP1)	Actin-binding Protein

A PPI network of the 22 cytoskeletal proteins highlighted known interactions between many of the proteins. Some of these proteins not only regulate the cytoskeleton but are also involved in cellular signalling and gene expression, for example LASP1 (LIM and SH3 domain protein 1), which is activated by the $G\alpha_i$ pathway and forms a complex with the tight junction protein zonula occludens-2 (ZO-2) (571) (Figure 7.34).

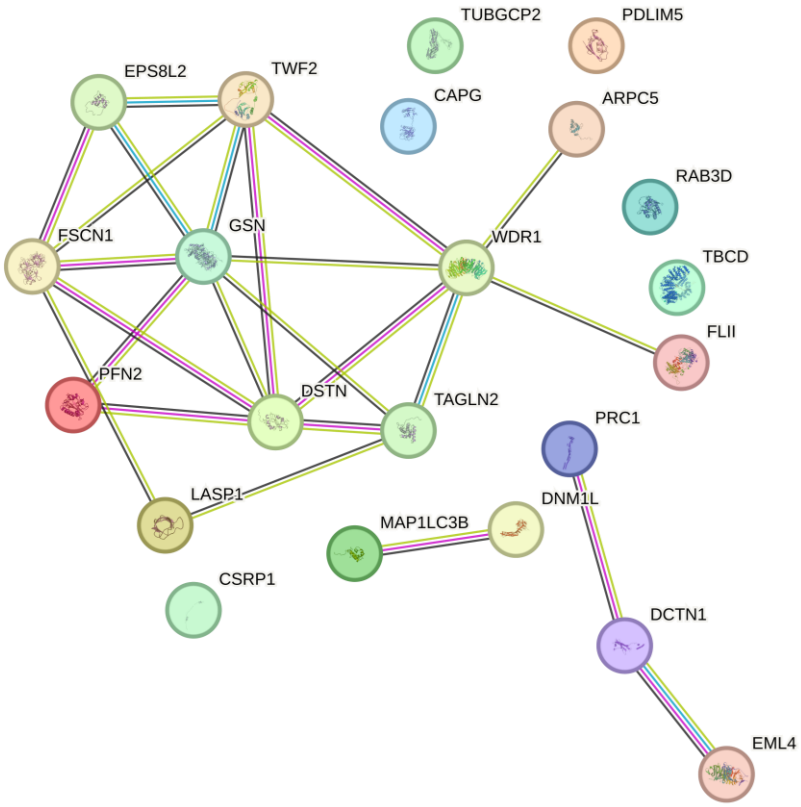

Figure 7.34 Protein-protein interaction network of the 22 cytoskeletal proteins with significantly altered abundance in VECs exposed to L-LA.

When VECs were exposed to L-LA, 72.7% (16/22) of the cytoskeletal proteins were upregulated, 13.6% (3/22) were downregulated and 13.6% (3/22) remained unchanged. MEK/ERK inhibition reduced the abundance of 56.3% (9/22) of these cytoskeletal proteins (Figure 7.35).

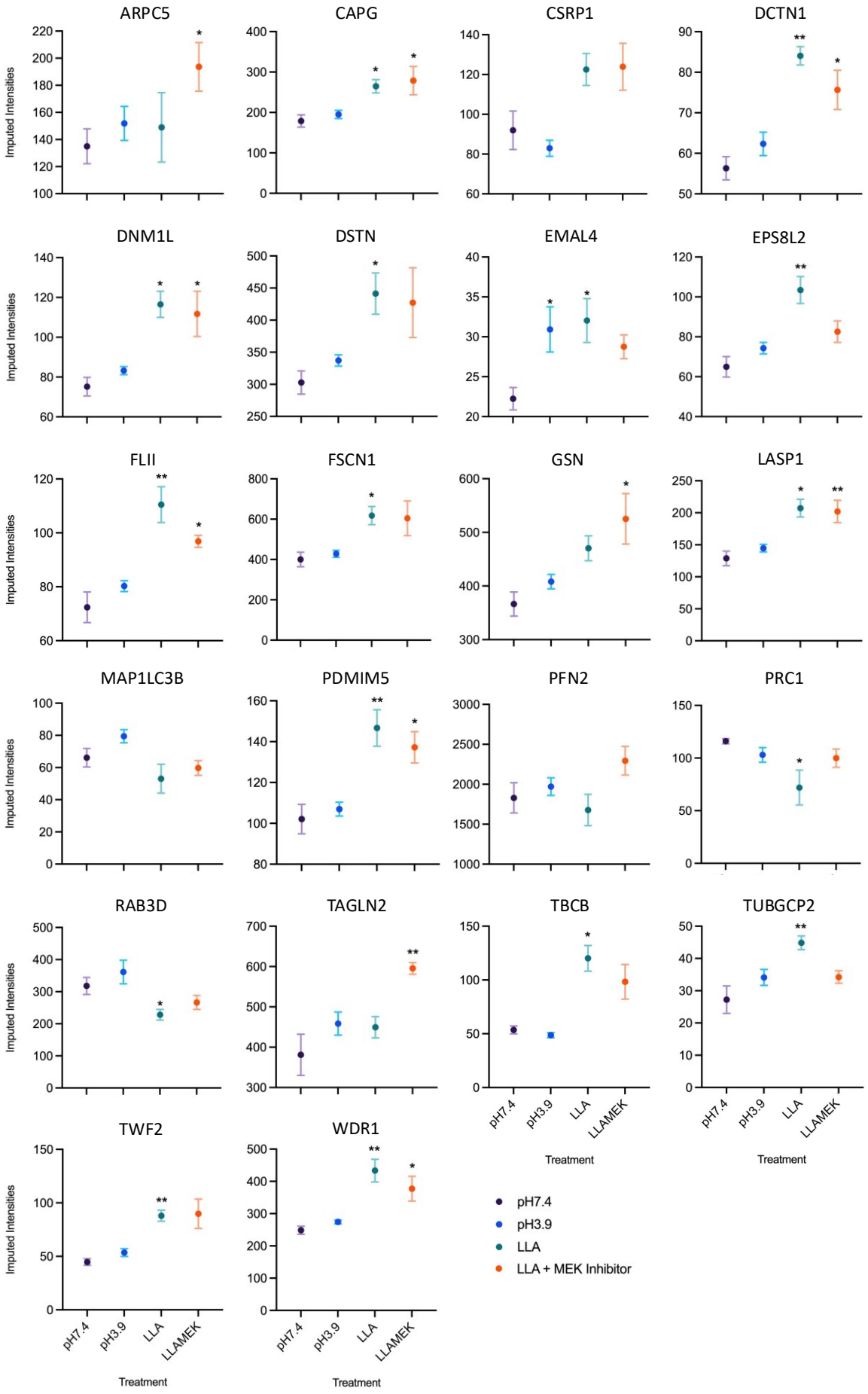
ARPC5
CAPG
CSRP1
DCTN1
DNM1L
DSTN
EMAL4
EPS8L2
FLII
FSCN1
GSN
LASP1
MAP1LC3B
PDMIM5
PFN2
PRC1
RAB3D
TAGLN2
TBCB
TUBGCP2
TWF2
WDR1
Imputed Intensities
Treatment
pH7.4
pH3.9
LLA
LLAMEK
LLA + MEK Inhibitor

Figure 7.35 Cytoskeletal protein abundance is differentially regulated by L-LA and MEK inhibition.

The abundance of 22 cytoskeletal proteins identified in the proteomics analysis was compared across the four different treatments. Graphs show mean ±SD from five independent experiments. Statistical significance was tested using one-way ANOVA Kruskal-Wallis test, with Dunn's *post hoc* test. * and ** denote $P < 0.05$ and 0.01, respectively.

7.2.5.2 Flightless I Protein (Flii)

Further assessment of the cytoskeletal protein, Flightless I (Flii), was undertaken because its abundance significantly increased with L-LA relative to pH 7.4 ($P < 0.01$) but decreased when the MEK/ERK pathway was inhibited ($P < 0.05$) (Figure 7.36A). Previously, it was reported that the association between Flii and the key TLR signalling mediator MyD88 required the adaptor protein nucleoredoxin (NXN) (572). In this proteomics experiment NXN was identified in VECs and, although it did not reach statistical significance, a trend towards increased abundance was observed in the presence of L-LA (Figure 7.36B).

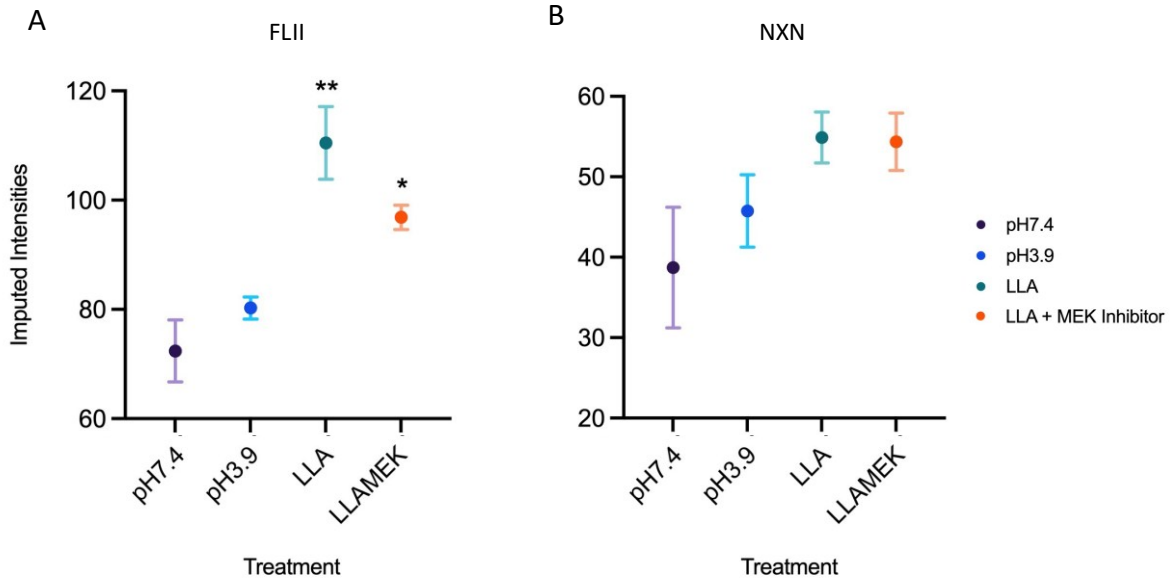

Figure 7.36 L-LA significantly increases the abundance of Flightless-I (Flii).

Following exposure to pH 7.4 or acidified medium (pH 3.9) with HCl or 30 mM L-LA, VECs were treated with MEK inhibitor U0126 (10 µM; 30 mins pre-treatment). Proteins were extracted and quantified using LC-MS. Abundance of **(A)** the actin-binding protein Flii (FLII) and **(B)** the adaptor protein nucleredoxin (NXN) was compared across the four treatments. Graphs show mean ±SD from five independent experiments. Statistical significance was tested using one-

way ANOVA Kruskal-Wallis test, with Dunn's *post hoc* test. * and ** denote $P < 0.05$ and 0.01, respectively.

Flii is also known to regulate cellular processes through interactions with integrin-binding proteins such as paxillin (PAXI), vinculin (VINC) and talin (TLN1) (573, 574). Using the proteomics data generated, talin abundance mirrored the trends seen with Flii, increasing significantly in the presence of L-LA ($P < 0.01$) and decreasing with MEK/ERK inhibition ($P < 0.05$) (Figure 7.37A). Vinculin levels also increased with L-LA ($P = 0.055$) and were further enriched when MEK was inhibited ($P < 0.01$) (Figure 7.37B). In contrast, paxillin abundance showed a general upward trend with acidity that was not specific to L-LA and did not reach statistical significance (Figure 7.37C).

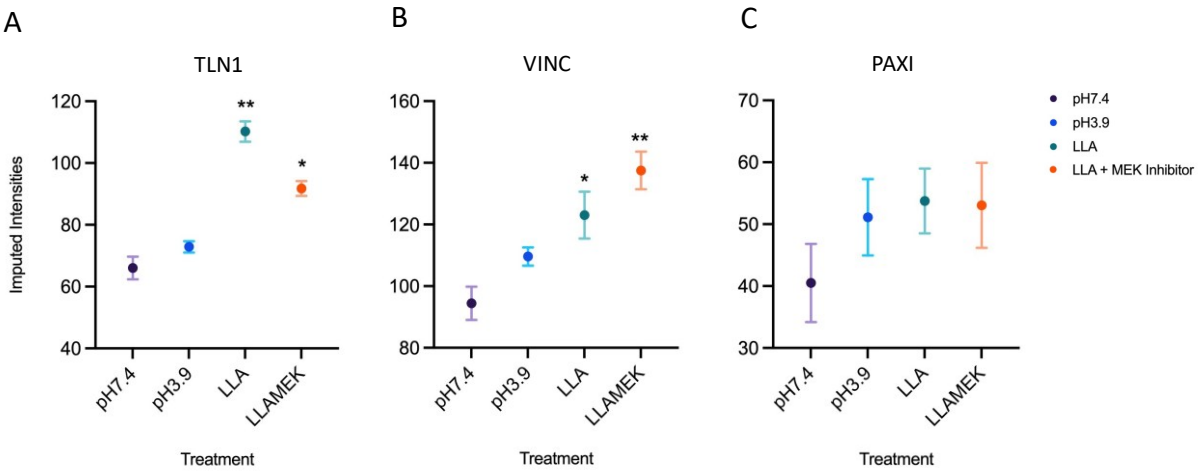

Figure 7.37 Changes in the abundance of integrin-binding proteins talin, vinculin and paxillin in response to L-LA.

Following exposure to pH 7.4 or acidified medium (pH 3.9) with HCl or 30 mM L-LA with/without MEK inhibitor U0126 (10 µM; 30 mins pre-treatment), proteins were extracted and quantified using LC-MS. The effects of L-LA and MEK inhibition on integrin-binding proteins **(A)** talin (TLN1), **(B)** vinculin (VINC) and **(C)** paxillin (PAXI) was analysed. Graphs show mean ±SD from five independent experiments. Statistical significance was tested using one-way ANOVA Kruskal-Wallis test, with Dunn's *post hoc* test. * and ** denote $P < 0.05$ and 0.01, respectively.

Talin is a transmembrane protein that links F-actin polymers to cytoplasmic integrins, such as integrin-β1 (ITB1). ITB1 was significantly downregulated when VECs were treated with L-LA compared to pH 3.9 ($P < 0.05$). Talin also recruits adaptor proteins such as focal adhesion

kinase (FAK) and Flii leucine rich repeat associated protein 1 (FLAP1), which are involved in cell adhesion and initiate FAK and integrin-linked signalling pathways (575, 576). Therefore, the effects of L-LA and MEK inhibition on the abundance of these proteins were also examined (Figure 7.38).

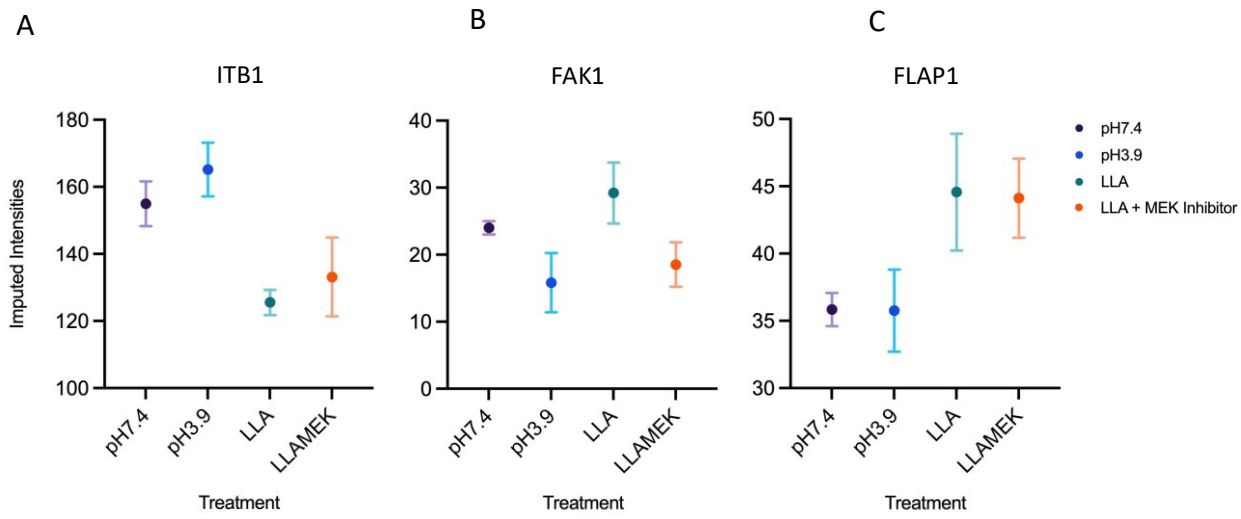

Figure 7.38 Changes in the abundance of integrin-binding proteins integrin-β1 (ITB1), focal adhesion kinase 1 (FAK1) and Flight I-associated protein 1 (FLAP1) with L-LA.

Following exposure to medium at pH 7.4 or acidified to pH 3.9 with HCl or 30 mM L-LA with/without MEK inhibitor U0126 (10 µM; 30 mins pre-treatment), proteins were extracted and quantified using LC-MS. The abundance of integrin-binding proteins **(A)** ITB1, **(B)** FAK1 and **(C)** FLAP1 was analysed. Graphs show mean ±SD from five independent experiments. Statistical significance was tested using one-way ANOVA Kruskal-Wallis test, with Dunn's *post hoc* test. * and ** denote $P < 0.05$ and 0.01, respectively.

7.3 Discussion

Using a proteomics approach, this chapter set out to identify pathways and proteins regulated by LA and to examine the statistical significance of ERK activation by LA in VECs. By analysing differential protein expression across different culture conditions and applying gene ontology classifications and pathway enrichment analyses, this approach helps generate novel hypotheses and enables a more comprehensive understanding of the biological processes and molecular functions affected by LA and ERK activation, potentially revealing new insights into cellular responses and adaptations.

Exposure to acidified culture media led to relatively few changes in VEC protein abundance. Of the 2555 proteins that were quantified, only 13 (0.51%) changed significantly over the 6-hour time frame of this experiment. This was unexpected, as a swift change in environmental pH often leads to cell death and rapid changes in stress and other early response proteins in intestinal epithelia (577). These results support the concept that VECs have evolved to tolerate the low pH environment of the vaginal niche, which is predominately acidified by bacterially derived LA (578, 579). Twelve of these proteins increased in abundance and were linked to pathways involving cytoskeletal regulation and signalling, such as Ras, integrin, Rho, and PDGF (indirectly through crosstalk with the Ras-MAPK signalling pathway). The Ras signalling pathway is involved in cell cycle regulation, wound healing, tissue repair, integrin signalling and cell migration (404, 580, 581). The upregulation of proteins in these interrelated pathways is consistent with the role of VECs in maintaining the mucosal barrier, where cytoskeletal remodelling is required to reinforce tight junctions and enhance cell-cell adhesion. This coordinated response may therefore contribute to both structural fortification of the epithelium and regulation of its immune functions in an acidic vaginal microenvironment.

Only one protein, RanB9, was downregulated with acidification. RanB9, a small GTP-binding protein of the Raf superfamily, has not been characterised in the context of VEC function. It is essential for the translocation of RNA and proteins through the nuclear pore complex, and plays an important role in regulating DNA-damaged cancerous cells in the lung, where increased levels of RanB9 correlates with an increase in DNA damage (582). Decreased levels of RanB9 in acidified VECs suggest that low pH does not induce DNA damage or stress in these cells.

However, when VECs were exposed to acidified media with LA, the number of significantly altered proteins increased 17-fold (223 proteins), with most increasing in abundance (80.7%) rather than decreasing (19.3%). This suggests that LA promotes changes across multiple functional pathways. Consistent with data from Chapters 3 and 4, proteins involved in inflammation were suppressed by LA. The results indicate a specific response to LA rather than a general response to acidification, providing evidence for receptor-mediated regulation of LA

signalling over generic proton transport mechanisms such as MCTs (310, 560, 583). The large number of regulated proteins involvement of multiple functional pathways suggests a complex cellular response and is more consistent with receptor-based signalling, which can trigger multiple signalling cascades, than with the simpler mechanism of proton transport (535, 583).

Two other regulatory signalling pathways were enriched in VECs exposed to LA: the Huntington disease pathway, involving inflammatory transcription factors (AP-1 and NF-κB), MAPKs (JNK and ERK), cytoskeletal proteins and inflammatory caspases; and the integrin signalling pathway (584, 585). The integrin signalling pathway proteins no longer increased in abundance when MEK/ERK was inhibited, suggesting regulation by the MEK/ERK. Integrins are cell surface receptors that play a crucial role in inflammation by mediating cell adhesion and signalling, influencing leukocyte migration, cytokine release and tissue remodelling (586). The β integrins regulate ERK and Rho GTPase signalling in other cell systems, such as tumour cells and polarised epithelia (587, 588), highlighting the integrin signalling pathway as an area warranting future research in the role of LA and increased levels of ERK in VECs.

Differentially regulated proteins in the presence of LA fell into similar functional groups at pH 7.4 or pH 3.9. Most upregulated proteins were involved in cytoskeletal organisation, cell adhesion, membrane trafficking, protein binding or enzymatic activities, such as modifying proteins or metabolite interconversion. Downregulated proteins also belonged to these categories but included more transporter or membrane trafficking proteins and RNA metabolism proteins. involved in cytoskeletal organisation and cell adhesion, transporter and membrane trafficking or protein binding, Fewer downregulated proteins were involved in cytoskeletal regulation. Some LA-induced downregulation affected proteins regulating the signal transduction pathways that link the plasma membrane receptors to the assembly of focal adhesions and actin stress fibres, such as small GTPases of the Ras-related Rho family. Rho GTPases,such as RhoA, RhoB, Ras and Cdc42, interact directly with protein kinases, controlling regulation of microfilament dynamics such as actin polymerisation, disassembly and contraction, gene expression and proliferation (589, 590), while Ras sub family regulates cell proliferation and differentiation (581, 591). Acidification with HCl significantly increased

these proteins, whereas LA reduced them. Similar mechanisms involving Rho GTPases regulate epithelial barrier functions in the gut (592, 593), but their role in VECs and response to LA remains poorly understood.

Several clusters of proteins were no longer abundant when MEK/ERK was inhibited. For example, CD47, a widely expressed glycoprotein found in most healthy cells and involved in immune responses, is upregulated in immune cells during infection (594). The proteomics data shows that CD47 was downregulated by LA but not when MEK was inhibited, suggesting that LA reduces CD47 levels, potentially dampening immune responses.

Proteins involved in cytoskeletal regulation also increased in abundance with LA. Inflammation disrupts intercellular junctions through myosin-dependent contractility, modulation of the actin cytoskeleton, and inflammatory signalling pathways that regulate reorganisation of actin filaments in the mucosal epithelia (595). Activated ERK has been observed in non-nuclear cellular compartments, where it interacts with cytoskeletal components, such as microtubules and actin filaments (596-598). This interaction can be direct or via adaptor proteins such as calponin which is an actin-binding protein. It is thought that this interaction restricts the entry of activated ERK into the nuclear compartment where it could activate transcription factors such as AP-1 and direct it to other locations within the cell (599). ERK is also directly recruited to specific membrane domains by scaffolding proteins, such as paxillin, β-arrestin and IQGAP1 (404, 408, 452, 600). Whether such mechanisms operate in VECs remains unknown and warrants further investigation, particularly concerning cellular junctions and regulation of interactions with neighbouring cells (595).

When MEK was inhibited, over a third of the upregulated proteins were enzymes modifying proteins or metabolites. ELKS, a membrane trafficking protein and regulatory subunit of IKK, increased in abundance, although phosphorylated levels of NF-κB remained unchanged (Chapter 4) (601). The importance of this being that when MEK/ERK is switched off, levels of ELKS are increasing which could result in an increase in activated NF-κB. But this does not correlate with our findings in where phosphorylated NF-κB levels remain the same when MEK inhibitor is in the system. Further characterisation of the phospho-proteome could enhance

understanding of key post-translational modifications known to regulate protein functions (602-605).

Proteins downregulated by MEK inhibition at pH 7.4, whilst not mapping onto any known pathways in PANTHER or Reactome, included transmembrane protein 33 (TMM33) and transmembrane protein 43 (TMM43), both of which are involved in the modulation of innate immune signalling via the cGAS-STING pathway (606, 607). Fenech *et al.* went on to show that loss of TMM33 or TMM43 increases the IFN response which is consistent with their roles as negative regulators of cGAS-STING signalling. TMM43 is also a critical signalling component in mediating NF-κB activation by acting downstream of the EGF receptor pathway. Rossi *et al.* observed in a breast cancer cell line that the increased lactate levels lead to EGFR activation and increased ERK1/2 phosphorylation (608).

In contrast, at pH 3.9 MEK/ERK inhibition caused greater protein abundance changes (n = 88) compared to pH 3.9 with LA (n = 8), where acidification is leading to a 7-fold increase in downregulated proteins compared to pH 7.4. Whereas LA diminishes this effect. Chapter 4 showed that the MEK inhibition targets a pathway modestly activated by acidification but more robustly by LA.

Several Rho family members, such as Rac1, RhoA, RhoB and RhoG proteins are downregulated by MEK inhibition. The Rho GTPases, particularly Rho, Rac and Cdc42, control polymerisation and depolymerisation of the actin cytoskeleton and the efficient turnover of adhesion sites. Integrin receptor signalling also initiates actin polymerisation and the formation of focal adhesion complexes which interact with the extracellular matrix. Several Rab proteins are also downregulated; these small GTPases are key regulators of intracellular membrane trafficking, immune activation and pathogen clearance (609, 610). Dysregulation of Rab protein functions can contribute to disease development ranging from neurological disorders, cancer, and infections (611). Intracellular pathogens can exploit disrupted Rab regulatory systems to evade host defences and promote their own replication. Both Rho GTPases and Rab proteins were not inhibited by LA.

Comparing LA-induced acidification with MEK/ERK inhibition demonstrates the importance of the MEK pathway. Few inflammatory proteins were regulated by MEK inhibition, but cytoskeletal remodelling proteins were increased. Proteins downregulated by LA via MEK/ERK primarily mediate cell-cell adhesion and epithelial polarisation (612-614). However, the phosphorylation states of these proteins are critical to their function and so a phospho-proteomics approach may uncover more relevant details.

Cytoskeletal proteins have emerged as key responders to LA exposure in VECs. Given that the ERK pathway is activated by LA and has been implicated in the regulation of cytoskeletal organisation and epithelial barrier integrity, this group of proteins was investigated in more detail. Tight junctions are critical for maintaining the mechanical integrity of the epithelial barrier and are regulated by numerous factors, including E-cadherin and Rho GTPases (615). Among the cytoskeletal proteins upregulated in response to LA, the actin-binding proteins Flii was selected for further investigation due to its established roles in both cytoskeletal regulation and inflammatory signalling. Flii belongs to the gelsolin family of actin-binding proteins, which regulate actin dynamics by severing existing filaments and capping filament ends to enable reassembly into new cytoskeletal structures (616). It plays a significant role in several cellular processes, including proliferation, adhesion, migration, and apoptosis (617-620). In addition, Flii has been shown to modulate key signalling processes involved in inflammation and inflammatory conditions. Structurally, in addition to its C-terminal gelsolin-like domain, Flii possesses an N-terminal leucine-rich repeat (LRR) region, which allows it to regulate cellular signalling events both synergistically and competitively (621). Through these domains, Flii interacts with multiple binding partners, implicating it in a wide range of cellular processes (622). Of particular interest is Flii's involvement in innate immune signalling. It interacts with two important inflammatory pathways - the MyD88-TLR signalling pathway as well as the NLRP3 inflammasome (622). Wang *et al.* demonstrated that Flii forms a complex with MyD88 which inhibits the assembly of the TLR4-MyD88 signalling complex and suppresses downstream activation of NF-κB and IRF3 (623). Furthermore, NXN a redox-sensitive regulatory, has been shown to interact with both Flii and MyD88, facilitating the recruitment of Flii to MyD88 (572, 624). Together, these findings suggest that Flii and NXN

suppress NF-κB activation by forming a complex with MyD88 and reducing MyD88 recruitment to TLRs.

Although the precise mechanism by which LA upregulates Flii levels remains unclear, several possibilities exist. LA may enhance Flii transcription, improve translational efficiency or prevent protein degradation, thereby increasing intracellular levels of Flii. These findings hold clinical relevance as they provide mechanistic insights into the anti-inflammatory effects of LA in the vaginal mucosa, particularly through modulation of TLR signalling and NF-κB activation.

As demonstrated in Chapter 3, LA suppresses activation of both NF-κB and AP-1 following TLR stimulation. This observation led to the hypothesis that Flii mediates, at least in part, the LA-induced suppression of NF-κB in VECs. When LA is present, it increases the abundance of both Flii and NXN. Flii forms a complex with NXN which interacts with MyD88 and prevents its recruitment to the TLR upon stimulation. This prevents the ubiquitination and subsequent degradation of IκBa, thereby inhibiting and NF-κB activation and nuclear translocation (Figure 7.39).

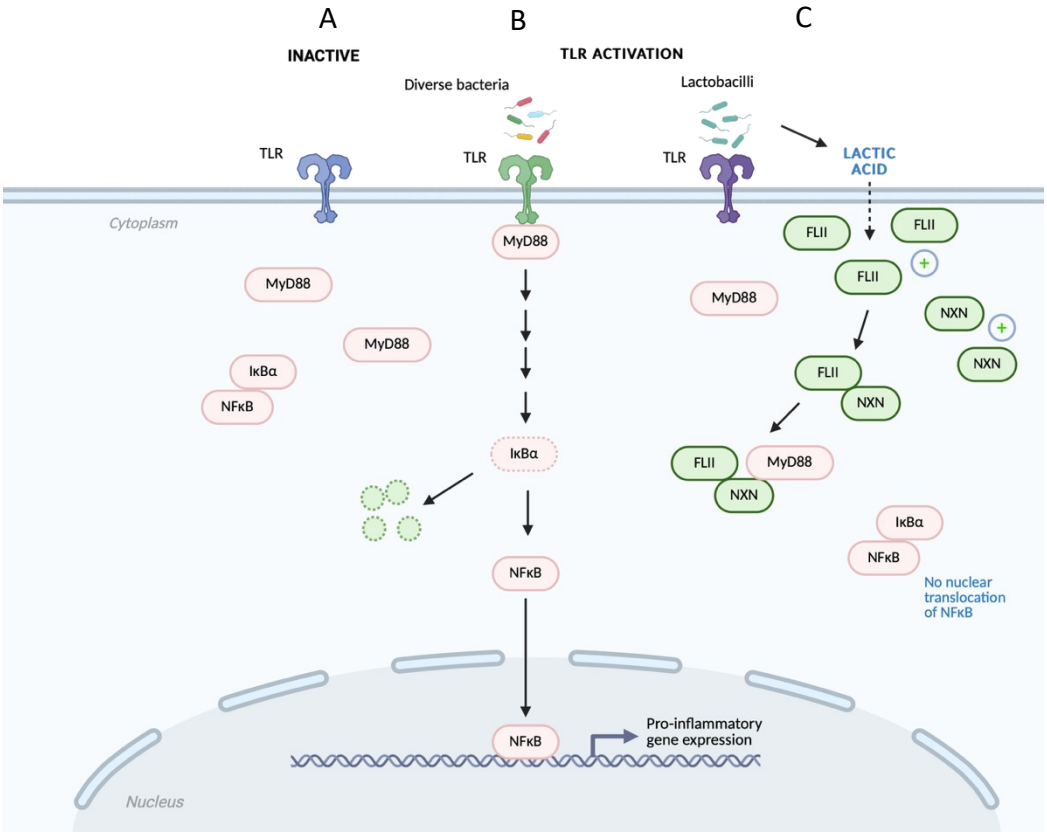

Figure 7.39 Putative role of LA, Flii, nucleoredoxin and MyD88 in TLR signalling in VECs.

(A) In the absence of TLR activation, MyD88 is not recruited to the receptor, IκBa remains intact and is not ubiquitinated and NF-κB remains sequestered in the cytosol. **(B)** Following TLR activation, MyD88 is recruited to the TLR, leading to IκBa degradation, NF-κB nuclear translocation, and transcription of pro-inflammatory genes. **(C)** Exposure of VECs to LA significantly increases the abundance of Flii ($P < 0.01$) as well as nucleoredoxin (NXN). These proteins form a complex with MyD88, which may reduce interfere with its to the TLR, thereby reducing IκB degradation and NF-κB activation. This suggests a potential anti-inflammatory effect of LA via modulation of the TLR-MyD88 signalling pathway. *Created with BioRender.*

Inhibition of the MEK pathway led to a reduction in Flii levels; however, these levels remained higher than those observed in cells at pH 7.4 or in acidic medium without LA (Figure 7.36). These findings suggest that while the MEK/ERK pathway may partially mediate Flii expression, it is not the primary pathway responsible for the LA-induced upregulation of this protein.

Results presented in Chapter 4 demonstrate that anti-inflammatory effect of LA persists even in the presence of a MEK inhibitor. This suggests that activation of the MEK pathway is not required for LA-mediated suppression of inflammation, implying the involvement of an

alternative pathway. The proteomics data identified the Flii protein, which is known to inhibit TLR signalling via MyD88, as a potential mediator. Furthermore, the findings indicate that acidification alone does not increase Flii and NXN levels to the same extent as LA. The MEK pathway appears to partially regulate Flii abundance, as MEK inhibition slightly reduces Flii levels, although they remain significantly higher than at pH 7.4 or pH 3.9. It remains unclear whether other pathways downstream of TAK1, such as JNK or p38, both of which are implicated in TLR signalling may contribute (404, 625). Previous studies of this pathway have not reported a role for MEK signalling.

Flii has been shown to interact with talin to activate integrins and promote integrin-mediated signalling (576). Integrins are transmembrane cell adhesion receptors that link the extracellular matrix to the cytoskeleton, playing a key role in cell-matrix interactions and barrier integrity (626). Talin, a key focal adhesion binding protein, initiates “inside-out” signalling by disrupting the interactions of integrin subunits, thereby modulating the affinity of integrins for extracellular ligands (627). Despite their known importance in epithelial biology, these proteins have not yet been studied in the context of the vaginal epithelium. In renal epithelial cells, for example, downregulation of ITB1 leads to increased expression of E-cadherin and claudin-7, and decreased claudin-2, resulting in a less permeable epithelial cell barrier (628). Similarly, Delgado-Diaz *et al.* reported that LA treatment ectocervical epithelial cells reduced claudin-2 and increased claudin-7 expression although they did not assess E-cadherin, which is known to be expressed in the vaginal epithelium (12, 383). These findings reinforce the potential significance of integrin signalling pathways and Flii in maintaining epithelial barrier integrity in the reproductive tract and warrant further investigation.

The power of a proteomics approach in identifying new pathways and proteins that would not have come to light using traditional methods was shown in this chapter. By capturing all the data simultaneously, another group of functional responses was obtained which had not been discovered in the more focused analysis of inflammatory pathway mediation by LA of the earlier chapters. It has revealed a whole new role for LA’s involvement in regulating cytoskeletal remodelling which is implicated in cell barrier and VEC function.

This chapter highlights the power of a proteomics-based approach in uncovering novel pathways and proteins that were not evident from earlier targeted analyses. By enabling a comprehensive unbiased examination of the proteome, this strategy revealed previously unrecognised functional responses to LA, including its unexpected role in regulating cytoskeletal remodelling, a process essential for maintaining epithelial barrier integrity and VEC function. These findings now require quantitative validation using traditional orthogonal methods. Western blotting remains a gold-standard technique for confirming the up- and downregulation of specific proteins identified through proteomics. Furthermore, because many of the proteins of interest are implicated in barrier function, functional assays such as TEER and FITC-dextran permeability tests should be employed to assess the biological impact of altered protein expression on epithelial integrity.

In conclusion, these findings highlight the ability of proteomics to elucidate new mechanisms by which LA modulates cytoskeletal dynamics, reinforcing barrier integrity and immune regulation in the vaginal mucosa, and opening a promising new area for future research.

Chapter 8: Final Summary and Discussion

8.1 Summary of key findings

In the 250 years since LA was first discovered and isolated from sour milk, major advances have been made in understanding the role of this molecule in the context of human health (629, 630). Initially regarded as a metabolic waste product generated during muscle contraction, lactate is now recognised as a signalling molecule involved in many cellular processes acting through both receptor-dependent or independent pathways. This thesis has explored the critical role of LA in modulating inflammation in VECS and its potential as a therapeutic target for inflammatory conditions and adverse pregnancy outcomes. Through a combination of hypothesis-driven and systems-based investigations in *in vitro* cell culture models and *in vivo* patient samples, key mechanisms by which LA exerts its anti-inflammatory effects have been elucidated, demonstrating its importance in maintaining reproductive health. This work contributes to a growing understanding of how the vaginal microbiome, specifically *Lactobacillus* dominance and its associated metabolic activity, can influence inflammation and potentially improve clinical outcomes in reproductive health.

8.1.1 Lactic acid's anti-inflammatory effects

One of the key findings of this thesis is the confirmation and further interpretation of LA's anti-inflammatory properties in the context of the lower FRT. LA was shown to significantly inhibit the activation of pro-inflammatory transcription factors, that regulate transcription of downstream pro-inflammatory mediators such as cytokines and chemokines. This was demonstrated in *in vitro* models with additional evidence from patient samples supporting the critical role of LA in suppressing inflammation in the lower FRT.

8.1.2 Role of microbiome modulation

As demonstrated in women receiving a biotherapeutic intervention as part of the FLIP-1 study, the transition from a *Lactobacillus*-depleted (CST IV) to a *Lactobacillus*-dominant (CST I) microbial composition increased LA levels and correspondingly reduced inflammation. This

finding demonstrates a tangible relationship between microbial composition, LA production and reduced pro-inflammatory markers, which has important clinical implications as discussed below (Figure 8.1).

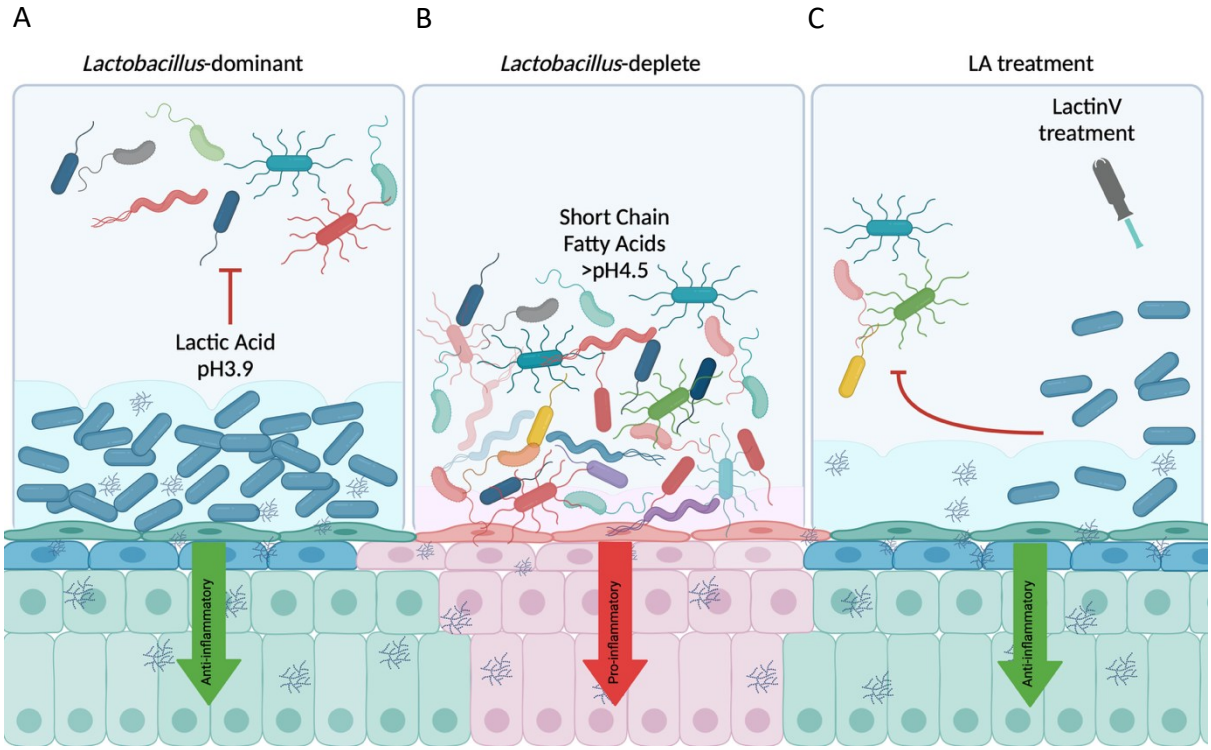

Figure 8.1 Overview of treating women with a Lactobacillus-deplete vaginal microbiome with Lactin-V.

(A) In a *Lactobacillus*-dominant vaginal microbiome (CST I, II, III or V), high levels of LA are produced which acidify the niche and protect against pathogens and associated inflammation. **(B)** In a *Lactobacillus*-deplete microbiome (CST IV), metabolites such as SCFAs are produced, leading to a higher vaginal pH, and increased inflammation. **(C)** Treatment of pregnant women with a *Lactobacillus*-deplete (CST IV) vaginal microbiome using Lactin-V resulted in successful colonisation of CST I in 62.5% of patients. Figure adapted from Wu 2022 (556). *Created with BioRender.com.*

8.1.3 Mechanistic insights into LA's action

Investigations into the molecular mechanisms underlying LA's anti-inflammatory effects have revealed several important findings. LA significantly suppressed the activation of NFκB, AP-1 and IRF3 in response to both bacterial and viral stimuli. This broad-spectrum inhibition suggests that LA acts as a key regulator of inflammatory responses in VECs. Specifically, LA

inhibited the phosphorylation of IKKα/β and TBK1, which are critical upstream regulators of NFκB, AP-1 and IRF3. These findings indicate that LA's anti-inflammatory effects are mediated, at least in part, through the suppression of these upstream signalling nodes. Furthermore, LA was found to differentially regulate MAPK pathways, strongly activating ERK signalling while suppressing p38 and JNK. This dichotomy suggests a nuanced role for LA in regulating cellular responses, potentially promoting cell survival and proliferation while simultaneously dampening inflammatory pathways. Both D-LA and L-LA isomers exhibited similar anti-inflammatory properties, indicating that the beneficial effects of LA are not restricted to a single isomer.

8.1.4 Receptor signalling

The identification of functional HCAR1 receptors in VECs represents a significant advancement in our understanding of LA signalling within the vaginal environment. This discovery provides a mechanistic explanation for the anti-inflammatory effects of LA. Specifically, our findings demonstrate that LA binding to HCAR1 reduces intracellular cAMP levels, consistent with a $G\alpha_i$-mediated response. This observation aligns with known HCAR1 signalling in other cell types but represents the first such demonstration of this pathway in VECs. Unexpectedly, the suppression of NFκB persisted despite the reduction in cAMP levels, highlighting the complex interplay between LA signalling and inflammatory pathways. Furthermore, the strong activation of ERK by LA appears to be independent of $G\alpha_i$ signalling, suggest the involvement of alternative mechanisms such as Gβγ- or β-arrestin-mediated pathways. These findings contribute to the growing body of evidence that GPCR signalling is more complex than previously thought, with a single receptor capable of activating multiple downstream signalling cascades.

8.1.5 Succinate and inflammatory pathways in VECs

Investigations of succinate, another key metabolite in the vaginal environment, revealed unexpected results. Contrary to its previously reported pro-inflammatory role in other tissues,

succinate was demonstrated anti-inflammatory effects in VECs, inhibiting the activation of NFκB and AP-1. This finding highlights the context-dependent nature of metabolite signalling and shows the unique properties of the vaginal niche. Succinate levels increased following the transition to *L. crispatus* dominance, challenging the assumption that elevated succinate levels are exclusively associated with dysbiosis.

8.1.6 Proteomics data

Our proteomics analysis of VECs exposed to LA and acidic conditions revealed that VECs are remarkably resilient to low pH, showing minimal changes in protein abundance following HCl-induced acidification. LA treatment induced more pronounced alterations in the VEC proteome compared to HCl alone, suggesting that LA's effects extend beyond simple acidification. These changes involved proteins related to cytoskeletal regulation, signalling and metabolism. Key proteins such as Flii and nucleoredoxin were implicated in LA-mediated suppression of inflammatory pathways, indicating a broader role for LA in maintaining cellular integrity and function.

8.2 Implications for reproductive health and translational outcomes

The findings presented in this thesis have significant implications for women's reproductive health with the vaginal microbiome playing a crucial role. In healthy reproductive age women, *Lactobacillus* species dominate and LA concentrations are high. The ability of LA to suppress inflammation suggests that its potential as a therapeutic agent for preventing PTB, STIs, and other conditions associated with chronic inflammation in the female reproductive tract following disruption of this microbiome.

During pregnancy, maintaining a balanced vaginal microbiome is critical, as dysbiosis has been linked to adverse outcomes such as PTB. Elevated levels of inflammatory cytokines can trigger early labour by promoting cervical ripening and uterine contractions. By suppressing pro-

inflammatory pathways, LA may reduce the risk of PTB by preserving a protective, low-inflammation environment. Additionally, LA may help maintain the integrity of the cervical mucus plug which acts as a barrier against ascending infections, further lowering the risk of premature labour. However, research in this area remains limited (30).

The acidic environment created by LA restricts the growth of pathogenic bacteria and viruses, including those that cause STIs, such as HIV and HPV (190, 280, 631). LA was been shown to inactivate HIV through multiple mechanisms: acidification of the environment disrupts the viral envelope and may inhibit viral protein function (250). When *L. crispatus* is present, elevated levels of D-LA increase the viscosity of the mucosal layer, enhancing the entrapment of bacterial and viral pathogens (632). Persistent HPV infection is the primary risk factor for cervical cancer. By reducing the persistence of HPV infections, through both direct inactivation of viral particles and suppression of inflammation-driven immune evasion, LA may help lower the risk of cervical carcinogenesis over time.

Pelvic inflammatory disease often arises from untreated STIs, leading to inflammation and infection of the upper reproductive tract (633-635). LA helps prevent the ascent of pathogens by strengthening the vaginal barrier, limiting the overgrowth of pathogenic bacteria, and maintaining a robust defence at the mucosal surface. Its anti-inflammatory properties may also reduce the severity of infection if it does occur by dampening the local immune response, limiting tissue damage caused by excessive inflammation, and supporting the resolution of the inflammatory process. This modulation of the host response could help preserve the integrity of the reproductive tract and reduce the risk of long-term sequelae such as scarring, infertility and chronic pelvic pain.

In endometriosis, chronic inflammation of the pelvic cavity promotes the growth of ectopic endometrial tissue. Although the exact role of the vaginal microbiome in endometriosis is not fully understood, emerging evidence suggests that LA's anti-inflammatory effects may help reduce the inflammatory milieu that supports endometrial lesion growth (636). By suppressing pro-inflammatory cytokines, LA could potentially slow disease progression and alleviate some symptoms.

8.2.1 Microbiome-targeted therapies

The *in vivo* data showing that Lactin-V treatment promoted a *Lactobacillus*-dominant microbiome, accompanied by increased LA levels and reduced inflammation, supports the development of further biotherapeutics aimed at enhancing *Lactobacillus* colonisation. However, Lactin-V contains only a single strain of *L. crispatus.* Ma *et al.* reported that the vaginal microbiota dominated by *Lactobacillus* species typically comprise of multiple strains of the same species (637). To mimic the ecology of these optimal vaginal microbiota treatments, a study reconstructed three *L. crispatus* multi-strain consortia which were used to compare microbiome-host interactions. It found that the multi-strain consortia outperformed the single *L. crispatus* strain, showing superior adhesion to vaginal tissue, D-LA production and immune suppression (54). This suggests that multi-strain *L. crispatus* biotherapeutics could be more effective. Furthermore, strategies could focus on selecting or bioengineering *Lactobacillus* species that produce higher LA levels, potentially reducing premature labour and other adverse pregnancy outcomes by lowering inflammation.

Lactobacillus biotherapeutics aim to restore the natural, living defence system of the vagina, by not only acidifying the environment but also providing a dynamic, multilayered barrier against infections. Lactic acid alone can mimic part of this effect temporarily, but it doesn't address the underlying ecological imbalance.

8.2.2 LA as a therapeutic agent

The anti-inflammatory and antimicrobial properties of LA make it a promising candidate for therapeutic interventions to reduce vaginal inflammation and restore microbial balance. LA-based treatments could benefit women with a CST IV vaginal microbiota by promoting a *Lactobacillus*-dominated state, thereby lowering the risk of infections and inflammation-related complications. Such interventions may also help prevent HPV infections, STIs, pelvic inflammatory disease, and adverse pregnancy outcomes, as previously discussed.

Several mechanisms have been proposed to explain how elevated microbially-derived LA concentrations could help prevent adverse pregnancy outcomes such as PTB and stillbirth. First, LA lowers vaginal pH to approximately 2.8 to 4.2, creating an environment that inhibits the growth of many pathogenic microbes (28). Second, LA suppresses pro-inflammatory transcription factors in the cervicovaginal niche, which in turn downregulates tissue remodelling genes, such as MMPs, that degrade collagenases involved in cervical remodelling, disrupt clotting and weaken the foetal membranes (251, 638). Since MMP release is driven by cytokine-mediated inflammation, reducing this pathway may be particularly beneficial in pregnant women with a *Lactobacillus*-depleted vaginal microbiome. Transitioning these women to a *Lactobacillus*-dominant state may improve both maternal and neonatal outcomes, given that infants exposed to high diversity CST IV microbiome, such as following PPROM, have increased risk of developing neonatal sepsis (194).

To develop LA as a therapeutic strategy, it must be delivered in a controlled, biocompatible manner that achieves effective local concentrations while avoiding tissue irritation. Given its established role in vaginal health and regulating inflammation, possible formulations include vaginal gels, suppositories, or sustained-release intravaginal devices designed for optimal delivery. Beyond gynaecological indications such as treating BV, preventing of PTB or reducing STIs, LA's anti-inflammatory and barrier-protective effects could also be explored in other mucosal diseases characterised by excessive inflammation and barrier disruption, such as inflammatory bowel disease or certain dermatological conditions.

The advantages of an LA-based therapy include its natural presence in the body, its dual antimicrobial and host-protective actions, and a potentially favourable safety profile. However, several limitations must be addressed. These include the challenge of maintaining effective and physiologically appropriate concentrations at the target site, possible irritation at high doses or low pH, and variability in patient response depending on underlying microbial or host factors (439, 639). Further research is needed to optimise LA formulation, determine appropriate dosing and identify the patient populations most likely to benefit.

8.3 Limitations

Despite the important findings of this thesis, several limitations must be acknowledged. First, the *in vivo* component of the study analysing metabolites in women transitioning from CST IV to CST I was underpowered, with only five of 28 women transitioning to CST I from CST IV microbiota. A larger sample size would enable a more robust examination of the relationship between LA concentrations and pregnancy outcomes, as the number of PTB and CST IV cases in this study was relatively small. Larger cohorts could also reveal additional insights.

The CST classification employed may have oversimplified key details as grouping all CST IV bacteria together potentially obscured species capable of producing LA. For example, *Bifidobacterium*, *Prevotella* and *Streptococcus* species can all produce LA, yet these communities still provoke a pro-inflammatory host response through alternative mechanisms, such as direct TLR activation on VECs, production of other inflammatory metabolites. Future studies should consider a more refined classification system that accounts for the LA-producing capacity of different bacterial species and identifies specific mechanisms driving inflammation.

The cell culture model used here was limited to studying VEC interactions with single metabolites (LA or succinate), whereas the vaginal mucosa is a much more complex system including immune cells, bacteria, viruses, and diverse metabolites. Future research should broaden the scope to include combinations of microbial metabolites that better mimic eubiotic and dysbiotic conditions and assess their impact on inflammation and barrier integrity. Moreover, affordable, reliable, and reproducible methods for co-culturing vaginal bacteria with VECs are needed.

Recent advances in cervicovaginal modelling offer powerful tools to better replicate the complexity of the vaginal mucosa *in vitro*. Several systems have been developed, each with distinct strengths and limitations (54, 55, 640). Organoids, derived from primary cervical cells,

form spherical structures and have been used to study viral infection susceptibility but not epithelial barrier function (641). They can be co-cultured with immune cells and microbiota to investigate FRT physiology and pathology (642, 643). However, robust human vaginal organoids so far are not yet available and have only been derived from murine stem cells (644). While these systems are more labour intensive and costly than standard cell culture, they offer greater physiological relevance. Microfluidic vagina-on-a-chip systems, by contrast enable co-culture of vaginal bacteria with stratified epithelial layers under dynamic flow and shear conditions, closely mimicking the vaginal microenvironment and supporting barrier function (54). They are particularly suited for studying microbiome-epithelial interactions and barrier integrity but require expertise in microfluidics and specialised equipment. Finally, a 3D epithelial tissue model, using a rotation wall vessel (RWV) bioreactor and cervicovaginal cell lines is more accessible and reproducible, producing mucus-secreting, stratified epithelia (645-649). While less complex than the other models and lacking dynamic flow or immune components, it offers a good compromise between physiological relevance and practicality. However, the choice of method should depend on the specific research question: for microbial interactions and barrier studies, the vagina-on-a-chip appears optimal; for crosstalk interactions between host and immune cells and the microbiome, organoids hold the most promise once established in human vaginal tissue; and for barrier and mucus studies with moderate complexity, 3D multilayered cultures remain a robust option.

This thesis primarily examined the MEK/ERK pathway in VECs, but other kinase pathways, including TBK1 and IKK, are also likely to contribute to LA-mediated modulation of inflammation. IKKs are pleiotropic signalling molecules involved in NF-κB activation and IFN gene transcription, thereby regulating cytokine production and innate immunity. Similarly, TBK1 coordinates activation of IRF3 and NF-κB in response to stimuli (650, 651). Future research should explore these pathways further.

8.4 Future Directions

An improved understanding of the role of LA in modulating inflammation within the FRT opens several promising avenues for further investigation.

Following our discovery of HCAR1 receptors in VECS, future research should aim to characterise LA signalling in greater detail, including the potential involvement of other receptors such as pH-sensitive GPCRs, for example GPR132, and SCFA receptors. A comprehensive understanding of the downstream signalling pathways mediating LA's anti-inflammatory effects may uncover novel therapeutic targets for maintaining vaginal health and preventing adverse reproductive outcomes.

Future studies investigating the synergistic or antagonistic effects of LA, SCFAs and succinate on inflammatory pathways in VECs could reveal additional mechanisms by which the vaginal microbiome influences local immune responses. Such work may also clarify how disruptions in metabolite profiles contribute to conditions such as BV, STIs and PTB.

Whilst the proteomics analyses presented in this thesis provided valuable insight into relative protein abundance changes in VECs exposed to LA, our findings suggest that post-translational modifications play a crucial role in modulating protein function and cellular responses. Specifically, the analyses revealed changes in proteins involved in cytoskeletal regulation and signalling pathways, including Ras, integrin and Rho, which are known to be extensively regulated by post-translational modifications such as phosphorylation. Moreover, the observed alterations in proteins related to cell-cell adhesion and barrier function indicate that glycosylation may also contribute to maintaining epithelial integrity under acidic conditions (652). These findings emphasise the need for future studies focusing on post-translational modifications, which could lead to a more comprehensive understanding of VEC biology and adaptation to the unique vaginal microenvironment, ultimately informing the development of targeted therapies to preserve vaginal health and prevent infection.

The impact of LA on cytoskeletal reorganisation and epithelial barrier integrity warrants further exploration. Elucidating how LA modulates these processes may provide novel insights into its protective role against infection and inflammation in the vaginal epithelium. This line

of research is particularly compelling considering the proteomic evidence that LA induces more substantial changes in the VEC proteome than HCl-induced acidification alone. Future studies should examine the effects of LA on tight junction formation and integrity and evaluate how LA-induced changes in cytoskeletal proteins and barrier function correlate with resistance to pathogen invasion and inflammatory responses. The consequences of transitioning from CST IV to CST I, for example following Lactin-V treatment, on other bacterial metabolites should also be investigated to gain a more comprehensive understanding of the vaginal metabolic landscape.

Finally, proteomics analyses identified the protein Flii as a potentially important regulator of LA's anti-inflammatory effects in VECs. LA treatment was associated with increased abundance of Flii, a protein known to act as a negative regulator of inflammation in other cellular contexts (623, 653, 654). Future work should investigate whether LA influences Flii at the transcriptional, translational or post-translational level, and the interpret the functional significance of this relationship in the vaginal epithelium.

8.5 Final Conclusions

This thesis has significantly advanced our understanding of the roles of LA and succinate in modulating inflammation within the vaginal environment. LA's ability to suppress key inflammatory pathways while promoting cellular survival and maintaining epithelial integrity positions it as a critical mediator of vaginal health (Figure 8.2).

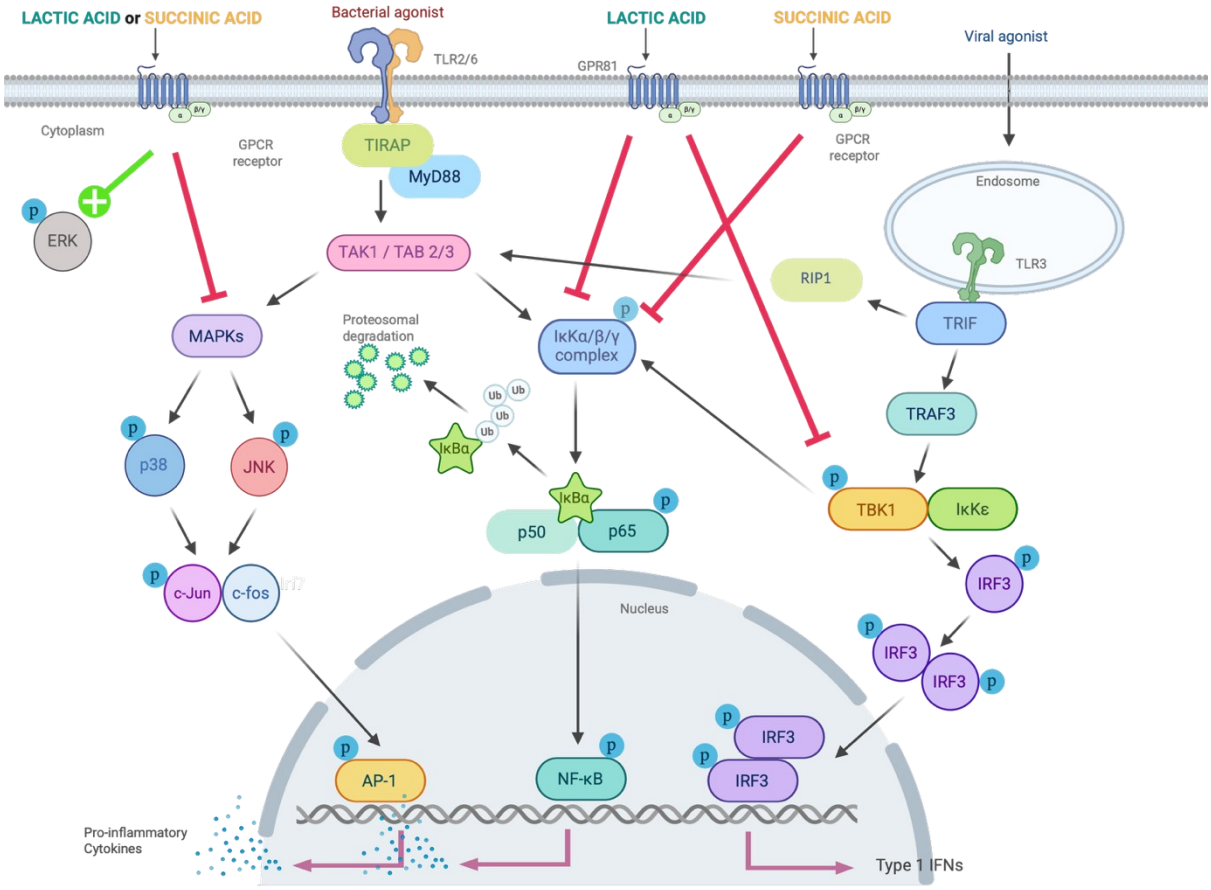

Figure 8.2 Schematic summarising the modulation of inflammatory signalling pathways in VECs by LA and succinic acid.

Created with BioRender.com.

These findings lay a strong foundation for future research and clinical applications aimed at harnessing this key metabolite to improve women's reproductive health. The transition of the vaginal microbiome toward *Lactobacillus* dominance, accompanied by increased LA production and reduced inflammation, shows promise as a therapeutic strategy to preventing adverse reproductive outcomes such as PTB. Moreover, the proteomic insights gained in this work open new avenues to explore how LA influences cellular functions beyond inflammation, particularly those related to cytoskeletal remodelling and barrier integrity.

Moving forward, larger scale *in vivo* studies, more sophisticated *in vitro* models, and deeper investigations into the molecular mechanism of LA will be essential to fully realise its therapeutic potential. Continued research into the complex interplay between LA, the vaginal

microbiome, and host inflammatory responses could lead to innovative strategies for preventing and treating a wide range of reproductive health conditions. This work contributes to the growing recognition of the intricate connections between microbes, metabolites, and host physiology, and sets the stage for future advancements in women's health.

Chapter 9: Supplementary

9.1 SWATH windows used in proteomics data

Table 9.1 SWATH windows used in proteomics data

START	STOP	Declustering Potential (V)	DP Spread	Collission Energy (V)	CE Spread (V)
399.5	406.5	80	0	19	0
405.5	412.5	80	0	19	0
411.5	418.5	80	0	19	0
417.5	424.5	80	0	20	0
423.5	430.5	80	0	20	0
429.5	436.5	80	0	20	0
435.5	442.5	80	0	20	0
441.5	448.5	80	0	21	0
447.5	454.5	80	0	21	0
453.5	459.5	80	0	21	0
458.5	464.5	80	0	22	0
463.5	469.5	80	0	22	0
468.5	474.5	80	0	22	0
473.5	479.5	80	0	22	0
478.5	484.5	80	0	23	0
483.5	489.5	80	0	23	0
488.5	494.5	80	0	23	0
493.5	499.5	80	0	23	0
498.5	504.5	80	0	23	0
503.5	509.5	80	0	24	0
508.5	514.5	80	0	24	0
513.5	519.5	80	0	24	0
518.5	524.5	80	0	24	0
523.5	529.5	80	0	25	0
528.5	534.5	80	0	25	0
533.5	539.5	80	0	25	0
538.5	544.5	80	0	25	0
543.5	549.5	80	0	26	0
548.5	554.5	80	0	26	0
553.5	559.5	80	0	26	0
558.5	564.5	80	0	26	0
563.5	569.5	80	0	27	0
568.5	574.5	80	0	27	0
573.5	579.5	80	0	27	0
578.5	584.5	80	0	27	0
583.5	589.5	80	0	28	0
588.5	594.5	80	0	28	0
593.5	599.5	80	0	28	0

598.5	604.5	80	0	28	0
603.5	609.5	80	0	29	0
608.5	614.5	80	0	29	0
613.5	619.5	80	0	29	0
618.5	624.5	80	0	29	0
623.5	629.5	80	0	30	0
628.5	634.5	80	0	30	0
633.5	639.5	80	0	30	0
638.5	644.5	80	0	30	0
643.5	649.5	80	0	31	0
648.5	654.5	80	0	31	0
653.5	660.5	80	0	31	0
659.5	666.5	80	0	31	0
665.5	672.5	80	0	32	0
671.5	678.5	80	0	32	0
677.5	684.5	80	0	32	0
683.5	690.5	80	0	33	0
689.5	696.5	80	0	33	0
695.5	702.5	80	0	33	0
701.5	708.5	80	0	33	0
707.5	714.5	80	0	34	0
713.5	720.5	80	0	34	0
719.5	726.5	80	0	34	0
725.5	732.5	80	0	35	0
731.5	738.5	80	0	35	0
737.5	744.5	80	0	35	0
743.5	750.5	80	0	35	0
749.5	756.5	80	0	36	0
755.5	763.5	80	0	36	0
762.5	770.5	80	0	36	0
769.5	777.5	80	0	37	0
776.5	784.5	80	0	37	0
783.5	791.5	80	0	37	0
790.5	798.5	80	0	38	0
797.5	805.5	80	0	38	0
804.5	812.5	80	0	38	0
811.5	819.5	80	0	39	0
818.5	826.5	80	0	39	0
825.5	834.5	80	0	40	0
833.5	842.5	80	0	40	0
841.5	850.5	80	0	40	0
849.5	858.5	80	0	41	0
857.5	867.5	80	0	41	0
866.5	876.5	80	0	42	0

875.5	885.5	80	0	42	0
884.5	894.5	80	0	42	0
893.5	903.5	80	0	43	0

9.2 FLIP-1 patient pregnancy outcome data for patients that transition from CST IV to CST I

Table 9.2 FLIP-1 patient pregnancy outcome data for women that transition from CST IV to CST I.

Patient ID	Pregnancy Outcome
F001	Term
F004	Term
F019	Term
F054	Term
F059	Term

9.3 FLIP-1 patient pregnancy outcome data for patients that do not transition following Lactin-V treatment

Table 9.3 FLIP-1 patient pregnancy outcome data for women that do not transition following Lactin-V treatment.

Patient ID	Pregnancy Outcome
F026	Term
F035	iPTB
F039	sPTB
F049	iPTB
F057	Term

sPTB = spontaneous preterm birth; iPTB = induced preterm birth.

9.4 IKK activation is suppressed by LA 1 hour after TLR agonist stimulation

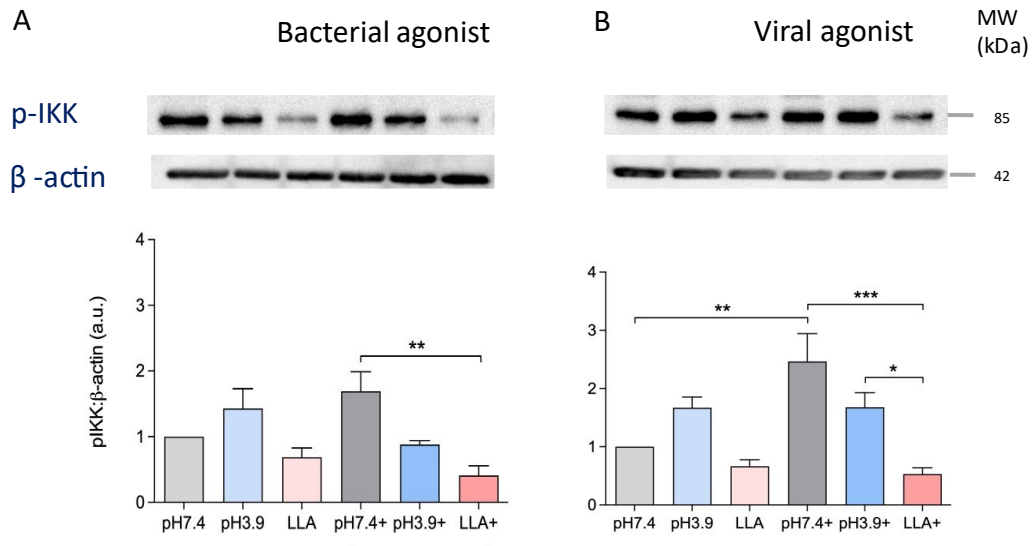

Figure 9.1 IKK activation continued to be suppressed by LA 1 hour after TLR agonist stimulation.

VECs were stimulated with **(A)** bacterial agonist fibroblast-stimulating lipopeptide (FSL-1) or **(B)** viral agonist (PIC) for 1 hour in the presence or absence of 30 mM L-LA (pH 3.9), or media alone (pH 7.4) as indicated. Whole cell protein extracts were probed for p-IKK. Graphs show mean ±SD from at least three independent experiments. Statistically significant differences between the different conditions and treatments were tested using one-way ANOVA and Tukey's *post hoc* test. *, **, and *** denote $P < 0.05$, 0.01, and 0.001, respectively. All data were standardised to untreated cells at pH 7.4.

9.5 LA-mediation of p38 phosphorylation following 30 minutes treatment with TLR agonists

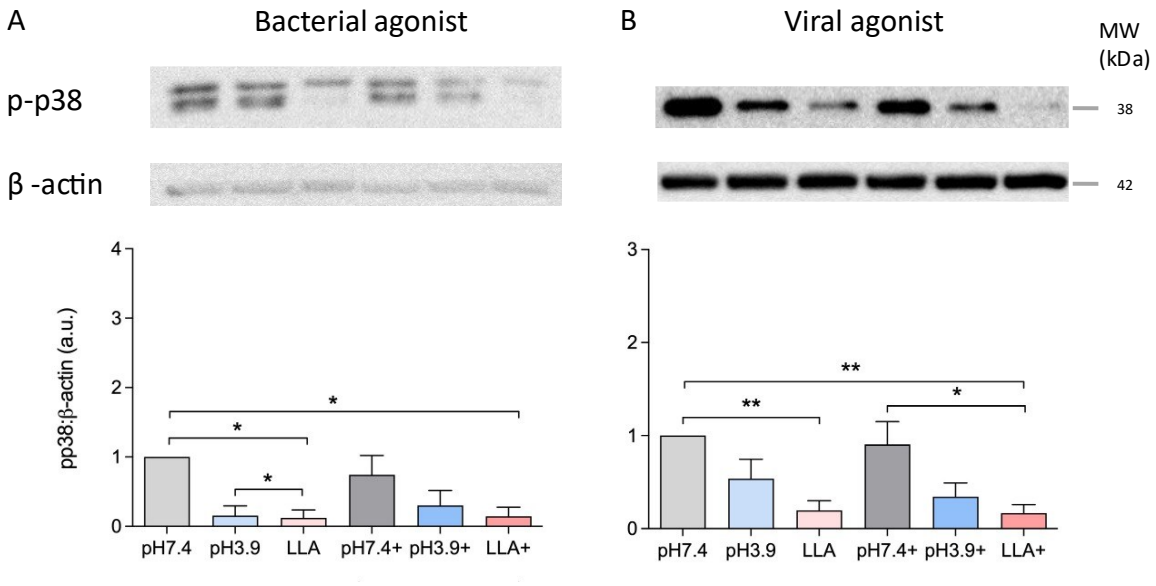

Figure 9.2 LA-mediation of p38 phosphorylation in VECs treated with FSL-1 or PIC for 30 minutes.

VECs were stimulated with **(A)** bacterial agonist fibroblast-stimulating lipopeptide (FSL-1; 1.0 µg ml^{-1}) or **(B)** viral agonist (PIC; 20 µg ml^{-1}) for 30 mins in the presence or absence of 30 mM L-LA (pH 3.9), or media alone (pH 7.4) as indicated. Whole cell protein extracts were probed for p-p38. Graphs show mean ±SD from at least three independent experiments. Statistically significant differences between the different conditions and treatments were tested using one-way ANOVA and Tukey's *post hoc* test. *and ** denote $P < 0.05$ and 0.01, respectively. All data were standardised to untreated cells at pH 7.4.

9.6 LA-induced ERK activation following bacterial agonist stimulation for 30 minutes, 1 hour and 2 hours treatments

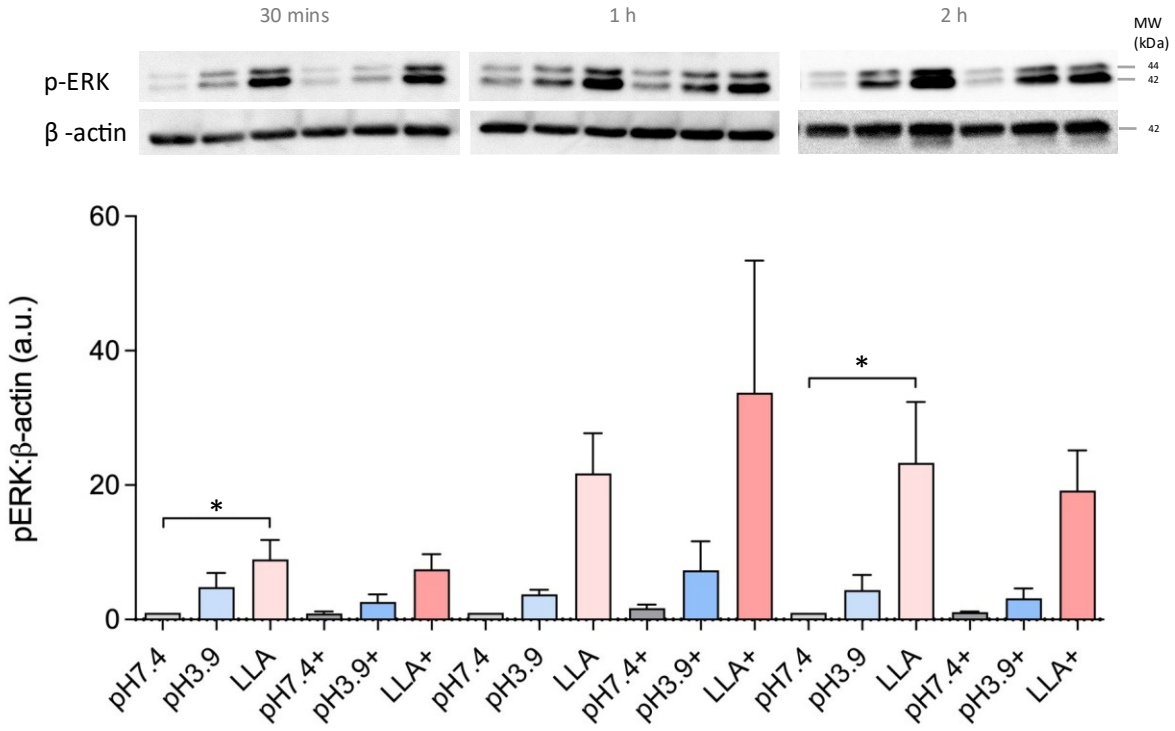

Figure 9.3 ERK continues to be strongly activated by LA after 4 hour's exposure.

VECs acclimatised for 2 hours in medium at pH 7.4 or acidified to pH 3.9 in the presence or absence of 30 mM L-LA were stimulated with bacterial agonist FSL-1 (1.0 µg ml^{-1}) 30 mins, 1 hour or 2 hours. Whole cell protein extracts were probed for p-ERK. Graphs show mean ±SD from five independent experiments. Statistically significant differences between the different conditions and treatments were assessed using one-way ANOVA and Tukey's *post hoc* test. * denotes $P < 0.05$. All data were standardised to untreated cells at pH 7.4.

Chapter 10: References

1. Anahtar MN, Byrne EH, Doherty KE, Bowman BA, Yamamoto HS, Soumillon M, et al. Cervicovaginal bacteria are a major modulator of host inflammatory responses in the female genital tract. Immunity. 2015;42(5):965-76.
2. Dong M, Dong Y, Bai J, Li H, Ma X, Li B, et al. Interactions between microbiota and cervical epithelial, immune, and mucus barrier. Front Cell Infect Microbiol. 2023;13:1124591.
3. Li H, Zang Y, Wang C, Fan A, Han C, Xue F. The Interaction Between Microorganisms, Metabolites, and Immune System in the Female Genital Tract Microenvironment. Front Cell Infect Microbiol. 2020;10:609488.
4. Costa-Fujishima M, Yazdanpanah A, Horne S, Lamont A, Lopez P, Farr Zuend C, et al. Nonoptimal bacteria species induce neutrophil-driven inflammation and barrier disruption in the female genital tract. Mucosal Immunol. 2023;16(3):341-56.
5. Pivarcsi A, Nagy I, Koreck A, Kis K, Kenderessy-Szabo A, Szell M, et al. Microbial compounds induce the expression of pro-inflammatory cytokines, chemokines and human beta-defensin-2 in vaginal epithelial cells. Microbes Infect. 2005;7(9-10):1117-27.
6. Plesniarski A, Siddik AB, Su RC. The Microbiome as a Key Regulator of Female Genital Tract Barrier Function. Front Cell Infect Microbiol. 2021;11:790627.
7. Anderson DJ, Marathe J, Pudney J. The structure of the human vaginal stratum corneum and its role in immune defense. Am J Reprod Immunol. 2014;71(6):618-23.
8. Zhao X, Jiang W, Jin X, Wang W, Shao Q, Liu T, et al. Role of Toll-Like Receptors in Common Infectious Diseases of the Female Lower Genital Tract. Front Biosci (Landmark Ed). 2023;28(9):232.
9. Elias PM, Friend DS. The permeability barrier in mammalian epidermis. J Cell Biol. 1975;65(1):180-91.
10. Asscher AW, De Boer CH, Turner CJ. Cornification of the human vaginal epithelium. J Anat. 1956;90(4):547-52.
11. Bragulla HH, Homberger DG. Structure and functions of keratin proteins in simple, stratified, keratinized and cornified epithelia. J Anat. 2009;214(4):516-59.
12. Blaskewicz CD, Pudney J, Anderson DJ. Structure and function of intercellular junctions in human cervical and vaginal mucosal epithelia. Biol Reprod. 2011;85(1):97-104.
13. Patton DL, Thwin SS, Meier A, Hooton TM, Stapleton AE, Eschenbach DA. Epithelial cell layer thickness and immune cell populations in the normal human vagina at different stages of the menstrual cycle. Am J Obstet Gynecol. 2000;183(4):967-73.
14. Farage MA, Neill S, MacLean AB. Physiological changes associated with the menstrual cycle: a review. Obstet Gynecol Surv. 2009;64(1):58-72.
15. Mirmonsef P, Hotton AL, Gilbert D, Gioia CJ, Maric D, Hope TJ, et al. Glycogen Levels in Undiluted Genital Fluid and Their Relationship to Vaginal pH, Estrogen, and Progesterone. PLoS One. 2016;11(4):e0153553.
16. Thompson IO, van der Bijl P, van Wyk CW, van Eyk AD. A comparative light-microscopic, electron-microscopic and chemical study of human vaginal and buccal epithelium. Arch Oral Biol. 2001;46(12):1091-8.
17. Nilsson K, Risberg B, Heimer G. The vaginal epithelium in the postmenopause--cytology, histology and pH as methods of assessment. Maturitas. 1995;21(1):51-6.

18. Langbein L, Grund C, Kuhn C, Praetzel S, Kartenbeck J, Brandner JM, et al. Tight junctions and compositionally related junctional structures in mammalian stratified epithelia and cell cultures derived therefrom. Eur J Cell Biol. 2002;81(8):419-35.
19. Green KJ, Simpson CL. Desmosomes: new perspectives on a classic. J Invest Dermatol. 2007;127(11):2499-515.
20. Garrod D, Chidgey M. Desmosome structure, composition and function. Biochim Biophys Acta. 2008;1778(3):572-87.
21. González-Mariscal L, Tapia R, Chamorro D. Crosstalk of tight junction components with signaling pathways. Biochim Biophys Acta. 2008;1778(3):729-56.
22. Matter K, Balda MS. Functional analysis of tight junctions. Methods. 2003;30(3):228-34.
23. Rao R. Occludin phosphorylation in regulation of epithelial tight junctions. Ann N Y Acad Sci. 2009;1165:62-8.
24. Gorodeski GI. Estrogen modulation of epithelial permeability in cervical-vaginal cells of premenopausal and postmenopausal women. Menopause. 2007;14(6):1012-9.
25. Oh KJ, Lee HS, Ahn K, Park K. Estrogen Modulates Expression of Tight Junction Proteins in Rat Vagina. Biomed Res Int. 2016;2016:4394702.
26. Averette HE, Weinstein GD, Frost P. Autoradiographic analysis of cell proliferation kinetics in human genital tissues. I. Normal cervix and vagina. Am J Obstet Gynecol. 1970;108(1):8-17.
27. Mirmonsef P, Gilbert D, Veazey RS, Wang J, Kendrick SR, Spear GT. A comparison of lower genital tract glycogen and lactic acid levels in women and macaques: implications for HIV and SIV susceptibility. AIDS Res Hum Retroviruses. 2012;28(1):76-81.
28. Boskey ER, Cone RA, Whaley KJ, Moench TR. Origins of vaginal acidity: high D/L lactate ratio is consistent with bacteria being the primary source. Hum Reprod. 2001;16(9):1809-13.
29. Wylie JG, Henderson A. Identity and glycogen-fermenting ability of lactobacilli isolated from the vagina of pregnant women. J Med Microbiol. 1969;2(3):363-6.
30. Lacroix G, Gouyer V, Gottrand F, Desseyn JL. The Cervicovaginal Mucus Barrier. Int J Mol Sci. 2020;21(21).
31. Zegels G, Van Raemdonck GA, Tjalma WA, Van Ostade XW. Use of cervicovaginal fluid for the identification of biomarkers for pathologies of the female genital tract. Proteome Sci. 2010;8:63.
32. Demouveaux B, Gouyer V, Gottrand F, Narita T, Desseyn JL. Gel-forming mucin interactome drives mucus viscoelasticity. Adv Colloid Interface Sci. 2018;252:69-82.
33. Andersch-Björkman Y, Thomsson KA, Holmén Larsson JM, Ekerhovd E, Hansson GC. Large scale identification of proteins, mucins, and their O-glycosylation in the endocervical mucus during the menstrual cycle. Mol Cell Proteomics. 2007;6(4):708-16.
34. Gipson IK. Mucins of the human endocervix. Front Biosci. 2001;6:D1245-55.
35. Valenti P, Rosa L, Capobianco D, Lepanto MS, Schiavi E, Cutone A, et al. Role of Lactobacilli and Lactoferrin in the Mucosal Cervicovaginal Defense. Front Immunol. 2018;9:376.
36. Boris S, Suarez J, Vazquez F, Barbes C. Adherence of human vaginal lactobacilli to vaginal epithelial cells and interaction with uropathogens. Infection and Immunity. 1998;66(5):1985-9.

37. Nakajima A, Vogelzang A, Maruya M, Miyajima M, Murata M, Son A, et al. IgA regulates the composition and metabolic function of gut microbiota by promoting symbiosis between bacteria. J Exp Med. 2018;215(8):2019-34.
38. Breedveld AC, Schuster HJ, van Houdt R, Painter RC, Mebius RE, van der Veer C, et al. Enhanced IgA coating of bacteria in women with Lactobacillus crispatus-dominated vaginal microbiota. Microbiome. 2022;10(1):15.
39. Fahrbach KM, Malykhina O, Stieh DJ, Hope TJ. Differential binding of IgG and IgA to mucus of the female reproductive tract. PLoS One. 2013;8(10):e76176.
40. Trifonova RT, Lieberman J, van Baarle D. Distribution of immune cells in the human cervix and implications for HIV transmission. Am J Reprod Immunol. 2014;71(3):252-64.
41. Pudney J, Quayle AJ, Anderson DJ. Immunological microenvironments in the human vagina and cervix: mediators of cellular immunity are concentrated in the cervical transformation zone. Biol Reprod. 2005;73(6):1253-63.
42. Chan D, Bennett PR, Lee YS, Kundu S, Teoh TG, Adan M, et al. Microbial-driven preterm labour involves crosstalk between the innate and adaptive immune response. Nat Commun. 2022;13(1):975.
43. Kutteh WH, Franklin RD. Quantification of immunoglobulins and cytokines in human cervical mucus during each trimester of pregnancy. Am J Obstet Gynecol. 2001;184(5):865-72; discussion 72-4.
44. Hein M, Petersen AC, Helmig RB, Uldbjerg N, Reinholdt J. Immunoglobulin levels and phagocytes in the cervical mucus plug at term of pregnancy. Acta Obstet Gynecol Scand. 2005;84(8):734-42.
45. Oh JE, Iijima N, Song E, Lu P, Klein J, Jiang R, et al. Migrant memory B cells secrete luminal antibody in the vagina. Nature. 2019;571(7763):122-6.
46. Franklin RD, Kutteh WH. Characterization of immunoglobulins and cytokines in human cervical mucus: influence of exogenous and endogenous hormones. J Reprod Immunol. 1999;42(2):93-106.
47. Wira CR, Rodriguez-Garcia M, Shen Z, Patel M, Fahey JV. The role of sex hormones and the tissue environment in immune protection against HIV in the female reproductive tract. Am J Reprod Immunol. 2014;72(2):171-81.
48. Fichorova RN, Rheinwald JG, Anderson DJ. Generation of papillomavirus-immortalized cell lines from normal human ectocervical, endocervical, and vaginal epithelium that maintain expression of tissue-specific differentiation proteins. Biol Reprod. 1997;57(4):847-55.
49. Pontes Soares C, Midlej V, de Oliveira ME, Benchimol M, Costa ML, Mermelstein C. 2D and 3D-organized cardiac cells shows differences in cellular morphology, adhesion junctions, presence of myofibrils and protein expression. PLoS One. 2012;7(5):e38147.
50. Chitcholtan K, Asselin E, Parent S, Sykes PH, Evans JJ. Differences in growth properties of endometrial cancer in three dimensional (3D) culture and 2D cell monolayer. Exp Cell Res. 2013;319(1):75-87.
51. Rose WA, McGowin CL, Spagnuolo RA, Eaves-Pyles TD, Popov VL, Pyles RB. Commensal bacteria modulate innate immune responses of vaginal epithelial cell multilayer cultures. PLoS One. 2012;7(3):e32728.
52. Lee Y, Dizzell SE, Leung V, Nazli A, Zahoor MA, Fichorova RN, et al. Effects of Female Sex Hormones on Susceptibility to HSV-2 in Vaginal Cells Grown in Air-Liquid Interface. Viruses. 2016;8(9).

53. Pyles RB, Vincent KL, Baum MM, Elsom B, Miller AL, Maxwell C, et al. Cultivated vaginal microbiomes alter HIV-1 infection and antiretroviral efficacy in colonized epithelial multilayer cultures. PLoS One. 2014;9(3):e93419.
54. Mahajan G, Doherty E, To T, Sutherland A, Grant J, Junaid A, et al. Vaginal microbiome-host interactions modeled in a human vagina-on-a-chip. Microbiome. 2022;10(1):201.
55. Stone L. A vagina on a chip to model microbiome-host interactions. Nat Rev Urol. 2023;20(2):64.
56. Aflatoonian R, Fazeli A. Toll-like receptors in female reproductive tract and their menstrual cycle dependent expression. J Reprod Immunol. 2008;77(1):7-13.
57. Hart KM, Murphy AJ, Barrett KT, Wira CR, Guyre PM, Pioli PA. Functional expression of pattern recognition receptors in tissues of the human female reproductive tract. J Reprod Immunol. 2009;80(1-2):33-40.
58. Ghosh M, Shen Z, Fahey JV, Crist SG, Patel M, Smith JM, et al. Pathogen recognition in the human female reproductive tract: expression of intracellular cytosolic sensors NOD1, NOD2, RIG-1, and MDA5 and response to HIV-1 and Neisseria gonorrhea. Am J Reprod Immunol. 2013;69(1):41-51.
59. Li D, Wu M. Pattern recognition receptors in health and diseases. Signal Transduct Target Ther. 2021;6(1):291.
60. Akira S, Hemmi H. Recognition of pathogen-associated molecular patterns by TLR family. Immunol Lett. 2003;85(2):85-95.
61. De Nardo D. Toll-like receptors: Activation, signalling and transcriptional modulation. Cytokine. 2015;74(2):181-9.
62. Kawai T, Akira S. Toll-like receptors and their crosstalk with other innate receptors in infection and immunity. Immunity. 2011;34(5):637-50.
63. Wira CR, Grant-Tschudy KS, Crane-Godreau MA. Epithelial cells in the female reproductive tract: a central role as sentinels of immune protection. Am J Reprod Immunol. 2005;53(2):65-76.
64. Cario E, Brown D, McKee M, Lynch-Devaney K, Gerken G, Podolsky DK. Commensal-associated molecular patterns induce selective toll-like receptor-trafficking from apical membrane to cytoplasmic compartments in polarized intestinal epithelium. Am J Pathol. 2002;160(1):165-73.
65. Carneiro LA, Magalhaes JG, Tattoli I, Philpott DJ, Travassos LH. Nod-like proteins in inflammation and disease. J Pathol. 2008;214(2):136-48.
66. Kufer TA, Banks DJ, Philpott DJ. Innate immune sensing of microbes by Nod proteins. Ann N Y Acad Sci. 2006;1072:19-27.
67. Abe T, Marutani Y, Shoji I. Cytosolic DNA-sensing immune response and viral infection. Microbiol Immunol. 2019;63(2):51-64.
68. Fazeli A, Bruce C, Anumba DO. Characterization of Toll-like receptors in the female reproductive tract in humans. Hum Reprod. 2005;20(5):1372-8.
69. Kumar H, Kawai T, Akira S. Toll-like receptors and innate immunity. Biochem Biophys Res Commun. 2009;388(4):621-5.
70. Akira S, Uematsu S, Takeuchi O. Pathogen recognition and innate immunity. Cell. 2006;124(4):783-801.
71. Schroder K, Tschopp J. The inflammasomes. Cell. 2010;140(6):821-32.
72. Takeuchi O, Akira S. Pattern recognition receptors and inflammation. Cell. 2010;140(6):805-20.

73. Eade CR, Diaz C, Wood MP, Anastos K, Patterson BK, Gupta P, et al. Identification and characterization of bacterial vaginosis-associated pathogens using a comprehensive cervical-vaginal epithelial coculture assay. PLoS One. 2012;7(11):e50106.
74. Gerson KD, Anton L, Ferguson B, Ravel J, Burris HH, Elovitz MA. Gardnerella vaginalis induces matrix metalloproteinases in the cervicovaginal epithelium through TLR-2 activation. J Reprod Immunol. 2022;152:103648.
75. Jensen MA, Wang YY, Lai SK, Forest MG, McKinley SA. Antibody-Mediated Immobilization of Virions in Mucus. Bull Math Biol. 2019;81(10):4069-99.
76. Kaisho T, Akira S. Toll-like receptor function and signaling. J Allergy Clin Immunol. 2006;117(5):979-87; quiz 88.
77. Barton GM. Viral recognition by Toll-like receptors. Semin Immunol. 2007;19(1):33-40.
78. Krieg AM, Vollmer J. Toll-like receptors 7, 8, and 9: linking innate immunity to autoimmunity. Immunol Rev. 2007;220:251-69.
79. Sellge G, Kufer TA. PRR-signaling pathways: Learning from microbial tactics. Semin Immunol. 2015;27(2):75-84.
80. Chang ZL. Important aspects of Toll-like receptors, ligands and their signaling pathways. Inflamm Res. 2010;59(10):791-808.
81. Kawai T, Akira S. The role of pattern-recognition receptors in innate immunity: update on Toll-like receptors. Nat Immunol. 2010;11(5):373-84.
82. Triantafilou M, Gamper FG, Haston RM, Mouratis MA, Morath S, Hartung T, et al. Membrane sorting of toll-like receptor (TLR)-2/6 and TLR2/1 heterodimers at the cell surface determines heterotypic associations with CD36 and intracellular targeting. J Biol Chem. 2006;281(41):31002-11.
83. Alexopoulou L, Holt AC, Medzhitov R, Flavell RA. Recognition of double-stranded RNA and activation of NF-kappaB by Toll-like receptor 3. Nature. 2001;413(6857):732-8.
84. Park BS, Song DH, Kim HM, Choi BS, Lee H, Lee JO. The structural basis of lipopolysaccharide recognition by the TLR4-MD-2 complex. Nature. 2009;458(7242):1191-5.
85. Yang J, Yan H. TLR5: beyond the recognition of flagellin. Cell Mol Immunol. 2017;14(12):1017-9.
86. Hayashi K, Yokozaki H, Goodison S, Oue N, Suzuki T, Lotan R, et al. Inactivation of retinoic acid receptor beta by promoter CpG hypermethylation in gastric cancer. Differentiation. 2001;68(1):13-21.
87. Oosting M, Cheng SC, Bolscher JM, Vestering-Stenger R, Plantinga TS, Verschueren IC, et al. Human TLR10 is an anti-inflammatory pattern-recognition receptor. Proc Natl Acad Sci U S A. 2014;111(42):E4478-84.
88. Su SB, Tao L, Deng ZP, Chen W, Qin SY, Jiang HX. TLR10: Insights, controversies and potential utility as a therapeutic target. Scand J Immunol. 2021;93(4):e12988.
89. Lee SM, Kok KH, Jaume M, Cheung TK, Yip TF, Lai JC, et al. Toll-like receptor 10 is involved in induction of innate immune responses to influenza virus infection. Proc Natl Acad Sci U S A. 2014;111(10):3793-8.
90. Mantovani S, Oliviero B, Varchetta S, Renieri A, Mondelli MU. TLRs: Innate Immune Sentries against SARS-CoV-2 Infection. Int J Mol Sci. 2023;24(9).
91. Aluri J, Cooper MA, Schuettpelz LG. Toll-Like Receptor Signaling in the Establishment and Function of the Immune System. Cells. 2021;10(6).

92. Kwissa M, Nakaya HI, Oluoch H, Pulendran B. Distinct TLR adjuvants differentially stimulate systemic and local innate immune responses in nonhuman primates. Blood. 2012;119(9):2044-55.
93. Takeda K, Akira S. Toll receptors and pathogen resistance. Cell Microbiol. 2003;5(3):143-53.
94. Kawasaki T, Kawai T. Toll-like receptor signaling pathways. Front Immunol. 2014;5:461.
95. Gay NJ, Symmons MF, Gangloff M, Bryant CE. Assembly and localization of Toll-like receptor signalling complexes. Nat Rev Immunol. 2014;14(8):546-58.
96. O'Neill LA, Fitzgerald KA, Bowie AG. The Toll-IL-1 receptor adaptor family grows to five members. Trends Immunol. 2003;24(6):286-90.
97. Fitzgerald KA, Rowe DC, Barnes BJ, Caffrey DR, Visintin A, Latz E, et al. LPS-TLR4 signaling to IRF-3/7 and NF-kappaB involves the toll adapters TRAM and TRIF. J Exp Med. 2003;198(7):1043-55.
98. Rajpoot S, Wary KK, Ibbott R, Liu D, Saqib U, Thurston TLM, et al. TIRAP in the Mechanism of Inflammation. Front Immunol. 2021;12:697588.
99. Chen YH, Wu KH, Wu HP. Unraveling the Complexities of Toll-like Receptors: From Molecular Mechanisms to Clinical Applications. Int J Mol Sci. 2024;25(9).
100. McGowin CL, Ma L, Martin DH, Pyles RB. Mycoplasma genitalium-encoded MG309 activates NF-kappaB via Toll-like receptors 2 and 6 to elicit proinflammatory cytokine secretion from human genital epithelial cells. Infect Immun. 2009;77(3):1175-81.
101. Lawrence T. The nuclear factor NF-kappaB pathway in inflammation. Cold Spring Harb Perspect Biol. 2009;1(6):a001651.
102. Nasu K, Narahara H. Pattern recognition via the toll-like receptor system in the human female genital tract. Mediators Inflamm. 2010;2010:976024.
103. Pudney J, He X, Masheeb Z, Kindelberger DW, Kuohung W, Ingalls RR. Differential expression of toll-like receptors in the human placenta across early gestation. Placenta. 2016;46:1-10.
104. Patni S, Wynen LP, Seager AL, Morgan G, White JO, Thornton CA. Expression and activity of Toll-like receptors 1-9 in the human term placenta and changes associated with labor at term. Biol Reprod. 2009;80(2):243-8.
105. Inohara N, Nuñez G. NODs: intracellular proteins involved in inflammation and apoptosis. Nat Rev Immunol. 2003;3(5):371-82.
106. Saxena M, Yeretssian G. NOD-Like Receptors: Master Regulators of Inflammation and Cancer. Front Immunol. 2014;5:327.
107. Chen G, Shaw MH, Kim YG, Nuñez G. NOD-like receptors: role in innate immunity and inflammatory disease. Annu Rev Pathol. 2009;4:365-98.
108. Girardin SE, Boneca IG, Viala J, Chamaillard M, Labigne A, Thomas G, et al. Nod2 is a general sensor of peptidoglycan through muramyl dipeptide (MDP) detection. J Biol Chem. 2003;278(11):8869-72.
109. Fensterl V, Sen GC. Interferons and viral infections. Biofactors. 2009;35(1):14-20.
110. Barral PM, Sarkar D, Su ZZ, Barber GN, DeSalle R, Racaniello VR, et al. Functions of the cytoplasmic RNA sensors RIG-I and MDA-5: key regulators of innate immunity. Pharmacol Ther. 2009;124(2):219-34.

111. Liu X, Cooper DE, Cluntun AA, Warmoes MO, Zhao S, Reid MA, et al. Acetate Production from Glucose and Coupling to Mitochondrial Metabolism in Mammals. Cell. 2018;175(2):502-13.e13.
112. Kok KH, Lui PY, Ng MH, Siu KL, Au SW, Jin DY. The double-stranded RNA-binding protein PACT functions as a cellular activator of RIG-I to facilitate innate antiviral response. Cell Host Microbe. 2011;9(4):299-309.
113. Lee JH, Chiang C, Gack MU. Endogenous Nucleic Acid Recognition by RIG-I-Like Receptors and cGAS. J Interferon Cytokine Res. 2019;39(8):450-8.
114. Zhang W, Wang G, Xu ZG, Tu H, Hu F, Dai J, et al. Lactate Is a Natural Suppressor of RLR Signaling by Targeting MAVS. Cell. 2019;178(1):176-89.e15.
115. Freeman SA, Grinstein S. Phagocytosis: receptors, signal integration, and the cytoskeleton. Immunol Rev. 2014;262(1):193-215.
116. Dambuza IM, Brown GD. C-type lectins in immunity: recent developments. Curr Opin Immunol. 2015;32:21-7.
117. Ebner S, Sharon N, Ben-Tal N. Evolutionary analysis reveals collective properties and specificity in the C-type lectin and lectin-like domain superfamily. Proteins. 2003;53(1):44-55.
118. Martinez-Pomares L. The mannose receptor. J Leukoc Biol. 2012;92(6):1177-86.
119. Bravo MF, Palanichamy K, Shlain MA, Schiro F, Naeem Y, Marianski M, et al. Synthesis and Binding of Mannose-Specific Synthetic Carbohydrate Receptors. Chemistry. 2020;26(51):11782-95.
120. Peters K, Peters M. The Role of Lectin Receptors and Their Ligands in Controlling Allergic Inflammation. Front Immunol. 2021;12:635411.
121. Decout A, Krasias I, Roberts L, Gimeno Molina B, Charenton C, Brown Romero D, et al. Lactobacillus crispatus S-layer proteins modulate innate immune response and inflammation in the lower female reproductive tract. Nat Commun. 2024;15(1):10879.
122. Feng S, Chen T, Lei G, Hou F, Jiang J, Huang Q, et al. Absent in melanoma 2 inflammasome is required for host defence against. Innate Immun. 2019;25(7):412-9.
123. Gray EE, Winship D, Snyder JM, Child SJ, Geballe AP, Stetson DB. The AIM2-like Receptors Are Dispensable for the Interferon Response to Intracellular DNA. Immunity. 2016;45(2):255-66.
124. Ishikawa H, Barber GN. STING is an endoplasmic reticulum adaptor that facilitates innate immune signalling. Nature. 2008;455(7213):674-8.
125. Ishikawa H, Ma Z, Barber GN. STING regulates intracellular DNA-mediated, type I interferon-dependent innate immunity. Nature. 2009;461(7265):788-92.
126. Sun L, Wu J, Du F, Chen X, Chen ZJ. Cyclic GMP-AMP synthase is a cytosolic DNA sensor that activates the type I interferon pathway. Science. 2013;339(6121):786-91.
127. Wu J, Sun L, Chen X, Du F, Shi H, Chen C, et al. Cyclic GMP-AMP is an endogenous second messenger in innate immune signaling by cytosolic DNA. Science. 2013;339(6121):826-30.
128. Decout A, Katz JD, Venkatraman S, Ablasser A. The cGAS-STING pathway as a therapeutic target in inflammatory diseases. Nat Rev Immunol. 2021;21(9):548-69.
129. Kumar V. The Trinity of cGAS, TLR9, and ALRs Guardians of the Cellular Galaxy Against Host-Derived Self-DNA. Front Immunol. 2020;11:624597.
130. Napetschnig J, Wu H. Molecular basis of NF-κB signaling. Annu Rev Biophys. 2013;42:443-68.

131. Hayden MS, Ghosh S. NF-κB, the first quarter-century: remarkable progress and outstanding questions. Genes Dev. 2012;26(3):203-34.
132. Hayden MS, Ghosh S. Signaling to NF-kappaB. Genes Dev. 2004;18(18):2195-224.
133. Israël A. The IKK complex, a central regulator of NF-kappaB activation. Cold Spring Harb Perspect Biol. 2010;2(3):a000158.
134. Bonizzi G, Karin M. The two NF-kappaB activation pathways and their role in innate and adaptive immunity. Trends Immunol. 2004;25(6):280-8.
135. Israël A. The IKK complex: an integrator of all signals that activate NF-kappaB? Trends Cell Biol. 2000;10(4):129-33.
136. Liu T, Zhang L, Joo D, Sun SC. NF-κB signaling in inflammation. Signal Transduct Target Ther. 2017;2:17023-.
137. Lindström TM, Bennett PR. The role of nuclear factor kappa B in human labour. Reproduction. 2005;130(5):569-81.
138. Traenckner EB, Baeuerle PA. Appearance of apparently ubiquitin-conjugated I kappa B-alpha during its phosphorylation-induced degradation in intact cells. J Cell Sci Suppl. 1995;19:79-84.
139. Oeckinghaus A, Ghosh S. The NF-kappaB family of transcription factors and its regulation. Cold Spring Harb Perspect Biol. 2009;1(4):a000034.
140. Kanarek N, Ben-Neriah Y. Regulation of NF-κB by ubiquitination and degradation of the IκBs. Immunol Rev. 2012;246(1):77-94.
141. Sun SC. Non-canonical NF-κB signaling pathway. Cell Res. 2011;21(1):71-85.
142. Richmond A. Nf-kappa B, chemokine gene transcription and tumour growth. Nat Rev Immunol. 2002;2(9):664-74.
143. Gómez-Chávez F, Correa D, Navarrete-Meneses P, Cancino-Diaz JC, Cancino-Diaz ME, Rodríguez-Martínez S. NF-κB and Its Regulators During Pregnancy. Front Immunol. 2021;12:679106.
144. Yu H, Lin L, Zhang Z, Zhang H, Hu H. Targeting NF-κB pathway for the therapy of diseases: mechanism and clinical study. Signal Transduct Target Ther. 2020;5(1):209.
145. Grimsey NJ, Lin Y, Narala R, Rada CC, Mejia-Pena H, Trejo J. G protein-coupled receptors activate p38 MAPK via a non-canonical TAB1-TAB2- and TAB1-TAB3-dependent pathway in endothelial cells. J Biol Chem. 2019;294(15):5867-78.
146. Guo YJ, Pan WW, Liu SB, Shen ZF, Xu Y, Hu LL. ERK/MAPK signalling pathway and tumorigenesis. Exp Ther Med. 2020;19(3):1997-2007.
147. Kyriakis JM, Avruch J. Mammalian MAPK signal transduction pathways activated by stress and inflammation: a 10-year update. Physiol Rev. 2012;92(2):689-737.
148. Cargnello M, Roux PP. Activation and function of the MAPKs and their substrates, the MAPK-activated protein kinases. Microbiol Mol Biol Rev. 2011;75(1):50-83.
149. Chalmers CJ, Gilley R, March HN, Balmanno K, Cook SJ. The duration of ERK1/2 activity determines the activation of c-Fos and Fra-1 and the composition and quantitative transcriptional output of AP-1. Cell Signal. 2007;19(4):695-704.
150. Gilley R, March HN, Cook SJ. ERK1/2, but not ERK5, is necessary and sufficient for phosphorylation and activation of c-Fos. Cell Signal. 2009;21(6):969-77.
151. Aggarwal S, Suzuki T, Taylor WL, Bhargava A, Rao RK. Contrasting effects of ERK on tight junction integrity in differentiated and under-differentiated Caco-2 cell monolayers. Biochem J. 2011;433(1):51-63.

152. Cui J, Zhang M, Zhang YQ, Xu ZH. JNK pathway: diseases and therapeutic potential. Acta Pharmacol Sin. 2007;28(5):601-8.
153. Ip YT, Davis RJ. Signal transduction by the c-Jun N-terminal kinase (JNK)--from inflammation to development. Curr Opin Cell Biol. 1998;10(2):205-19.
154. Erlanson DA, Chytil M, Verdine GL. The leucine zipper domain controls the orientation of AP-1 in the NFAT.AP-1.DNA complex. Chem Biol. 1996;3(12):981-91.
155. Pattison MJ, Naik RJ, Reyskens KMSE, Arthur JSC. Loss of Mef2D function enhances TLR induced IL-10 production in macrophages. Biosci Rep. 2020;40(8).
156. Han J, Jiang Y, Li Z, Kravchenko VV, Ulevitch RJ. Activation of the transcription factor MEF2C by the MAP kinase p38 in inflammation. Nature. 1997;386(6622):296-9.
157. Zhao M, New L, Kravchenko VV, Kato Y, Gram H, di Padova F, et al. Regulation of the MEF2 family of transcription factors by p38. Mol Cell Biol. 1999;19(1):21-30.
158. Yang SH, Galanis A, Sharrocks AD. Targeting of p38 mitogen-activated protein kinases to MEF2 transcription factors. Mol Cell Biol. 1999;19(6):4028-38.
159. Curran T, Franza BR. Fos and Jun: the AP-1 connection. Cell. 1988;55(3):395-7.
160. Shaulian E, Karin M. AP-1 as a regulator of cell life and death. Nat Cell Biol. 2002;4(5):E131-6.
161. Shaulian E, Karin M. AP-1 in cell proliferation and survival. Oncogene. 2001;20(19):2390-400.
162. Eferl R, Wagner EF. AP-1: a double-edged sword in tumorigenesis. Nat Rev Cancer. 2003;3(11):859-68.
163. Milde-Langosch K. The Fos family of transcription factors and their role in tumourigenesis. Eur J Cancer. 2005;41(16):2449-61.
164. Hernandez JM, Floyd DH, Weilbaecher KN, Green PL, Boris-Lawrie K. Multiple facets of junD gene expression are atypical among AP-1 family members. Oncogene. 2008;27(35):4757-67.
165. Oeckinghaus A, Hayden MS, Ghosh S. Crosstalk in NF-κB signaling pathways. Nat Immunol. 2011;12(8):695-708.
166. Lucas RM, Luo L, Stow JL. ERK1/2 in immune signalling. Biochem Soc Trans. 2022;50(5):1341-52.
167. Fang R, Jiang Q, Zhou X, Wang C, Guan Y, Tao J, et al. MAVS activates TBK1 and IKKε through TRAFs in NEMO dependent and independent manner. PLoS Pathog. 2017;13(11):e1006720.
168. Liu S, Cai X, Wu J, Cong Q, Chen X, Li T, et al. Phosphorylation of innate immune adaptor proteins MAVS, STING, and TRIF induces IRF3 activation. Science. 2015;347(6227):aaa2630.
169. Kawai T, Akira S. Signaling to NF-kappaB by Toll-like receptors. Trends Mol Med. 2007;13(11):460-9.
170. Rathinam VA, Fitzgerald KA. Inflammasome Complexes: Emerging Mechanisms and Effector Functions. Cell. 2016;165(4):792-800.
171. Elliott EI, Sutterwala FS. Initiation and perpetuation of NLRP3 inflammasome activation and assembly. Immunol Rev. 2015;265(1):35-52.
172. Zhao C, Zhao W. NLRP3 Inflammasome-A Key Player in Antiviral Responses. Front Immunol. 2020;11:211.
173. Abdel-Nour M, Tsalikis J, Kleinman D, Girardin SE. The emerging role of mTOR signalling in antibacterial immunity. Immunol Cell Biol. 2014;92(4):346-53.

174. Luo Y, Li L, Zou P, Wang J, Shao L, Zhou D, et al. Rapamycin enhances long-term hematopoietic reconstitution of ex vivo expanded mouse hematopoietic stem cells by inhibiting senescence. Transplantation. 2014;97(1):20-9.
175. Berard AR, Brubaker DK, Birse K, Lamont A, Mackelprang RD, Noël-Romas L, et al. Vaginal epithelial dysfunction is mediated by the microbiome, metabolome, and mTOR signaling. Cell Rep. 2023;42(5):112474.
176. Donders GG, Bosmans E, Dekeersmaecker A, Vereecken A, Van Bulck B, Spitz B. Pathogenesis of abnormal vaginal bacterial flora. Am J Obstet Gynecol. 2000;182(4):872-8.
177. Ma B, Forney LJ, Ravel J. Vaginal microbiome: rethinking health and disease. Annu Rev Microbiol. 2012;66:371-89.
178. van de Wijgert JH, Borgdorff H, Verhelst R, Crucitti T, Francis S, Verstraelen H, et al. The vaginal microbiota: what have we learned after a decade of molecular characterization? PLoS One. 2014;9(8):e105998.
179. McKinnon LR, Achilles SL, Bradshaw CS, Burgener A, Crucitti T, Fredricks DN, et al. The Evolving Facets of Bacterial Vaginosis: Implications for HIV Transmission. AIDS Res Hum Retroviruses. 2019;35(3):219-28.
180. Sumati AH, Saritha NK. Association of urinary tract infection in women with bacterial vaginosis. J Glob Infect Dis. 2009;1(2):151-2.
181. Stapleton AE. The Vaginal Microbiota and Urinary Tract Infection. Microbiol Spectr. 2016;4(6).
182. Taha TE, Hoover DR, Dallabetta GA, Kumwenda NI, Mtimavalye LA, Yang LP, et al. Bacterial vaginosis and disturbances of vaginal flora: association with increased acquisition of HIV. AIDS. 1998;12(13):1699-706.
183. Martin HL, Richardson BA, Nyange PM, Lavreys L, Hillier SL, Chohan B, et al. Vaginal lactobacilli, microbial flora, and risk of human immunodeficiency virus type 1 and sexually transmitted disease acquisition. J Infect Dis. 1999;180(6):1863-8.
184. Lai SK, Hida K, Shukair S, Wang YY, Figueiredo A, Cone R, et al. Human immunodeficiency virus type 1 is trapped by acidic but not by neutralized human cervicovaginal mucus. J Virol. 2009;83(21):11196-200.
185. Cone RA. Vaginal microbiota and sexually transmitted infections that may influence transmission of cell-associated HIV. J Infect Dis. 2014;210 Suppl 3:S616-21.
186. Gosmann C, Anahtar MN, Handley SA, Farcasanu M, Abu-Ali G, Bowman BA, et al. Lactobacillus-Deficient Cervicovaginal Bacterial Communities Are Associated with Increased HIV Acquisition in Young South African Women. Immunity. 2017;46(1):29-37.
187. Brotman RM, Bradford LL, Conrad M, Gajer P, Ault K, Peralta L, et al. Association between Trichomonas vaginalis and vaginal bacterial community composition among reproductive-age women. Sex Transm Dis. 2012;39(10):807-12.
188. Mastromarino P, Di Pietro M, Schiavoni G, Nardis C, Gentile M, Sessaa R. Effects of vaginal lactobacilli in Chlamydia trachomatis infection. International Journal of Medical Microbiology. 2014;304(5-6):654-61.
189. Nardis C, Mosca L, Mastromarino P. Vaginal microbiota and viral sexually transmitted diseases. Ann Ig. 2013;25(5):443-56.
190. Gong Z, Luna Y, Yu P, Fan H. Lactobacilli inactivate Chlamydia trachomatis through lactic acid but not H2O2. PLoS One. 2014;9(9):e107758.

191. Nene N, Reisel D, Leimbach A. Association between the cervicovaginal microbiome, BRCA1 mutation status, and risk of ovarian cancer: a case-control study (vol 20, pg 1171, 2019). Lancet Oncology. 2019;20(9):E468-E.
192. Wilson JD, Ralph SG, Rutherford AJ. Rates of bacterial vaginosis in women undergoing in vitro fertilisation for different types of infertility. BJOG. 2002;109(6):714-7.
193. Donders GG, Van Calsteren K, Bellen G, Reybrouck R, Van den Bosch T, Riphagen I, et al. Predictive value for preterm birth of abnormal vaginal flora, bacterial vaginosis and aerobic vaginitis during the first trimester of pregnancy. BJOG. 2009;116(10):1315-24.
194. Brown RG, Marchesi JR, Lee YS, Smith A, Lehne B, Kindinger LM, et al. Vaginal dysbiosis increases risk of preterm fetal membrane rupture, neonatal sepsis and is exacerbated by erythromycin. BMC Med. 2018;16(1):9.
195. Hočevar K, Maver A, Vidmar Šimic M, Hodžić A, Haslberger A, Premru Seršen T, et al. Vaginal Microbiome Signature Is Associated With Spontaneous Preterm Delivery. Front Med (Lausanne). 2019;6:201.
196. Borgdorff H, Tsivtsivadze E, Verhelst R, Marzorati M, Jurriaans S, Ndayisaba GF, et al. Lactobacillus-dominated cervicovaginal microbiota associated with reduced HIV/STI prevalence and genital HIV viral load in African women. ISME J. 2014;8(9):1781-93.
197. Farr A, Kiss H, Hagmann M, Machal S, Holzer I, Kueronya V, et al. Role of Lactobacillus Species in the Intermediate Vaginal Flora in Early Pregnancy: A Retrospective Cohort Study. Plos One. 2015;10(12).
198. Correia GD, Marchesi JR, MacIntyre DA. Moving beyond DNA: towards functional analysis of the vaginal microbiome by non-sequencing-based methods. Curr Opin Microbiol. 2023;73:102292.
199. Ravel J, Gajer P, Abdo Z, Schneider GM, Koenig SS, McCulle SL, et al. Vaginal microbiome of reproductive-age women. Proc Natl Acad Sci U S A. 2011;108 Suppl 1:4680-7.
200. Gajer P, Brotman RM, Bai G, Sakamoto J, Schütte UM, Zhong X, et al. Temporal dynamics of the human vaginal microbiota. Sci Transl Med. 2012;4(132):132ra52.
201. France MT, Ma B, Gajer P, Brown S, Humphrys MS, Holm JB, et al. VALENCIA: a nearest centroid classification method for vaginal microbial communities based on composition. Microbiome. 2020;8(1):166.
202. Molina MA, Andralojc KM, Huynen MA, Leenders WPJ, Melchers WJG. In-depth insights into cervicovaginal microbial communities and hrHPV infections using high-resolution microbiome profiling. NPJ Biofilms Microbiomes. 2022;8(1):75.
203. Ma LN, Huang XB, Muyayalo KP, Mor G, Liao AH. Lactic Acid: A Novel Signaling Molecule in Early Pregnancy? Front Immunol. 2020;11:279.
204. Mitra A, MacIntyre DA, Marchesi JR, Lee YS, Bennett PR, Kyrgiou M. The vaginal microbiota, human papillomavirus infection and cervical intraepithelial neoplasia: what do we know and where are we going next? Microbiome. 2016;4(1):58.
205. Mitra A, MacIntyre DA, Ntritsos G, Smith A, Tsilidis KK, Marchesi JR, et al. The vaginal microbiota associates with the regression of untreated cervical intraepithelial neoplasia 2 lesions. Nat Commun. 2020;11(1):1999.
206. Mitra A, MacIntyre DA, Lee YS, Smith A, Marchesi JR, Lehne B, et al. Cervical intraepithelial neoplasia disease progression is associated with increased vaginal microbiome diversity. Sci Rep. 2015;5:16865.

207. Elovitz MA, Gajer P, Riis V, Brown AG, Humphrys MS, Holm JB, et al. Cervicovaginal microbiota and local immune response modulate the risk of spontaneous preterm delivery. Nat Commun. 2019;10(1):1305.
208. Fettweis JM, Serrano MG, Brooks JP, Edwards DJ, Girerd PH, Parikh HI, et al. The vaginal microbiome and preterm birth. Nat Med. 2019;25(6):1012-21.
209. van de Wijgert JHHM. The vaginal microbiome and sexually transmitted infections are interlinked: Consequences for treatment and prevention. PLoS Med. 2017;14(12):e1002478.
210. Kindinger LM, Bennett PR, Lee YS, Marchesi JR, Smith A, Cacciatore S, et al. The interaction between vaginal microbiota, cervical length, and vaginal progesterone treatment for preterm birth risk. Microbiome. 2017;5(1):6.
211. Jespers V, van de Wijgert J, Cools P, Verhelst R, Verstraelen H, Delany-Moretlwe S, et al. The significance of Lactobacillus crispatus and L. vaginalis for vaginal health and the negative effect of recent sex: a cross-sectional descriptive study across groups of African women. BMC Infect Dis. 2015;15:115.
212. Grace JB, Anderson TM, Seabloom EW, Borer ET, Adler PB, Harpole WS, et al. Integrative modelling reveals mechanisms linking productivity and plant species richness. Nature. 2016;529(7586):390-3.
213. Wang S, Wang Q, Yang E, Yan L, Li T, Zhuang H. Antimicrobial Compounds Produced by Vaginal Lactobacillus crispatus Are Able to Strongly Inhibit Candida albicans Growth, Hyphal Formation and Regulate Virulence-related Gene Expressions. Front Microbiol. 2017;8:564.
214. Argentini C, Fontana F, Alessandri G, Lugli GA, Mancabelli L, Ossiprandi MC, et al. Evaluation of Modulatory Activities of Lactobacillus crispatus Strains in the Context of the Vaginal Microbiota. Microbiol Spectr. 2022;10(2):e0273321.
215. Petrova MI, Reid G, Vaneechoutte M, Lebeer S. Lactobacillus iners: Friend or Foe? Trends Microbiol. 2017;25(3):182-91.
216. Vaneechoutte M. Lactobacillus iners, the unusual suspect. Res Microbiol. 2017;168(9-10):826-36.
217. Macklaim JM, Fernandes AD, Di Bella JM, Hammond JA, Reid G, Gloor GB. Comparative meta-RNA-seq of the vaginal microbiota and differential expression by Lactobacillus iners in health and dysbiosis. Microbiome. 2013;1(1):12.
218. France MT, Mendes-Soares H, Forney LJ. Genomic Comparisons of Lactobacillus crispatus and Lactobacillus iners Reveal Potential Ecological Drivers of Community Composition in the Vagina. Appl Environ Microbiol. 2016;82(24):7063-73.
219. Macklaim JM, Gloor GB, Anukam KC, Cribby S, Reid G. At the crossroads of vaginal health and disease, the genome sequence of Lactobacillus iners AB-1. Proc Natl Acad Sci U S A. 2011;108 Suppl 1:4688-95.
220. Campisciano G, Iebba V, Zito G, Luppi S, Martinelli M, Fischer L, et al. Lactobacillus iners and gasseri, Prevotella bivia and HPV Belong to the Microbiological Signature Negatively Affecting Human Reproduction. Microorganisms. 2020;9(1).
221. Spear GT, Gilbert D, Landay AL, Zariffard R, French AL, Patel P, et al. Pyrosequencing of the genital microbiotas of HIV-seropositive and -seronegative women reveals Lactobacillus iners as the predominant Lactobacillus Species. Appl Environ Microbiol. 2011;77(1):378-81.
222. Fettweis JM, Brooks JP, Serrano MG, Sheth NU, Girerd PH, Edwards DJ, et al. Differences in vaginal microbiome in African American women versus women of European ancestry. Microbiology. 2014;160(Pt 10):2272-82.

223. Jie Z, Xia H, Zhong SL, Feng Q, Li S, Liang S, et al. The gut microbiome in atherosclerotic cardiovascular disease. Nat Commun. 2017;8(1):845.
224. Romero R, Hassan SS, Gajer P, Tarca AL, Fadrosh DW, Nikita L, et al. The composition and stability of the vaginal microbiota of normal pregnant women is different from that of non-pregnant women. Microbiome. 2014;2(1):4.
225. Baud A, Hillion KH, Plainvert C, Tessier V, Tazi A, Mandelbrot L, et al. Microbial diversity in the vaginal microbiota and its link to pregnancy outcomes. Sci Rep. 2023;13(1):9061.
226. Rasmussen MA, Thorsen J, Dominguez-Bello MG, Blaser MJ, Mortensen MS, Brejnrod AD, et al. Ecological succession in the vaginal microbiota during pregnancy and birth. ISME J. 2020;14(9):2325-35.
227. Muhleisen AL, Herbst-Kralovetz MM. Menopause and the vaginal microbiome. Maturitas. 2016;91:42-50.
228. Hugenholtz F, van der Veer C, Terpstra ML, Borgdorff H, van Houdt R, Bruisten S, et al. Urine and vaginal microbiota compositions of postmenopausal and premenopausal women differ regardless of recurrent urinary tract infection and renal transplant status. Sci Rep. 2022;12(1):2698.
229. Petricevic L, Domig KJ, Nierscher FJ, Sandhofer MJ, Fidesser M, Krondorfer I, et al. Characterisation of the vaginal Lactobacillus microbiota associated with preterm delivery. Sci Rep. 2014;4:5136.
230. Tabatabaei N, Eren AM, Barreiro LB, Yotova V, Dumaine A, Allard C, et al. Vaginal microbiome in early pregnancy and subsequent risk of spontaneous preterm birth: a case-control study. BJOG. 2019;126(3):349-58.
231. DiGiulio DB, Callahan BJ, McMurdie PJ, Costello EK, Lyell DJ, Robaczewska A, et al. Temporal and spatial variation of the human microbiota during pregnancy. Proc Natl Acad Sci U S A. 2015;112(35):11060-5.
232. Kindinger LM, MacIntyre DA, Lee YS, Marchesi JR, Smith A, McDonald JA, et al. Relationship between vaginal microbial dysbiosis, inflammation, and pregnancy outcomes in cervical cerclage. Sci Transl Med. 2016;8.
233. Brown RG, Al-Memar M, Marchesi JR, Lee YS, Smith A, Chan D, et al. Establishment of vaginal microbiota composition in early pregnancy and its association with subsequent preterm prelabor rupture of the fetal membranes. Transl Res. 2019;207:30-43.
234. Gimeno-Molina B, Muller I, Kropf P, Sykes L. The Role of Neutrophils in Pregnancy, Term and Preterm Labour. Life (Basel). 2022;12(10).
235. Zevin AS, Xie IY, Birse K, Arnold K, Romas L, Westmacott G, et al. Microbiome Composition and Function Drives Wound-Healing Impairment in the Female Genital Tract. PLoS Pathog. 2016;12(9):e1005889.
236. Borgdorff H, Gautam R, Armstrong SD, Xia D, Ndayisaba GF, van Teijlingen NH, et al. Cervicovaginal microbiome dysbiosis is associated with proteome changes related to alterations of the cervicovaginal mucosal barrier. Mucosal Immunol. 2016;9(3):621-33.
237. Lewis WG, Robinson LS, Gilbert NM, Perry JC, Lewis AL. Degradation, foraging, and depletion of mucus sialoglycans by the vagina-adapted Actinobacterium Gardnerella vaginalis. J Biol Chem. 2013;288(17):12067-79.
238. De Seta F, Campisciano G, Zanotta N, Ricci G, Comar M. The Vaginal Community State Types Microbiome-Immune Network as Key Factor for Bacterial Vaginosis and Aerobic Vaginitis. Front Microbiol. 2019;10:2451.

239. Ravel J, Moreno I, Simón C. Bacterial vaginosis and its association with infertility, endometritis, and pelvic inflammatory disease. Am J Obstet Gynecol. 2021;224(3):251-7.
240. Jamieson DJ, Duerr A, Klein RS, Paramsothy P, Brown W, Cu-Uvin S, et al. Longitudinal analysis of bacterial vaginosis: findings from the HIV epidemiology research study. Obstet Gynecol. 2001;98(4):656-63.
241. Martins BCT, Guimarães RA, Alves RRF, Saddi VA. Bacterial vaginosis and cervical human papillomavirus infection in young and adult women: a systematic review and meta-analysis. Rev Saude Publica. 2023;56:113.
242. Mitchell C, Marrazzo J. Bacterial vaginosis and the cervicovaginal immune response. Am J Reprod Immunol. 2014;71(6):555-63.
243. Doerflinger SY, Throop AL, Herbst-Kralovetz MM. Bacteria in the vaginal microbiome alter the innate immune response and barrier properties of the human vaginal epithelia in a species-specific manner. J Infect Dis. 2014;209(12):1989-99.
244. Libby EK, Pascal KE, Mordechai E, Adelson ME, Trama JP. Atopobium vaginae triggers an innate immune response in an in vitro model of bacterial vaginosis. Microbes Infect. 2008;10(4):439-46.
245. Baldewijns S, Sillen M, Palmans I, Vandecruys P, Van Dijck P, Demuyser L. The Role of Fatty Acid Metabolites in Vaginal Health and Disease: Application to Candidiasis. Front Microbiol. 2021;12:705779.
246. Pruski P, MacIntyre DA, Lewis HV, Inglese P, Correia GD, Hansel TT, et al. Medical Swab Analysis Using Desorption Electrospray Ionization Mass Spectrometry: A Noninvasive Approach for Mucosal Diagnostics. Anal Chem. 2017;89(3):1540-50.
247. Pruski P, Correia GDS, Lewis HV, Capuccini K, Inglese P, Chan D, et al. Direct on-swab metabolic profiling of vaginal microbiome host interactions during pregnancy and preterm birth. Nat Commun. 2021;12(1):5967.
248. McMillan A, Rulisa S, Sumarah M, Macklaim JM, Renaud J, Bisanz JE, et al. A multi-platform metabolomics approach identifies highly specific biomarkers of bacterial diversity in the vagina of pregnant and non-pregnant women. Sci Rep. 2015;5:14174.
249. Vitali B, Cruciani F, Picone G, Parolin C, Donders G, Laghi L. Vaginal microbiome and metabolome highlight specific signatures of bacterial vaginosis. Eur J Clin Microbiol Infect Dis. 2015;34(12):2367-76.
250. Tachedjian G, Aldunate M, Bradshaw CS, Cone RA. The role of lactic acid production by probiotic Lactobacillus species in vaginal health. Res Microbiol. 2017;168(9-10):782-92.
251. Łaniewski P, Herbst-Kralovetz MM. Bacterial vaginosis and health-associated bacteria modulate the immunometabolic landscape in 3D model of human cervix. NPJ Biofilms Microbiomes. 2021;7(1):88.
252. Brooks GA. Lactate as a fulcrum of metabolism. Redox Biol. 2020;35:101454.
253. Brooks GA, Arevalo JA, Osmond AD, Leija RG, Curl CC, Tovar AP. Lactate in contemporary biology: a phoenix risen. J Physiol. 2022;600(5):1229-51.
254. Brooks GA. The Science and Translation of Lactate Shuttle Theory. Cell Metab. 2018;27(4):757-85.
255. Gladden LB. Lactate metabolism: a new paradigm for the third millennium. J Physiol. 2004;558(Pt 1):5-30.
256. Wisneski JA, Gertz EW, Neese RA, Gruenke LD, Morris DL, Craig JC. Metabolic fate of extracted glucose in normal human myocardium. J Clin Invest. 1985;76(5):1819-27.

257. Mason S. Lactate Shuttles in Neuroenergetics-Homeostasis, Allostasis and Beyond. Front Neurosci. 2017;11:43.
258. Pucino V, Bombardieri M, Pitzalis C, Mauro C. Lactate at the crossroads of metabolism, inflammation, and autoimmunity. Eur J Immunol. 2017;47(1):14-21.
259. Certo M, Tsai CH, Pucino V, Ho PC, Mauro C. Lactate modulation of immune responses in inflammatory versus tumour microenvironments. Nat Rev Immunol. 2021;21(3):151-61.
260. Amabebe E, Anumba DOC. The Vaginal Microenvironment: The Physiologic Role of *Lactobacilli*. Front Med (Lausanne). 2018;5:181.
261. O'Hanlon DE, Moench TR, Cone RA. Vaginal pH and microbicidal lactic acid when lactobacilli dominate the microbiota. PLoS One. 2013;8(11):e80074.
262. Spear GT, French AL, Gilbert D, Zariffard MR, Mirmonsef P, Sullivan TH, et al. Human α-amylase present in lower-genital-tract mucosal fluid processes glycogen to support vaginal colonization by Lactobacillus. J Infect Dis. 2014;210(7):1019-28.
263. Petrova MI, Lievens E, Malik S, Imholz N, Lebeer S. Lactobacillus species as biomarkers and agents that can promote various aspects of vaginal health. Front Physiol. 2015;6:81.
264. Mirmonsef P, Spear GT. The barrier to HIV transmission provided by genital tract Lactobacillus colonization. Am J Reprod Immunol. 2014;71(6):531-6.
265. van der Veer C, Hertzberger RY, Bruisten SM, Tytgat HLP, Swanenburg J, de Kat Angelino-Bart A, et al. Comparative genomics of human Lactobacillus crispatus isolates reveals genes for glycosylation and glycogen degradation: implications for in vivo dominance of the vaginal microbiota. Microbiome. 2019;7(1):49.
266. Ojala T, Kankainen M, Castro J, Cerca N, Edelman S, Westerlund-Wikström B, et al. Comparative genomics of Lactobacillus crispatus suggests novel mechanisms for the competitive exclusion of Gardnerella vaginalis. BMC Genomics. 2014;15:1070.
267. Nunn KL, Forney LJ. Unraveling the Dynamics of the Human Vaginal Microbiome. Yale J Biol Med. 2016;89(3):331-7.
268. Nunn KL, Clair GC, Adkins JN, Engbrecht K, Fillmore T, Forney LJ. Amylases in the Human Vagina. mSphere. 2020;5(6).
269. Navarro S, Abla H, Delgado B, Colmer-Hamood JA, Ventolini G, Hamood AN. Glycogen availability and pH variation in a medium simulating vaginal fluid influence the growth of vaginal Lactobacillus species and Gardnerella vaginalis. BMC Microbiol. 2023;23(1):186.
270. Jenkins DJ, Woolston BM, Hood-Pishchany MI, Pelayo P, Konopaski AN, Quinn Peters M, et al. Bacterial amylases enable glycogen degradation by the vaginal microbiome. Nat Microbiol. 2023;8:1641–52.
271. Witkin SS, Mendes-Soares H, Linhares IM, Jayaram A, Ledger WJ, Forney LJ. Influence of vaginal bacteria and D- and L-lactic acid isomers on vaginal extracellular matrix metalloproteinase inducer: implications for protection against upper genital tract infections. MBio. 2013;4(4):e00460-13.
272. Aldunate M, Srbinovski D, Hearps AC, Latham CF, Ramsland PA, Gugasyan R, et al. Antimicrobial and immune modulatory effects of lactic acid and short chain fatty acids produced by vaginal microbiota associated with eubiosis and bacterial vaginosis. Front Physiol. 2015;6:164.
273. O'Hanlon DE, Moench TR, Cone RA. In vaginal fluid, bacteria associated with bacterial vaginosis can be suppressed with lactic acid but not hydrogen peroxide. BMC Infect Dis. 2011;11:200.

274. Aldunate M, Tyssen D, Johnson A, Zakir T, Sonza S, Moench T, et al. Vaginal concentrations of lactic acid potently inactivate HIV. J Antimicrob Chemother. 2013;68(9):2015-25.
275. Tyssen D, Wang YY, Hayward JA, Agius PA, DeLong K, Aldunate M, et al. Anti-HIV-1 Activity of Lactic Acid in Human Cervicovaginal Fluid. mSphere. 2018;3(4):e00055-18.
276. Hearps AC, Tyssen D, Srbinovski D, Bayigga L, Diaz DJD, Aldunate M, et al. Vaginal lactic acid elicits an anti-inflammatory response from human cervicovaginal epithelial cells and inhibits production of pro-inflammatory mediators associated with HIV acquisition. Mucosal Immunol. 2017;10(6):1480-90.
277. Alakomi HL, Skyttä E, Saarela M, Mattila-Sandholm T, Latva-Kala K, Helander IM. Lactic acid permeabilizes gram-negative bacteria by disrupting the outer membrane. Appl Environ Microbiol. 2000;66(5):2001-5.
278. Butler D, Silvestroni A, Stapleton A. Cytoprotective Effect of Lactobacillus crispatus CTV-05 against Uropathogenic E. coli. Pathogens. 2016;5(1):27–38.
279. McGroarty JA, Reid G. Detection of a Lactobacillus substance that inhibits Escherichia coli. Can J Microbiol. 1988;34(8):974-8.
280. Conti C, Malacrino C, Mastromarino P. Inhibition of herpes simplex virus type 2 by vaginal lactobacilli. J Physiol Pharmacol. 2009;60 Suppl 6:19-26.
281. Isaacs C, Xu W. Theaflavin-3,3 '-Digallate and Lactic Acid Combinations Reduce Herpes Simplex Virus Infectivity. Antimicrobial Agents and Chemotherapy. 2013;57(8):3806-14.
282. Frąszczak K, Barczyński B, Kondracka A. Does Lactobacillus Exert a Protective Effect on the Development of Cervical and Endometrial Cancer in Women? Cancers (Basel). 2022;14(19).
283. Graver MA, Wade JJ. The role of acidification in the inhibition of Neisseria gonorrhoeae by vaginal lactobacilli during anaerobic growth. Ann Clin Microbiol Antimicrob. 2011;10:8.
284. Edwards VL, Smith SB, McComb EJ, Tamarelle J, Ma B, Humphrys MS, et al. The Cervicovaginal Microbiota-Host Interaction Modulates Chlamydia trachomatis Infection. mBio. 2019;10(4):e01548-19.
285. Hearps A, Gugasyan R, Srbinovski D, Tyssen D, Aldunate M, Anderson D, et al. Lactic Acid, a Vaginal Microbiota Metabolite, Elicits an Anti-inflammatory Response from Vaginal and Cervical Epithelial Cells. Aids Research and Human Retroviruses. 2014;30:A238-A9.
286. Nunn KL, Wang YY, Harit D, Humphrys MS, Ma B, Cone R, et al. Enhanced Trapping of HIV-1 by Human Cervicovaginal Mucus Is Associated with Lactobacillus crispatus-Dominant Microbiota. MBio. 2015;6(5):e01084-15.
287. Iacono KT, Brown AL, Greene MI, Saouaf SJ. CD147 immunoglobulin superfamily receptor function and role in pathology. Exp Mol Pathol. 2007;83(3):283-95.
288. Mossop H, Linhares IM, Bongiovanni AM, Ledger WJ, Witkin SS. Influence of lactic acid on endogenous and viral RNA-induced immune mediator production by vaginal epithelial cells. Obstet Gynecol. 2011;118(4):840-6.
289. Becher N, Hein M, Danielsen CC, Uldbjerg N. Matrix metalloproteinases in the cervical mucus plug in relation to gestational age, plug compartment, and preterm labor. Reprod Biol Endocrinol. 2010;8:113.
290. Koh A, De Vadder F, Kovatcheva-Datchary P, Bäckhed F. From Dietary Fiber to Host Physiology: Short-Chain Fatty Acids as Key Bacterial Metabolites. Cell. 2016;165(6):1332-45.

291. Tungland B. Chapter 2: Short-chain fatty acid production and functional aspects on host metabolism. Human Microbiota in Health and Disease. 2018:37-106.
292. Amabebe E, Anumba DOC. Female Gut and Genital Tract Microbiota-Induced Crosstalk and Differential Effects of Short-Chain Fatty Acids on Immune Sequelae. Front Immunol. 2020;11:2184.
293. Al-Mushrif S, Eley A, Jones BM. Inhibition of chemotaxis by organic acids from anaerobes may prevent a purulent response in bacterial vaginosis. J Med Microbiol. 2000;49(11):1023-30.
294. Chaudry AN, Travers PJ, Yuenger J, Colletta L, Evans P, Zenilman JM, et al. Analysis of vaginal acetic acid in patients undergoing treatment for bacterial vaginosis. J Clin Microbiol. 2004;42(11):5170-5.
295. Srinivasan S, Morgan MT, Fiedler TL, Djukovic D, Hoffman NG, Raftery D, et al. Metabolic signatures of bacterial vaginosis. MBio. 2015;6(2):e00204-15.
296. Schwecht I, Nazli A, Gill B, Kaushic C. Lactic acid enhances vaginal epithelial barrier integrity and ameliorates inflammatory effects of dysbiotic short chain fatty acids and HIV-1. Sci Rep. 2023;13(1):20065.
297. Rudiansyah M, Abdalkareem Jasim S, S Azizov B, Samusenkov V, Kamal Abdelbasset W, Yasin G, et al. The emerging microbiome-based approaches to IBD therapy: From SCFAs to urolithin A. J Dig Dis. 2022;23(8-9):412-34.
298. Macia L, Thorburn AN, Binge LC, Marino E, Rogers KE, Maslowski KM, et al. Microbial influences on epithelial integrity and immune function as a basis for inflammatory diseases. Immunol Rev. 2012;245(1):164-76.
299. Arpaia N, Rudensky AY. Microbial metabolites control gut inflammatory responses. Proc Natl Acad Sci U S A. 2014;111(6):2058-9.
300. Zhao Y, Chen F, Wu W, Sun M, Bilotta AJ, Yao S, et al. GPR43 mediates microbiota metabolite SCFA regulation of antimicrobial peptide expression in intestinal epithelial cells via activation of mTOR and STAT3. Mucosal Immunol. 2018;11(3):752-62.
301. Peng L, Li ZR, Green RS, Holzman IR, Lin J. Butyrate enhances the intestinal barrier by facilitating tight junction assembly via activation of AMP-activated protein kinase in Caco-2 cell monolayers. J Nutr. 2009;139(9):1619-25.
302. Ewaschuk JB, Diaz H, Meddings L, Diederichs B, Dmytrash A, Backer J, et al. Secreted bioactive factors from Bifidobacterium infantis enhance epithelial cell barrier function. Am J Physiol Gastrointest Liver Physiol. 2008;295(5):G1025-34.
303. Willemsen LE, Koetsier MA, van Deventer SJ, van Tol EA. Short chain fatty acids stimulate epithelial mucin 2 expression through differential effects on prostaglandin E(1) and E(2) production by intestinal myofibroblasts. Gut. 2003;52(10):1442-7.
304. Sun S, Li H, Chen J, Qian Q. Lactic Acid: No Longer an Inert and End-Product of Glycolysis. Physiology (Bethesda). 2017;32(6):453-63.
305. Stafford GP, Parker JL, Amabebe E, Kistler J, Reynolds S, Stern V, et al. Spontaneous Preterm Birth Is Associated with Differential Expression of Vaginal Metabolites by Lactobacilli-Dominated Microflora. Front Physiol. 2017;8:615.
306. Kaneuchi C, Seki M, Komagata K. Production of succinic Acid from citric Acid and related acids by lactobacillus strains. Appl Environ Microbiol. 1988;54(12):3053-6.
307. Farr Zuend C, Lamont A, Noel-Romas L, Knodel S, Birse K, Kratzer K, et al. Increased genital mucosal cytokines in Canadian women associate with higher antigen-presenting cells,

inflammatory metabolites, epithelial barrier disruption, and the depletion of L. crispatus. Microbiome. 2023;11(1):159.
308. Delgado-Diaz DJ, Tyssen D, Hayward JA, Gugasyan R, Hearps AC, Tachedjian G. Distinct Immune Responses Elicited From Cervicovaginal Epithelial Cells by Lactic Acid and Short Chain Fatty Acids Associated With Optimal and Non-optimal Vaginal Microbiota. Front Cell Infect Microbiol. 2019;9:446.
309. Cai TQ, Ren N, Jin L, Cheng K, Kash S, Chen R, et al. Role of GPR81 in lactate-mediated reduction of adipose lipolysis. Biochem Biophys Res Commun. 2008;377(3):987-91.
310. Liu C, Wu J, Zhu J, Kuei C, Yu J, Shelton J, et al. Lactate inhibits lipolysis in fat cells through activation of an orphan G-protein-coupled receptor, GPR81. J Biol Chem. 2009;284(5):2811-22.
311. Morland C, Lauritzen KH, Puchades M, Holm-Hansen S, Andersson K, Gjedde A, et al. The lactate receptor, G-protein-coupled receptor 81/hydroxycarboxylic acid receptor 1: Expression and action in brain. J Neurosci Res. 2015;93(7):1045-55.
312. Ishihara S, Hata K, Hirose K, Okui T, Toyosawa S, Uzawa N, et al. The lactate sensor GPR81 regulates glycolysis and tumor growth of breast cancer. Sci Rep. 2022;12(1):6261.
313. Manoharan I, Prasad PD, Thangaraju M, Manicassamy S. Lactate-Dependent Regulation of Immune Responses by Dendritic Cells and Macrophages. Front Immunol. 2021;12:691134.
314. Colucci ACM, Tassinari ID, Loss EDS, de Fraga LS. History and Function of the Lactate Receptor GPR81/HCAR1 in the Brain: A Putative Therapeutic Target for the Treatment of Cerebral Ischemia. Neuroscience. 2023;526:144-63.
315. Kennedy L, Glesaaen ER, Palibrk V, Pannone M, Wang W, Al-Jabri A, et al. Lactate receptor HCAR1 regulates neurogenesis and microglia activation after neonatal hypoxia-ischemia. Elife. 2022;11:e76451.
316. Bosshart PD, Charles RP, Garibsingh RA, Schlessinger A, Fotiadis D. SLC16 Family: From Atomic Structure to Human Disease. Trends Biochem Sci. 2021;46(1):28-40.
317. Sun X, Wang M, Yao L, Li X, Dong H, Li M, et al. Role of Proton-Coupled Monocarboxylate Transporters in Cancer: From Metabolic Crosstalk to Therapeutic Potential. Front Cell Dev Biol. 2020;8:651.
318. Ganapathy V, Thangaraju M, Gopal E, Martin PM, Itagaki S, Miyauchi S, et al. Sodium-coupled monocarboxylate transporters in normal tissues and in cancer. AAPS J. 2008;10(1):193-9.
319. Thangaraju M, Cresci G, Itagaki S, Mellinger J, Browning DD, Berger FG, et al. Sodium-coupled transport of the short chain fatty acid butyrate by SLC5A8 and its relevance to colon cancer. J Gastrointest Surg. 2008;12(10):1773-81; discussion 81-2.
320. Martin PM, Gopal E, Ananth S, Zhuang L, Itagaki S, Prasad BM, et al. Identity of SMCT1 (SLC5A8) as a neuron-specific Na+-coupled transporter for active uptake of L-lactate and ketone bodies in the brain. J Neurochem. 2006;98(1):279-88.
321. van der Hee B, Wells JM. Microbial Regulation of Host Physiology by Short-chain Fatty Acids. Trends Microbiol. 2021;29(8):700-12.
322. Husted AS, Trauelsen M, Rudenko O, Hjorth SA, Schwartz TW. GPCR-Mediated Signaling of Metabolites. Cell Metab. 2017;25(4):777-96.
323. Lauritzen KH, Morland C, Puchades M, Holm-Hansen S, Hagelin EM, Lauritzen F, et al. Lactate receptor sites link neurotransmission, neurovascular coupling, and brain energy metabolism. Cereb Cortex. 2014;24(10):2784-95.

324. Ahmed K, Tunaru S, Tang C, Müller M, Gille A, Sassmann A, et al. An autocrine lactate loop mediates insulin-dependent inhibition of lipolysis through GPR81. Cell Metab. 2010;11(4):311-9.
325. Ge H, Weiszmann J, Reagan JD, Gupte J, Baribault H, Gyuris T, et al. Elucidation of signaling and functional activities of an orphan GPCR, GPR81. J Lipid Res. 2008;49(4):797-803.
326. Feng J, Yang H, Zhang Y, Wei H, Zhu Z, Zhu B, et al. Tumor cell-derived lactate induces TAZ-dependent upregulation of PD-L1 through GPR81 in human lung cancer cells. Oncogene. 2017;36(42):5829-39.
327. Bohn T, Rapp S, Luther N, Klein M, Bruehl TJ, Kojima N, et al. Tumor immunoevasion via acidosis-dependent induction of regulatory tumor-associated macrophages. Nat Immunol. 2018;19(12):1319-29.
328. Chen P, Zuo H, Xiong H, Kolar MJ, Chu Q, Saghatelian A, et al. Gpr132 sensing of lactate mediates tumor-macrophage interplay to promote breast cancer metastasis. Proc Natl Acad Sci U S A. 2017;114(3):580-5.
329. Parks SK, Mueller-Klieser W, Pouysségur J. Lactate and Acidity in the Cancer Microenvironment. Annual Review of Cancer Biology. 2020;4(Volume 4, 2020):141-58.
330. Li X, Yang Y, Zhang B, Lin X, Fu X, An Y, et al. Lactate metabolism in human health and disease. Signal Transduct Target Ther. 2022;7(1):305.
331. Fang Y, Li Z, Yang L, Li W, Wang Y, Kong Z, et al. Emerging roles of lactate in acute and chronic inflammation. Cell Commun Signal. 2024;22(1):276.
332. Caslin HL, Abebayehu D, Pinette JA, Ryan JJ. Lactate Is a Metabolic Mediator That Shapes Immune Cell Fate and Function. Front Physiol. 2021;12:688485.
333. Manosalva C, Quiroga J, Teuber S, Cárdenas S, Carretta MD, Morán G G, et al. D-Lactate Increases Cytokine Production in Bovine Fibroblast-Like Synoviocytes via MCT1 Uptake and the MAPK, PI3K/Akt, and NFκB Pathways. Animals (Basel). 2020;10(11):2105.
334. Ippolito L, Morandi A, Giannoni E, Chiarugi P. Lactate: A Metabolic Driver in the Tumour Landscape. Trends Biochem Sci. 2019;44(2):153-66.
335. Wang ZH, Peng WB, Zhang P, Yang XP, Zhou Q. Lactate in the tumour microenvironment: From immune modulation to therapy. EBioMedicine. 2021;73:103627.
336. Zhang L, Luo J, Wen H, Zhang T, Zuo X, Li X. MDM2 promotes rheumatoid arthritis via activation of MAPK and NF-κB. Int Immunopharmacol. 2016;30:69-73.
337. Rosser EC, Piper CJM, Matei DE, Blair PA, Rendeiro AF, Orford M, et al. Microbiota-Derived Metabolites Suppress Arthritis by Amplifying Aryl-Hydrocarbon Receptor Activation in Regulatory B Cells. Cell Metab. 2020;31(4):837-51.e10.
338. Yi O, Lin Y, Hu M, Hu S, Su Z, Liao J, et al. Lactate metabolism in rheumatoid arthritis: Pathogenic mechanisms and therapeutic intervention with natural compounds. Phytomedicine. 2022;100:154048.
339. Manosalva C, Quiroga J, Hidalgo AI, Alarcón P, Anseoleaga N, Hidalgo MA, et al. Role of Lactate in Inflammatory Processes: Friend or Foe. Frontiers in Immunology. 2022;12:808799.
340. Caslin HL, Abebayehu D, Abdul Qayum A, Haque TT, Taruselli MT, Paez PA, et al. Lactic Acid Inhibits Lipopolysaccharide-Induced Mast Cell Function by Limiting Glycolysis and ATP Availability. J Immunol. 2019;203(2):453-64.
341. Yang K, Xu J, Fan M, Tu F, Wang X, Ha T, et al. Lactate Suppresses Macrophage Pro-Inflammatory Response to LPS Stimulation by Inhibition of YAP and NF-κB Activation. Front Immunol. 2020;11:587913.

342. Hoque R, Farooq A, Ghani A, Gorelick F, Mehal WZ. Lactate reduces liver and pancreatic injury in Toll-like receptor- and inflammasome-mediated inflammation via GPR81-mediated suppression of innate immunity. Gastroenterology. 2014;146(7):1763-74.
343. Peter K, Rehli M, Singer K, Renner-Sattler K, Kreutz M. Lactic acid delays the inflammatory response of human monocytes. Biochem Biophys Res Commun. 2015;457(3):412-8.
344. Shime H, Yabu M, Akazawa T, Kodama K, Matsumoto M, Seya T, et al. Tumor-secreted lactic acid promotes IL-23/IL-17 proinflammatory pathway. J Immunol. 2008;180(11):7175-83.
345. Silva YP, Bernardi A, Frozza RL. The Role of Short-Chain Fatty Acids From Gut Microbiota in Gut-Brain Communication. Front Endocrinol (Lausanne). 2020;11:25.
346. Zhang Z, Zhang H, Chen T, Shi L, Wang D, Tang D. Regulatory role of short-chain fatty acids in inflammatory bowel disease. Cell Commun Signal. 2022;20(1):64.
347. Sam QH, Ling H, Yew WS, Tan Z, Ravikumar S, Chang MW, et al. The Divergent Immunomodulatory Effects of Short Chain Fatty Acids and Medium Chain Fatty Acids. Int J Mol Sci. 2021;22(12).
348. Feng Y, Wang Y, Wang P, Huang Y, Wang F. Short-Chain Fatty Acids Manifest Stimulative and Protective Effects on Intestinal Barrier Function Through the Inhibition of NLRP3 Inflammasome and Autophagy. Cell Physiol Biochem. 2018;49(1):190-205.
349. Hsieh CY, Osaka T, Moriyama E, Date Y, Kikuchi J, Tsuneda S. Strengthening of the intestinal epithelial tight junction by Bifidobacterium bifidum. Physiol Rep. 2015;3(3):e12327.
350. Didusch S, Madern M, Hartl M, Baccarini M. amica: an interactive and user-friendly web-platform for the analysis of proteomics data. BMC Genomics. 2022;23(1):817.
351. Rasheed ZBM, Lee YS, Kim SH, Rai RK, Ruano CSM, Anucha E, et al. Differential Response of Gestational Tissues to TLR3 Viral Priming Prior to Exposure to Bacterial TLR2 and TLR2/6 Agonists. Front Immunol. 2020;11:1899.
352. Camp JE, Nyamini SB, Scott FJ. Cyrene™ is a green alternative to DMSO as a solvent for antibacterial drug discovery against ESKAPE pathogens. RSC Med Chem. 2020;11(1):111-7.
353. Livak KJ, Schmittgen TD. Analysis of relative gene expression data using real-time quantitative PCR and the 2(-Delta Delta C(T)) Method. Methods. 2001;25(4):402-8.
354. Hidalgo IJ, Raub TJ, Borchardt RT. Characterization of the human colon carcinoma cell line (Caco-2) as a model system for intestinal epithelial permeability. Gastroenterology. 1989;96(3):736-49.
355. Srinivasan B, Kolli AR, Esch MB, Abaci HE, Shuler ML, Hickman JJ. TEER measurement techniques for in vitro barrier model systems. J Lab Autom. 2015;20(2):107-26.
356. MacIntyre DA, Chandiramani M, Lee YS, Kindinger L, Smith A, Angelopoulos N, et al. The vaginal microbiome during pregnancy and the postpartum period in a European population. Sci Rep. 2015;5:8988.
357. Kindinger L, MacIntyre D, Lee Y, Teoh TG, Bennett P. Understanding the interaction between the cervix and the vaginal microbiome underlying specific aetiologies of preterm birth. Bjog-an International Journal of Obstetrics and Gynaecology. 2016;123(13):E5-E6.
358. Pruski P, Lewis HV, Lee YS, Marchesi JR, Bennett PR, Takats Z, et al. Assessment of microbiota:host interactions at the vaginal mucosa interface. Methods. 2018;149:74-84.
359. Kessner D, Chambers M, Burke R, Agus D, Mallick P. ProteoWizard: open source software for rapid proteomics tools development. Bioinformatics. 2008;24(21):2534-6.

360. Bayar E, MacIntyre DA, Sykes L, Mountain K, Parks TP, Lee PP, et al. Safety, tolerability, and acceptability of Lactobacillus crispatus CTV-05 (LACTIN-V) in pregnant women at high-risk of preterm birth. Benef Microbes. 2023;14(1):45-56.
361. Ludwig C, Gillet L, Rosenberger G, Amon S, Collins BC, Aebersold R. Data-independent acquisition-based SWATH-MS for quantitative proteomics: a tutorial. Mol Syst Biol. 2018;14(8):e8126.
362. Thomas PD, Ebert D, Muruganujan A, Mushayahama T, Albou LP, Mi H. PANTHER: Making genome-scale phylogenetics accessible to all. Protein Sci. 2022;31(1):8-22.
363. Griss J, Viteri G, Sidiropoulos K, Nguyen V, Fabregat A, Hermjakob H. ReactomeGSA - Efficient Multi-Omics Comparative Pathway Analysis. Mol Cell Proteomics. 2020;19(12):2115-25.
364. Jassal B, Matthews L, Viteri G, Gong C, Lorente P, Fabregat A, et al. The reactome pathway knowledgebase. Nucleic Acids Res. 2020;48(D1):D498-D503.
365. Milacic M, Beavers D, Conley P, Gong C, Gillespie M, Griss J, et al. The Reactome Pathway Knowledgebase 2024. Nucleic Acids Res. 2023;52((D1)):D672-D8.
366. Szklarczyk D, Kirsch R, Koutrouli M, Nastou K, Mehryary F, Hachilif R, et al. The STRING database in 2023: protein-protein association networks and functional enrichment analyses for any sequenced genome of interest. Nucleic Acids Res. 2023;51(D1):D638-D46.
367. Team RC. R: A Language and Environment for Statistical Computing.: R Foundation for Statistical Computing; 2018 [Available from: https://www.R-project.org/.
368. R K. Pheatmap: pretty heatmaps: R package version 1.0.12.; 2022 [Available from: https://cran.r-project.org/web/packages/pheatmap/index.html.
369. Amabebe E, Anumba DOC. Mechanistic Insights into Immune Suppression and Evasion in Bacterial Vaginosis. Curr Microbiol. 2022;79(3):84.
370. Anton L, Ferguson B, Friedman ES, Gerson KD, Brown AG, Elovitz MA. Gardnerella vaginalis alters cervicovaginal epithelial cell function through microbe-specific immune responses. Microbiome. 2022;10(1):119.
371. Anton L, Sierra LJ, DeVine A, Barila G, Heiser L, Brown AG, et al. Common Cervicovaginal Microbial Supernatants Alter Cervical Epithelial Function: Mechanisms by Which. Front Microbiol. 2018;9:2181.
372. Mares D, Simoes JA, Novak RM, Spear GT. TLR2-mediated cell stimulation in bacterial vaginosis. J Reprod Immunol. 2008;77(1):91-9.
373. Rahman MM, McFadden G. Modulation of NF-κB signalling by microbial pathogens. Nat Rev Microbiol. 2011;9(4):291-306.
374. Fichorova R, Yamamoto H, Delaney M, Onderdonk A, Doncel G. Novel Vaginal Microflora Colonization Model Providing New Insight into Microbicide Mechanism of Action. Mbio. 2011;2(6):e00168-11.
375. Aroutcheva A, Gariti D, Simon M, Shott S, Faro J, Simoes JA, et al. Defense factors of vaginal lactobacilli. Am J Obstet Gynecol. 2001;185(2):375-9.
376. Feng T, Liu Y. Microorganisms in the reproductive system and probiotic's regulatory effects on reproductive health. Comput Struct Biotechnol J. 2022;20:1541-53.
377. Nardini P, Ñahui Palomino RA, Parolin C, Laghi L, Foschi C, Cevenini R, et al. Lactobacillus crispatus inhibits the infectivity of Chlamydia trachomatis elementary bodies, in vitro study. Sci Rep. 2016;6:29024.
378. Gupta SC, Singh R, Pochampally R, Watabe K, Mo YY. Acidosis promotes invasiveness of breast cancer cells through ROS-AKT-NF-κB pathway. Oncotarget. 2014;5(23):12070-82.

379. Peppicelli S, Bianchini F, Contena C, Tombaccini D, Calorini L. Acidic pH via NF-κB favours VEGF-C expression in human melanoma cells. Clin Exp Metastasis. 2013;30(8):957-67.
380. Chen B, Liu J, Ho TT, Ding X, Mo YY. ERK-mediated NF-κB activation through ASIC1 in response to acidosis. Oncogenesis. 2016;5(12):e279.
381. Lester SN, Li K. Toll-like receptors in antiviral innate immunity. J Mol Biol. 2014;426(6):1246-64.
382. Sartorius R, Trovato M, Manco R, D'Apice L, De Berardinis P. Exploiting viral sensing mediated by Toll-like receptors to design innovative vaccines. NPJ Vaccines. 2021;6(1):127.
383. Delgado-Diaz DJ, Jesaveluk B, Hayward JA, Tyssen D, Alisoltani A, Potgieter M, et al. Lactic acid from vaginal microbiota enhances cervicovaginal epithelial barrier integrity by promoting tight junction protein expression. Microbiome. 2022;10(1):141.
384. Lim R, Lappas M. Differential expression of AP-1 proteins in human myometrium after spontaneous term labour onset. Eur J Obstet Gynecol Reprod Biol. 2014;177:100-5.
385. Florova V, Romero R, Tarca AL, Galaz J, Motomura K, Ahmad MM, et al. Vaginal host immune-microbiome interactions in a cohort of primarily African-American women who ultimately underwent spontaneous preterm birth or delivered at term. Cytokine. 2021;137:155316.
386. Novak J, Ferreira CST, Golim MA, Silva MG, Marconi C. Covariates of vaginal microbiota and pro-inflammatory cytokine levels in women of reproductive age. Benef Microbes. 2023;14(2):131-42.
387. Bellocq A, Suberville S, Philippe C, Bertrand F, Perez J, Fouqueray B, et al. Low environmental pH is responsible for the induction of nitric-oxide synthase in macrophages. Evidence for involvement of nuclear factor-kappaB activation. J Biol Chem. 1998;273(9):5086-92.
388. Gerry AB, Leake DS. Effect of low extracellular pH on NF-κB activation in macrophages. Atherosclerosis. 2014;233(2):537-44.
389. Krebs FC, Miller SR, Catalone BJ, Fichorova R, Anderson D, Malamud D, et al. Comparative in vitro sensitivities of human immune cell lines, vaginal and cervical epithelial cell lines, and primary cells to candidate microbicides nonoxynol 9, C31G, and sodium dodecyl sulfate. Antimicrob Agents Chemother. 2002;46(7):2292-8.
390. Collins TS, Lee LF, Ting JP. Paclitaxel up-regulates interleukin-8 synthesis in human lung carcinoma through an NF-kappaB- and AP-1-dependent mechanism. Cancer Immunol Immunother. 2000;49(2):78-84.
391. Devary Y, Rosette C, DiDonato JA, Karin M. NF-kappa B activation by ultraviolet light not dependent on a nuclear signal. Science. 1993;261(5127):1442-5.
392. Yasumoto K, Okamoto S, Mukaida N, Murakami S, Mai M, Matsushima K. Tumor necrosis factor alpha and interferon gamma synergistically induce interleukin 8 production in a human gastric cancer cell line through acting concurrently on AP-1 and NF-kB-like binding sites of the interleukin 8 gene. J Biol Chem. 1992;267(31):22506-11.
393. Fujioka S, Niu J, Schmidt C, Sclabas GM, Peng B, Uwagawa T, et al. NF-kappaB and AP-1 connection: mechanism of NF-kappaB-dependent regulation of AP-1 activity. Mol Cell Biol. 2004;24(17):7806-19.
394. Roselletti E, Sabbatini S, Perito S, Mencacci A, Vecchiarelli A, Monari C. Apoptosis of vaginal epithelial cells in clinical samples from women with diagnosed bacterial vaginosis. Sci Rep. 2020;10(1):1978.

395. Mokoena MP. Lactic Acid Bacteria and Their Bacteriocins: Classification, Biosynthesis and Applications against Uropathogens: A Mini-Review. Molecules. 2017;22(8):1255.
396. Zheng J, Wittouck S, Salvetti E, Franz CMAP, Harris HMB, Mattarelli P, et al. A taxonomic note on the genus Lactobacillus: Description of 23 novel genera, emended description of the genus Lactobacillus Beijerinck 1901, and union of Lactobacillaceae and Leuconostocaceae. Int J Syst Evol Microbiol. 2020;70(4):2782-858.
397. George SD, Van Gerwen OT, Dong C, Sousa LGV, Cerca N, Elnaggar JH, et al. The Role of Prevotella Species in Female Genital Tract Infections. Pathogens. 2024;13(5):364.
398. Abou Chacra L, Fenollar F, Diop K. Bacterial Vaginosis: What Do We Currently Know? Front Cell Infect Microbiol. 2021;11:672429.
399. Zhou R, Lu J, Wang J, Xiao B. Vaginal Lactobacillus iners abundance is associated with outcome in antibiotic treatment of bacterial vaginosis and capable of inhibiting Gardnerella. Front Cell Infect Microbiol. 2022;12:1033431.
400. Karin M. How NF-kappaB is activated: the role of the IkappaB kinase (IKK) complex. Oncogene. 1999;18(49):6867-74.
401. Zhang Q, Lenardo MJ, Baltimore D. 30 Years of NF-κB: A Blossoming of Relevance to Human Pathobiology. Cell. 2017;168(1-2):37-57.
402. Dong C, Davis RJ, Flavell RA. MAP kinases in the immune response. Annu Rev Immunol. 2002;20:55-72.
403. Liu Y, Shepherd EG, Nelin LD. MAPK phosphatases--regulating the immune response. Nat Rev Immunol. 2007;7(3):202-12.
404. Lavoie H, Gagnon J, Therrien M. ERK signalling: a master regulator of cell behaviour, life and fate. Nat Rev Mol Cell Biol. 2020;21(10):607-32.
405. Pearson G, Robinson F, Beers Gibson T, Xu BE, Karandikar M, Berman K, et al. Mitogen-activated protein (MAP) kinase pathways: regulation and physiological functions. Endocr Rev. 2001;22(2):153-83.
406. Arthur JS, Ley SC. Mitogen-activated protein kinases in innate immunity. Nat Rev Immunol. 2013;13(9):679-92.
407. Kolch W. Coordinating ERK/MAPK signalling through scaffolds and inhibitors. Nat Rev Mol Cell Biol. 2005;6(11):827-37.
408. Dhanasekaran DN, Kashef K, Lee CM, Xu H, Reddy EP. Scaffold proteins of MAP-kinase modules. Oncogene. 2007;26(22):3185-202.
409. Owens DM, Keyse SM. Differential regulation of MAP kinase signalling by dual-specificity protein phosphatases. Oncogene. 2007;26(22):3203-13.
410. Raman M, Chen W, Cobb MH. Differential regulation and properties of MAPKs. Oncogene. 2007;26(22):3100-12.
411. Zhang Y, Dong C. Regulatory mechanisms of mitogen-activated kinase signaling. Cell Mol Life Sci. 2007;64(21):2771-89.
412. Knight T, Irving JA. Ras/Raf/MEK/ERK Pathway Activation in Childhood Acute Lymphoblastic Leukemia and Its Therapeutic Targeting. Front Oncol. 2014;4:160.
413. Shaul YD, Seger R. The MEK/ERK cascade: from signaling specificity to diverse functions. Biochim Biophys Acta. 2007;1773(8):1213-26.
414. Chambard JC, Lefloch R, Pouysségur J, Lenormand P. ERK implication in cell cycle regulation. Biochim Biophys Acta. 2007;1773(8):1299-310.
415. Kolch W. Meaningful relationships: the regulation of the Ras/Raf/MEK/ERK pathway by protein interactions. Biochem J. 2000;351 Pt 2(Pt 2):289-305.

416. Johnson GL, Lapadat R. Mitogen-activated protein kinase pathways mediated by ERK, JNK, and p38 protein kinases. Science. 2002;298(5600):1911-2.
417. Yang Y, Kim SC, Yu T, Yi YS, Rhee MH, Sung GH, et al. Functional roles of p38 mitogen-activated protein kinase in macrophage-mediated inflammatory responses. Mediators Inflamm. 2014;2014:352371.
418. Cuadrado A, Nebreda AR. Mechanisms and functions of p38 MAPK signalling. Biochem J. 2010;429(3):403-17.
419. Lin A. Activation of the JNK signaling pathway: breaking the brake on apoptosis. Bioessays. 2003;25(1):17-24.
420. Liu J, Lin A. Role of JNK activation in apoptosis: a double-edged sword. Cell Res. 2005;15(1):36-42.
421. Bogoyevitch MA, Kobe B. Uses for JNK: the many and varied substrates of the c-Jun N-terminal kinases. Microbiol Mol Biol Rev. 2006;70(4):1061-95.
422. Goldenberg RL, Hauth JC, Andrews WW. Intrauterine infection and preterm delivery. N Engl J Med. 2000;342(20):1500-7.
423. Sommers CD, Thompson JM, Guzova JA, Bonar SL, Rader RK, Mathialagan S, et al. Novel tight-binding inhibitory factor-kappaB kinase (IKK-2) inhibitors demonstrate target-specific anti-inflammatory activities in cellular assays and following oral and local delivery in an in vivo model of airway inflammation. J Pharmacol Exp Ther. 2009;330(2):377-88.
424. Li H, Han W, Polosukhin V, Yull FE, Segal BH, Xie CM, et al. NF-κB inhibition after cecal ligation and puncture reduces sepsis-associated lung injury without altering bacterial host defense. Mediators Inflamm. 2013;2013:503213.
425. Contreras-Nuñez E, Blancas-Flores G, Cruz M, Almanza-Perez JC, Gomez-Zamudio JH, Ventura-Gallegosc JL, et al. Participation of the IKK-α/β complex in the inhibition of the TNF-α/NF-κB pathway by glycine: Possible involvement of a membrane receptor specific to adipocytes. Biomed Pharmacother. 2018;102:120-31.
426. Duan H, Wang L, Huangfu M, Li H. The impact of microbiota-derived short-chain fatty acids on macrophage activities in disease: Mechanisms and therapeutic potentials. Biomed Pharmacother. 2023;165:115276.
427. Barbie DA, Tamayo P, Boehm JS, Kim SY, Moody SE, Dunn IF, et al. Systematic RNA interference reveals that oncogenic KRAS-driven cancers require TBK1. Nature. 2009;462(7269):108-12.
428. Zhao T, Yang L, Sun Q, Arguello M, Ballard DW, Hiscott J, et al. The NEMO adaptor bridges the nuclear factor-kappaB and interferon regulatory factor signaling pathways. Nat Immunol. 2007;8(6):592-600.
429. Shin CH, Choi DS. Essential Roles for the Non-Canonical IκB Kinases in Linking Inflammation to Cancer, Obesity, and Diabetes. Cells. 2019;8(2).
430. Wietek C, Cleaver CS, Ludbrook V, Wilde J, White J, Bell DJ, et al. IkappaB kinase epsilon interacts with p52 and promotes transactivation via p65. J Biol Chem. 2006;281(46):34973-81.
431. Clément JF, Bibeau-Poirier A, Gravel SP, Grandvaux N, Bonneil E, Thibault P, et al. Phosphorylation of IRF-3 on Ser 339 generates a hyperactive form of IRF-3 through regulation of dimerization and CBP association. J Virol. 2008;82(8):3984-96.
432. Clément JF, Meloche S, Servant MJ. The IKK-related kinases: from innate immunity to oncogenesis. Cell Res. 2008;18(9):889-99.

433. Panne D, McWhirter SM, Maniatis T, Harrison SC. Interferon regulatory factor 3 is regulated by a dual phosphorylation-dependent switch. J Biol Chem. 2007;282(31):22816-22.
434. Zhao P, Wong KI, Sun X, Reilly SM, Uhm M, Liao Z, et al. TBK1 at the Crossroads of Inflammation and Energy Homeostasis in Adipose Tissue. Cell. 2018;172(4):731-43.e12.
435. Bodur C, Kazyken D, Huang K, Ekim Ustunel B, Siroky KA, Tooley AS, et al. The IKK-related kinase TBK1 activates mTORC1 directly in response to growth factors and innate immune agonists. EMBO J. 2018;37(1):19-38.
436. Pirianov G, MacIntyre DA, Lee Y, Waddington SN, Terzidou V, Mehmet H, et al. Specific inhibition of c-Jun N-terminal kinase delays preterm labour and reduces mortality. Reproduction. 2015;150(4):269-77.
437. Petrova MI, van den Broek M, Balzarini J, Vanderleyden J, Lebeer S. Vaginal microbiota and its role in HIV transmission and infection. FEMS Microbiol Rev. 2013;37(5):762-92.
438. Witkin SS, Linhares IM. Why do lactobacilli dominate the human vaginal microbiota? BJOG. 2017;124(4):606-11.
439. Tyssen D, Hearps AC, Guntur K, Masson L, Cook S, Moulton SE, et al. The Impact of Over-The-Counter Lactic Acid Containing Vaginal Gels on the Integrity and Inflammatory State of the Vaginal Epithelium. Front Reprod Health. 2022;4:915948.
440. Forney LJ, Foster JA, Ledger W. The vaginal flora of healthy women is not always dominated by Lactobacillus species. J Infect Dis. 2006;194(10):1468-9; author reply 9-70.
441. Krog MC, Hugerth LW, Fransson E, Bashir Z, Nyboe Andersen A, Edfeldt G, et al. The healthy female microbiome across body sites: effect of hormonal contraceptives and the menstrual cycle. Hum Reprod. 2022;37(7):1525-43.
442. Auriemma RS, Scairati R, Del Vecchio G, Liccardi A, Verde N, Pirchio R, et al. The Vaginal Microbiome: A Long Urogenital Colonization Throughout Woman Life. Front Cell Infect Microbiol. 2021;11:686167.
443. Brusselaers N, Shrestha S, van de Wijgert J, Verstraelen H. Vaginal dysbiosis and the risk of human papillomavirus and cervical cancer: systematic review and meta-analysis. Am J Obstet Gynecol. 2019;221(1):9-18.e8.
444. Norenhag J, Du J, Olovsson M, Verstraelen H, Engstrand L, Brusselaers N. The vaginal microbiota, human papillomavirus and cervical dysplasia: a systematic review and network meta-analysis. BJOG. 2020;127(2):171-80.
445. Blair L, Pattison MJ, Chakravarty P, Papoutsopoulou S, Bakiri L, Wagner EF, et al. TPL-2 Inhibits IFN-β Expression via an ERK1/2-TCF-FOS Axis in TLR4-Stimulated Macrophages. J Immunol. 2022;208(4):941-54.
446. Vuong B, Hogan-Cann AD, Alano CC, Stevenson M, Chan WY, Anderson CM, et al. NF-κB transcriptional activation by TNFα requires phospholipase C, extracellular signal-regulated kinase 2 and poly(ADP-ribose) polymerase-1. J Neuroinflammation. 2015;12:229.
447. Li G, Wang HQ, Wang LH, Chen RP, Liu JP. Distinct pathways of ERK1/2 activation by hydroxy-carboxylic acid receptor-1. PLoS One. 2014;9(3):e93041.
448. Wagner W, Ciszewski WM, Kania KD. L- and D-lactate enhance DNA repair and modulate the resistance of cervical carcinoma cells to anticancer drugs via histone deacetylase inhibition and hydroxycarboxylic acid receptor 1 activation. Cell Commun Signal. 2015;13:36.
449. Maeng YS, Min JK, Kim JH, Yamagishi A, Mochizuki N, Kwon JY, et al. ERK is an anti-inflammatory signal that suppresses expression of NF-kappaB-dependent inflammatory genes by inhibiting IKK activity in endothelial cells. Cell Signal. 2006;18(7):994-1005.

450. Ogata T, Naito D, Nakanishi N, Hayashi YK, Taniguchi T, Miyagawa K, et al. MURC/Cavin-4 facilitates recruitment of ERK to caveolae and concentric cardiac hypertrophy induced by α1-adrenergic receptors. Proc Natl Acad Sci U S A. 2014;111(10):3811-6.
451. Vomastek T, Schaeffer HJ, Tarcsafalvi A, Smolkin ME, Bissonette EA, Weber MJ. Modular construction of a signaling scaffold: MORG1 interacts with components of the ERK cascade and links ERK signaling to specific agonists. Proc Natl Acad Sci U S A. 2004;101(18):6981-6.
452. Roy M, Li Z, Sacks DB. IQGAP1 is a scaffold for mitogen-activated protein kinase signaling. Mol Cell Biol. 2005;25(18):7940-52.
453. Lavoie H, Therrien M. Regulation of RAF protein kinases in ERK signalling. Nat Rev Mol Cell Biol. 2015;16(5):281-98.
454. Samson SC, Khan AM, Mendoza MC. ERK signaling for cell migration and invasion. Front Mol Biosci. 2022;9:998475.
455. Ryan DG, Peace CG, Hooftman A. Basic Mechanisms of Immunometabolites in Shaping the Immune Response. J Innate Immun. 2023;15(1):925-43.
456. Richardson ET, Shukla S, Nagy N, Boom WH, Beck RC, Zhou L, et al. ERK Signaling Is Essential for Macrophage Development. PLoS One. 2015;10(10):e0140064.
457. Kim B, Breton S. The MAPK/ERK-Signaling Pathway Regulates the Expression and Distribution of Tight Junction Proteins in the Mouse Proximal Epididymis. Biol Reprod. 2016;94(1):22.
458. Samak G, Aggarwal S, Rao RK. ERK is involved in EGF-mediated protection of tight junctions, but not adherens junctions, in acetaldehyde-treated Caco-2 cell monolayers. Am J Physiol Gastrointest Liver Physiol. 2011;301(1):G50-9.
459. Sekar A, Ho B. Role of ERK activation in H. pylori-induced disruption of cell-cell tight junctions. 2020.
460. Chongchong Feng and Chengxun Jin and Kexin Liu and Zecheng Y. Microbiota-derived short chain fatty acids: Their role and mechanisms in viral infections. Biomedicine & Pharmacotherapy. 2023;160:114414.
461. Wirusanti NI, Baldridge MT, Harris VC. Microbiota regulation of viral infections through interferon signaling. Trends Microbiol. 2022;30(8):778-92.
462. Kim CH. Control of lymphocyte functions by gut microbiota-derived short-chain fatty acids. Cell Mol Immunol. 2021;18(5):1161-71.
463. Segain JP, Raingeard de la Blétière D, Bourreille A, Leray V, Gervois N, Rosales C, et al. Butyrate inhibits inflammatory responses through NFkappaB inhibition: implications for Crohn's disease. Gut. 2000;47(3):397-403.
464. Lührs H, Gerke T, Müller JG, Melcher R, Schauber J, Boxberge F, et al. Butyrate inhibits NF-kappaB activation in lamina propria macrophages of patients with ulcerative colitis. Scand J Gastroenterol. 2002;37(4):458-66.
465. Mirmonsef P, Zariffard MR, Gilbert D, Makinde H, Landay AL, Spear GT. Short-chain fatty acids induce pro-inflammatory cytokine production alone and in combination with toll-like receptor ligands. Am J Reprod Immunol. 2012;67(5):391-400.
466. Huggins GR, Preti G. Volatile constituents of human vaginal secretions. Am J Obstet Gynecol. 1976;126(1):129-36.
467. Spiegel CA, Amsel R, Eschenbach D, Schoenknecht F, Holmes KK. Anaerobic bacteria in nonspecific vaginitis. N Engl J Med. 1980;303(11):601-7.

468. Piot P, Van Dyck E, Godts P, Vanderheyden J. The vaginal microbial flora in non-specific vaginitis. Eur J Clin Microbiol. 1982;1(5):301-6.
469. Ison CA, Easmon CS, Dawson SG, Southerton G, Harris JW. Non-volatile fatty acids in the diagnosis of non-specific vaginitis. J Clin Pathol. 1983;36(12):1367-70.
470. Krohn MA, Hillier SL, Eschenbach DA. Comparison of methods for diagnosing bacterial vaginosis among pregnant women. J Clin Microbiol. 1989;27(6):1266-71.
471. Stanek R, Gain RE, Glover DD, Larsen B. High performance ion exclusion chromatographic characterization of the vaginal organic acids in women with bacterial vaginosis. Biomed Chromatogr. 1992;6(5):231-5.
472. Nazli A, Chan O, Dobson-Belaire WN, Ouellet M, Tremblay MJ, Gray-Owen SD, et al. Exposure to HIV-1 directly impairs mucosal epithelial barrier integrity allowing microbial translocation. PLoS Pathog. 2010;6(4):e1000852.
473. Ansari A, Lee H, You YA, Jung Y, Park S, Kim SM, et al. Identification of Potential Biomarkers in the Cervicovaginal Fluid by Metabolic Profiling for Preterm Birth. Metabolites. 2020;10(9):349.
474. Bai G, Gajer P, Nandy M, Ma B, Yang H, Sakamoto J, et al. Comparison of storage conditions for human vaginal microbiome studies. PLoS One. 2012;7(5):e36934.
475. Harber KJ, de Goede KE, Verberk SGS, Meinster E, de Vries HE, van Weeghel M, et al. Succinate Is an Inflammation-Induced Immunoregulatory Metabolite in Macrophages. Metabolites. 2020;10(9):1-14.
476. Peruzzotti-Jametti L, Bernstock JD, Vicario N, Costa ASH, Kwok CK, Leonardi T, et al. Macrophage-Derived Extracellular Succinate Licenses Neural Stem Cells to Suppress Chronic Neuroinflammation. Cell Stem Cell. 2018;22(3):355-68.e13.
477. Keiran N, Ceperuelo-Mallafré V, Calvo E, Hernández-Alvarez MI, Ejarque M, Núñez-Roa C, et al. SUCNR1 controls an anti-inflammatory program in macrophages to regulate the metabolic response to obesity. Nat Immunol. 2019;20(5):581-92.
478. Murphy MP, O'Neill LAJ. Krebs Cycle Reimagined: The Emerging Roles of Succinate and Itaconate as Signal Transducers. Cell. 2018;174(4):780-4.
479. Marsal-Beltran A, Rodríguez-Castellano A, Astiarraga B, Calvo E, Rada P, Madeira A, et al. Protective effects of the succinate/SUCNR1 axis on damaged hepatocytes in NAFLD. Metabolism. 2023;145:155630.
480. Mills E, O'Neill LA. Succinate: a metabolic signal in inflammation. Trends Cell Biol. 2014;24(5):313-20.
481. Wu JY, Huang TW, Hsieh YT, Wang YF, Yen CC, Lee GL, et al. Cancer-Derived Succinate Promotes Macrophage Polarization and Cancer Metastasis via Succinate Receptor. Mol Cell. 2020;77(2):213-27.e5.
482. Trauelsen M, Hiron TK, Lin D, Petersen JE, Breton B, Husted AS, et al. Extracellular succinate hyperpolarizes M2 macrophages through SUCNR1/GPR91-mediated Gq signaling. Cell Rep. 2021;35(11):109246.
483. Fremder M, Kim SW, Khamaysi A, Shimshilashvili L, Eini-Rider H, Park IS, et al. A transepithelial pathway delivers succinate to macrophages, thus perpetuating their pro-inflammatory metabolic state. Cell Rep. 2021;36(6):109521.
484. Hyman RW, Fukushima M, Jiang H, Fung E, Rand L, Johnson B, et al. Diversity of the vaginal microbiome correlates with preterm birth. Reprod Sci. 2014;21(1):32-40.
485. Stout MJ, Zhou Y, Wylie KM, Tarr PI, Macones GA, Tuuli MG. Early pregnancy vaginal microbiome trends and preterm birth. Am J Obstet Gynecol. 2017;217(3):356.e1-.e18.

486. Uhlén M, Fagerberg L, Hallström BM, Lindskog C, Oksvold P, Mardinoglu A, et al. Proteomics. Tissue-based map of the human proteome. Science. 2015;347(6220):1260419.
487. Rubic T, Lametschwandtner G, Jost S, Hinteregger S, Kund J, Carballido-Perrig N, et al. Triggering the succinate receptor GPR91 on dendritic cells enhances immunity. Nat Immunol. 2008;9(11):1261-9.
488. He W, Miao FJ, Lin DC, Schwandner RT, Wang Z, Gao J, et al. Citric acid cycle intermediates as ligands for orphan G-protein-coupled receptors. Nature. 2004;429(6988):188-93.
489. Aguiar CJ, Rocha-Franco JA, Sousa PA, Santos AK, Ladeira M, Rocha-Resende C, et al. Succinate causes pathological cardiomyocyte hypertrophy through GPR91 activation. Cell Commun Signal. 2014;12:78.
490. Hu J, Li T, Du S, Chen Y, Wang S, Xiong F, et al. The MAPK signaling pathway mediates the GPR91-dependent release of VEGF from RGC-5 cells. Int J Mol Med. 2015;36(1):130-8.
491. Tannahill GM, Curtis AM, Adamik J, Palsson-McDermott EM, McGettrick AF, Goel G, et al. Succinate is an inflammatory signal that induces IL-1β through HIF-1α. Nature. 2013;496(7444):238-42.
492. Sturm AW. Chemotaxis inhibition by Gardnerella vaginalis and succinate producing vaginal anaerobes: composition of vaginal discharge associated with G vaginalis. Genitourin Med. 1989;65(2):109-12.
493. Wang JQ, Mao L. The ERK Pathway: Molecular Mechanisms and Treatment of Depression. Mol Neurobiol. 2019;56(9):6197-205.
494. Morrill S, Gilbert NM, Lewis AL. as a Cause of Bacterial Vaginosis: Appraisal of the Evidence From. Front Cell Infect Microbiol. 2020;10:168.
495. Amsel R, Totten PA, Spiegel CA, Chen KC, Eschenbach D, Holmes KK. Nonspecific vaginitis. Diagnostic criteria and microbial and epidemiologic associations. Am J Med. 1983;74(1):14-22.
496. Burkett JB, Doran AC, Gannon M. Harnessing prostaglandin E. Trends Immunol. 2023;44(3):162-71.
497. Awasthi D, Nagarkoti S, Sadaf S, Chandra T, Kumar S, Dikshit M. Glycolysis dependent lactate formation in neutrophils: A metabolic link between NOX-dependent and independent NETosis. Biochim Biophys Acta Mol Basis Dis. 2019;1865(12):165542.
498. Kellum JA, Song M, Li J. Lactic and hydrochloric acids induce different patterns of inflammatory response in LPS-stimulated RAW 264.7 cells. Am J Physiol Regul Integr Comp Physiol. 2004;286(4):R686-92.
499. Végran F, Boidot R, Michiels C, Sonveaux P, Feron O. Lactate influx through the endothelial cell monocarboxylate transporter MCT1 supports an NF-κB/IL-8 pathway that drives tumor angiogenesis. Cancer Res. 2011;71(7):2550-60.
500. Haas R, Smith J, Rocher-Ros V, Nadkarni S, Montero-Melendez T, D'Acquisto F, et al. Lactate Regulates Metabolic and Pro-inflammatory Circuits in Control of T Cell Migration and Effector Functions. PLoS Biol. 2015;13(7):e1002202.
501. Zou Y, Zeng S, Huang M, Qiu Q, Xiao Y, Shi M, et al. Inhibition of 6-phosphofructo-2-kinase suppresses fibroblast-like synoviocytes-mediated synovial inflammation and joint destruction in rheumatoid arthritis. Br J Pharmacol. 2017;174(9):893-908.
502. Srinivas SR, Gopal E, Zhuang L, Itagaki S, Martin PM, Fei YJ, et al. Cloning and functional identification of slc5a12 as a sodium-coupled low-affinity transporter for monocarboxylates (SMCT2). Biochem J. 2005;392(Pt 3):655-64.

503. Halestrap AP, Wilson MC. The monocarboxylate transporter family--role and regulation. IUBMB Life. 2012;64(2):109-19.
504. Wang T, Li Z, Cvijic M. Measurement of cAMP for Gαs- and Gαi Protein-Coupled Receptors (GPCRs). https://www.ncbi.nlm.nih.gov/books/NBK464633/2017.
505. Kurose H, Katada T, Amano T, Ui M. Specific uncoupling by islet-activating protein, pertussis toxin, of negative signal transduction via alpha-adrenergic, cholinergic, and opiate receptors in neuroblastoma x glioma hybrid cells. J Biol Chem. 1983;258(8):4870-5.
506. Katada T, Tamura M, Ui M. The A protomer of islet-activating protein, pertussis toxin, as an active peptide catalyzing ADP-ribosylation of a membrane protein. Arch Biochem Biophys. 1983;224(1):290-8.
507. Goldsmith ZG, Dhanasekaran DN. G protein regulation of MAPK networks. Oncogene. 2007;26(22):3122-42.
508. Tavares LP, Negreiros-Lima GL, Lima KM, E Silva PMR, Pinho V, Teixeira MM, et al. Blame the signaling: Role of cAMP for the resolution of inflammation. Pharmacol Res. 2020;159:105030.
509. Ahmed K, Tunaru S, Offermanns S. GPR109A, GPR109B and GPR81, a family of hydroxy-carboxylic acid receptors. Trends Pharmacol Sci. 2009;30(11):557-62.
510. Kuchiiwa T, Nio-Kobayashi J, Takahashi-Iwanaga H, Yajima T, Iwanaga T. Cellular expression of monocarboxylate transporters in the female reproductive organ of mice: implications for the genital lactate shuttle. Histochem Cell Biol. 2011;135(4):351-60.
511. Kashket ER. Bioenergetics of lactic acid bacteria: cytoplasmic pH and osmotolerance. FEMS Microbiology Letters. 1987;46:233-44.
512. O'Hanlon DE, Come RA, Moench TR. Vaginal pH measured in vivo: lactobacilli determine pH and lactic acid concentration. BMC Microbiol. 2019;19(1):13.
513. Felmlee MA, Jones RS, Rodriguez-Cruz V, Follman KE, Morris ME. Monocarboxylate Transporters (SLC16): Function, Regulation, and Role in Health and Disease. Pharmacol Rev. 2020;72(2):466-85.
514. Martin PM, Dun Y, Mysona B, Ananth S, Roon P, Smith SB, et al. Expression of the sodium-coupled monocarboxylate transporters SMCT1 (SLC5A8) and SMCT2 (SLC5A12) in retina. Invest Ophthalmol Vis Sci. 2007;48(7):3356-63.
515. Ahmed K, Tunaru S, Langhans CD, Hanson J, Michalski CW, Kölker S, et al. Deorphanization of GPR109B as a receptor for the beta-oxidation intermediate 3-OH-octanoic acid and its role in the regulation of lipolysis. J Biol Chem. 2009;284(33):21928-33.
516. Zhang D, Jian YP, Zhang YN, Li Y, Gu LT, Sun HH, et al. Short-chain fatty acids in diseases. Cell Commun Signal. 2023;21(1):212.
517. Li X, Xie L, Qu X, Zhao B, Fu W, Wu B, et al. GPR91, a critical signaling mechanism in modulating pathophysiologic processes in chronic illnesses. FASEB J. 2020;34(10):13091-105.
518. Gilissen J, Jouret F, Pirotte B, Hanson J. Insight into SUCNR1 (GPR91) structure and function. Pharmacol Ther. 2016;159:56-65.
519. Eishingdrelo H, Kongsamut S. Minireview: Targeting GPCR Activated ERK Pathways for Drug Discovery. Curr Chem Genom Transl Med. 2013;7:9-15.
520. Jin L, Guo Y, Chen J, Wen Z, Jiang Y, Qian J. Lactate receptor HCAR1 regulates cell growth, metastasis and maintenance of cancer-specific energy metabolism in breast cancer cells. Mol Med Rep. 2022;26(2):268.

521. Kamthong PJ, Wu M. Inhibitor of nuclear factor-kappaB induction by cAMP antagonizes interleukin-1-induced human macrophage-colony-stimulating-factor expression. Biochem J. 2001;356(Pt 2):525-30.
522. Neumann M, Grieshammer T, Chuvpilo S, Kneitz B, Lohoff M, Schimpl A, et al. RelA/p65 is a molecular target for the immunosuppressive action of protein kinase A. EMBO J. 1995;14(9):1991-2004.
523. Sousa LP, Carmo AF, Rezende BM, Lopes F, Silva DM, Alessandri AL, et al. Cyclic AMP enhances resolution of allergic pleurisy by promoting inflammatory cell apoptosis via inhibition of PI3K/Akt and NF-kappaB. Biochem Pharmacol. 2009;78(4):396-405.
524. Hollomon JM, Grahl N, Willger SD, Koeppen K, Hogan DA. Global Role of Cyclic AMP Signaling in pH-Dependent Responses in Candida albicans. mSphere. 2016;1(6):e00283-16.
525. Wang Y, Yin, J., Weng, W., Liu, Z., & Huang, J. Kinetic study of the degradation of forskolin in aqueous systems by stability-indicating HPLC method and identification of its degradation products. Journal of Liquid Chromatography & Related Technologies. 2016;39(1):44-9.
526. Mangmool S, Kurose H. G(i/o) protein-dependent and -independent actions of Pertussis Toxin (PTX). Toxins (Basel). 2011;3(7):884-99.
527. Fields TA, Casey PJ. Signalling functions and biochemical properties of pertussis toxin-resistant G-proteins. Biochem J. 1997;321 (Pt 3)(Pt 3):561-71.
528. Xu Y, Barbieri JT. Pertussis toxin-mediated ADP-ribosylation of target proteins in Chinese hamster ovary cells involves a vesicle trafficking mechanism. Infect Immun. 1995;63(3):825-32.
529. Xu Y, Barbieri JT. Pertussis toxin-catalyzed ADP-ribosylation of Gi-2 and Gi-3 in CHO cells is modulated by inhibitors of intracellular trafficking. Infect Immun. 1996;64(2):593-9.
530. Locht C, Coutte L, Mielcarek N. The ins and outs of pertussis toxin. FEBS J. 2011;278(23):4668-82.
531. Hausman SZ, Burns DL. Interaction of pertussis toxin with cells and model membranes. J Biol Chem. 1992;267(19):13735-9.
532. Zhang Y, Liu L, Qi Y, Lou J, Chen Y, Liu C, et al. Lactic acid promotes nucleus pulposus cell senescence and corresponding intervertebral disc degeneration via interacting with Akt. Cell Mol Life Sci. 2024;81(1):24.
533. Lanahan SM, Wymann MP, Lucas CL. The role of PI3Kγ in the immune system: new insights and translational implications. Nat Rev Immunol. 2022;22(11):687-700.
534. Ozes ON, Mayo LD, Gustin JA, Pfeffer SR, Pfeffer LM, Donner DB. NF-kappaB activation by tumour necrosis factor requires the Akt serine-threonine kinase. Nature. 1999;401(6748):82-5.
535. de Castro Abrantes H, Briquet M, Schmuziger C, Restivo L, Puyal J, Rosenberg N, et al. The Lactate Receptor HCAR1 Modulates Neuronal Network Activity through the Activation of G. J Neurosci. 2019;39(23):4422-33.
536. Tang F, Lane S, Korsak A, Paton JF, Gourine AV, Kasparov S, et al. Lactate-mediated glia-neuronal signalling in the mammalian brain. Nat Commun. 2014;5:3284.
537. Vardjan N, Chowdhury HH, Horvat A, Velebit J, Malnar M, Muhič M, et al. Enhancement of Astroglial Aerobic Glycolysis by Extracellular Lactate-Mediated Increase in cAMP. Front Mol Neurosci. 2018;11:148.
538. Morland C, Andersson KA, Haugen Ø, Hadzic A, Kleppa L, Gille A, et al. Exercise induces cerebral VEGF and angiogenesis via the lactate receptor HCAR1. Nat Commun. 2017;8:15557.

539. Ohno Y, Oyama A, Kaneko H, Egawa T, Yokoyama S, Sugiura T, et al. Lactate increases myotube diameter via activation of MEK/ERK pathway in C2C12 cells. Acta Physiol (Oxf). 2018;223(2):e13042.
540. Wu Y, Wang M, Zhang K, Li Y, Xu M, Tang S, et al. Lactate enhanced the effect of parathyroid hormone on osteoblast differentiation via GPR81-PKC-Akt signaling. Biochem Biophys Res Commun. 2018;503(2):737-43.
541. Weissinger EM, Eissner G, Grammer C, Fackler S, Haefner B, Yoon LS, et al. Inhibition of the Raf-1 kinase by cyclic AMP agonists causes apoptosis of v-abl-transformed cells. Mol Cell Biol. 1997;17(6):3229-41.
542. Jiang H, Galtes D, Wang J, Rockman HA. G protein-coupled receptor signaling: transducers and effectors. Am J Physiol Cell Physiol. 2022;323(3):C731-C48.
543. Crespo P, Xu N, Simonds WF, Gutkind JS. Ras-dependent activation of MAP kinase pathway mediated by G-protein beta gamma subunits. Nature. 1994;369(6479):418-20.
544. Koch WJ, Hawes BE, Allen LF, Lefkowitz RJ. Direct evidence that Gi-coupled receptor stimulation of mitogen-activated protein kinase is mediated by G beta gamma activation of p21ras. Proc Natl Acad Sci U S A. 1994;91(26):12706-10.
545. Koch WJ, Hawes BE, Inglese J, Luttrell LM, Lefkowitz RJ. Cellular expression of the carboxyl terminus of a G protein-coupled receptor kinase attenuates G beta gamma-mediated signaling. J Biol Chem. 1994;269(8):6193-7.
546. Ahn S, Shenoy SK, Luttrell LM, Lefkowitz RJ. SnapShot: β-Arrestin Functions. Cell. 2020;182(5):1362-.e1.
547. Lefkowitz RJ, Shenoy SK. Transduction of receptor signals by beta-arrestins. Science. 2005;308(5721):512-7.
548. Srivastava A, Gupta B, Gupta C, Shukla AK. Emerging Functional Divergence of β-Arrestin Isoforms in GPCR Function. Trends Endocrinol Metab. 2015;26(11):628-42.
549. Hu J, Cai M, Liu Y, Liu B, Xue X, Ji R, et al. The roles of GRP81 as a metabolic sensor and inflammatory mediator. J Cell Physiol. 2020;235(12):8938-50.
550. Harun-Or-Rashid M, Inman DM. Reduced AMPK activation and increased HCAR activation drive anti-inflammatory response and neuroprotection in glaucoma. J Neuroinflammation. 2018;15(1):313.
551. Ma K, Ding X, Song Q, Han Z, Yao H, Ding J, et al. Lactate enhances Arc/arg3.1 expression through hydroxycarboxylic acid receptor 1-β-arrestin2 pathway in astrocytes. Neuropharmacology. 2020;171:108084.
552. Yan Y, Jiang W, Spinetti T, Tardivel A, Castillo R, Bourquin C, et al. Omega-3 fatty acids prevent inflammation and metabolic disorder through inhibition of NLRP3 inflammasome activation. Immunity. 2013;38(6):1154-63.
553. Oh DY, Talukdar S, Bae EJ, Imamura T, Morinaga H, Fan W, et al. GPR120 is an omega-3 fatty acid receptor mediating potent anti-inflammatory and insulin-sensitizing effects. Cell. 2010;142(5):687-98.
554. Kahsai AW, Shah KS, Shim PJ, Lee MA, Shreiber BN, Schwalb AM, et al. Signal transduction at GPCRs: Allosteric activation of the ERK MAPK by β-arrestin. Proc Natl Acad Sci U S A. 2023;120(43):e2303794120.
555. Baidya M, Kumari P, Dwivedi-Agnihotri H, Pandey S, Sokrat B, Sposini S, et al. Genetically encoded intrabody sensors report the interaction and trafficking of β-arrestin 1 upon activation of G-protein-coupled receptors. J Biol Chem. 2020;295(30):10153-67.

556. Wu Y, Ma W, Liu W, Zhang S. Lactate: a pearl dropped in the ocean-an overlooked signal molecule in physiology and pathology. Cell Biol Int. 2023;47((2)):295-307.
557. Vadevoo SMP, Gunassekaran GR, Lee C, Lee N, Lee J, Chae S, et al. The macrophage odorant receptor Olfr78 mediates the lactate-induced M2 phenotype of tumor-associated macrophages. Proc Natl Acad Sci U S A. 2021;118(37).
558. Nakashima A, Nakashima N, Nakashima K, Takano M. Olfactory receptor 78 is expressed in hypothalamic vasopressin/oxytocin neurons, parenchymal microglia and choroidal macrophages in mice. Mol Brain. 2022;15(1):29.
559. Chang AJ, Ortega FE, Riegler J, Madison DV, Krasnow MA. Oxygen regulation of breathing through an olfactory receptor activated by lactate. Nature. 2015;527(7577):240-4.
560. Cornell J, Rea S, Neitzel LR, Williams CH, Hong CC. Proton Sensing GPCR's: The missing link to Warburg's Oncogenic Legacy? J Cancer Biol. 2024;5(2):65-75.
561. Mohammad Nezhady MA, Chemtob S. 3-OBA Is Not an Antagonist of GPR81. Front Pharmacol. 2021;12:803907.
562. Blad CC, Tang C, Offermanns S. G protein-coupled receptors for energy metabolites as new therapeutic targets. Nat Rev Drug Discov. 2012;11(8):603-19.
563. Offermanns S, Colletti SL, Lovenberg TW, Semple G, Wise A, IJzerman AP. International Union of Basic and Clinical Pharmacology. LXXXII: Nomenclature and Classification of Hydroxy-carboxylic Acid Receptors (GPR81, GPR109A, and GPR109B). Pharmacol Rev. 2011;63(2):269-90.
564. Chen S, Zhou X, Li W, Yang X, Niu X, Hu Z, et al. Development of a novel peptide targeting GPR81 to suppress adipocyte-mediated tumor progression. Biochem Pharmacol. 2023;217:115800.
565. Al-Amrani S, Al-Jabri Z, Al-Zaabi A, Alshekaili J, Al-Khabori M. Proteomics: Concepts and applications in human medicine. World J Biol Chem. 2021;12(5):57-69.
566. Johnston HE, Yadav K, Kirkpatrick JM, Biggs GS, Oxley D, Kramer HB, et al. Solvent Precipitation SP3 (SP4) Enhances Recovery for Proteomics Sample Preparation without Magnetic Beads. Anal Chem. 2022;94(29):10320-8.
567. Kar UK, Simonian M, Whitelegge JP. Integral membrane proteins: bottom-up, top-down and structural proteomics. Expert Rev Proteomics. 2017;14(8):715-23.
568. Gillet LC, Leitner A, Aebersold R. Mass Spectrometry Applied to Bottom-Up Proteomics: Entering the High-Throughput Era for Hypothesis Testing. Annu Rev Anal Chem (Palo Alto Calif). 2016;9(1):449-72.
569. Aebersold R, Mann M. Mass-spectrometric exploration of proteome structure and function. Nature. 2016;537(7620):347-55.
570. Chen C, Hou J, Tanner JJ, Cheng J. Bioinformatics Methods for Mass Spectrometry-Based Proteomics Data Analysis. Int J Mol Sci. 2020;21(8).
571. Butt E, Howard CM, Raman D. LASP1 in Cellular Signaling and Gene Expression: More than Just a Cytoskeletal Regulator. Cells. 2022;11(23).
572. Hayashi T, Funato Y, Terabayashi T, Morinaka A, Sakamoto R, Ichise H, et al. Nucleoredoxin negatively regulates Toll-like receptor 4 signaling via recruitment of flightless-I to myeloid differentiation primary response gene (88). J Biol Chem. 2010;285(24):18586-93.
573. Kopecki Z, Arkell R, Powell BC, Cowin AJ. Flightless I regulates hemidesmosome formation and integrin-mediated cellular adhesion and migration during wound repair. J Invest Dermatol. 2009;129(8):2031-45.

574. Lin CH, Waters JM, Powell BC, Arkell RM, Cowin AJ. Decreased expression of Flightless I, a gelsolin family member and developmental regulator, in early-gestation fetal wounds improves healing. Mamm Genome. 2011;22(5-6):341-52.
575. Lee YH, Stallcup MR. Interplay of Fli-I and FLAP1 for regulation of beta-catenin dependent transcription. Nucleic Acids Res. 2006;34(18):5052-9.
576. Das M, Ithychanda S, Qin J, Plow EF. Mechanisms of talin-dependent integrin signaling and crosstalk. Biochim Biophys Acta. 2014;1838(2):579-88.
577. Cartwright IM, Dowdell AS, Lanis JM, Brink KR, Mu A, Kostelecky RE, et al. Mucosal acidosis elicits a unique molecular signature in epithelia and intestinal tissue mediated by GPR31-induced CREB phosphorylation. Proc Natl Acad Sci U S A. 2021;118(20):e2023871118.
578. Miller EA, Beasley DE, Dunn RR, Archie EA. Lactobacilli Dominance and Vaginal pH: Why Is the Human Vaginal Microbiome Unique? Front Microbiol. 2016;7:1936.
579. Wei X, Tsai MS, Liang L, Jiang L, Hung CJ, Jelliffe-Pawlowski L, et al. Vaginal microbiomes show ethnic evolutionary dynamics and positive selection of Lactobacillus adhesins driven by a long-term niche-specific process. Cell Rep. 2024;43(4):114078.
580. Vega FM, Ridley AJ. Rho GTPases in cancer cell biology. FEBS Lett. 2008;582(14):2093-101.
581. Mendoza MC, Er EE, Blenis J. The Ras-ERK and PI3K-mTOR pathways: cross-talk and compensation. Trends Biochem Sci. 2011;36(6):320-8.
582. Palmieri D, Scarpa M, Tessari A, Uka R, Amari F, Lee C, et al. Ran Binding Protein 9 (RanBP9) is a novel mediator of cellular DNA damage response in lung cancer cells. Oncotarget. 2016;7(14):18371-83.
583. Certo M, Llibre A, Lee W, Mauro C. Understanding lactate sensing and signalling. Trends Endocrinol Metab. 2022;33(10):722-35.
584. Bodai L, Marsh JL. A novel target for Huntington's disease: ERK at the crossroads of signaling. The ERK signaling pathway is implicated in Huntington's disease and its upregulation ameliorates pathology. Bioessays. 2012;34(2):142-8.
585. Valadão PAC, Santos KBS, Ferreira E Vieira TH, Macedo E Cordeiro T, Teixeira AL, Guatimosim C, et al. Inflammation in Huntington's disease: A few new twists on an old tale. J Neuroimmunol. 2020;348:577380.
586. Mezu-Ndubuisi OJ, Maheshwari A. The role of integrins in inflammation and angiogenesis. Pediatr Res. 2021;89(7):1619-26.
587. Canel M, Serrels A, Frame MC, Brunton VG. E-cadherin-integrin crosstalk in cancer invasion and metastasis. J Cell Sci. 2013;126(Pt 2):393-401.
588. Del Pozo MA, Schwartz MA. Rac, membrane heterogeneity, caveolin and regulation of growth by integrins. Trends Cell Biol. 2007;17(5):246-50.
589. Gad AK, Nehru V, Ruusala A, Aspenström P. RhoD regulates cytoskeletal dynamics via the actin nucleation-promoting factor WASp homologue associated with actin Golgi membranes and microtubules. Mol Biol Cell. 2012;23(24):4807-19.
590. Guan G, Cannon RD, Coates DE, Mei L. Effect of the Rho-Kinase/ROCK Signaling Pathway on Cytoskeleton Components. Genes (Basel). 2023;14(2).
591. Crespo P, León J. Ras proteins in the control of the cell cycle and cell differentiation. Cell Mol Life Sci. 2000;57(11):1613-36.
592. López-Posadas R, Stürzl M, Atreya I, Neurath MF, Britzen-Laurent N. Interplay of GTPases and Cytoskeleton in Cellular Barrier Defects during Gut Inflammation. Front Immunol. 2017;8:1240.

593. Pradhan R, Ngo PA, Martínez-Sánchez LD, Neurath MF, López-Posadas R. Rho GTPases as Key Molecular Players within Intestinal Mucosa and GI Diseases. Cells. 2021;10(1):66.
594. Doyen V, Rubio M, Braun D, Nakajima T, Abe J, Saito H, et al. Thrombospondin 1 is an autocrine negative regulator of human dendritic cell activation. J Exp Med. 2003;198(8):1277-83.
595. Akhmanova A, Kapitein LC. Mechanisms of microtubule organization in differentiated animal cells. Nat Rev Mol Cell Biol. 2022;23(8):541-58.
596. Yao Z, Seger R. The ERK signaling cascade--views from different subcellular compartments. Biofactors. 2009;35(5):407-16.
597. Pullikuth AK, Catling AD. Scaffold mediated regulation of MAPK signaling and cytoskeletal dynamics: a perspective. Cell Signal. 2007;19(8):1621-32.
598. Reszka AA, Seger R, Diltz CD, Krebs EG, Fischer EH. Association of mitogen-activated protein kinase with the microtubule cytoskeleton. Proc Natl Acad Sci U S A. 1995;92(19):8881-5.
599. Perlson E, Hanz S, Ben-Yaakov K, Segal-Ruder Y, Seger R, Fainzilber M. Vimentin-dependent spatial translocation of an activated MAP kinase in injured nerve. Neuron. 2005;45(5):715-26.
600. Eishingdrelo H, Sun W, Li H, Wang L, Eishingdrelo A, Dai S, et al. ERK and β-arrestin interaction: a converging point of signaling pathways for multiple types of cell surface receptors. J Biomol Screen. 2015;20(3):341-9.
601. Ducut Sigala JL, Bottero V, Young DB, Shevchenko A, Mercurio F, Verma IM. Activation of transcription factor NF-kappaB requires ELKS, an IkappaB kinase regulatory subunit. Science. 2004;304(5679):1963-7.
602. Ramazi S, Zahiri J. Posttranslational modifications in proteins: resources, tools and prediction methods. Database (Oxford). 2021;2021:baab012.
603. Duchovni L, Shmunis G, Lobel L. Posttranslational modifications: an emerging functional layer of diet-host-microbe interactions. mBio. 2024;15(10):e0238724.
604. Karve TM, Cheema AK. Small changes huge impact: the role of protein posttranslational modifications in cellular homeostasis and disease. J Amino Acids. 2011;2011:207691.
605. Aebersold R, Agar JN, Amster IJ, Baker MS, Bertozzi CR, Boja ES, et al. How many human proteoforms are there? Nat Chem Biol. 2018;14(3):206-14.
606. Fenech M, Kirsch-Volders M, Natarajan AT, Surralles J, Crott JW, Parry J, et al. Molecular mechanisms of micronucleus, nucleoplasmic bridge and nuclear bud formation in mammalian and human cells. Mutagenesis. 2011;26(1):125-32.
607. Basit A, Cho MG, Kim EY, Kwon D, Kang SJ, Lee JH. The cGAS/STING/TBK1/IRF3 innate immunity pathway maintains chromosomal stability through regulation of p21 levels. Exp Mol Med. 2020;52(4):643-57.
608. Rossi V, Hochkoeppler A, Govoni M, Di Stefano G. Lactate-Induced HBEGF Shedding and EGFR Activation: Paving the Way to a New Anticancer Therapeutic Opportunity. Cells. 2024;13(18):1533.
609. Hutagalung AH, Novick PJ. Role of Rab GTPases in membrane traffic and cell physiology. Physiol Rev. 2011;91(1):119-49.
610. Prashar A, Schnettger L, Bernard EM, Gutierrez MG. Rab GTPases in Immunity and Inflammation. Front Cell Infect Microbiol. 2017;7:435.
611. Guadagno NA, Progida C. Rab GTPases: Switching to Human Diseases. Cells. 2019;8(8).

612. Jiang Y, Tsoi LC, Billi AC, Ward NL, Harms PW, Zeng C, et al. Cytokinocytes: the diverse contribution of keratinocytes to immune responses in skin. JCI Insight. 2020;5(20):e142067.
613. Adarska P, Wong-Dilworth L, Bottanelli F. ARF GTPases and Their Ubiquitous Role in Intracellular Trafficking Beyond the Golgi. Front Cell Dev Biol. 2021;9:679046.
614. Junutula JR, Schonteich E, Wilson GM, Peden AA, Scheller RH, Prekeris R. Molecular characterization of Rab11 interactions with members of the family of Rab11-interacting proteins. J Biol Chem. 2004;279(32):33430-7.
615. Rübsam M, Mertz AF, Kubo A, Marg S, Jüngst C, Goranci-Buzhala G, et al. E-cadherin integrates mechanotransduction and EGFR signaling to control junctional tissue polarization and tight junction positioning. Nat Commun. 2017;8(1):1250.
616. Campbell HD, Fountain S, Young IG, Claudianos C, Hoheisel JD, Chen KS, et al. Genomic structure, evolution, and expression of human FLII, a gelsolin and leucine-rich-repeat family member: overlap with LLGL. Genomics. 1997;42(1):46-54.
617. Cowin AJ, Adams DH, Strudwick XL, Chan H, Hooper JA, Sander GR, et al. Flightless I deficiency enhances wound repair by increasing cell migration and proliferation. J Pathol. 2007;211(5):572-81.
618. Kopecki Z, Cowin AJ. Flightless I: an actin-remodelling protein and an important negative regulator of wound repair. Int J Biochem Cell Biol. 2008;40(8):1415-9.
619. Jin J, Yu Q, Han C, Hu X, Xu S, Wang Q, et al. LRRFIP2 negatively regulates NLRP3 inflammasome activation in macrophages by promoting Flightless-I-mediated caspase-1 inhibition. Nat Commun. 2013;4:2075.
620. Marei H, Carpy A, Woroniuk A, Vennin C, White G, Timpson P, et al. Differential Rac1 signalling by guanine nucleotide exchange factors implicates FLII in regulating Rac1-driven cell migration. Nat Commun. 2016;7:10664.
621. Silacci P, Mazzolai L, Gauci C, Stergiopulos N, Yin HL, Hayoz D. Gelsolin superfamily proteins: key regulators of cellular functions. Cell Mol Life Sci. 2004;61(19-20):2614-23.
622. Strudwick XL, Cowin AJ. Multifunctional Roles of the Actin-Binding Protein Flightless I in Inflammation, Cancer and Wound Healing. Front Cell Dev Biol. 2020;8:603508.
623. Wang T, Chuang TH, Ronni T, Gu S, Du YC, Cai H, et al. Flightless I homolog negatively modulates the TLR pathway. J Immunol. 2006;176(3):1355-62.
624. Idelfonso-García OG, Alarcón-Sánchez BR, Vásquez-Garzón VR, Baltiérrez-Hoyos R, Villa-Treviño S, Muriel P, et al. Is Nucleoredoxin a Master Regulator of Cellular Redox Homeostasis? Its Implication in Different Pathologies. Antioxidants (Basel). 2022;11(4):670.
625. Rodrigues M, Petrova T, Tibbs B, Arthur JSC, Cohen P. TAK1 protein kinase activity is required for TLR signalling and cytokine production in myeloid cells. Biochem J. 2022;479(17):1891-907.
626. Pang X, He X, Qiu Z, Zhang H, Xie R, Liu Z, et al. Targeting integrin pathways: mechanisms and advances in therapy. Signal Transduct Target Ther. 2023;8(1):1.
627. Kim C, Schmidt T, Cho EG, Ye F, Ulmer TS, Ginsberg MH. Basic amino-acid side chains regulate transmembrane integrin signalling. Nature. 2011;481(7380):209-13.
628. Elias BC, Mathew S, Srichai MB, Palamuttam R, Bulus N, Mernaugh G, et al. The integrin β1 subunit regulates paracellular permeability of kidney proximal tubule cells. J Biol Chem. 2014;289(12):8532-44.
629. Poole DC, Rossiter HB, Brooks GA, Gladden LB. The anaerobic threshold: 50+ years of controversy. J Physiol. 2021;599(3):737-67.

630. Von Muralt A. The development of muscle-chemistry, a lesson in neurophysiology. Biochim Biophys Acta. 1950;4(1-3):126-9.
631. Shukair SA, Allen SA, Cianci GC, Stieh DJ, Anderson MR, Baig SM, et al. Human cervicovaginal mucus contains an activity that hinders HIV-1 movement. Mucosal Immunol. 2013;6(2):427-34.
632. Witkin SS, Linhares IM. HIV inhibition by lactobacilli: easier in a test tube than in real life. MBio. 2015;6(5):e01485-15.
633. Carey AJ, Beagley KW. Chlamydia trachomatis, a hidden epidemic: effects on female reproduction and options for treatment. Am J Reprod Immunol. 2010;63(6):576-86.
634. Simms I, Eastick K, Mallinson H, Thomas K, Gokhale R, Hay P, et al. Associations between Mycoplasma genitalium, Chlamydia trachomatis and pelvic inflammatory disease. J Clin Pathol. 2003;56(8):616-8.
635. Molenaar MC, Singer M, Ouburg S. The two-sided role of the vaginal microbiome in Chlamydia trachomatis and Mycoplasma genitalium pathogenesis. J Reprod Immunol. 2018;130:11-7.
636. Jiang I, Yong PJ, Allaire C, Bedaiwy MA. Intricate Connections between the Microbiota and Endometriosis. Int J Mol Sci. 2021;22(11):5644.
637. Ma B, France MT, Crabtree J, Holm JB, Humphrys MS, Brotman RM, et al. A comprehensive non-redundant gene catalog reveals extensive within-community intraspecies diversity in the human vagina. Nat Commun. 2020;11(1):940.
638. Short CS, Quinlan RA, Wang X, Preda VG, Smith A, Marchesi JR, et al. Vaginal Microbiota, Genital Inflammation and Extracellular Matrix Remodelling Collagenase: MMP-9 in Pregnant Women With HIV, a Potential Preterm Birth Mechanism Warranting Further Exploration. Front Cell Infect Microbiol. 2021;11:750103.
639. Tidbury F, Brülhart G, Müller G, Pavicic E, Weidlinger S, Eichner G, et al. Effectiveness and tolerability of lactic acid vaginal gel compared to oral metronidazole in the treatment of acute symptomatic bacterial vaginosis: a multicenter, randomized-controlled, head-to-head pilot study. BMC Womens Health. 2025;25(1):7.
640. Edwards VL, McComb E, Gleghorn JP, Forney L, Bavoil PM, Ravel J. Three-dimensional models of the cervicovaginal epithelia to study host-microbiome interactions and sexually transmitted infections. Pathog Dis. 2022;80(1):ftac026.
641. Lõhmussaar K, Oka R, Espejo Valle-Inclan J, Smits MHH, Wardak H, Korving J, et al. Patient-derived organoids model cervical tissue dynamics and viral oncogenesis in cervical cancer. Cell Stem Cell. 2021;28(8):1380-96.e6.
642. Li J, Zhou M, Xie J, Chen J, Yang M, Ye C, et al. Organoid modeling meets cancers of female reproductive tract. Cell Death Discov. 2024;10(1):410.
643. Alzamil L, Nikolakopoulou K, Turco MY. Organoid systems to study the human female reproductive tract and pregnancy. Cell Death Differ. 2021;28(1):35-51.
644. Ali A, Syed SM, Jamaluddin MFB, Colino-Sanguino Y, Gallego-Ortega D, Tanwar PS. Cell Lineage Tracing Identifies Hormone-Regulated and Wnt-Responsive Vaginal Epithelial Stem Cells. Cell Rep. 2020;30(5):1463-77.e7.
645. Barrila J, Crabbé A, Yang J, Franco K, Nydam SD, Forsyth RJ, et al. Modeling Host-Pathogen Interactions in the Context of the Microenvironment: Three-Dimensional Cell Culture Comes of Age. Infect Immun. 2018;86(11):e00282-18.

646. Barrila J, Radtke AL, Crabbé A, Sarker SF, Herbst-Kralovetz MM, Ott CM, et al. Organotypic 3D cell culture models: using the rotating wall vessel to study host-pathogen interactions. Nat Rev Microbiol. 2010;8(11):791-801.
647. Jackson R, Maarsingh JD, Herbst-Kralovetz MM, Van Doorslaer K. 3D Oral and Cervical Tissue Models for Studying Papillomavirus Host-Pathogen Interactions. Curr Protoc Microbiol. 2020;59(1):e129.
648. Łaniewski P, Herbst-Kralovetz MM. Analysis of Host Responses to Neisseria gonorrhoeae Using a Human Three-Dimensional Endometrial Epithelial Cell Model. Methods Mol Biol. 2019;1997:347-61.
649. Łaniewski P, Ilhan ZE, Herbst-Kralovetz MM. The microbiome and gynaecological cancer development, prevention and therapy. Nat Rev Urol. 2020;17(4):232-50.
650. Runde AP, Mack R, S J PB, Zhang J. The role of TBK1 in cancer pathogenesis and anticancer immunity. J Exp Clin Cancer Res. 2022;41(1):135.
651. Helgason E, Phung QT, Dueber EC. Recent insights into the complexity of Tank-binding kinase 1 signaling networks: the emerging role of cellular localization in the activation and substrate specificity of TBK1. FEBS Lett. 2013;587(8):1230-7.
652. Varki A, Cummings RD, Esko JD, Stanley P, Hart GW, Aebi M, et al. Essentials of Glycobiology [internet]. 4th edition ed: Cold Spring Harbor (NY): Cold Spring Harbor Laboratory Press; 2022.
653. Dai P, Jeong SY, Yu Y, Leng T, Wu W, Xie L, et al. Modulation of TLR signaling by multiple MyD88-interacting partners including leucine-rich repeat Fli-I-interacting proteins. J Immunol. 2009;182(6):3450-60.
654. Wang T, Gu S, Ronni T, Du YC, Chen X. In vivo dual-tagging proteomic approach in studying signaling pathways in immune response. J Proteome Res. 2005;4(3):941-9.